Tomy J. Gutiérrez *Editor*

Reactive and Functional Polymers Volume Four

Surface, Interface, Biodegradability, Compostability and Recycling

Springer

Reactive and Functional Polymers Volume Four

Tomy J. Gutiérrez
Editors

Reactive and Functional Polymers Volume Four

Surface, Interface, Biodegradability, Compostability and Recycling

Springer

Editor
Tomy J. Gutiérrez
National Scientific and Technical Research Council (CONICET)
Institute of Research in Materials Science and Technology (INTEMA)
Thermoplastic Composite Materials (CoMP) Group
Mar del Plata, Argentina

ISBN 978-3-030-52051-9 ISBN 978-3-030-52052-6 (eBook)
https://doi.org/10.1007/978-3-030-52052-6

© The Editor(s) (if applicable) and The Author(s), under exclusive license to Springer Nature Switzerland AG 2020, Corrected Publication 2020
This work is subject to copyright. All rights are reserved by the Publisher, whether the whole or part of the material is concerned, specifically the rights of translation, reprinting, reuse of illustrations, recitation, broadcasting, reproduction on microfilms or in any other physical way, and transmission or information storage and retrieval, electronic adaptation, computer software, or by similar or dissimilar methodology now known or hereafter developed.
The use of general descriptive names, registered names, trademarks, service marks, etc. in this publication does not imply, even in the absence of a specific statement, that such names are exempt from the relevant protective laws and regulations and therefore free for general use.
The publisher, the authors, and the editors are safe to assume that the advice and information in this book are believed to be true and accurate at the date of publication. Neither the publisher nor the authors or the editors give a warranty, expressed or implied, with respect to the material contained herein or for any errors or omissions that may have been made. The publisher remains neutral with regard to jurisdictional claims in published maps and institutional affiliations.

This Springer imprint is published by the registered company Springer Nature Switzerland AG
The registered company address is: Gewerbestrasse 11, 6330 Cham, Switzerland

I would like to dedicate this book:

To my God (Father, Son and Holy Spirit), to the Virgin Mary and to my Guardian Angel,
Its energy stimulates me to enjoy the landscape we call life and its peace encourages me to always continue towards the future, a place where we will all go and each one will be under the law of the creative father.
To my Mother (Dr. Mirian Arminda Carmona Rodríguez),
For forming my character and attitude towards life.
To my Grandmother (Mrs. Arminda Teresa Rodríguez Romero),
A person who unfortunately left before this world’s time, but I am sure that she is up watching me and supporting me in all facets of my life. You are in my most beautiful memories.
To my firstborn daughter (Miranda V. Gutiérrez),
I will give you a lot of love!!!🤗♡.
To all anonymous people,
Those who give me their love, friendship, patience and support in various situations.

To Venezuela and Argentina,
The first for giving me my academic and professional training, and the second for welcoming me with love and friendship before the dictatorship that my country (Venezuela) is experiencing today.

Tomy J. Gutiérrez, Ph.D.
Editor

Preface

Reactive and functional polymers are essentially linked to the chemistry of polymers and their applications. The multiple tasks that they have accomplished in our recent history, and how they will help new advances in different crucial fields are indisputable. Volume 4 has been focused on surface reactions, interfacial interactions and reactive processes for recycling polymers and their biodegradability and compostability. I appreciate the valuable contribution of each of the contributing authors to this book from nine different countries.

Tomy J. Gutiérrez, Ph.D
National Scientific and Technical Research Council (CONICET)
Institute of Research in Materials Science and Technology (INTEMA)
Thermoplastic Composite Materials (CoMP) Group
Mar del Plata, Argentina

Contents

1 Surfaces, Interfaces and Recycling from Reactive and Functional Polymers: Editor's Insights 1
Tomy J. Gutiérrez

2 Surface Functionalization of Polymers 5
Deval Prasad Bhattarai, Pashupati Pokharel, and Dequan Xiao

3 Surface Reactive and Active Polymers 35
Saeed Ghanooni, Nasser Nikfarjam, and Pooyan Makvandi

4 Polymer Interface Reactions 55
Michael Cordin, Judith R. Büttler, Thomas Bechtold, and Tung Pham

5 Design of Switchable and Supramolecular Polymers for Biointerface Applications 97
Luanda Lins

6 Recycling of Reactive and Functional Polymers 129
A. M. M. Saleh and Reem K. Farag

7 Readily Recyclable Thermosets Based on Dynamic Covalent Bonds 159
Sheng Wang, Songqi Ma, and Jin Zhu

8 A Review to Guide Eco-Design of Reactive Polymer-Based Materials 207
Emma Delamarche, Valérie Massardier, Remy Bayard, and Edson Dos Santos

Correction to: Surface Functionalization of Polymers C1

Index 243

About the Editor

Tomy J. Gutiérrez received his degrees in Chemistry (Geochemical Option) and in Education (Chemical Mention) from the Central University of Venezuela (UCV) in December 2007 and July 2008, respectively. He completed his specialization in International Negotiation of Hydrocarbons from the National Polytechnic Experimental University of the National Armed Force (UNEFA), Venezuela, in July 2011, and his Master's and PhD degrees in Food Science and Technology in October 2013 and April 2015, respectively, both from the UCV. He has also PhD studies in Metallurgy and Materials Science from the UCV and postdoctoral studies in the Research Institute in Materials Science and Technology (INTEMA). He has been a Professor/Researcher both at the Institute of Food Science and Technology (ICTA) and the School of Pharmacy at the UCV. Currently, he is an Adjunct Researcher in the INTEMA, National Scientific and Technical Research Council (CONICET), Argentina. Dr. Gutiérrez has at least 20 book chapters, 40 publications in international journals of high-impact factor, and 5 published books. He has been a Lead Guest Editor of several international journals such as *Journal of Food Quality*, *Polymers for Advanced Technologies* and *Current Pharmaceutical Design*. He is also an Editorial Board Member of different international journals such as *Food and Bioprocess Technology* (from April 2019 to the present, 2019 impact factor 3.356), *Current Nutraceuticals* (from May 2019 to the present), and *Journal of Renewable Materials* (from June 2019 to the present, 2019 impact factor 1.341). Currently, he is developing a line of research in nanostructured materials based on polymers (composite materials), which are obtained on a pilot scale to be transferred to the agricultural, food, pharmaceutical and polymer industries. He is also a collaborator of international projects between Argentina and Brazil, Colombia, France, Poland, Spain, Italy, Sweden, and Venezuela.

Chapter 1
Surfaces, Interfaces and Recycling from Reactive and Functional Polymers: Editor's Insights

Tomy J. Gutiérrez

Abstract Surface modifications and reactions on polymer systems have achieved to improve their performance as reactive and functional materials, compatibility of polymer blends, among others. Likewise, there is a great interest in the reduction of plastic waste or its reuse. This has been more recently addressed by reactive polymer processing or the use of reactive and functional polymers *per se* with the aim of reducing pollution from conventional petroleum-derived polymers. With this chapter, we open these main topics that will be analyzed in this volume.

Keywords Biodegradability · Composting

1.1 Editor's Insights

The future of the new materials will go through the development of reactive and functional polymers with the objective of obtaining polymers with outstanding and extravagant properties to be used in different domestic, industrial and extraordinary applications. With this in mind, the superficial modifications and reactions will give a great guideline in this case, as well as with the aim of avoiding environmental pollution. Keeping this in view, these aspects will be exhaustively analyzed in this book (Gutiérrez 2017a, b, 2018a, b; Gutiérrez and Álvarez 2016, 2017a, b, c, d, 2018; Gutiérrez and González 2016, 2017; Gutiérrez et al. 2015a, b, 2016a, b, 2017, 2018a, b, 2019; Herniou–Julien et al. 2019; Merino et al. 2018a, b, 2019a, b; Toro-Márquez et al. 2018; Zarrintaj et al. 2019).

T. J. Gutiérrez (✉)
National Scientific and Technical Research Council (CONICET), Institute of Research in Materials Science and Technology (INTEMA), Thermoplastic Composite Materials (CoMP) Group, Mar del Plata, Argentina
e-mail: tomy.gutierrez@fi.mdp.edu.ar

T. J. Gutiérrez (ed.), *Reactive and Functional Polymers Volume Four*,
https://doi.org/10.1007/978-3-030-52052-6_1

Acknowledgements The author would like to thank the Consejo Nacional de Investigaciones Científicas y Técnicas (CONICET) (Postdoctoral fellowship internal PDTS-Resolution 2417), Agencia Nacional de Promoción Científica y Tecnológica (ANPCyT) (grant PICT-2017-1362), Universidad Nacional de Mar del Plata (UNMdP) for financial support, and Dr. Mirian Carmona-Rodríguez.

Conflicts of Interest The author declares no conflict of interest.

References

Gutiérrez, T. J. (2017a). Effects of exposure to pulsed light on molecular aspects of edible films made from cassava and taro starch. *Innovative Food Science and Emerging Technologies, 41*, 387–396. https://doi.org/10.1016/j.ifset.2017.04.014.

Gutiérrez, T. J. (2017b). Surface and nutraceutical properties of edible films made from starchy sources with and without added blackberry pulp. *Carbohydrate Polymers, 165*, 169–179. https://doi.org/10.1016/j.carbpol.2017.02.016.

Gutiérrez, T. J. (2018a). Active and intelligent films made from starchy sources/blackberry pulp. *Journal of Polymers and the Environment, 26*(6), 2374–2391. https://doi.org/10.1007/s10924-017-1134-y.

Gutiérrez, T. J. (2018b). Are modified pumpkin flour/plum flour nanocomposite films biodegradable and compostable? *Food Hydrocolloids, 83*, 397–410. https://doi.org/10.1016/j.foodhyd.2018.05.035.

Gutiérrez, T. J., & Álvarez, K. (2016). Physico-chemical properties and *in vitro* digestibility of edible films made from plantain flour with added *Aloe vera* gel. *Journal of Functional Foods, 26*, 750–762. https://doi.org/10.1016/j.jff.2016.08.054.

Gutiérrez, T. J., & Alvarez, V. A. (2017a). Cellulosic materials as natural fillers in starch-containing matrix-based films: A review. *Polymer Bulletin, 74*(6), 2401–2430. https://doi.org/10.1007/s00289-016-1814-0.

Gutiérrez, T. J., & Alvarez, V. A. (2017b). Data on physicochemical properties of active films derived from plantain flour/PCL blends developed under reactive extrusion conditions. *Data in Brief, 15*, 445–448. https://doi.org/10.1016/j.dib.2017.09.071.

Gutiérrez, T. J., & Alvarez, V. A. (2017c). Eco-friendly films prepared from plantain flour/PCL blends under reactive extrusion conditions using zirconium octanoate as a catalyst. *Carbohydrate Polymers, 178*, 260–269. https://doi.org/10.1016/j.carbpol.2017.09.026.

Gutiérrez, T. J., & Alvarez, V. A. (2017d). Properties of native and oxidized corn starch/polystyrene blends under conditions of reactive extrusion using zinc octanoate as a catalyst. *Reactive and Functional Polymers, 112*, 33–44. https://doi.org/10.1016/j.reactfunctpolym.2017.01.002.

Gutiérrez, T. J., & Alvarez, V. A. (2018). Bionanocomposite films developed from corn starch and natural and modified nano-clays with or without added blueberry extract. *Food Hydrocolloids, 77*, 407–420. https://doi.org/10.1016/j.foodhyd.2017.10.017.

Gutiérrez, T. J., & González, G. (2016). Effects of exposure to pulsed light on surface and structural properties of edible films made from cassava and taro starch. *Food and Bioprocess Technology, 9*(11), 1812–1824. https://doi.org/10.1007/s11947-016-1765-3.

Gutiérrez, T. J., & González, G. (2017). Effect of cross-linking with *Aloe vera* gel on surface and physicochemical properties of edible films made from plantain flour. *Food Biophysics, 12*(1), 11–22. https://doi.org/10.1007/s11483-016-9458-z.

Gutiérrez, T. J., Morales, N. J., Pérez, E., Tapia, M. S., & Famá, L. (2015a). Physico-chemical properties of edible films derived from native and phosphated cush-cush yam and cassava starches. *Food Packaging and Shelf Life, 3*, 1–8. https://doi.org/10.1016/j.fpsl.2014.09.002.

Gutiérrez, T. J., Tapia, M. S., Pérez, E., & Famá, L. (2015b). Structural and mechanical properties of native and modified cush-cush yam and cassava starch edible films. *Food Hydrocolloids, 45*, 211–217. https://doi.org/10.1016/j.foodhyd.2014.11.017.

Gutiérrez, T. J., Guzmán, R., Medina Jaramillo, C., & Famá, L. (2016a). Effect of beet flour on films made from biological macromolecules: Native and modified plantain flour. *International Journal of Biological Macromolecules, 82*, 395–403. https://doi.org/10.1016/j.ijbiomac.2015.10.020.

Gutiérrez, T. J., Suniaga, J., Monsalve, A., & García, N. L. (2016b). Influence of beet flour on the relationship surface-properties of edible and intelligent films made from native and modified plantain flour. *Food Hydrocolloids, 54*, 234–244. https://doi.org/10.1016/j.foodhyd.2015.10.012.

Gutiérrez, T. J., Guarás, M. P., & Vera, A. A. (2017). Chapter 9. Reactive extrusion for the production of starch-based biopackaging. In M. A. Masuelli (Ed.), *Biopackaging* (pp. 287–315). Miami, FL: CRC, Taylor & Francis Group. EE.UU. ISBN: 978-1-4987-4968-8. https://doi.org/10.1201/9781315152349-9.

Gutiérrez, T. J., Herniou-Julien, C., Álvarez, K., & Alvarez, V. A. (2018a). Structural properties and *in vitro* digestibility of edible and pH-sensitive films made from Guinea arrowroot starch and wastes from wine manufacture. *Carbohydrate Polymers, 184*, 135–143. https://doi.org/10.1016/j.carbpol.2017.12.039.

Gutiérrez, T. J., Ollier, R., & Alvarez, V. A. (2018b). Chapter 5. Surface properties of thermoplastic starch materials reinforced with natural fillers. In V. K. Thakur & M. K. Thakur (Eds.), *Functional biopolymers* (pp. 131–158). Cham: Springer International. EE.UU. ISBN: 978-3-319-66416-3. eISBN: 978-3-319-66417-0. https://doi.org/10.1007/978-3-319-66417-0_5.

Gutiérrez, T. J., Toro-Márquez, L. A., Merino, D., & Mendieta, J. R. (2019). Hydrogen-bonding interactions and compostability of bionanocomposite films prepared from corn starch and nano-fillers with and without added Jamaica flower extract. *Food Hydrocolloids, 89*, 283–293. https://doi.org/10.1016/j.foodhyd.2018.10.058.

Herniou--Julien, C., Mendieta, J. R., & Gutiérrez, T. J. (2019). Characterization of biodegradable/non-compostable films made from cellulose acetate/corn starch blends processed under reactive extrusion conditions. *Food Hydrocolloids, 89*, 67–79. https://doi.org/10.1016/j.foodhyd.2018.10.024.

Merino, D., Gutiérrez, T. J., Mansilla, A. Y., Casalongué, C. A., & Alvarez, V. A. (2018a). Critical evaluation of starch-based antibacterial nanocomposites as agricultural mulch films: Study on their interactions with water and light. *ACS Sustainable Chemistry & Engineering, 6*(11), 15662–15672. https://doi.org/10.1021/acssuschemeng.8b04162.

Merino, D., Mansilla, A. Y., Gutiérrez, T. J., Casalongué, C. A., & Alvarez, V. A. (2018b). Chitosan coated-phosphorylated starch films: Water interaction, transparency and antibacterial properties. *Reactive and Functional Polymers, 131*, 445–453. https://doi.org/10.1016/j.reactfunctpolym.2018.08.012.

Merino, D., Gutiérrez, T. J., & Alvarez, V. A. (2019a). Potential agricultural mulch films based on native and phosphorylated corn starch with and without surface functionalization with chitosan. *Journal of Polymers and the Environment, 27*(1), 97–105. https://doi.org/10.1007/s10924-018-1325-1.

Merino, D., Gutiérrez, T. J., & Alvarez, V. A. (2019b). Structural and thermal properties of agricultural mulch films based on native and oxidized corn starch nanocomposites. *Starch-Stärke, 71*(7–8), 1800341. https://doi.org/10.1002/star.201800341.

Toro-Márquez, L. A., Merino, D., & Gutiérrez, T. J. (2018). Bionanocomposite films prepared from corn starch with and without nanopackaged Jamaica (*Hibiscus sabdariffa*) flower extract. *Food and Bioprocess Technology, 11*(11), 1955–1973. https://doi.org/10.1007/s11947-018-2160-z.

Zarrintaj, P., Jouyandeh, M., Ganjali, M. R., Hadavand, B. S., Mozafari, M., Sheiko, S. S., Vatankhah-Varnoosfaderani, M., Gutiérrez, T. J., & Saeb, M. R. (2019). Thermo-sensitive polymers in medicine: A review. *European Polymer Journal, 117*, 402–423. https://doi.org/10.1016/j.eurpolymj.2019.05.024.

Chapter 2
Surface Functionalization of Polymers

Deval Prasad Bhattarai, Pashupati Pokharel, and Dequan Xiao

Abstract The wide range of inherent and tunable physicochemical properties of polymers made them ubiquitous and unavoidable materials in the physical and biological world. Both natural and synthetic polymers find their wide range of applications from everyday life to technical innovations. The unique physicochemical properties dependent on the morphology of the polymers have led its wide range of applications in therapies and diagnostic options. The inherent and tunable surface characteristics of polymers are used for technical applications with specific surface specialties. The polymers used for biomaterial application must meet some criteria, such as non-cytotoxicity, high drug loading capacity and improved cellular internalization. However, the polymer may have some special surface properties due to its performance according to its application design. In these perspectives, the surface functionalization of polymers is necessary to take advantage of their properties and achieve the selective and specific recognition required for biomedical applications. The surface functionalization of polymers is a promising technique to introduce and monitor some specific surface properties, such as adhesion, adsorption, biocompatibility, electrical conductivity, optical properties and wettability to target their corresponding applications. In this chapter, the chemistry, scope and current trends of surface functionalization will be discussed in terms of chemical, physical, and nanotechnological methods.

Keywords Advanced materials · Macromolecule · Nanotechnology · Surface properties

---

The original version of this chapter was revised. The correction to this chapter is available at https://doi.org/10.1007/978-3-030-52052-6_9

D. P. Bhattarai
Department of Chemistry, Amrit Campus, Tribhuvan University, Kathmandu, Nepal

P. Pokharel (✉) · D. Xiao
Department of Chemistry and Chemical Engineering, Center for Integrative Materials Discovery, University of New Haven, West Haven, CT, USA
e-mail: ppokharel@newhaven.edu

T. J. Gutiérrez (ed.), *Reactive and Functional Polymers Volume Four*,
https://doi.org/10.1007/978-3-030-52052-6_2

Abbreviations

AA	Acrylic acid
APTES	3-Aminopropyltriethoxysilane
CNC	Cellulose nanocrystal
DMSO	Dimethylsulphoxide
GO	Graphene oxide
HAp	Hydroxyapatite
MDI	4,4′-methylene diphenyl diisocyanate
$NaBH_4$	Sodium borohydride
NPs	Nanoparticles
P3HT	Poly(3-hexylthiophene)
PAN	Poly(acrylonitrile)
PAPMA	Poly(*N*-3-aminopropylmethacrylamide)
PBTP	Poly(butylene terephthalate)
PC	Poly(carbonate)
PCL	Poly(ε-caprolactone)
PDA	Poly(dopamine)
PDMS	Poly(dimethylsiloxane)
PE	Poly(ethylene)
PEEK	Polyetheretherketone
PEG	Poly(ethylene glycol)
PEO	Poly(ethylene oxide)
PES	Poly(ether sulfone)
PET	Poly(ethylene terephthalate)
PGA	Poly(glycolide)
PLA	Poly(lactide)
PLGA	Poly(lactic-*co*-glycolic acid)
PLGA-*b*-PEG-NH_2	Poly(D,L-lactic-*co*-glycolic acid)-poly(ethylene glycol)-NH_2
PLLA	Poly(L-lactic acid)
PLLC	Poly(L-lactide-*co*-caprolactone)
PMAA	Poly(methacrylic acid)
PMMA	Poly(methyl methacrylate)
PNIPAAm	Poly(*N*-isopropylacrylamide)
PP	Poly(propylene)
PS	Poly(styrene)
PSBMA	Poly(sulfobetaine methacrylate)
PtBuA	Poly(*tert*-butyl acrylate)
PU	Poly(urethane)
PVDF	Poly(vinylidene fluoride)

2.1 Introduction: Fundamentals of Surface Functionalization of Polymer

Various polymeric substances have been designed in different nano-forms (polymeric NPs, nanofibers, nanorods, nanospheres, nanotubes, electro-spun fibers, etc.) and have been used in various aspects of research and commercial applications (Bhattarai et al. 2019b, 2020). The properties of the polymeric nanomaterial are the synergistic effect of its bulk properties, surface properties, formulation and engineering. The nanomaterials endowed with the intended bulk and surface properties could be the material chosen for their applications as advanced materials with desirable characteristics. The high surface/volume ratio of nanomaterials and quantum confinement have triggered its scope and dynamics in various research fields, as well as trades and commerce. A wide range of materials and their performance depend largely on their surface characteristics. In biological settings, surface functionalization of polymer is intended to influence on the implant biocompatibility, thus reducing thrombogenicity and tuning the adhesion of proteins and cells (Tang et al. 2008). Some properties such as thermal stability, mechanical strength, behavior towards solvent, polymer degradation, swelling/deswelling properties are more related with bulk properties of polymer, while other properties such as surface adhesion, chemistry and wettability, as well as behavior towards harsh chemical/environmental agents are more concerned with surface characteristics. In most cases, the polymers of choice may be lower than the intended properties required for particular applications. To fill these gaps, the polymerization surface functionalization strategy can be a way of implementation (Penn and Wang 1994).

The understanding of the material surfaces and their engineering has increased significantly with a greater capacity to tailor and modulate the surface characteristics for specific application. Especially, such surface modifications of polymers *via* surface functionalization would change the fate of surface hydrophilicity, cellular behavior and physicochemical platforms such as antibacterial or photothermal properties (Tiwari et al. 2019).

Different types of polymers are used for several types of physical applications. The electric charge transfer process through the polymer film and metal electrode interfaces plays a key role in many polymeric optoelectronic devices, including light-emitting diodes, photovoltaic cells and thin film transistors. Polymers such as PBTP, PC, PDMS, PMMA, polyolefins (e.g. PE and PP), etc. can be used in the manufacture of thermosetting materials (Zarrintaj et al. 2019). However, the polymers used can capture some specific types compounds from the solution passing through it. In order to inhibit such undesired molecular adsorptions, it is required to functionalize the surface of such polymers (Rohr et al. 2003).

Polymers, in different forms and designs, are being used in different fields of bio-applications. Whatever the polymeric materials or their design, it is the surface of the biomaterials which comes into contact with physiological environment immediately after their accommodation into the body (Dai et al. 2003). To improve the surface effectiveness of the engineered material, it is a common practice to carry out surface functionalization of the material. However, the approaches of surface functionalization might be different. The surface of electro-spun fibers can be modified or functionalized by various ways to introduce new functionalities. In some cases, even after surface functionalization, cell-recognizable ligands can be chemically immobilized on the substrate surface for anchoring (Gutiérrez et al. 2018). The surface functionalization of polymers can be linked to different fields of applications including drug delivery, gene delivery and various aspects of tissue engineering. The high surface area of nanomaterials could provide platforms for the immobilization of bioactive molecules such as antibodies, DNA, enzymes and peptides (Kim and Park 2006). In view of the bio-application of any polymer, the cellular interaction and cytotoxicity of the materials depends on the physicochemical properties and the surface modification of material (Dowding et al. 2013). Once nanomaterials enter the body's administration, they come into immediate contact with various plasma constitutes. The initial interaction of nanomaterials with body environment induces the formation of protein coronas which influences the subsequent immunological cascade and can either stimulate or mitigate the immune response. For this reason, *in vivo* therapeutics requires the evaluation of the nanomaterial/protein corona formation and their subsequent destination towards the physicochemical properties of the substrate (Lee et al. 2015). The surface of polymeric substrates (electro-spun mats, NPs, nanorods, etc.) can be chemically or physically modified with bioactive molecules (carbohydrates, nucleic acid and proteins) and cell-recognizable ligands (Yoo et al. 2009). Such types of biologically modified synthetic nanofibers can further support the specific cell phenotype and cell organization due to diverse biochemical signals on the cell contact surface.

The chemical functionalities of the surface influence the adsorption of proteins, cell behavior and subsequent tissue responses. Common functionalities in relation to biomaterial interactions are the amino ($-NH_2$), carboxyl (–COOH), hydroxyl (–OH) and methyl ($-CH_3$) groups. The hydrophilic surface provides low interfacial free energy resulting in less protein adsorption and cell adhesion. Reduction of protein adsorption influence on subsequent cellular responses. The interactions between protein and biomaterial can be modulated by the nature of functional groups and their density. Increasing the density of –OH and $-NH_2$ groups onto the polymeric substrate can improve the surface hydrophilicity and the influence on immunoglobulin G (IgG) adsorption from serum. Fibrinogen can be linked to the hydroxyl and amino surfaces, as well as fibrinogen can be linked to methyl-functionalized surface *via* hydrophobic interactions (Tang et al. 2008). The functional group of polymeric surfaces characterized by hydrophilic nature, presence of hydrogen bond acceptors (no hydrogen bond donor) and electrically neutral charge can resist the protein adsorption (Ostuni et al. 2001).

All in all, the inherent surface properties of the polymer may not meet all the requirements for specific physical or biomedical applications. However, it is possible to induce and monitor the desired interfacial properties of a substrate by some chemical or physical means. In this context, it has been commendable to modify the outermost layers of polymer by introducing some types of functional groups onto the polymer surface. The approaches of surface functionalization may be different for each case and particularly depends on the interplay between functionalized materials and anchor molecules. For example, aminolysis, hydrolysis, and plasma treatment can be adopted for surface functionalization of non-degradable synthetic polymers (Croll et al. 2004).

2.2 Scope of Surface Functionalization of Polymers

Surface functionalization of polymers paves the way for their novel applications in different research fields, including biomedical applications, electronics, protective coatings, textiles, thin film technology and others (Fig. 2.1) (Iijima et al. 2016). Different fields of research involving surface functionalization of polymers are described briefly below.

2.2.1 Surface Functionalization of the Polymer in Microfluidic Channels

Surface chemistry plays an important role in the interactions of flowing liquid to the inner surface of the microfluidic channels. The polymers commonly used in microfluidic channels are PC, PDMS, PMMA, etc. These polymers exhibit hydrophobic nature and can capture some specific molecules during the solution flow through the channels. The capture of specific molecules can change the concentration of the solution by denying the precise quantitation of the analytes, as a result, the adsorbed molecules on the wall of channels continuously change the surface chemistry, thus affecting the reliability of quantitative assays. Appropriate functionalization of the

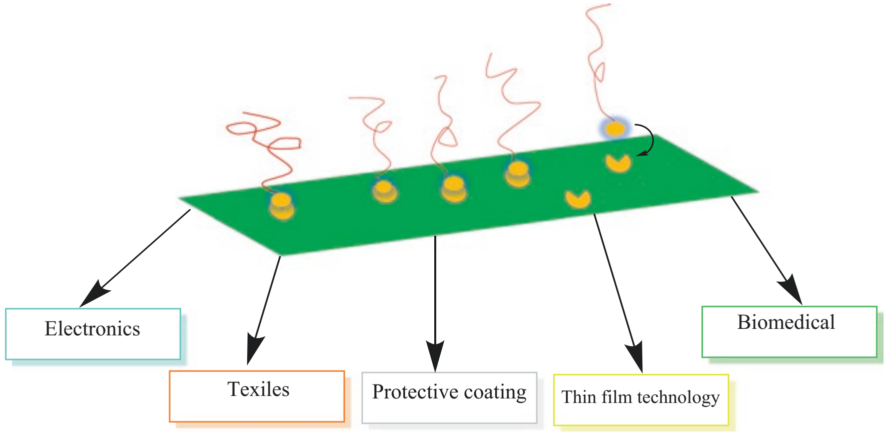

Fig. 2.1 Scope of surface functionalization of polymer

polymeric microchannel surface could control the undesired adsorption process causing better reliability in the tests (Rohr et al. 2003).

2.2.2 *Surface Functionalization of the Polymer in Ultrafiltration*

Ultrafiltration is a kind of membrane filtration that is used to separate high molecular weight solute (1–1000 kD, retentate) from low molecular weight solute and water (permeate) through a semipermeable membrane under the effect of gradient of pressure or concentration. Adsorption and permeation are two main events that can occur in biological filtration. During the filtration process, the protein molecules are adsorbed and deposited onto the porous membrane. Researches have shown that hydrophilic polymers adsorbed on the surface of membranes relieve fouling of proteins during the time of ultrafiltration and microfiltration (Chen and Belfort 1999). In such cases, the polymer layers can be functionalized on the surface to obtain more stability and durable surface properties to support the ultrafiltration process.

2.2.3 *Surface Functionalization of the Polymer in Drug Delivery*

Recent studies have suggested that the surface functionality of drug delivery vehicles influence on rate and mechanism of cellular absorption. Polymeric nanomaterials can be a good drug delivery depot and form a vehicle for slow drug molecule release, thus obtaining a sustained therapeutic effect. The surface functionalization of polymeric nanomaterials by hydrophilic polymer (e.g. PEG) can increase the residence time of polymeric NPs in the systemic circulation. The tailor of tissue-recognizable ligands can also help drug delivery to targets (Patil et al. 2009; Otsuka et al. 2003). Surface functionalization of the polymer can complement some additional tunable characteristics of polymeric materials and can make them responsive to external stimuli such as light (e.g. near infrared (NIR) and ultraviolet (UV) radiation), pH, temperature, ultrasound, etc. to trigger the controlled release of drugs. Surface functionalization can significantly change the biological response beyond the mere performance of the polymer's core structure (Masserini 2013). The pH-responsive drug delivery systems can mediate the drug release rate according to the pathophysiological need demand. For example, Jiang et al. (2014) reported that PDA coating can load and release the rate of charged molecules from PCL nanofibers with different pH values. In this work, the positively charged molecules triggered the quick release of the drug in acidic medium compared to the neutral and basic medium under the same incubation conditions. In addition, polymer NPs must be biodegradable and biocompatible, as well as non-inflammatory and non-immunogenic for medical use. They should be nontoxic to bloodstream cells or to

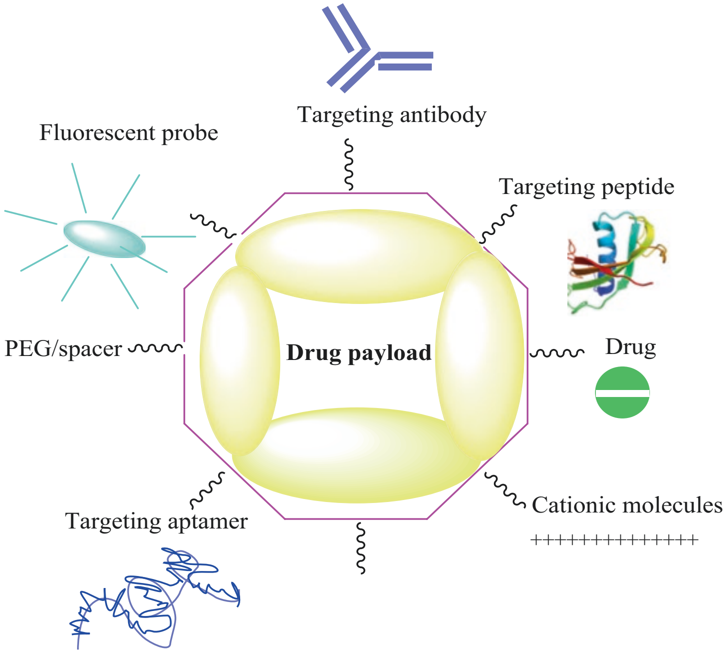

Fig. 2.2 Graphical representation of surface functionalized NPs with cationic molecules, targeting aptamer and peptide, fluorescent and PEG spacer, and drug

stationary cells. Figure 2.2 shows the graphic representation of surface modified NPs with drugs for brain drug delivery (Masserini 2013; Jiang et al. 2014).

2.2.4 Surface Functionalization of the Polymer in Electronics

Uniform dispersion of NPs into polymer nanocomposites for polymer matrix formulation in order to tune the desired electrical, mechanical opto-electronic and thermal properties is a challenging task. One of the solutions for such complications could be surface functionalization of particles with organic surfactant molecules to develop compatible polarity in mixing solutions. Polymer composite materials with low temperature processability and various functionalities are good materials for optoelectronic applications. For example, functionalized GO nanosheets with hydrophobic brushes (e.g. PtBuA-grafted GO nanosheet) can be tailored onto an electroactive polymer matrix for switching behavior of bistable electrical conductivity (Jiang et al. 2006; Li et al. 2010). Dopamine-functionalized PMMA has also been shown to improve dielectric properties compared to pristine PMMA films (Thakur et al. 2014). Functionalized conductive polymers could be used to improve performance, selectivity and sensitivity of sensors beyond the level of their pristine form (Anantha-Iyengar et al. 2019).

2.2.5 *Surface Functionalization of the Polymer in Textiles*

Superhydrophobic surfaces offer a self-cleaning mechanism in compliance with lotus effect. The concept of superhydrophobicity arose in the field of textile industry since about 1940. For example, amine functionalized SiO_2 coating onto cotton fibers followed by dipping into epoxy functionalized silica (particles solution) was performed to avail epoxy group for surface grafting (Hao et al. 2012). Stearic acid grafting can also impart superhydrophobic property to the cotton fabric (Gao and McCarthy 2006; Xue et al. 2008). Zemljič et al. (2018) also reported the encapsulation of iodine with chitosan (Cs) on cellulose viscose fabrics to exhibit an antimicrobial and antioxidative function.

2.2.6 *Surface Functionalization of the Polymer in Food Packaging Process*

The application of novel technique in the food packaging process could reduce discomfort related to operating conditions and processing costs, which reduces environmental and financial costs. Plasma-induced effects can exploit the surface functionalization of food packaging polymers to promote adhesion or anti-adhesion, printing and sealing capacity, adhesion of antibacterial coatings. PP is a polymer commonly used to develop packaging films which are often coated with acrylic to improve durability, flexibility and resistance to degradability caused by UV rays (Vukušić et al. 2018). PEGylated CNCs *via* PDA chemistry have been shown to significantly improve the crystallization, mechanical and barrier properties of PLLA bio-nanocomposites, thus exhibiting great promise for potential applications in packaging fields (Li et al. 2019).

2.2.7 *Surface Functionalization of the Polymer in Protective Coatings*

Only a polymer coating on a substrate may not satisfy the anticorrosive action, but the surface functionalization of polymer could support this. PDA, which contains the catechol and amine groups, can be used to modify a wide variety of material surface to support protein immobilization (Kang et al. 2010; Cho et al. 2009). Keeping this in view, Tian et al. (2016) demonstrated that the PEO/PCL coating on the AZ31 magnesium alloy can improve bioactivity, cytocompatibility and corrosion resistivity of the substrate.

2.2.8 Surface Functionalization of the Polymer to Influence Particle Stability

Zeta potential value of NPs allows to know the fate of the stability of the particles (Bhattarai et al. 2019b). Some polymeric NPs need to improve their stability for their sound stability under a physiological pH value. Under such requirements, a greater zeta potential magnitude can be achieved by surface functionalization. The research results shown, e.g. that the zeta potential magnitude of PLGA NPs can be increased by surface functionalization using heparin- or Cs-pluronic conjugates (Chung et al. 2010). Zeta potential of polymeric NPs can also be tuned by varying the nature of surfactants (anionic, cationic or non-ionic) and, consequently, changes the stability of the particles (Sis and Birinci 2009).

2.2.9 Surface Functionalization of the Polymer in Biomedical Applications

The applications of polymer varieties in different forms and functions are ubiquitous and wonderful in the biological world. It would be commendable in most of the cases to functionalize the polymer surface by inducing some desired physicochemical properties. The surface functionalization of polymers for bio-application can be multipurpose. For example, the surface functionalization of polymers is carried out not only to develop hydrophilicity, or to develop a conducive environment to protein adhesion, but also to develop antimicrobial and antifouling properties (Zeng et al. 2018).

Metallic implants are prone to corrosion under physiological environment. It is usual to develop a coating of anticorrosive polymer on the substrate to solve the corrosion problem. Under such conditions, the surface functionalization of polymers plays a crucial and promising role in the field of materials science. Surface functionalization of polymers for biomedical applications is considered under the tuning possibilities of the physicochemical properties of the polymer capable of working within a physiological niche. The reduced dimensions, the high surface area/volume ratio and the high drug loading efficiency of biocompatible NPs also make them attractive for drug delivery (Wang et al. 2017). These NPs may have the ability to respond quickly to environmental stimuli, such as magnetic field, pH, temperature or ultrasound. Different synthetic polymers such as PGA, PLA and PLGA copolymers have been used for the manufacture of NPs to control drug release due to its established safety profile, its long history of clinical applications and its well-understood degradation mechanism. Figure 2.3 shows the multiple nanocarriers for the encapsulation and release of growth factors.

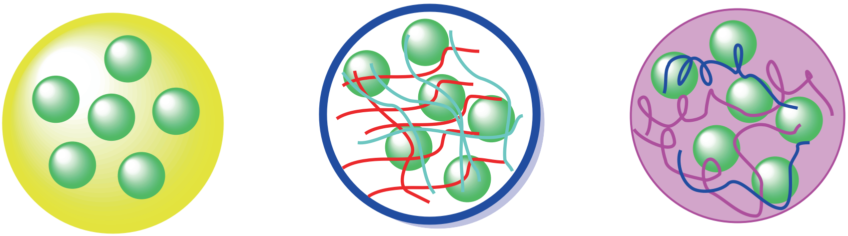

Synthetic polymer NPs Protein-based nanoparticles Polysaccharide-based NPs

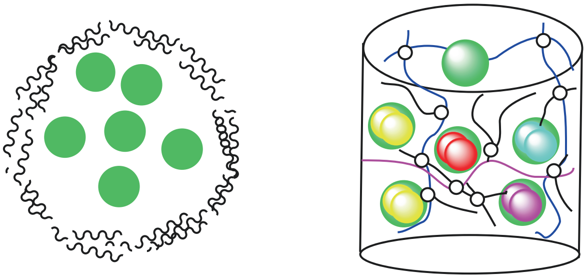

Polymer nanocapsule Functionalized scaffolds

Fig. 2.3 Multiple nanocarriers for the encapsulation and release of growth factors. Adapted with permission from Wang et al. (2017)

2.3 Classification of Surface Functionalization of Polymer

Surface functionalization of polymer can be classified into different bases. Some of the classification approaches are given below:

2.3.1 Classification According to the Surface Charge

- **Cationic surface functionalization:**
  In this type of functionalization, cationic moieties are tailored onto the polymer surfaces. As an example, a large number of hydroxyl groups present onto CNCs make it a space for diverse chemical functionalization possibilities with the generation of relevant surface properties. In addition, the extent of surface functionalization and the nature of tailored functional group onto the substrate can influence the surface charge density and impact the physic-chemical properties of the substrate. Wide varieties of surface functionalization of polymers have been made possible to interact with the corresponding biomolecules for multiple biomedical applications. With this in mind, Despres et al. (2019) obtained a CNC-PAPMA polymer with cationic surface functionalization. The cationic or

anionic surface charge of the synthesized polymer can be determined by zeta potential measurements, while functionalized chemical structure can be determined by Fourier transform infrared (FTIR), energy-dispersive X-ray (EDX), X-ray photoelectron spectra (XPS) or nuclear magnetic resonance (NMR) analysis. Such types functionalized polymer on different surfaces behave differently towards cell interaction.

- **Anionic surface functionalization:**
  In this type of surface modification, the anionic groups are tailored onto the polymer surface. This can be done by acid hydrolysis process or by some other methods. For example, hydrolysis of cellulose by using sulphuric acid incorporates anionic sulphate half-ester (OSO_3^-) (Fig. 2.4) (Sunasee and Hemraz 2018) and hydrolysis by using phosphoric acid incorporates phosphate groups onto the surface of CNCs (Eyley and Thielemans 2014). In such cases, the extent of the sulphate or phosphate groups onto the polymer can be estimated by elemental detection or functional group identification. Similarly, CNC-PNIPAAm is a polymer with anionic surface functionalization.
- **Zwitter-ionic surface functionalization:**
  Zwitterion is a chemical moiety that has at least one positive and one negative electric charge. The net charge of the entire chemical species is zero. The surface charge of such molecules is a function of the pH value of the solution. It means

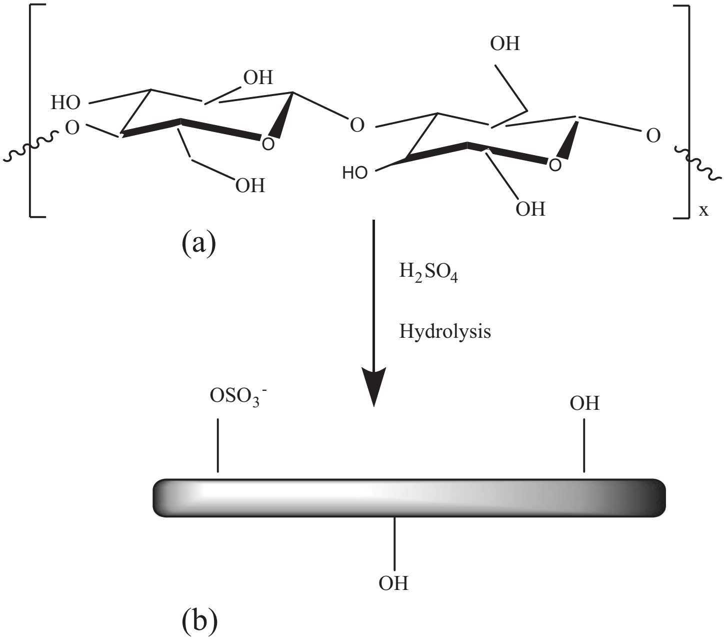

Fig. 2.4 Hydrolysis of cellulose through the use of sulfuric acid incorporating anionic sulfate half-ester (OSO_3^-). Adapted with permission from Sunasee and Hemraz (2018)

that they behave like cationic or anionic molecules below or above a particular pH value. However, the molecule behaves like a neutral molecule at a particular pH value, called an isoelectric point. At the isoelectric point, the zwitterionic molecule does not migrate at all, even under the application of electric field. Such zwitterionic molecules can be exploited to functionalize the polymer surface. Wu et al. (2018) reported the grafting of zwitterionic PSBMA onto the cotton fabrics *via* intermediate reaction of reactive dye and a surface-initiated atom transfer radical polymerization method to develop a non-fouling property.

2.3.2 Classification on the Basis of Functional Group Modification

- **Amine functionalization:**
  It is the tailoring of the amine groups onto the polymer surface. For example, the amine functionalized PS NPs can be synthesized by a copolymerization of styrene miniemulsion and a different amount of amine functionalized monomer such as 2-aminoethylmethacrylate hydrochloride (Fig. 2.5) (Holzapfel et al. 2005).
- **Amide functionalization (Amidation):**
  It is the tailoring or insertion of amide groups onto the polymer surface. Amide-functionalized polymers have shown substantial electron mobility and have gained the most encouraging device performance in the field of organic optoelectronics and polymer semiconductors (Guo et al. 2014). Suresh et al. (2014) synthesized amide-functionalized microporous organic polymers from trimesic acid and *p*-phenylenediamine in the presence of thionyl chloride. The amide group in the polymer helps, e.g. to adsorb carbon dioxide molecules *via* Lewis acid-base type interaction.

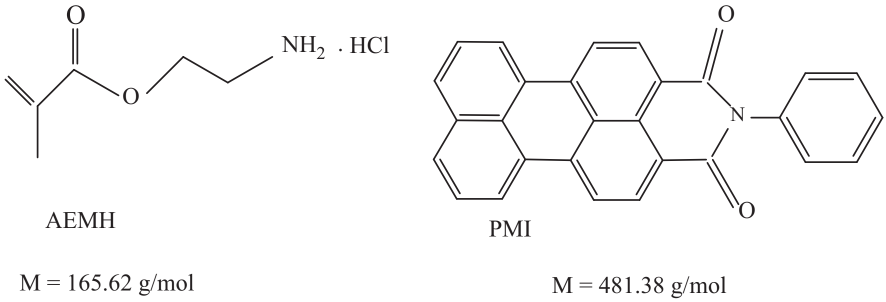

Fig. 2.5 Amine-functionalized PS NPs. Adapted with permission from Holzapfel et al. (2005)

- **Carboxylate functionalization:**
  It is the tailoring of carboxylate groups onto the polymer surface. For example, the carboxylate functionalized PS NPs can be synthesized by mini-emulsion copolymerization of styrene and a different amount of carboxylic functionalized monomers such as AA (Holzapfel et al. 2005). Murphy et al. (2005) reported the increased stability of polythiophene against oxidative doping due to the addition of an electron-withdrawing alkyl carboxylate substitute.
- **Ester functionalization (esterification):**
  Esterification is the process of introducing the ester group onto the polymer surface. Esterification by substituting hydroxyl groups of polymers introduce less polar ester group onto the polymer surface. The hydroxyl substituted esterification is applied to hydrophobize polymer. For bio-application, natural α-hydroxy acids such as citric acid, glyceric acid, glycolic acid, lactic acid, malic acid, mandelic acid, tartaric acid, etc. can be used to catalyze the esterification of CNC (hydroxyl rich molecule). CNCs can, for example, be esterified by treatment with acetic anhydride in presence of citric acid. Here, the hydroxyl group of α-hydroxy acid presumably induce a nucleophilic attack on the acylating agent (Ávila Ramírez et al. 2014, 2017).
- **Surface acetylation:**
  The acetyl group can be introduced onto the polymer surface by an acetylation process. For example, surface acetylation of CNC can be carried out by treating the CNC with acetic anhydride in presence of pyridine (Eyley and Thielemans 2014).
- **Surface acylation:**
  It is the tailoring of acyl (RCO-) group onto the polymer by chemical method. For example, alkenyl succinic anhydride can be used as an acylating agent for polysaccharide nanocrystals in non-polar media (Gopalan Nair et al. 2003; Angellier et al. 2005).
- **Catechol functionalization:**
  Catechol group of a molecule imparts water solubility, which makes it a useful candidate in the design of biomimetic materials. Catechol functionalization onto polymer such as Cs increases the bio-adhesiveness and antioxidant properties (Zhang et al. 2018; Ryu et al. 2015; Faure et al. 2013).
- **Oxidation:**
  The oxidation modification of the functional groups on the surface significantly affects the surface charge density, hydrophilicity/hydrophobicity of polymer which influences the cellular interactions accordingly. For example, the primary hydroxyl (hydroxymethyl) group of cellulose into carboxyl group is possible by 2,2,6,6-tetramethylpiperidinyloxyl radical-mediated oxidation process (Habibi et al. 2006). However, the oxidation of CNCs by sodium periodate can develop aldehyde functional group (Sun et al. 2015).

2.3.3 Classification Based on the Polymer Grafting/Spraying

- **Polymer grafting:**
  The results of current research have suggested the grafting of conjugated polymers into biopolymers to introduce novel functionalities with new features. Conductive polymer grafting over the specified polymer introduces conductivity in the polymer composite. Surface functionalization of cellulose can, for example, be performed by direct grafting of P3HT *via* oxidative polymerization. The grafting of P3HT onto the cellulose surface increases the hydrophobic properties with lotus effect and also increases conductivity (Hai and Sugimoto 2018).
- **Spray coating:**
  The antibacterial or antimicrobial properties can be developed onto a polymer by a spray coating method. For example, mussel-inspired polyglycerol (MI-PG) can be successfully functionalized to impart antibacterial activities *via* the spray coating of an aqueous solution of silver nitrate (Schlaich et al. 2018).
- **PEGylation:**
  PEG is an amphiphilic polymer composed of a repetitive unit of ethylene glycol. PEG is activated for polymer conjugation by substituting its terminal –OH functional group by appropriate group retaining its biological activities. The activated PEG may be PEG-aldehyde, PEG-alkyne, PEG-amine, PEG-hydrazine, PEG-NHS ester, PEG-thiol, etc. (Giorgi et al. 2014). This process links the PEG polymer chain to the target molecules *via* covalent or non-covalent bonding. PEGylation is most commonly adopted to functionalize proteins and anticancer drugs. Generally, PEGylation is carried out to improve the water solubility of substances such as drugs, proteins, etc. and to improve colloidal stability to polymers (Lin et al. 2008; Veronese and Pasut 2005; Pelaz et al. 2015).
- **Silylation (silane grafting)**:
  It is the process of introducing a substituted silyl group (R3Si) to a molecule such as alcohol, amine, carboxylic acid, phosphate, thiol, etc. of a particular polymer. The silane group can be introduced onto CNCs to increase hydrophobicity. APTES is a commonly used silane, and can functionalize the CNC surface for silylation. For example, Khanjanzadeh et al. (2018) linked the APTES hydrocarbon chain to the surface of the CNC *via* an Si-O-C bond by the condensation reaction between the hydroxyl group of CNC and the silanol group of APTES. This type of surface modification promotes the dispersion of the polymer into non-polar media. The surface properties of polymers can change with the incorporation of functionalized nanomaterials and, consequently, improve the effectiveness of the material for a specific application (Pokharel and Lee 2014; Pokharel et al. 2015a; Pant et al. 2015; Pokharel and Truong 2014). Figure 2.6 shows the schematic diagram for grafting of PU chains onto the APTES-treated GO surface (Pokharel et al. 2015b). The epoxide groups of GO react with the amine group of aminosilane in aqueous medium *via* S_N^2 nucleophilic displacement (Pokharel et al. 2015b). Following Pokharel et al. (2015b), the GO-grafted APTES methoxy groups underwent hydrolysis and this was

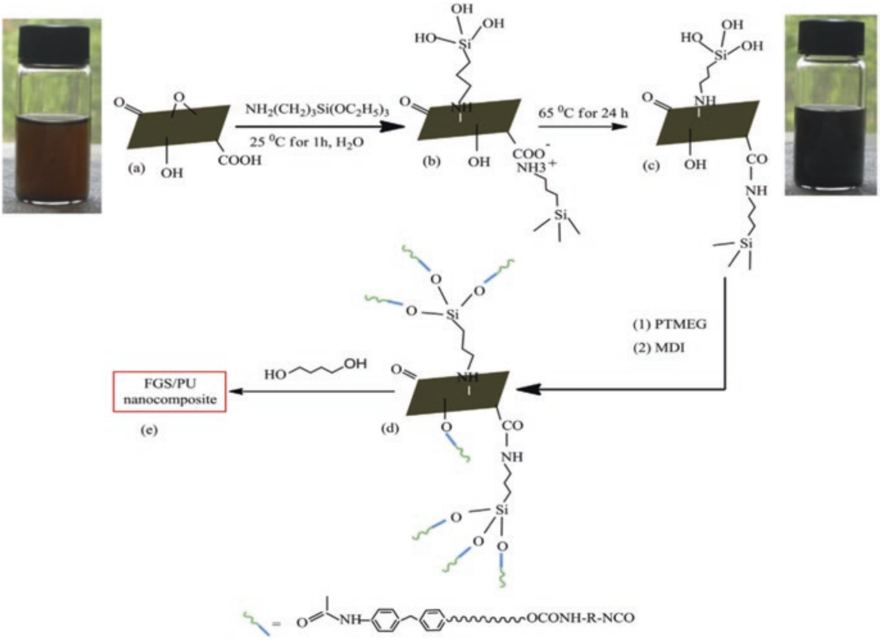

Fig. 2.6 Schematic diagram to illustrate the functionalization of polymers during the preparation of GO-based PU nanocomposites. *BD* 1,4-butanediol, *FGSs* functionalized graphene sheets, *MDI* 4,4′-methylene diphenyl diisocyanate, *PTMEG* poly(tetramethylene glycol) (average Mw = 1000 g/mol). Reprinted with permission from Pokharel et al. (2015b)

responsible for increasing the number of hydroxyl groups onto the GO surface. The hydroxyl and carboxyl groups onto GO surface can also react with the -NCO groups of MDI and the PU pre-polymer (Pokharel et al. 2015c, 2019; Pokharel and Choi 2015; Pokharel 2014). As a result, the electrical, mechanical, surface and thermal properties of the nanocomposite are completely changed during the preparation of PU nanocomposites by *in-situ* polymerization (Pokharel et al. 2015c, 2019; Pokharel and Choi 2015; Pokharel 2014).

2.4 Methods of Surface Functionalization of Polymers

The surface functionalization of polymer depends on several factors, such as the material used in the surface functionalization, the functional group intended to bind onto the polymer and purpose of the specific application. Although several methods of surface functionalization of polymers are theoretically possible, practically some methods are limited by some types of technical problems and aspects of applicability. Basically, the surface modification/functionalization of polymer can be carried out by covalent fixation of chemical moieties, plasma treatment, wet chemical oxidation, and functionalization based on classical organic chemistry (Penn and Wang 1994). Some commonly used methods of the surface functionalization of polymers are given below:

2.4.1 Plasma Treatment

Plasma is considered the fourth state of matter, it is a mixture of highly-excited molecular, atomic, ionic and radical species (Chu et al. 2002). Plasma treatment can be used to etch the polymer surface, develop a certain functional group and thin layer coat of polymer on the substrate. For surface functionalization of polymer, plasma sources are selected to direct a particular functional group on the polymer surface to introduce the desired functionality without compromising their bulk properties. Plasma treatment with oxygen, ammonia or air can generate amine and carboxyl groups on the surface of the substrate. Air, water vapor and oxygen plasma are used to introduce oxygen-containing functional groups, while alkyl amine, ammonia, nitrogen, etc. are used to introduce nitrogen-containing functional groups.

Plasma treatment can also modify the polymer surface *via* different ways such as activation, cleaning, crosslinking, etching, etc. Chemical etching is promoted by radicals such as O_2 and CF_4 discharge, while physical etching is promoted by strong ion bombardment (e.g. argon plasma). Plasma treatment on polymer refines the surface and also leaves some post-reaction-active sites (Hegemann et al. 2003). Plasma treatment can increase or decrease the surface hydrophilicity of polymer. For example, oxygen plasma (mixing several reactive oxygen species) can improve the hydrophilicity while fluorocarbon treatment increases the surface hydrophobicity to the polymer. According to Park et al. (2007a) the hydrophilicity of electrospun PLGA nanofibers can be increased by the gas plasma treatment method. The increase in hydrophilicity could be associated with the intrusion of polar functional moieties (Park et al. 2007a), whereas air plasma treatment on PCL nanofibers can, for example, introduce –COOH functional groups which can help gelatin grafting in the presence of carbodiimide cross-linker (Ma et al. 2005a).

Plasma treatment followed by grafting of hydrophilic moieties could also be an alternative approach to polymer surface modification. For example, the surface of biodegradable polymers such as PGA, PLGA and PLLA can be chemically modified by an oxygen plasma treatment which makes a room for grafting hydrophilic acid such as AA. Such grafting of hydrophilic moieties can be evidenced by a higher ratio of oxygen to carbon, a lower contact angle and the presence of a carboxylic acid group. Such surface-functionalized scaffolds improve the cell attachment and proliferation (Park et al. 2007b). The surface of the electro-spun PVDF fibers can also be treated to argon plasma followed by graft-copolymerization with methacrylic acid, thus increasing material hydrophilicity (Kaur et al. 2007). Hetemi and Pinson (2017) showed that the surface functionalization of S-Nitrosated

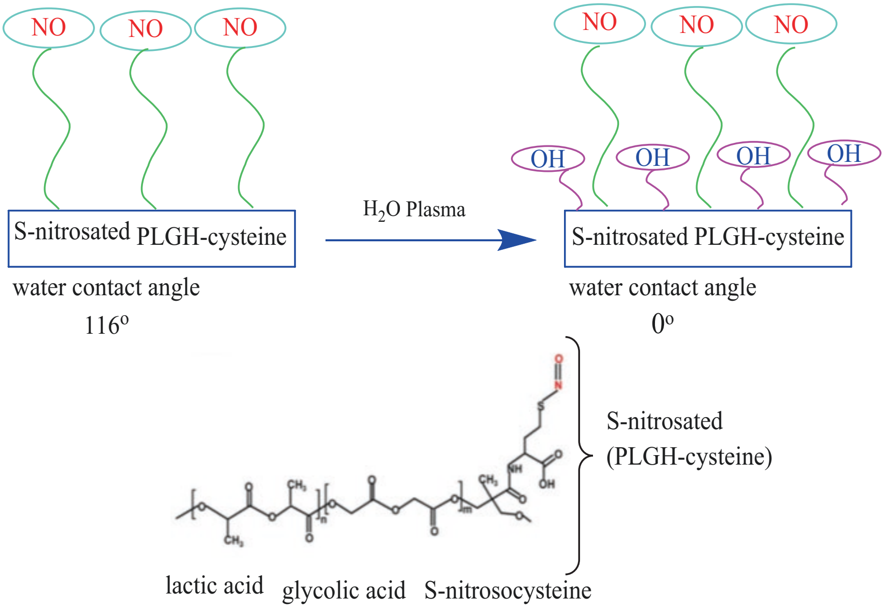

Fig. 2.7 Surface functionalization of S-Nitrosated PLGA-cysteine (PLGH-cysteine) by water plasma treatment without disturbing the active NO group. Adapted with permission from Hetemi and Pinson (2017)

PLGA-cysteine (PLGH-cysteine) by water plasma treatment without disturbing the active NO group can also decrease water contact angle values from 116° to 0° (Fig. 2.7).

2.4.2 UV Treatment

Surface functionalization of polymer can be made feasible by UV treatment (~200–400 nm of radiation). The effect of UV treatment depends on the UV irradiation parameters (distance, power and time of UV irradiation), room temperature, concentration of functionalizing and oxidizing agent (Gutiérrez and González 2016). UV treatment can cause surface functionalization of polymer *via* radical formations, or oxidation of the polymer or some types of bond cleavage (Hetemi and Pinson 2017). For example, surface functionalization of PES nanofibers can be carried out by UV irradiation into the PES nanofibers immersed in an aqueous solution of functionalizing agent (e.g. AA) in the presence of oxidant (e.g. sodium periodate solution) (Chua et al. 2006). The functionalization of AA onto the substrate introduces a functional group of carboxylic acid, while the poly(acrylic acid)-grafted PES can further be conjugated with other chemical moieties (such as the amino groups) by using different spacers (butylene, ethylene, hexylene, etc.) ethylene diamine employing carbodiimide crosslinking technique (Chua et al. 2007).

2.4.3 Ozone Treatment

Surface functionalization of polymer by ozone treatment method is also a type of oxidation process. This can develop the peroxide formation on or within the polymer, making a space for the binding of the active group. For example, an active group can be linked onto PE *via* ozone treatment (Hetemi and Pinson 2017).

2.4.4 Electrospinning

The desired functional group in the polymer can be introduced by electrospinning of the mixing solution. For example, the primary amino groups can be introduced onto the polymer surface by electrospinning of the PLGA and PLGA-*b*-PEG-NH_2 diblock copolymer mixture. Such surface-aminated polymeric fibers offer rich sites for enzyme or peptide immobilization, which lead to greater cell attachment and proliferation (Kim and Park 2006).

2.4.5 Enzyme Immobilization

In some cases, polymer nanofibers are activated and processed for a chemical reaction with enzyme such as lipase. For example, hydrogen chloride gas can be bubbled into the PAN fiber immersed in an absolute ethanol solution to introduce imidoester (R-CNH-OR′) functionalities which impart the sites for conjugation with amine moieties of lipase (Fig. 2.8) (Li et al. 2007).

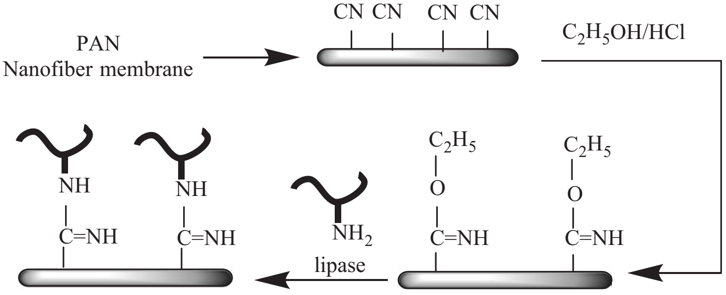

Fig. 2.8 Modification of PAN fiber by enzymatic immobilization of lipase. Adapted with permission from Li et al. (2007)

2.4.6 Hydrolysis

Hydrolysis of the esters produces carboxylic acid and hydroxyl groups. The carboxylic acid groups can be introduced into the ester bond polymer by hydrolysis, which would be beneficial for further processing. For example, partial hydrolysis of PCL fibers develops carboxylate groups which promotes the nucleation of calcium ions during the biomineralization process (Fig. 2.9) (Araujo et al. 2008). Similarly, the hydrolysis of PET produces a polymer surface with functionality of the carboxyl and hydroxyl groups (Chen and McCarthy 1998).

2.4.7 Grafting

It is the method of chemical immobilization of molecular moieties or polymer chain onto the polymer surface. The polymer chain can be linked onto the polymer either by graft polymerization (synthesis of polymer chains from the reactive sites of the polymer substrate) or by polymer grafting (attachment of polymer segment previously synthesized onto the polymer substrate). Proteins or some types of monomers are covalently conjugated onto the material surface to alter surface chemistry. The polymer surfaces are activated with some types of reactive groups followed by grafting of the desired functionality. The polymer surface activation can be carried out by ozone exposure, plasma treatment, UV irradiation, etc. Chemical grafting method is more prone to toxicity compared to the physical adsorption method (Tang et al. 2008).

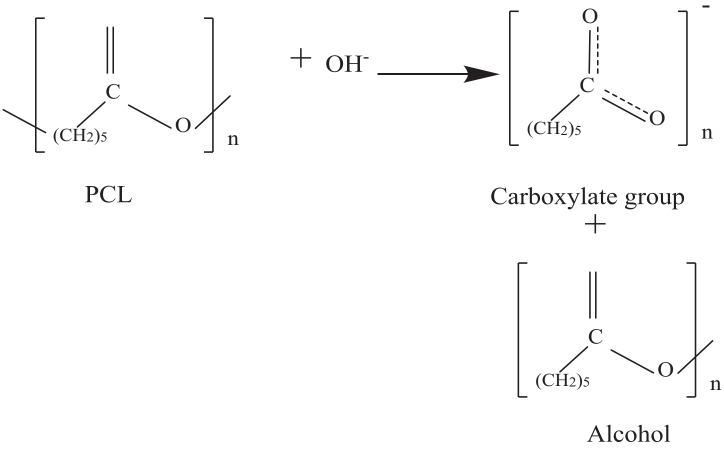

Fig. 2.9 Hydrolysis of PCL using sodium hydroxide. Adapted with permission from Araujo et al. (2008)

2.4.8 Chemical Reduction

The functional groups of some polymer can be reduced to other types by treating the polymer with some types of reducers such as $NaBH_4$. For example, the ketone functional group of PEEK polymer can be reduced to hydroxyl functional group by treating the polymer with $NaBH_4$ in DMSO at 120 °C (Fig. 2.10) (Park et al. 2007b). The –OH group can further be transformed into other desired functionalities by some types of chemical treatment (Hetemi and Pinson 2017; Diez-Pascual et al. 2009). Similarly, the alcohol functionality can be introduced onto PET by reducing it with lithium aluminum hydride (Chen and McCarthy 1998).

Some specific polymers and approaches for surface functionalization, as well as their advantages are briefly presented in Table 2.1.

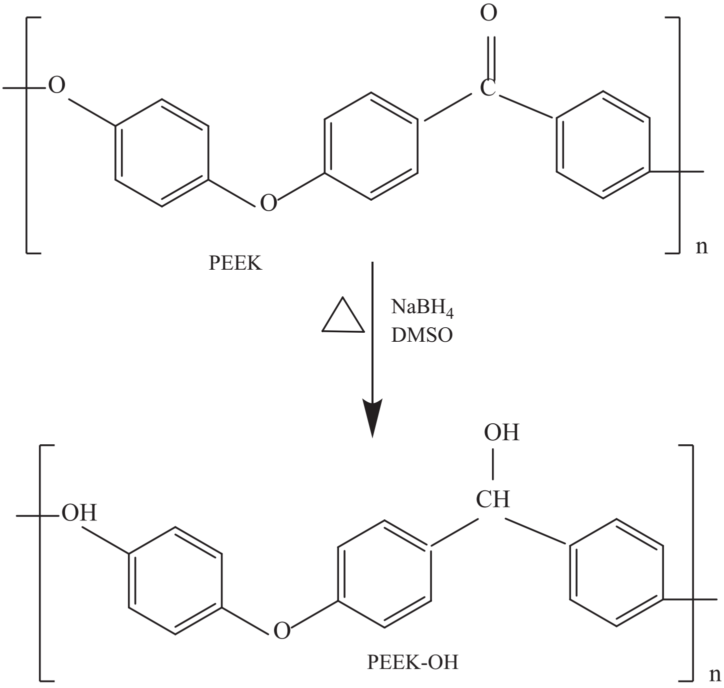

Fig. 2.10 Surface functionalization of PEEK polymers by transforming its carbonyl group into hydroxyl group by the reducing action of $NaBH_4$ in DMSO medium. Adapted with permission from Hetemi and Pinson (2017)

Table 2.1 Surface functionalization approaches for some polymers

Surface functionalization of polymers			References
Polymers	Approaches	Achievements	
PCL	Immobilization of soluble eggshell membrane on PCL electros-pun mat	Increases hydrophilicity and proliferation of human dermal fibroblasts	Jia et al. (2008)
PCL	Plasma treatment on PCL mat	Increases hydrophilicity and improves Schwann cell adhesion and proliferation	Prabhakaran et al. (2008)
PCL	Plasma treatment on PCL mat followed by immersion in a synthetic body fluid solution	Increases biomineralization and hydrophilicity	Yang et al. (2008)
PCL	Alkaline hydrolysis followed by peptide coupling	Carboxylic acid group is introduced by ester hydrolysis, peptide coupling can increase the cell attachment and proliferation	Sun and Önneby (2006)
PET	Formaldehyde treatment on PET nanofibers to introduce hydroxyl group on the surface of the substrate	Improves the viability of endothelial cells	Ma et al. (2005b)
PES	Helium plasma or UV treatment on PES mat	Improves stability in acetonitrile medium where amination can be carried out efficiently	Chen and Belfort (1999)
PLA	Surface functionalization by heparin or hyaluronic acid	Sustained drug delivery for growth factors	Kim and Park (2008)
PLA, PLGA, PS, silk fibroin	Plasma treatment	Increases hydrophilicity and improves the cellular affinity of porous scaffolds	Yang et al. (2002) and Cheon et al. (2010)
PLLA, PCL	Alkaline hydrolysis	Increases biomineralization and hydrophilicity	Yoo et al. (2009)
Ester, PLLC	Surface aminolysis	Develops surface positive charge and creates amine functionalized surface	
PET nanofibers	Modification of PET nanofibers with PMAC by graft polymerization in mild condition	Increases surface hydrophilicity Introduces multifunctional groups on the surface which support for the covalent immobilization of bioactive molecules. This enhances the cell adhesion, proliferation, and differentiation	
PU nanofibers	Modification of PU nanofibers with poly(4-vinyl-*N*-hexyl pyridinium bromide) on the surface	Improves antibacterial properties	

(continued)

Table 2.1 (continued)

Surface functionalization of polymers			
Polymers	Approaches	Achievements	References
PDA	Amines (Schiffs base reaction) or thiols (Michael addition)	Organic ad-layer formation	Lee et al. (2007)
PLLA	Co-electrospinning (electrospinning of the HAp/PLLA mixture)	High surface free energy, increases hydrophilicity and decreases degradation rate	
PP, PE	Water vapor plasma treatment	Increase hydrophilicity	Lee et al. (1991)
PP, PE, polyester	Wet chemical oxidation	Introduces carbonyl, hydroxyl and carboxylic group onto the polymer surface	Penn and Wang (1994)

2.5 Analytical Techniques for Surface Characterization

The surface functionalization of polymer causes some types of chemical and physical changes associated to surface chemistry, morphology and topography, as well as hydrophilicity or hydrophobicity, crystallinity and functional group on the polymer surface. Accurate evaluations of such modifications are required in relation to physicochemical characterizations and their targeted objectives. However, the characterization is a bit sensitive because the mass or volume of the functionalizing species is extremely low in relation to bulk mass. In addition, the spectroscopic signal from the bulk mass overwhelms the contribution from the surface. No single method of characterization can provide a complete evaluation of the surface. Many of the characterizations in concert can give supporting evidence on surface characterization. The techniques commonly used for the assessment of surface functionalization of polymers are given in Table 2.2.

2.6 Recent Trends in the Surface Functionalization of Polymers

Several approaches of surface functionalization of polymers have been practiced for some decades. In this sense, surface functionalization of polymer should be carried out without compromising their inherent biocompatibility, biodegradability concerns, non-cytotoxicity and bulk properties. Until now, the surface functionalization of polymers has expanded the various promising aspects of the polymer, from physical applications to biomedical applications. Currently, research is not limited to only reducing or increasing the hydrophilicity of polymers, but are expanding for multipurpose applications. In addition, modulation of the degree of surface functionalization has been achieved based on the polymer nature and the flux of reactive

Table 2.2 Surface characterization methods commonly employed

Measurement properties	Characterization method	References
Surface morphology and roughness	Field emission scanning electron microscopy (FESEM)/atomic force microscopy (AFM)	Pant et al. (2011)
Surface hydrophilicity	Water contact angle	Croll et al. (2004) and Tiwari et al. (2017)
Functional group insertion or modification	FTIR	Tiwari et al. (2018)
Crystallinity	XRD	Bhattarai et al. (2019a)
Elemental detection	EDX	Bhattarai et al. (2019a)
Surface composition and elemental analysis	XPS	Weibel (2010)
D/G ratio in carbon materials	Raman spectra	Pokharel et al. (2019)
Hyperthermia	Photothermal performance	Tiwari et al. (2018, 2019) and Bhattarai et al. (2019a)
Chemical analysis	NMR	
Surface charge measurement	Zeta potential	Bhattarai et al. (2019b)

plasma species (Vesel and Mozetic 2017). Selective synchrotron radiations can be applied to functionalize the polymer in presence of reactive gas species (Weibel 2010). Medical implants are more susceptible to microbial attack and embedding. Polymer-coated implants must retain certain specific properties for their targeted applications. Sterilization and other material processing events should not deteriorate the properties of polymers. For this reason, surface functionalization of polymer should be seen as a holistic approach rather than as a stereotype. Today, surface functionalization of polymers has developed new properties on the simple state of the polymer. For example, Tiwari et al. (2018) functionalized the PCL electro-spun mat by using poly(pyrrole) *via* chemical polymerization to induce photothermal property for hyperthermia applications targeted at cancer treatment. PDA surface functionalization onto PCL mat unveils an efficient photothermal chemotherapy route (Tiwari et al. 2019).

Although there have been several types of surface functionalization approaches in practice, surface functionalization by plasma treatment has played a leading role among many other methods. The reasons behind the main role of plasma treatment in surface functionalization is that plasma treatment can introduce various functional groups with different concentrations (Zille et al. 2015; Kajjout et al. 2019). For example, oxygen plasma treatment can introduce several oxygenated functional groups, such as carbonyl (>C=O), ether (C–O–C), hydroxyl (–OH), peroxy (–C–O–O–), etc. As plasma treatment does not involve the maximum use of harsh chemicals, it is more applicable in industrial sectors.

2.7 Conclusion

Regarding the various aspects of surface functionalization of polymers, the crucial issue is to tune the surface functionalities without compromising the inherent bulk properties, targeted for a specific application. Specifically, the related nanotoxicology and cytotoxicity issues are the main concerns regarding their bioapplication in clinical trials. However, it may get some exemption of toxicity concerns for physical applications. To date, significant progress has been made in the field of surface functionalization of polymers. A large number of polymer surface functionalization approaches have been designed, formulated and employed in recent decades. Successes in surface functionalization of polymers has led to progress in the design and formulation of multifunctional platforms to recapitulate the complex functioning process both in biological and physical fields. The surface functionalization of polymer has not only modified the polymer surface, but also provides efficiencies of differential immobilization and release kinetics of growth factors and drugs. The surface functionalized polymer can be used for a wide range of nanocarriers to improve the therapeutic efficacy. Future research directions related to surface functionalization of polymer should be focused on a comprehensive understanding of surface functionalized polymer-tissue interactions and optimization for long-term performance.

Acknowledgments D. Xiao sincerely acknowledges the Jacob F. Buckman Chair endowment fund at the University of New Haven. P. Pokharel and D. Xiao gratefully acknowledge the Higasket Research Fund.

Conflicts of Interest The authors declare no conflict of interest.

References

Anantha-Iyengar, G., Shanmugasundaram, K., Nallal, M., Lee, K. P., Whitcombe, M. J., Lakshmi, D., & Sai-Anand, G. (2019). Functionalized conjugated polymers for sensing and molecular imprinting applications. *Progress in Polymer Science, 88*, 1–129. https://doi.org/10.1016/j.progpolymsci.2018.08.001.

Angellier, H., Molina-Boisseau, S., Belgacem, M. N., & Dufresne, A. (2005). Surface chemical modification of waxy maize starch nanocrystals. *Langmuir, 21*(6), 2425–2433. https://doi.org/10.1021/la047530j.

Araujo, J. V., Martins, A., Leonor, I. B., Pinho, E. D., Reis, R. L., & Neves, N. M. (2008). Surface controlled biomimetic coating of polycaprolactone nanofiber meshes to be used as bone extracellular matrix analogues. *Journal of Biomaterials Science, Polymer Edition, 19*(10), 1261–1278. https://doi.org/10.1163/156856208786052335.

Ávila Ramírez, J. A., Suriano, C. J., Cerrutti, P., & Foresti, M. L. (2014). Surface esterification of cellulose nanofibers by a simple organocatalytic methodology. *Carbohydrate Polymers, 114*, 416–423. https://doi.org/10.1016/j.carbpol.2014.08.020.

Ávila Ramírez, J. A., Fortunati, E., Kenny, J. M., Torre, L., & Foresti, M. L. (2017). Simple citric acid-catalyzed surface esterification of cellulose nanocrystals. *Carbohydrate Polymers, 157*, 1358–1364. https://doi.org/10.1016/j.carbpol.2016.11.008.

Bhattarai, D. P., Tiwari, A. P., Maharjan, B., Tumurbaatar, B., Park, C. H., & Kim, C. S. (2019a). Sacrificial template-based synthetic approach of polypyrrole hollow fibers for photothermal therapy. *Journal of Colloid and Interface Science, 534*, 447–458. https://doi.org/10.1016/j.jcis.2018.09.047.

Bhattarai, D. P., Awasthi, G. P., Maharjan, B., Lee, J., Kim, B. S., Park, C. H., & Kim, C. S. (2019b). Synthesis of polythiophene nanoparticles by surfactant-free chemical oxidative polymerization method: Characterization, *in vitro* biomineralization, and cytotoxicity evaluation. *Journal of Industrial and Engineering Chemistry, 77*, 243–252. https://doi.org/10.1016/j.jiec.2019.04.045.

Bhattarai, D. P., Hwang, T. I., Kim, J. I., Lee, J. H., Chun, S., Kim, B. S., Park, C. H., & Kim, C. S. (2020). Synthesis of polypyrrole nanorods by sacrificial removal of aluminum oxide nanopore template: A study on cell viability, electrical stimulation and neuronal differentiation of PC12 cells. *Materials Science and Engineering: C, 107*, 110325. https://doi.org/10.1016/j.msec.2019.110325.

Chen, H., & Belfort, G. (1999). Surface modification of poly(ether sulfone) ultrafiltration membranes by low-temperature plasma-induced graft polymerization. *Journal of Applied Polymer Science, 72*(13), 1699–1711. https://doi.org/10.1002/(sici)1097-4628(19990624)72:13<1699::aid-app6>3.0.co;2-9.

Chen, W., & McCarthy, T. J. (1998). Chemical surface modification of poly(ethylene terephthalate). *Macromolecules, 31*(11), 3648–3655. https://doi.org/10.1021/ma9710601.

Cheon, Y. W., Lee, W. J., Baek, H. S., Lee, Y. D., Park, J.-C., Park, Y. H., Ki, C. S., Chung, K.-H., & Rah, D. K. (2010). Enhanced chondrogenic responses of human articular chondrocytes onto silk fibroin/wool keratose scaffolds treated with microwave-induced argon plasma. *Artificial Organs, 34*(5), 384–392. https://doi.org/10.1111/j.1525-1594.2009.00871.x.

Cho, S. H., White, S. R., & Braun, P. V. (2009). Self-healing polymer coatings. *Advanced Materials, 21*(6), 645–649. https://doi.org/10.1002/adma.200802008.

Chu, P. K., Chen, J. Y., Wang, L. P., & Huang, N. (2002). Plasma-surface modification of biomaterials. *Materials Science & Engineering R: Reports, 36*(5–6), 143–206. https://doi.org/10.1016/s0927-796x(02)00004-9.

Chua, K. N., Chai, C., Lee, P. C., Tang, Y. N., Ramakrishna, S., Leong, K. W., & Mao, H. Q. (2006). Surface-aminated electrospun nanofibers enhance adhesion and expansion of human umbilical cord blood hematopoietic stem/progenitor cells. *Biomaterials, 27*(36), 6043–6051. https://doi.org/10.1016/j.biomaterials.2006.06.017.

Chua, K.-N., Chai, C., Lee, P.-C., Ramakrishna, S., Leong, K. W., & Mao, H.-Q. (2007). Functional nanofiber scaffolds with different spacers modulate adhesion and expansion of cryopreserved umbilical cord blood hematopoietic stem/progenitor cells. *Experimental Hematology, 35*(5), 771–781. https://doi.org/10.1016/j.exphem.2007.02.002.

Chung, Y.-I., Kim, J. C., Kim, Y. H., Tae, G., Lee, S.-Y., Kim, K., & Kwon, I. C. (2010). The effect of surface functionalization of PLGA nanoparticles by heparin-or chitosan-conjugated Pluronic on tumor targeting. *Journal of Controlled Release, 143*(3), 374–382. https://doi.org/10.1016/j.jconrel.2010.01.017.

Croll, T. I., O'Connor, A. J., Stevens, G. W., & Cooper-White, J. J. (2004). Controllable surface modification of poly(lactic-*co*-glycolic acid)(PLGA) by hydrolysis or aminolysis I: Physical, chemical, and theoretical aspects. *Biomacromolecules, 5*(2), 463–473. https://doi.org/10.1021/bm0343040.

Dai, L., He, P., & Li, S. (2003). Functionalized surfaces based on polymers and carbon nanotubes for some biomedical and optoelectronic applications. *Nanotechnology, 14*(10), 1081–1097. https://doi.org/10.1088/0957-4484/14/10/305.

Despres, H. W., Sabra, A., Anderson, P., Hemraz, U. D., Boluk, Y., Sunasee, R., & Ckless, K. (2019). Mechanisms of the immune response cause by cationic and anionic surface functionalized cellulose nanocrystals using cell-based assays. *Toxicology In Vitro, 55*, 124–133. https://doi.org/10.1016/j.tiv.2018.12.009.

Diez-Pascual, A. M., Martinez, G., & Gomez, M. A. (2009). Synthesis and characterization of poly(ether ether ketone) derivatives obtained by carbonyl reduction. *Macromolecules, 42*(18), 6885–6892. https://doi.org/10.1021/ma901208e.

Dowding, J. M., Das, S., Kumar, A., Dosani, T., McCormack, R., Gupta, A., Sayle, T. X. T., Sayle, D. C., von Kalm, L., Seal, S., & Self, W. T. (2013). Cellular interaction and toxicity depend on physicochemical properties and surface modification of redox-active nanomaterials. *ACS Nano, 7*(6), 4855–4868. https://doi.org/10.1021/nn305872d.

Eyley, S., & Thielemans, W. (2014). Surface modification of cellulose nanocrystals. *Nanoscale, 6*(14), 7764–7779. https://doi.org/10.1039/c4nr01756k.

Faure, E., Falentin-Daudré, C., Jérôme, C., Lyskawa, J., Fournier, D., Woisel, P., & Detrembleur, C. (2013). Catechols as versatile platforms in polymer chemistry. *Progress in Polymer Science, 38*(1), 236–270. https://doi.org/10.1016/j.progpolymsci.2012.06.004.

Gao, L., & McCarthy, T. J. (2006). "Artificial lotus leaf" prepared using a 1945 patent and a commercial textile. *Langmuir, 22*(14), 5998–6000. https://doi.org/10.1021/la061237x.

Giorgi, M. E., Agusti, R., & de Lederkremer, R. M. (2014). Carbohydrate PEGylation, an approach to improve pharmacological potency. *Beilstein Journal of Organic Chemistry, 10*(1), 1433–1444. https://doi.org/10.3762/bjoc.10.147.

Gopalan Nair, K., Dufresne, A., Gandini, A., & Belgacem, M. N. (2003). Crab shell chitin whiskers reinforced natural rubber nanocomposites. 3. Effect of chemical modification of chitin whiskers. *Biomacromolecules, 4*(6), 1835–1842. https://doi.org/10.1021/bm030058g.

Guo, X., Facchetti, A., & Marks, T. J. (2014). Imide-and amide-functionalized polymer semiconductors. *Chemical Reviews, 114*(18), 8943–9021. https://doi.org/10.1021/cr500225d.

Gutiérrez, T. J., & González, G. (2016). Effects of exposure to pulsed light on surface and structural properties of edible films made from cassava and taro starch. *Food and Bioprocess Technology, 9*(11), 1812–1824. https://doi.org/10.1007/s11947-016-1765-3.

Gutiérrez, T. J., Ollier, R., & Alvarez, V. A. (2018). Chapter 5. Surface properties of thermoplastic starch materials reinforced with natural fillers. In V. K. Thakur & M. K. Thakur (Eds.), *Functional biopolymers* (pp. 131–158). Cham: Editorial Springer International. EE.UU. ISBN: 978-3-319-66416-3. eISBN: 978-3-319-66417-0. https://doi.org/10.1007/978-3-319-66417-0_5.

Habibi, Y., Chanzy, H., & Vignon, M. R. (2006). TEMPO-mediated surface oxidation of cellulose whiskers. *Cellulose, 13*(6), 679–687. https://doi.org/10.1007/s10570-006-9075-y.

Hai, T. A. P., & Sugimoto, R. (2018). Surface functionalization of cellulose with poly(3-hexylthiophene) via novel oxidative polymerization. *Carbohydrate Polymers, 179*, 221–227. https://doi.org/10.1016/j.carbpol.2017.09.067.

Hao, L., An, Q., & Xu, W. (2012). Facile fabrication of superhydrophobic cotton fabric from stearyl methacrylate modified polysiloxane/silica nanocomposite. *Fibers and Polymers, 13*(9), 1145–1153. https://doi.org/10.1007/s12221-012-1145-1.

Hegemann, D., Brunner, H., & Oehr, C. (2003). Plasma treatment of polymers for surface and adhesion improvement. *Nuclear Instruments and Methods in Physics Research Section B: Beam Interactions with Materials and Atoms, 208*, 281–286. https://doi.org/10.1016/s0168-583x(03)00644-x.

Hetemi, D., & Pinson, J. (2017). Surface functionalisation of polymers. *Chemical Society Reviews, 46*(19), 5701–5713. https://doi.org/10.1039/c7cs00150a.

Holzapfel, V., Musyanovych, A., Landfester, K., Lorenz, M. R., & Mailänder, V. (2005). Preparation of fluorescent carboxyl and amino functionalized polystyrene particles by miniemulsion polymerization as markers for cells. *Macromolecular Chemistry and Physics, 206*(24), 2440–2449. https://doi.org/10.1002/macp.200500372.

Iijima, K., Nagahama, H., Takada, A., Sawada, T., Serizawa, T., & Hashizume, M. (2016). Surface functionalization of polymer substrates with hydroxyapatite using polymer-binding peptides. *Journal of Materials Chemistry B, 4*(21), 3651–3659. https://doi.org/10.1039/c6tb00624h.

Jia, J., Duan, Y.-Y., Yu, J., & Lu, J.-W. (2008). Preparation and immobilization of soluble eggshell membrane protein on the electrospun nanofibers to enhance cell adhesion and growth. *Journal of Biomedical Materials Research Part A, 86*(2), 364–373. https://doi.org/10.1002/jbm.a.31606.

Jiang, H., Moon, K. S., Li, Y., & Wong, C. P. (2006). Surface functionalized silver nanoparticles for ultrahigh conductive polymer composites. *Chemistry of Materials, 18*(13), 2969–2973. https://doi.org/10.1021/cm0527773.

Jiang, J., Xie, J., Ma, B., Bartlett, D. E., Xu, A., & Wang, C. H. (2014). Mussel-inspired protein-mediated surface functionalization of electrospun nanofibers for pH-responsive drug delivery. *Acta Biomaterialia, 10*(3), 1324–1332. https://doi.org/10.1016/j.actbio.2013.11.012.

Kajjout, M., Lemmouchi, Y., Jama, C., Rolando, C., Villasmunta, F., Heinrich, F., & Mazzah, A. (2019). Grafting of amine functions on cellulose acetate fibers by plasma processing. *Reactive and Functional Polymers, 134*, 40–48. https://doi.org/10.1016/j.reactfunctpolym.2018.11.004.

Kang, S. M., You, I., Cho, W. K., Shon, H. K., Lee, T. G., Choi, I. S., Choi, I. S., & Lee, H. (2010). One-step modification of superhydrophobic surfaces by a mussel-inspired polymer coating. *Angewandte Chemie International Edition, 49*(49), 9401–9404. https://doi.org/10.1002/anie.201004693.

Kaur, S., Ma, Z., Gopal, R., Singh, G., Ramakrishna, S., & Matsuura, T. (2007). Plasma-induced graft copolymerization of poly(methacrylic acid) on electrospun poly(vinylidene fluoride) nanofiber membrane. *Langmuir, 23*(26), 13085–13092. https://doi.org/10.1021/la701329r.

Khanjanzadeh, H., Behrooz, R., Bahramifar, N., Gindl-Altmutter, W., Bacher, M., Edler, M., & Griesser, T. (2018). Surface chemical functionalization of cellulose nanocrystals by 3-aminopropyltriethoxysilane. *International Journal of Biological Macromolecules, 106*, 1288–1296. https://doi.org/10.1016/j.ijbiomac.2017.08.136.

Kim, T. G., & Park, T. G. (2006). Surface functionalized electrospun biodegradable nanofibers for immobilization of bioactive molecules. *Biotechnology Progress, 22*(4), 1108–1113. https://doi.org/10.1021/bp060039t.

Kim, T. G., & Park, T. G. (2008). Biodegradable polymer nanocylinders fabricated by transverse fragmentation of electrospun nanofibers through aminolysis. *Macromolecular Rapid Communications, 29*(14), 1231–1236. https://doi.org/10.1002/marc.200800094.

Lee, J. H., Park, J. W., & Lee, H. B. (1991). Cell adhesion and growth on polymer surfaces with hydroxyl groups prepared by water vapour plasma treatment. *Biomaterials, 12*(5), 443–448. https://doi.org/10.1016/0142-9612(91)90140-6.

Lee, H., Dellatore, S. M., Miller, W. M., & Messersmith, P. B. (2007). Mussel-inspired surface chemistry for multifunctional coatings. *Science, 318*(5849), 426–430. https://doi.org/10.1126/science.1147241.

Lee, Y. K., Choi, E. J., Webster, T. J., Kim, S. H., & Khang, D. (2015). Effect of the protein corona on nanoparticles for modulating cytotoxicity and immunotoxicity. *International Journal of Nanomedicine, 10*, 97–113. https://doi.org/10.2147/ijn.s72998.

Li, S.-F., Chen, J. P., & Wu, W.-T. (2007). Electrospun polyacrylonitrile nanofibrous membranes for lipase immobilization. *Journal of Molecular Catalysis B: Enzymatic, 47*(3–4), 117–124. https://doi.org/10.1016/j.molcatb.2007.04.010.

Li, G. L., Liu, G., Li, M., Wan, D., Neoh, K. G., & Kang, E. T. (2010). Organo-and water-dispersible graphene oxide-polymer nanosheets for organic electronic memory and gold nanocomposites. *The Journal of Physical Chemistry C, 114*(29), 12742–12748. https://doi.org/10.1021/jp102640s.

Li, L., Bao, R. Y., Gao, T., Liu, Z. Y., Xie, B. H., Yang, M. B., & Yang, W. (2019). Dopamine-induced functionalization of cellulose nanocrystals with polyethylene glycol towards poly(L-lactic acid) bionanocomposites for green packaging. *Carbohydrate Polymers, 203*, 275–284. https://doi.org/10.1016/j.carbpol.2018.09.057.

Lin, C. A. J., Sperling, R. A., Li, J. K., Yang, T. Y., Li, P. Y., Zanella, M., Chang, W. H., & Parak, W. J. (2008). Design of an amphiphilic polymer for nanoparticle coating and functionalization. *Small, 4*(3), 334–341. https://doi.org/10.1002/smll.200700654.

Ma, Z., He, W., Yong, T., & Ramakrishna, S. (2005a). Grafting of gelatin on electrospun poly(caprolactone) nanofibers to improve endothelial cell spreading and proliferation and to control cell orientation. *Tissue Engineering, 11*(7–8), 1149–1158. https://doi.org/10.1089/ten.2005.11.1149.

Ma, Z., Kotaki, M., Yong, T., He, W., & Ramakrishna, S. (2005b). Surface engineering of electrospun polyethylene terephthalate (PET) nanofibers towards development of a new material for blood vessel engineering. *Biomaterials, 26*(15), 2527–2536. https://doi.org/10.1016/j.biomaterials.2004.07.026.

Masserini, M. (2013). Nanoparticles for brain drug delivery. *ISRN Biochemistry*, 238428. 18 pages. https://doi.org/10.1155/2013/238428.

Murphy, A. R., Liu, J., Luscombe, C., Kavulak, D., Fréchet, J. M., Kline, R. J., & McGehee, M. D. (2005). Synthesis, characterization, and field-effect transistor performance of carboxylate-functionalized polythiophenes with increased air stability. *Chemistry of Materials, 17*(20), 4892–4899. https://doi.org/10.1021/cm050911d.

Ostuni, E., Chapman, R. G., Holmlin, R. E., Takayama, S., & Whitesides, G. M. (2001). A survey of structure-property relationships of surfaces that resist the adsorption of protein. *Langmuir, 17*(18), 5605–5620. https://doi.org/10.1021/la010384m.

Otsuka, H., Nagasaki, Y., & Kataoka, K. (2003). PEGylated nanoparticles for biological and pharmaceutical applications. *Advanced Drug Delivery Reviews, 55*(3), 403–419. https://doi.org/10.1016/s0169-409x(02)00226-0.

Pant, H. R., Baek, W. I., Nam, K. T., Jeong, I. S., Barakat, N. A., & Kim, H. Y. (2011). Effect of lactic acid on polymer crystallization chain conformation and fiber morphology in an electrospun nylon-6 mat. *Polymer, 52*(21), 4851–4856. https://doi.org/10.1016/j.polymer.2011.08.059.

Pant, H. R., Pokharel, P., Joshi, M. K., Adhikari, S., Kim, H. J., Park, C. H., & Kim, C. S. (2015). Processing and characterization of electrospun graphene oxide/polyurethane composite nanofibers for stent coating. *Chemical Engineering Journal, 270*, 336–342. https://doi.org/10.1016/j.cej.2015.01.105.

Park, H., Lee, K. Y., Lee, S. J., Park, K. E., & Park, W. H. (2007a). Plasma-treated poly(lactic-*co*-glycolic acid) nanofibers for tissue engineering. *Macromolecular Research, 15*(3), 238–243. https://doi.org/10.1007/bf03218782.

Park, K., Ju, Y. M., Son, J. S., Ahn, K. D., & Han, D. K. (2007b). Surface modification of biodegradable electrospun nanofiber scaffolds and their interaction with fibroblasts. *Journal of Biomaterials Science, Polymer Edition, 18*(4), 369–382. https://doi.org/10.1163/156856207780424997.

Patil, Y. B., Toti, U. S., Khdair, A., Ma, L., & Panyam, J. (2009). Single-step surface functionalization of polymeric nanoparticles for targeted drug delivery. *Biomaterials, 30*(5), 859–866. https://doi.org/10.1016/j.biomaterials.2008.09.056.

Pelaz, B., del Pino, P., Maffre, P., Hartmann, R., Gallego, M., Rivera-Fernández, S., de la Fuente, J. M., Ulrich Nienhaus, G., & Parak, W. J. (2015). Surface functionalization of nanoparticles with polyethylene glycol: Effects on protein adsorption and cellular uptake. *ACS Nano, 9*(7), 6996–7008. https://doi.org/10.1021/acsnano.5b01326.

Penn, L. S., & Wang, H. (1994). Chemical modification of polymer surfaces: A review. *Polymers for Advanced Technologies, 5*(12), 809–817. https://doi.org/10.1002/pat.1994.220051207.

Pokharel, P. (2014). High performance polyurethane nanocomposite films prepared from a masterbatch of graphene oxide in polyether polyol. *Chemical Engineering Journal, 253*, 356–365. https://doi.org/10.1016/j.cej.2014.05.046.

Pokharel, P., & Choi, S. (2015). The effect of hard segment length on the thermal and mechanical properties of polyurethane/graphene oxide nanocomposites. *Composites Part A: Applied Science and Manufacturing, 69*, 168–177. https://doi.org/10.1016/j.compositesa.2014.11.010.

Pokharel, P., & Lee, D. S. (2014). Thermal and mechanical properties of reduced graphene oxide/polyurethane nanocomposite. *Journal of Nanoscience and Nanotechnology, 14*(8), 5718–5721. https://doi.org/10.1166/jnn.2014.8824.

Pokharel, P., & Truong, Q. T. (2014). Multi-step microwave reduction of graphite oxide and its use in the formation of electrically conductive graphene/epoxy composites. *Composites Part B: Engineering, 64*, 187–193. https://doi.org/10.1016/j.compositesb.2014.04.013.

Pokharel, P., Bae, H., Lim, J.-G., Lee, K. Y., & Choi, S. (2015a). Effects of titanate treatment on morphology and mechanical properties of graphene nanoplatelets/high density polyethylene nanocomposites. *Journal of Applied Polymer Science, 132*(23). https://doi.org/10.1002/app.42073.

Pokharel, P., Pant, B., Pokhrel, K., Pant, H. R., Lim, J. G., Kim, H. Y., & Choi, S. (2015b). Effects of functional groups on the graphene sheet for improving the thermomechanical properties of polyurethane nanocomposites. *Composites Part B: Engineering, 78*, 192–201. https://doi.org/10.1016/j.compositesb.2015.03.089.

Pokharel, P., Lee, S. H., & Lee, D. S. (2015c). Thermal, mechanical, and electrical properties of graphene nanoplatelet/graphene oxide/polyurethane hybrid nanocomposite. *Journal of Nanoscience and Nanotechnology, 15*(1), 211–214. https://doi.org/10.1166/jnn.2015.8353.

Pokharel, P., Xiao, D., Erogbogbo, F., & Keles, O. (2019). A hierarchical approach for creating electrically conductive network structure in polyurethane nanocomposites using a hybrid of graphene nanoplatelets, carbon black and multi-walled carbon nanotubes. *Composites Part B: Engineering, 161*, 169–182. https://doi.org/10.1016/j.compositesb.2018.10.057.

Prabhakaran, M. P., Venugopal, J., Chan, C. K., & Ramakrishna, S. (2008). Surface modified electrospun nanofibrous scaffolds for nerve tissue engineering. *Nanotechnology, 19*(45), 455102. https://doi.org/10.1088/0957-4484/19/45/455102.

Rohr, T., Ogletree, D. F., Svec, F., & Fréchet, J. M. (2003). Surface functionalization of thermoplastic polymers for the fabrication of microfluidic devices by photoinitiated grafting. *Advanced Functional Materials, 13*(4), 264–270. https://doi.org/10.1002/adfm.200304229.

Ryu, J. H., Hong, S., & Lee, H. (2015). Bio-inspired adhesive catechol-conjugated chitosan for biomedical applications: A mini review. *Acta Biomaterialia, 27*, 101–115. https://doi.org/10.1016/j.actbio.2015.08.043.

Schlaich, C., Li, M., Cheng, C., Donskyi, I. S., Yu, L., Song, G., Osorio, E., & Haag, R. (2018). Mussel-inspired polymer-based universal spray coating for surface modification: Fast fabrication of antibacterial and superhydrophobic surface coatings. *Advanced Materials Interfaces, 5*(5), 1701254. https://doi.org/10.1002/admi.201701254.

Sis, H., & Birinci, M. (2009). Effect of nonionic and ionic surfactants on zeta potential and dispersion properties of carbon black powders. *Colloids and Surfaces A: Physicochemical and Engineering Aspects, 341*(1–3), 60–67. https://doi.org/10.1016/j.colsurfa.2009.03.039.

Sun, H., & Önneby, S. (2006). Facile polyester surface functionalization via hydrolysis and cell-recognizing peptide attachment. *Polymer International, 55*(11), 1336–1340. https://doi.org/10.1002/pi.2090.

Sun, B., Hou, Q., Liu, Z., & Ni, Y. (2015). Sodium periodate oxidation of cellulose nanocrystal and its application as a paper wet strength additive. *Cellulose, 22*(2), 1135–1146. https://doi.org/10.1007/s10570-015-0575-5.

Sunasee, R., & Hemraz, U. D. (2018). Synthetic strategies for the fabrication of cationic surface-modified cellulose nanocrystals. Fibers, 6(1), 15. https://doi.org/10.3390/fib6010015.

Suresh, V. M., Bonakala, S., Atreya, H. S., Balasubramanian, S., & Maji, T. K. (2014). Amide functionalized microporous organic polymer (Am-MOP) for selective CO_2 sorption and catalysis. *ACS Applied Materials & Interfaces, 6*(7), 4630–4637. https://doi.org/10.1021/am500057z.

Tang, L., Thevenot, P., & Hu, W. (2008). Surface chemistry influences implant biocompatibility. *Current Topics in Medicinal Chemistry, 8*(4), 270–280. https://doi.org/10.2174/156802608783790901.

Thakur, V. K., Vennerberg, D., Madbouly, S. A., & Kessler, M. R. (2014). Bio-inspired green surface functionalization of PMMA for multifunctional capacitors. *RSC Advances, 4*(13), 6677–6684. https://doi.org/10.1039/c3ra46592f.

Tian, P., Xu, D., & Liu, X. (2016). Mussel-inspired functionalization of PEO/PCL composite coating on a biodegradable AZ31 magnesium alloy. *Colloids and Surfaces B: Biointerfaces, 141*, 327–337. https://doi.org/10.1016/j.colsurfb.2016.02.004.

Tiwari, A. P., Joshi, M. K., Lee, J., Maharjan, B., Ko, S. W., Park, C. H., & Kim, C. S. (2017). Heterogeneous electrospun polycaprolactone/polyethylene glycol membranes with improved wettability, biocompatibility, and mineralization. *Colloids and Surfaces A: Physicochemical and Engineering Aspects, 520*, 105–113. https://doi.org/10.1016/j.colsurfa.2017.01.054.

Tiwari, A. P., Hwang, T. I., Oh, J. M., Maharjan, B., Chun, S., Kim, B. S., Joshi, M. K., Park, C. H., & Kim, C. S. (2018). pH/NIR-responsive polypyrrole-functionalized fibrous localized drug-delivery platform for synergistic cancer therapy. *ACS Applied Materials & Interfaces, 10*(24), 20256–20270. https://doi.org/10.1021/acsami.7b17664.

Tiwari, A. P., Bhattarai, D. P., Maharjan, B., Ko, S. W., Kim, H. Y., Park, C. H., & Kim, C. S. (2019). Polydopamine-based implantable multifunctional nanocarpet for highly efficient photothermal-chemo therapy. *Scientific Reports, 9*(1), 2943. https://doi.org/10.1038/s41598-019-39457-y.

Veronese, F. M., & Pasut, G. (2005). PEGylation, successful approach to drug delivery. *Drug Discovery Today, 10*(21), 1451–1458. https://doi.org/10.1016/s1359-6446(05)03575-0.

Vesel, A., & Mozetic, M. (2017). New developments in surface functionalization of polymers using controlled plasma treatments. *Journal of Physics D: Applied Physics, 50*(29), 293001. https://doi.org/10.1088/1361-6463/aa748a.

Vukušić, T., Vesel, A., Holc, M., Ščetar, M., Jambrak, A., & Mozetič, M. (2018). Modification of physico-chemical properties of acryl-coated polypropylene foils for food packaging by reactive particles from oxygen plasma. *Materials, 11*(3), 372. https://doi.org/10.3390/ma11030372.

Wang, Z., et al. (2017) Novel biomaterial strategies for controlled growth factor delivery for biomedical applications. *NPG Asia Materials, 9*(10), e435–e435.

Weibel, D. E. (2010). Polymer surface functionalization using plasma, ultraviolet and synchrotron radiation. *Composite Interfaces, 17*(2–3), 127–136. https://doi.org/10.1163/092764410x490545.

Wu, J., Zhang, C., Xu, S., Pang, X., Cai, G., & Wang, J. (2018). Preparation of zwitterionic polymer-functionalized cotton fabrics and the performance of anti-biofouling and long-term biofilm resistance. *Colloid and Interface Science Communications, 24*, 98–104. https://doi.org/10.1016/j.colcom.2018.02.001.

Xue, C. H., Jia, S.-T., Zhang, J., Tian, L.-Q., Chen, H.-Z., & Wang, M. (2008). Preparation of superhydrophobic surfaces on cotton textiles. *Science and Technology of Advanced Materials, 9*(3), 035008. https://doi.org/10.1088/1468-6996/9/3/035008.

Yang, J., Shi, G., Bei, J., Wang, S., Cao, Y., Shang, Q., Yang, G., & Wang, W. (2002). Fabrication and surface modification of macroporous poly(L-lactic acid) and poly(L-lactic-co-glycolic acid)(70/30) cell scaffolds for human skin fibroblast cell culture. *Journal of Biomedical Materials Research, 62*(3), 438–446. https://doi.org/10.1002/jbm.10318.

Yang, F., Wolke, J. G. C., & Jansen, J. A. (2008). Biomimetic calcium phosphate coating on electrospun poly(ε-caprolactone) scaffolds for bone tissue engineering. *Chemical Engineering Journal, 137*(1), 154–161. https://doi.org/10.1016/j.cej.2007.07.076.

Yoo, H. S., Kim, T. G., & Park, T. G. (2009). Surface-functionalized electrospun nanofibers for tissue engineering and drug delivery. *Advanced Drug Delivery Reviews, 61*(12), 1033–1042. https://doi.org/10.1016/j.addr.2009.07.007.

Zarrintaj, P., Jouyandeh, M., Ganjali, M. R., Hadavand, B. S., Masoud Mozafari, M., Sheiko, S. S., Vatankhah-Varnoosfaderani, M., Gutiérrez, T. J., & Saeb, M. R. (2019). Thermo-sensitive polymers in medicine: A review. *European Polymer Journal, 117*, 402–423. https://doi.org/10.1016/j.eurpolymj.2019.05.024.

Zemljič, L. F., Peršin, Z., Šauperl, O., Rudolf, A., & Kostić, M. (2018). Medical textiles based on viscose rayon fabrics coated with chitosan-encapsulated iodine: Antibacterial and antioxidant properties. *Textile Research Journal, 88*(22), 2519–2531. https://doi.org/10.1177/0040517517725117.

Zeng, Q., Zhu, Y., Yu, B., Sun, Y., Ding, X., Xu, C., Wu, Y.-W., Tang, Z., & Xu, F.-J. (2018). Antimicrobial and antifouling polymeric agents for surface functionalization of medical implants. *Biomacromolecules, 19*(7), 2805–2811. https://doi.org/10.1021/acs.biomac.8b00399.

Zhang, H., Zhao, T., Newland, B., Liu, W., Wang, W., & Wang, W. (2018). Catechol functionalized hyperbranched polymers as biomedical materials. *Progress in Polymer Science, 78*, 47–55. https://doi.org/10.1016/j.progpolymsci.2017.09.002.

Zille, A., Oliveira, F. R., & Souto, A. P. (2015). Plasma treatment in textile industry. *Plasma Processes and Polymers, 12*(2), 98–131. https://doi.org/10.1002/ppap.201400052.

Chapter 3
Surface Reactive and Active Polymers

Saeed Ghanooni, Nasser Nikfarjam, and Pooyan Makvandi

Abstract Modified polymer surfaces have experienced rapid growth over the past decade in industries such as biomedical, bioprocessing, food packaging, microelectronics and textiles. Although the final use of the bio-functionalized polymer varies with each application, the general concept is the same. The first step is to design or select a polymer with bulk properties matching the needs of the final applications, such as conductivity, degradability, elasticity, optical clarity, origin (natural *vs*. synthetic) and strength. The second step is, therefore, to optimize surface functionalization techniques in order to introduce the desired type and amount of reactive functional groups. This chapter aims to introduce the advances in the covalent bonding to functionalized polymer surfaces, including the relevant techniques in the modification of the polymeric surface.

Keywords Antibacterial · Functional polymers · Functionalization · Surface modification

3.1 Introduction

The inert nature of most commercial polymers cannot be developed for specific applications in various industries, and therefore, must undergo surface modification to improve their adhesion, printing and wetting by bringing a variety of polar groups on polymer surfaces. Several surface modification methods have been established during the past decade, and generally follow a general path: first the binding of

---

S. Ghanooni · N. Nikfarjam
Polymer Chemistry Division, Department of Chemistry, Institute for Advanced Studies in Basic Sciences (IASBS), Zanjan, Iran

P. Makvandi (✉)
Institute for Polymers, Composites, and Biomaterials (IPCB), National Research Council (CNR), Naples, Italy
e-mail: pooyan.makvandi@ipcb.cnr.it

T. J. Gutiérrez (ed.), *Reactive and Functional Polymers Volume Four*,
https://doi.org/10.1007/978-3-030-52052-6_3

primary reactive functional groups to the polymer chain ends at the surface, followed by modifying the reactive surface with active/bioactive agents, hydrophobic and hydrophilic monomers, oligomers or polymers to achieve specific surface characteristics matching the needs of the end use. The immobilization of active/bioactive agents on a polymeric surface are generally performed by covalent bonds, electrostatic interactions and ligand-receptor pairing. Non-covalent physical adsorption is desirable for some applications such as certain drug delivery systems (Richey et al. 2000) and regenerable antimicrobial textiles (Kim and Sun 2001; Sun et al. 2001). However, immobilization of the agent *via* covalent bonding leads to the more stable bond between the active/bioactive agent and the functionalized polymer surface. The covalent immobilizations also offer some other advantages by providing the durability of active/bioactive agents, the extended half-life for biomolecules and preventing their quick metabolism (Harris; Alferiev et al. 2006), as well as preventing the migration of bioactive agents to food from the active food packaging films. Grafting of polyfunctional and anchoring compounds *via* a spacer molecule onto the surface of the solid substrate leads to an increase in the number of available active/bioactive agents *per* unit area and improves the efficiency of active/bioactive agents by reducing steric restrictions. Therefore, this chapter focuses on recent advances in the modification of solid surfaces, mainly polymer surfaces, through the covalent bonding of active/bioactive agents targeted for various applications.

3.2 Surface Reactive and Active Polymers for Several Applications

3.2.1 Surface Modifications for Antimicrobial Applications

There are two main strategies to inhibit microbiological growth on the surface of nanocomposite polymers: (1) release of antibacterial agents embedded into polymers and (2) fixation of antibacterial compounds on their surfaces (contact-killing). As for the first strategy, nanomaterials are able to inhibit the bacteriological by releasing them from the matrix (Makvandi et al. 2019a, b; Zare et al. 2019a). In the second strategy, the surface modification of polymer (or metallic) is performed to chemically or physically link various agents with antimicrobial activities, resulting in direct contact with microorganisms. For example, the functionalization of implants by antimicrobial peptides (AMPs) can improve the microbicidal properties of implants (Makvandi et al. 2019c; Zare et al. 2019b). Zhan et al. (2018) conjugated a polydopamine-coated titanium (Ti) substrate using AMPs through a ‘click’ chemistry reaction (Fig. 3.1). The AMPs can reduce the infection of different types of microbes, including bacteria and fungi. AMPs can penetrate the bacterial cell membrane and even fatally damage the drug-resistant bacteria (Zhan et al. 2018). Zhan et al. (2018) indicated that AMP-functionalized surfaces showed high microbicidal effects with low cytotoxicity.

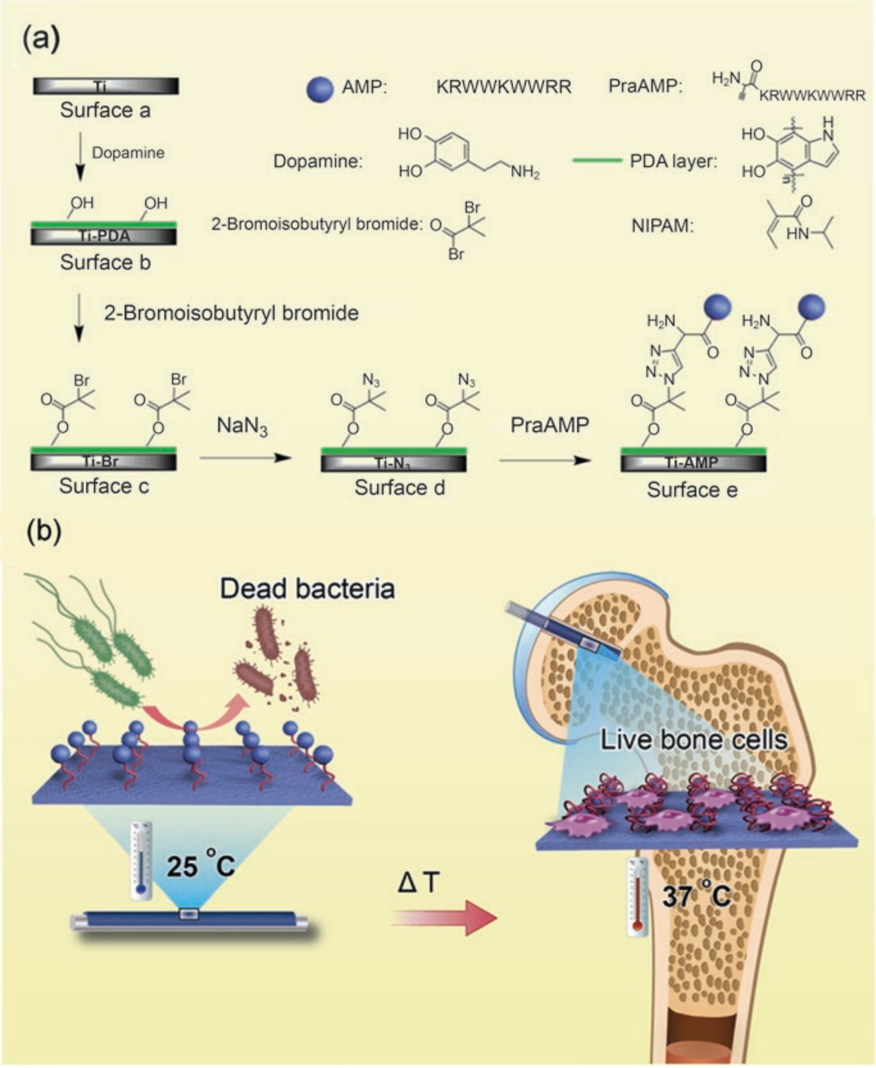

Fig. 3.1 (a) Schematic preparation antibacterial implants by conjugation of antimicrobial peptides (AMPs) on Ti substrates. (b) Temperature-sensitive behavior of the platform. Adapted with permission from Zhan et al. (2018)

Quaternary ammonium compounds (QACs) have also been widely used to improve the antimicrobial efficacy of various surfaces through a contact-killing mechanism. QACs, especially those possessing long alkyl chains, are frequently used as antimicrobial materials and disinfectants against fungi, amoebas and enveloped viruses (Makvandi et al. 2016, 2018a, b). In this context, another example that can be mentioned is the grafting modification onto the surface of the

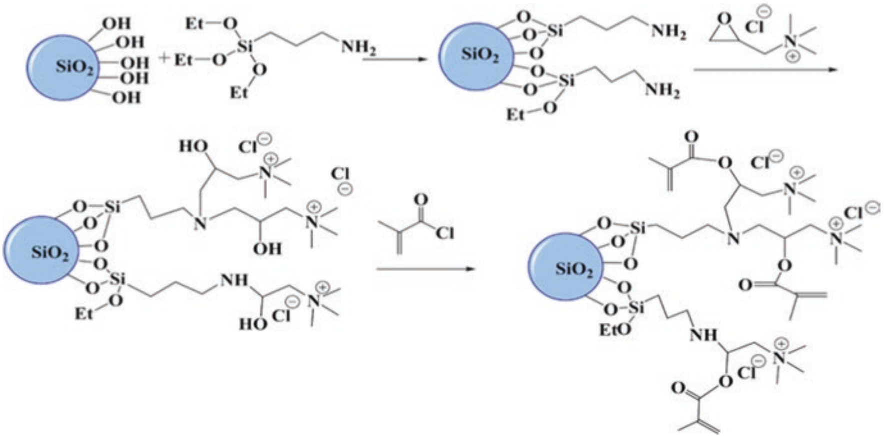

Fig. 3.2 Surface modification of SiO_2 NPs. Adapted with permission from Makvandi et al. (2015)

polysaccharides (cellulose and chitosan) using glycidyl trimethylammonium chloride (Kim et al. 1998; Fu et al. 2011; Pour et al. 2015; Chaker and Boufi 2015).

Some ceramic nanocompounds, e.g. hydroxyapatite and silica nanoparticles (SiO_2 NPs) do not possess antimicrobial activity, and therefore, they can be modified with polymers to generate surface microbicidal materials (Makvandi et al. 2018). Makvandi et al. (2015) functionalized SiO_2 NPs with quaternary ammonium methacrylate using a bisphenol A glycerolate dimethacrylate/triethylene glycol dimethacrylate blend, thus creating a polymerized nanocomposite with antimicrobial properties (Fig. 3.2). The photocurable SiO_2 NPs containing two functional segments: QAC as an antimicrobial agent and methacrylate monomers that are copolymerized with the organic polymer matrix can also be development to obtain polymer-functionalized particles (Makvandi et al. 2015).

The hydrophobic nature of some polymers containing surface-free functional groups, such as polyethylene (PE), polypropylene (PP), polystyrene (PS) and etc., in contact with biological systems are susceptible to microbial growth. Chemical etching *via* surface oxidation and morphological changes is a way to alter the hydrophobicity of the polymer surfaces mentioned above. In addition, several radiation sources such as gamma (γ), infrared, ultraviolet and visible light radiation, as well as microwave plasma and high-energy electrons have been primarily used to graft species and monomer to/from the surface (Pearson and Urban 2014). Microwave plasma-mediated surface reactions is a fast, solvent-free and sterile approach, which provides covalent bonds from carboxylic groups on almost any polymer substrate (Pearson and Urban 2014). Several researchers have also employed an excited ionized gas to produce reactive functional groups onto the surface of the polymers, thus providing controllable conditions to covalently bond desirable compounds (Pearson and Urban 2014). For example, maleic anhydride when applied as a monomer, the modification of the resulting surface produces '–COOH' entities which are linked to a polymer main chain (backbone). Figure 3.3 schematically represents this simple

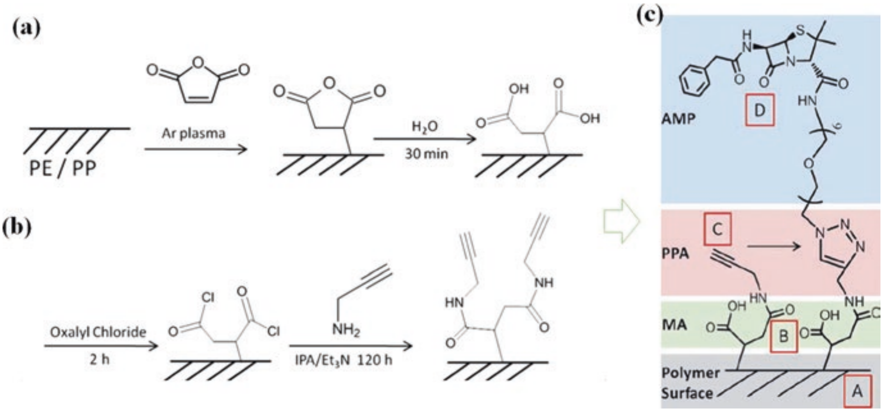

Fig. 3.3 Functionalization of the PE/PP surface through microwave plasma in the presence of maleic anhydride (**a**), followed by alkyne fixation using propargylamine (**b**) and then ampicillin grafting *via* ‘click’ reaction (**c**). Adapted with permission from Pearson and Urban (2014)

two-step process: (a) microwave plasma reactions lead to the formation of ‘–COOH’ on the surface and (b) covalent bonding of alkyne moieties. The polymer surface after this surface treatment is ready for further modifications and to link antimicrobial agents. This approach was used by Pearson and Urban (2014) for the fixation of antibiotics, such as ampicillin, to provide microbicidal properties on the surface of PP and PE substrates. These authors indicated that these modified surfaces revealed strong antibacterial effects against *Staphylococcus aureus* (Pearson and Urban 2014). Some of the other antibiotics such as amoxicillin, cephalexin, methicillin and vancomycin have also been linked to various surfaces to provide active surfaces (Gu et al. 2003; Ye et al. 2018). For example, Ye et al. (2018) prepared amoxicillin-grafted bacterial cellulose sponges for antibacterial materials and wound healing applications.

Poly(propylene carbonate) (PPC) is a partially renewable polymer, since it is produced by carbon dioxide (CO_2), and can be degraded into CO_2 and water (Bahramian et al. 2017). The functionalization of PPC surface increases its applications in food industry as biodegradable packaging (Bahramian et al. 2017). The plasma coating has been used for the chemical immobilization of thymol, a natural microbiocide, on the surface of the PPC. Bahramian et al. (2017) reported a greater antibacterial effect for coatings containing thymol superficially (1.25 mg/cm^2) immobilized with high-intensity plasma for 15 min. The antibacterial effect of the thymol-decorated PPC was preserved for a week in aqueous medium, while under dry conditions the antimicrobial properties were maintained for several months (Bahramian et al. 2017).

Other polymers such as polydopamine have been used for surface modification of other polymers such as polyurethane (PU). For example, Liu and Huang (2016) reported that polydopamine-coated PU films and then modified with perfluoroalkyl exhibited strong antifouling properties, while coatings containing silver NPs (Ag

NPs) showed biocidal activity. In addition, polydopamine-coated PU films decorated with Ag NPs and perfluoroalkyl exhibited a synergistic effect, thus showing a high antibacterial effect against Gram-positive and -negative bacteria (Liu and Huang 2016).

The antibacterial surfaces of PE and PS have also been exploited through the use of dimethyloctadecyl [3-(trimethoxysilyl) propyl] ammonium chloride as QACs. According to Fadida et al. (2014) the QAC-decorated PE and PS surfaces exhibited antibacterial activity against *Salmonella enterica* (Gram negative bacterium). However, the antibacterial effects of the QACs-decorated PS was higher compared to QAC-decorated PE, which was attributed to the higher density of active sites (Fadida et al. 2014). It should be noted that the surface functionalization with short alkyl chain, e.g. methyl (C_1) consists of trimethyl [3-(trimethoxysilyl) propyl] ammonium chloride, did not show a considerable antibacterial effect, thus suggesting the importance of the length of the alkyl chain. Therefore, this technique presents an adequate approach to develop antibacterial hydrocarbons with contact active sites (Fadida et al. 2014).

The stainless steel surfaces have also been functionalized by antimicrobial moieties. With this in mind, Bastarrachea and Goddard (2013) prepared the covalent functionalization of the stainless steel surface to have *N*-halamine antibacterial groups. The multiple layers of poly(acrylic acid) (PAA) and polyethylenimine (PEI) were linked to the surface of stainless steel by a layer-by-layer technique. *N*-halamine-functionalized steel exhibited an antibacterial effect (99.7% reduction) against *Listeria monocytogenes* (Bastarrachea and Goddard 2013).

3.2.2 Drug Delivery Applications

For a successful delivery of a drug or other biomolecules, the desired dose of drug/biomolecule should be delivered at the targeted site for a desired period. A successful methodology to comply with the controlled and targeted release of the drug has been the use of polymeric membranes. However, surface modification of nanomaterials has also been used for this purpose, e.g. polymeric or metallic NPs modified by organic compounds, thus improving drug release in the human body. Several studies have shown the improvement of delivery efficiency using surface functionalized nanostructures. The surface functionalization of polymeric nanomaterials can be classified into two categories (Fig. 3.4). In the first approach, a coupling agent is used for the modification of the nanostructure and, consequently, at least one reactive group must be available onto the surface of NPs. The second approach is similar to the micellar formation of the amphiphilic block copolymers which have hydrophilic and hydrophobic segments such as Pluronic, which is a polyethylene oxide-polypropylene oxide-polyethylene oxide (PPO-PEO-PPO) copolymer. It is worth noting that such amphiphilic copolymers are used for the preparation of thermosensitive injectable hydrogels for biomedical applications (Yang et al. 2011; Zarrintaj et al. 2019).

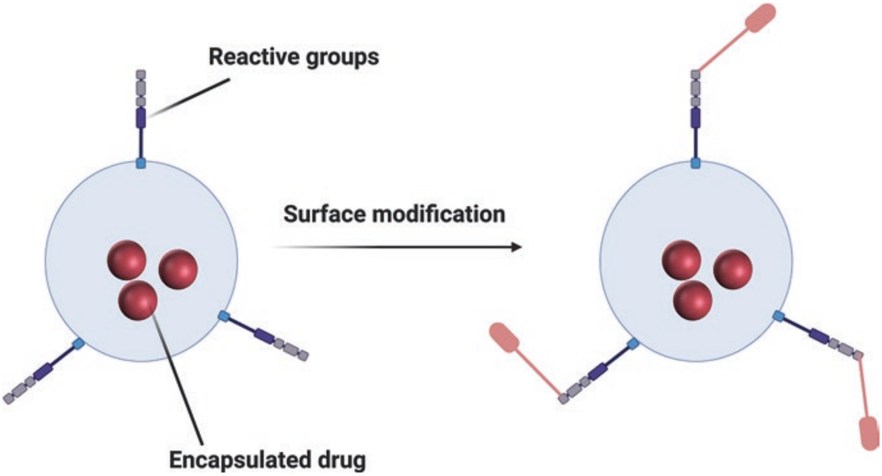

Fig. 3.4 Schematic presentation for the surface functionalization of polymeric nanomaterials. Adapted with permission from Delfi et al. (2020) and Choi et al. (2003)

In general, the hydrophobic core provides a domain for encapsulation of hydrophobic biomolecules, such as diclofenac, while the shell layer is in direct contact with body fluids and organs, which are used for site-specific delivery. For example, polylactic-*co*-glycolic acid (PLGA) NPs have been functionalized using poly(ethylene)glycol (PEG) for various purposes, including improved diffusion of PLGA NPs into human cervical mucus or better delivery of drugs/biomolecules (Cu and Saltzman 2008; Park et al. 2009).

In addition to surface functionalization by covalent bonds, another method is surface coating by chemical interactions between the coated compounds and polymeric NPs. For example, the main drawback to the use of PLGA NPs for DNA/RNA delivery is its negative charge, which restricts the interaction with negatively charged DNA, as well as the poor transportability of the DNA-loaded PLGA NPs through the cell membrane. With this in mind, many researchers have coated PLGA NPs using cationic polymers such as chitosan to overcome or reduce the aforementioned problems (Nafee et al. 2007).

Some other types of nanostructures based on natural polymers, such as hyaluronic acid (HA), have been decorated to improve their drug delivery capability. In addition to polymeric nanomaterials, some metallic and ceramic particles have also been extensively researched as delivery vehicles for various biopharmaceuticals. However, to improve their biocompatibility and properties, the surface of these nanostructures has been modified. For example, gold NPs (Au NPs) have been functionalized using HA. HA is a natural glycosaminoglycan, which is presents in the connective tissues of mammals, such as the dermis, synovial fluids, the vitreous body and the nucleus pulposus, where it fulfills important physiochemical and biological functions. As a drug delivery vehicle, a biocompatible linear polysaccharide of HA is highly efficient for site-specific delivery to tissues with HA receptors such as the hyaluronan receptor for endocytosis (HARE) and the cluster determinant 44 (CD44) (Lee et al. 2012; Mayol et al. 2014).

3.2.3 Textile Applications

Naturally derived materials, such as cotton fiber, have been widely applied as solid phase extraction absorbents for sample preparation due to their high adsorption capacity of hydrophobic materials (He et al. 2014). This type of adsorbents exhibits high mechanical strength, good biocompatibility and desired stability in non-aqueous or aqueous solutions. However, the versatile application of cotton-based materials is restricted due to their monotonous functional groups. In thi sentes, He et al. (2014) functionalized sulfhydryl cotton fiber-based (SCF) materials by using 'thiol-ene' click chemistry *via* the abundant thiol groups onto sulfhydryl cotton (Fig. 3.5). The reaction consists of the esterification of solid cotton to prepare SCF followed by the reaction of the sulfide groups with vinyl functionality (He et al. 2014).

Surface modification of the cotton can also be carried out *via* graft polymerization by using the hydroxyl groups on its surface. Grafting copolymerization is a versatile and attractive technique to provide several chains with different functionalities to the polymer backbone. The polysaccharide graft copolymerization is based on three common methods namely 'grafting to', 'grafting from' and 'grafting through' (Fig. 3.6) (He et al. 2017). In the 'grafting to' method, the precursors of tele-functional side chains made individually react with a complementary functionality distributed in the polymer backbone. In contrast, the 'grafting through', macromonomers are polymerized using an appropriate initiator, while in the 'grafting from', polymerization of the second monomer occurs from functionalities induced

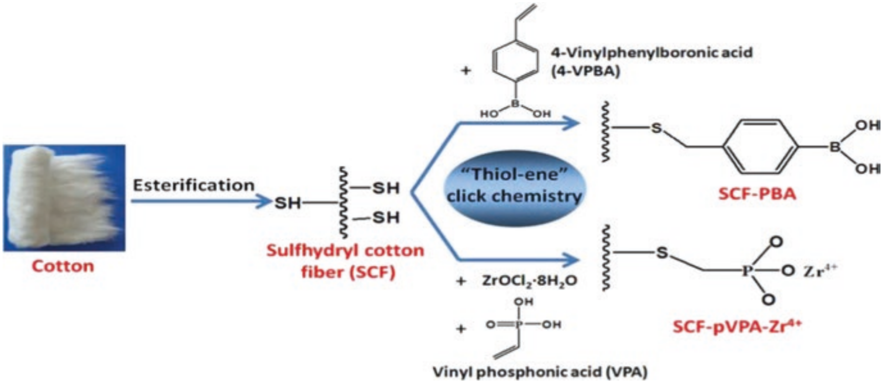

Fig. 3.5 Scheme for the preparation of zirconium phosphonate-modified (SCF-pVPA-Zr^{4+}) and phenylboronic acid-grafted (SCF-PBA) sulfhydryl cotton fibers. Adapted with permission from He et al. (2014)

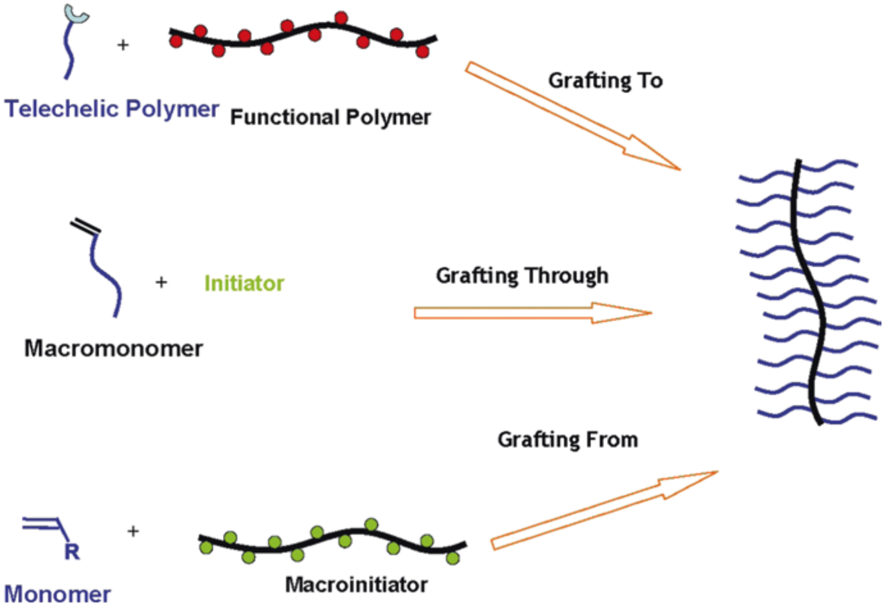

Fig. 3.6 Scheme for the different types of graft reactions. Adapted with permission from Van Camp et al. (2007)

into the polymer backbone which can initiate polymerization (Sumerlin et al. 2005; Gao and Matyjaszewski 2007; Tsarevsky et al. 2007; Van Camp et al. 2007).

3.2.4 *Water Desalination/Purification Applications*

One of the most practical and viable approaches to achieve high metal removal efficiency is the surface modification of natural polymer adsorbents with functional polymeric materials (Kobayashi and Uyama 2003). In line with this, superficially modified cellulose has been used for environmental remediation and water purification in industrial processes (Wang 2019). It should be noted that cellulose is the most abundant polysaccharide in nature (Bracone et al. 2016; Gutiérrez and Alvarez 2017; Herniou-Julien et al. 2019). Unlike the bulk form, the cellulose nanomaterials show improved properties, such as large surface area and high strength, which make them very promising materials for the manufacture of high performance filters and membranes. These properties allow them to be used in numerous applications for the removal of contaminants and the purification of drinking water and industrial wastewater systems (Wang 2019). Different cellulose materials such as cellulose nanofibers (CNFs), cellulose nanocrystals (CNCs, also known as cellulose nanowhiskers, CNW) and bacterial cellulose nanocrystals (BCN) with an excellent capacity have been used for water purification (Wang 2019). The CNCs is isolated from the monocrystalline region of cellulose with an almost perfect crystalline structure. It has rod-like morphology with 10–20 nm in width and several hundred nanometers in length. The nanoscale advantages of CNCs along with properties such as high aspect ratio and high specific strength make it a desirable reinforcing agent for different polymers. The CNFs are longer than CNCs, and therefore, have a much larger aspect ratio and a stronger percolation network, which generally exhibit stronger reinforcing effects than CNCs (Wang 2019). Surface modification of CNFs by using 2,2,6,6-tetramethyl-1-piperidinyloxy (TEMPO)-mediated oxidation, coupling agents, acetylation, polymer grafting and cationic modification are commonly performed to extend their applications for hydrophobic polymers, as well as to promote its compatibility and dispersion in other polymers (Wang 2019). Reactive molecules can also be grafted onto the nanocellulose surfaces by means of functional groups from chemical reactions such as amidation, carboxylation, esterification, etherification, oxidation, phosphorylation and sulfonation (Fig. 3.7). The resulting materials can be used for the removal of heavy toxic metals from contaminated water. In particular, Wang (2019) demonstrated that carboxyl, phosphonate and sulfonate groups present on nanocellulose surfaces can exhibit selective absorption of contaminants in water, such as dyes, metal ions and microbes for water purification.

Yang et al. (2013) and Sheikhi et al. (2015) created carboxyl groups through selective oxidation of the hydroxyl groups located at C_2 and C_3 positions of the nanocellulose to give rise to aldehyde groups, and then to 2,3-dicarboxyl groups in

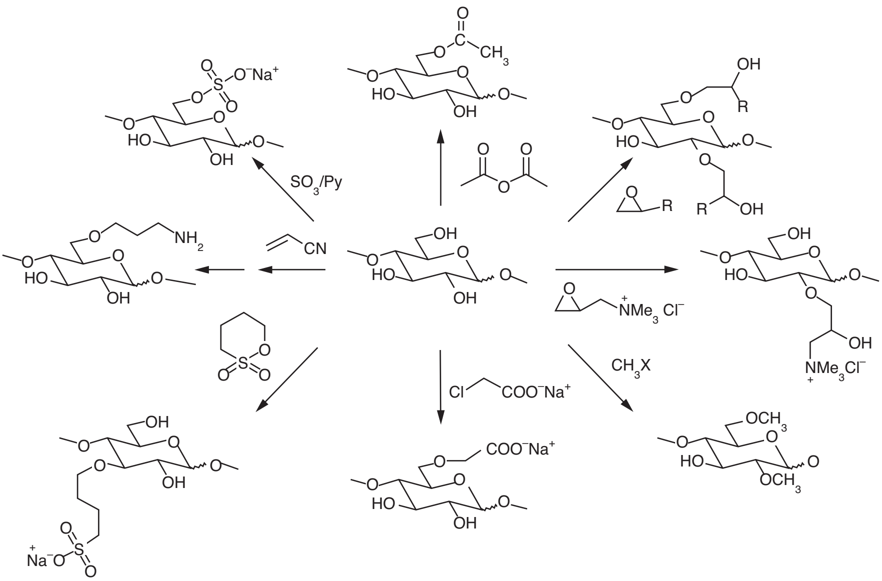

Fig. 3.7 The main chemical modifications/functionalizations of the nanocellulose surface for water purification. Reprinted with permission from Kobayashi and Uyama (2003)

acidic media. The succinylation of CNC (Yu et al. 2013) and CNF (Srivastava et al. 2012) has resulted in efficient, stable and recyclable adsorbents to be use for the removal of Pb^{2+}, Cd^{2+}, Ni^{2+} and Cr^{3+}. According to Yu et al. (2013), sulfated CNCs grafted by amide-bearing polymers have shown a very high mercury absorption (710 mg/g) at pH 6.2. In addition, carboxylate bearing polymers grafted onto diverse CNCs have also helped in the removal of numerous cations. For example, PAA-grafted CNCs (obtained from bamboo) can be used for the removal of Cu^{2+} ions from aqueous solutions (Zhang et al. 2014), while sulphated CNCs have also been used for adsorption of drugs such as doxorubicin hydrochloride (DOX) and tetracycline hydrochloride (TC) from the water (Jackson et al. 2011).

Hong et al. (2018) recently efficiently immobilized carboxymethylated cellulose nanofibrils (CMCNFs) onto PU foams in a cost-effective manner. The PU foam structure was developed simultaneously due to the release of CO_2 gas formed from the reaction between water and isocyanate (R-NCO) in the prepolymer (Eq. 3.1).

$$R-NCO+H_2O\rightarrow\left[R-NHCOOH\right]\rightarrow R-NH_2\left(\text{amine}\right)+CO_2 \tag{3.1}$$

During the formation of amine groups into the PU foam structure, the CMCNFs are naturally bound to the surface of the PU foam to form a 3D porous PU/CMCNF composite (Ram and Chauhan 2018). These composite foams have exhibited high mechanical strength, recyclability and greater adsorption efficiency of 78.7, 98 and 216.1 mg/g for Cu^{2+}, Cd^{2+} and Pb^{2+} cations, respectively (Wang 2019).

Ram and Chauhan (2018) synthesized and demonstrated that a new thiolated spherical nanocellulose (CNS) obtained *via* acid hydrolysis, followed by esterification with 3-mercaptopropionic acid (3-MPA) by lipase catalysis (Fig. 3.8) can be used as an efficient and selective absorbent of Hg^{2+} ions. The results obtained revealed a high adsorption capacity with rapid adsorption: 98.6% in 20 min. Functionally-induced thiol groups led to an increase in the selectivity of SNC-3-MPA towards Hg^{2+} ions, while adsorption capacity remained very high even in the presence of competitive ions (Ram and Chauhan 2018).

Cellulose nanomaterials can also be functionalized with positively charged groups in order to adsorb anionic organic pollutants and metal species such as arseniates and chromates. The positively charged CNCs can be obtained by treating the sulfated CNCs with epoxypropyl trimethylammonium chloride (EPTMAC) (Hasani et al. 2008), or by synthesizing bisphosphonated nanocellulose by oxidation with sodium periodate followed by the reaction with sodium alendronate and then used to absorb vanadium in the form of metavanadate (VO^{3-}) (Sirviö et al. 2016).

With respect to the absorption of dyes, carboxylated CNCs can also be prepared by the TEMPO oxidation method with high carboxylic acid content for adsorption and removal of methylene blue (a well known contaminant dye) with an adsorption capacity of 769 mg/g at pH 9 (Batmaz et al. 2014). Qiao et al. (2015) indicated that the esterification of existing hydroxyl groups on the surface of CNCs by using maleic anhydride makes that carboxylated CNCs have a greater absorption efficiency towards a variety of cationic dyes such as malachite green, methylene blue and crystal violet. Jin et al. (2015) also prepared cationic nanocellulose as follows:

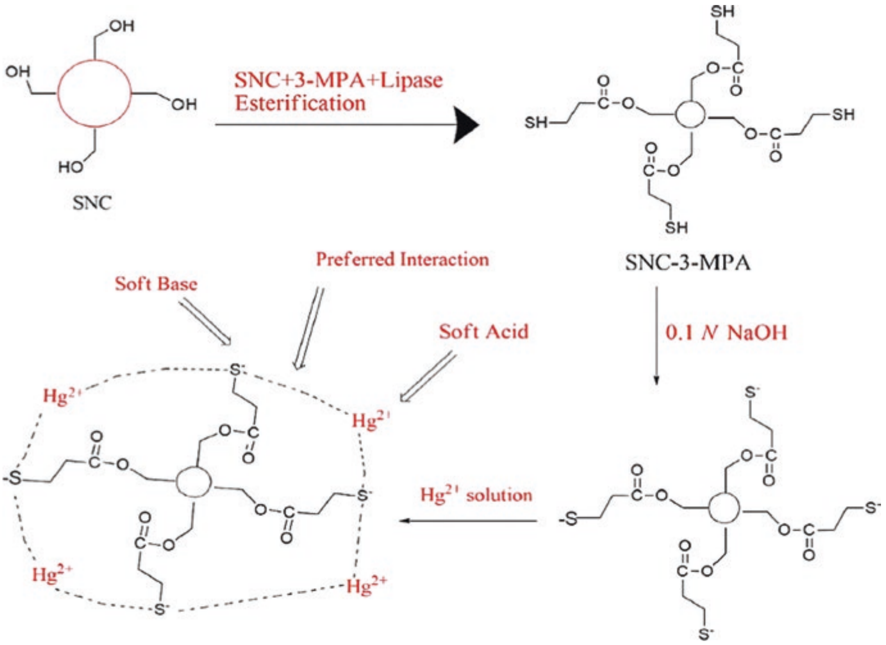

Fig. 3.8 Scheme for the synthesis of SNC-3-MPA and its mechanism for adsorption of Hg^{2+} ions. Reprinted with permission from Ram and Chauhan (2018)

the CNCs were oxidized by sodium periodate and subsequently reacted with ethylenediamine with the aim of removing the acid red GR dye (anionic dye), the resulting material showed a maximum absorption of 556 mg/g for acid red GR.

Other non-dye anionic water pollutants can be fluorides, nitrates, phosphates and sulfates. With this in mind, cationic CNFs can be used for the removal of these anionic species. For this reason, surface modification can improve the absorption capacity of a dye selectively. In line with this, Pei et al. (2013) manufactured cationic CNF *via* quaternization through the use of glycidyltrimethylammonium chloride (GTAC) and then the material was used for the removal of green acid 25 and Congo red. In contrast, anionic CNF can be used for cationic dye adsorption (Selkälä et al. 2018).

Polyester films based on polyethylene terephthalate (PET) have also been superficially modified for water treatment. For example, the cyclodextrin polymer (CDP) was coated on electro-spun PET nanofibers by polymerization of cyclodextrin in the presence of citric acid (crosslinking agent) (Fig. 3.9) (Kayaci et al. 2013). The prepared materials were targeted for removal of polycyclic aromatic hydrocarbons such as phenanthrene (Kayaci et al. 2013).

New chelating thiosemicarbazide (TSC) moietie-functionalized PET fibers (PET-TSC) were also made by Monier and Abdel-Latif (2013) for the removal of heavy metal ions, such as Co^{2+}, Cu^{2+} and Hg^{2+} from water. The material was manufactured in three stages: (1) graft copolymerization of polyacrylonitrile (PAN) onto PET backbone, (2) modification of PET-*g*-PAN fibers by using an alcoholic

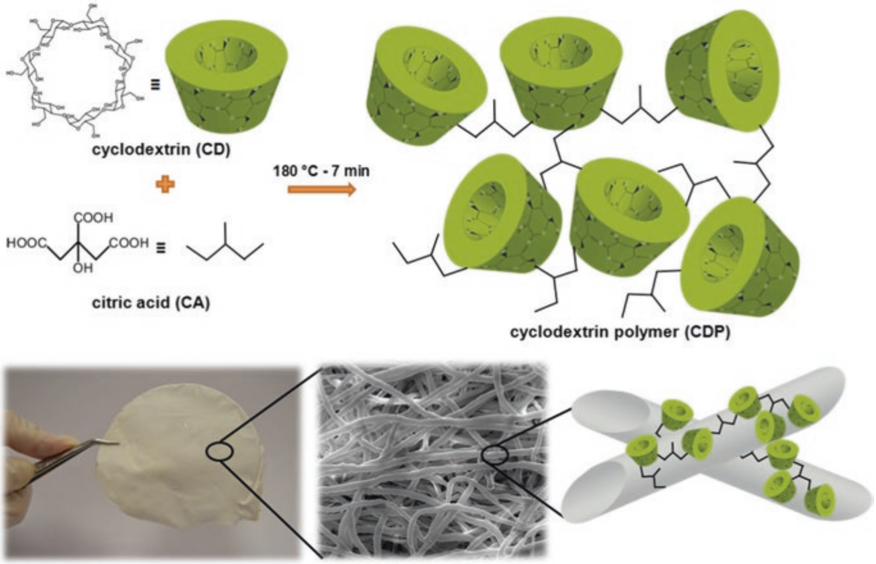

Fig. 3.9 Mechanism of the schematic formation of CDP-coated electrospun PET nanofibers and the illustrative photograph of PET/CDP nanofibrous mat and its SEM micrograph showing schematic representation of PET/CDP nanofibers. Adapted with permission from Kayaci et al. (2013)

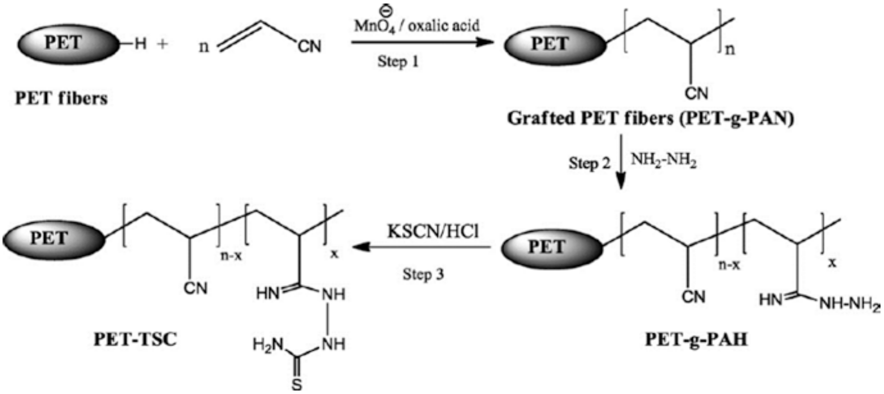

Fig. 3.10 Synthesis of PET-TSC chelating fibers. Adapted with permission from Monier and Abdel-Latif (2013)

hydrazine hydrate solution to prepare PET-grafted poly(acrylic hydrazidine) (PET-*g*-PAH) and (3) chelating PET-TSC fibers were obtained by treating PET-*g*-PAH fibers with a aqueous solution of potassium thiocyanate and HCl (Fig. 3.10) (Monier and Abdel-Latif 2013).

Bayramoglu et al. (2015) modified the algal biomass with PEI and amidoxime ligand by using glutaraldehyde as a coupling agent with the objective of removing

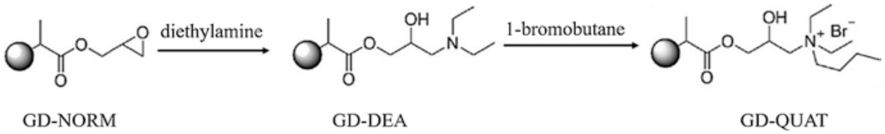

Fig. 3.11 Preparation of two resin beads including a weakly basic anionic exchange group (GD-DEA) and a weakly basic anionic exchange group (GD-QUAT). Adapted with permission from Aversa et al. (2016)

U^{4+} from aqueous solutions. It was discovered in this study that the interactions between uranium cations and amine groups played an important role in the adsorption process (Bayramoglu et al. 2015).

On the other hand, polymeric resins due to easy regeneration and reuse have also been widely used for the adsorption of phenol and its derivatives. In this sense, Aversa et al. (2016) prepared polymer resin beads *via* suspension polymerization and copolymerization of glycidyl methacrylate (GD-NORM), and were then prepared two resin beads containing a weakly basic anionic exchange group (GD-DEA) and a strongly basic group (GD-QUAT) by reaction of diethylamine using GD-NORM beads and reaction of 1-bromobutane with GD-DEA beads, respectively (Fig. 3.11). These authors found that the resin containing a tertiary amine group (GD-DEA) was able to efficiently adsorb phenols more than the resin containing a quaternary ammonium salt (GD-QUAT). The greater availability of the electron pair in the resin with the weakly basic donor group was the main reason for improving the interaction of the resin with the phenoxide ions (Aversa et al. 2016).

Kwak and Lee (2018) grafted PEI onto the surface of silk sericin beads by using glutaraldehyde as a coupling agent. These authors reported the possible application of the materials made for the removal of Cr^{6+} from aqueous solutions. Interestingly, Tripathi et al. (2013) also grafted multilayers of polyelectrolytes into pores and surfaces of PET membranes. Poly(sodium 4-styrenesulfonate), as negatively charged polyelectrolyte, and poly(diallyldimethylammonium chloride), as positively charged polyelectrolyte, were alternately assembled to make polyelectrolyte multilayers *via* the convective flow method (Tripathi et al. 2013). These membranes showed an almost complete rejection of the Congo red pollutant dye with adequate flows (Tripathi et al. 2013).

3.2.5 Improved Coating Applications

Diene elastomers have been widely used as suspension elements in cars, sport goods and for the manufacture of plastic toys. The important synthetic diene elastomers are acrylonitrile-butadiene-styrene (ABS), nitrile-butadiene rubber (NBR), polybutadiene (PBD), polychloroprene (CR), polyisoprene (IR), styrene-butadiene rubber (SBR) and styrene-isoprene-styrene (SIS). In general, additives are added to these polymers to improve their properties. However, these non-reactive additives can seep from materials over time. One way to solve this problem is to graft additives

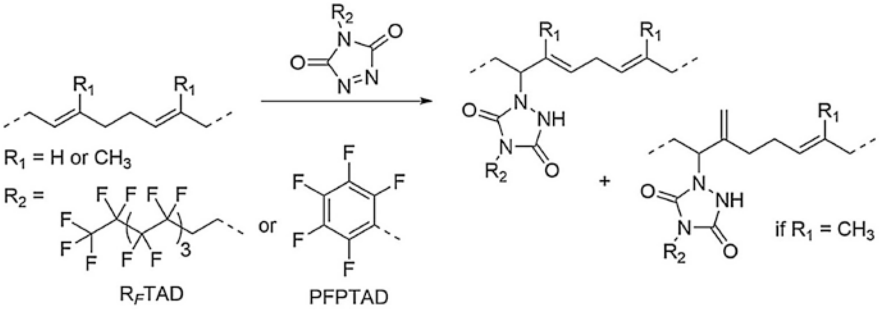

Fig. 3.12 Schematic illustration of grafting 1*H*,1*H*,2*H*,2*H*-perfluorodecyl triazolinedione (R_FTAD) and perfluorophenyl triazolinedione (PFPTAD) onto polyisoprene and polybutadiene. Adapted with permission from De Bruycker et al. (2017)

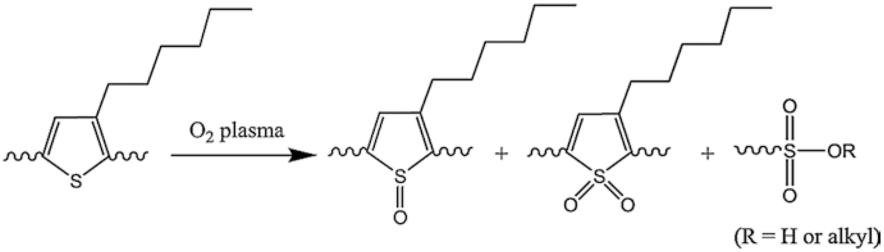

Fig. 3.13 Oxidation mechanism of P3HT films *via* O_2 plasma treatment. Adapted with permission from Tountas et al. (2018)

into the polymer backbone. With this in mind, De Bruycker et al. (2017) synthesized fluorinated triazolinedione (TAD) derivatives and then grafted onto the SIS, SBR and SBS backbone (Fig. 3.12). Specifically, grafting 4-perfluorophenyl-TAD introduces polarity in the polymer backbone, and therefore, the strong intra-intermolecular hydrogen-bonding interactions can affect the properties of the material (De Bruycker et al. 2017).

Poly(3-hexylthiophene) (P3HT) is one of the most attractive materials for preparing field-effect transistors, organic photovoltaics and photodetectors. Generally, the surface modification strategy is applied to increase the device efficiency of P3HT materials. In this concept, the oxygen (O_2) plasma treatment allows hydroxylation of the surface of polymers, thus leading to the roughness of the nanoscale interface in order to solve with the problem of the limited contact area of the acceptor and the donor. Direct oxidation of sulfur atoms in the thiophene ring *via* O_2 plasma converts the hydrophobic surfaces of P3HT into hydrophilic ones by anchoring polar groups on the surfaces (Fig. 3.13) In addition, an increase in the work function is driven due to the change in the faction of the oxidized surface species which in turn effectively increases the ionization potential *via* oxidative p-type doping (Tountas et al. 2018).

It is worth remembering that most surfaces of biopolymeric materials are naturally hydrophobic, and therefore, many efforts have been made to solve this problem. For example, El-Saftawy et al. (2018) adapted the surface chemistry of the ethylene-vinyl alcohol (EVOH) copolymer by using electron beam followed by grafting of fucoidan. The fucoidan-coated EVOH samples exhibited a great improvement in surface wettability and a reduction in the recovery effect compared to pristine EVOH samples (El-Saftawy et al. 2018). The surface of the porous PE substrates was also modified by Chen et al. (2018) through the use of polymers bearing phosphorylcholine groups, known as antifouling agents, by generating photochemical generation followed by photoirradiation. According to Chen et al. (2018) the modified porous PE exhibited an increase in hydrophilicity and the rate of water penetration through the pores. Finally, the antifouling properties of this material can be useful for biomedical applications (Chen et al. 2018).

3.3 Conclusions

Polymer modifications have become another important area of polymer science and technology. Functionalized polymer have experienced rapid growth over the recent years in various fields, including biomedical sectors and different industries such as foods, microelectronics and textiles. These modified polymers have been used in coatings, drug delivery, textiles and water treatments. The functionalization can be done to impart various properties or improve existing features. Surface modification of synthetic and natural polymers can obtain desirable properties, such as antimicrobial activity and biocompatibility, which are highly debated and researched properties in modern times.

Acknowledgments Does not declare.

Conflicts of Interest The authors declare no conflict of interest.

References

Alferiev, I. S., Connolly, J. M., Stachelek, S. J., Ottey, A., Rauova, L., & Levy, R. J. (2006). Surface heparinization of polyurethane via bromoalkylation of hard segment nitrogens. *Biomacromolecules, 7*(1), 317–322. https://doi.org/10.1021/bm0506694.

Aversa, T. M., da Silva, C. M. F., da Rocha, P. C. S., & Lucas, E. F. (2016). Influence of exchange group of modified glycidyl methacrylate polymer on phenol removal: A study by batch and continuous flow processes. *Journal of Environmental Management, 182*, 301–307. https://doi.org/10.1016/j.jenvman.2016.07.082.

Bahramian, B., Chrzanowski, W., Kondyurin, A., Thomas, N., & Dehghani, F. (2017). Fabrication of antimicrobial poly(propylene carbonate) film by plasma surface modification. *Industrial & Engineering Chemistry Research, 56*(44), 12578–12587. https://doi.org/10.1021/acs.iecr.7b01185.

Bastarrachea, L. J., & Goddard, J. M. (2013). Development of antimicrobial stainless steel via surface modification with N-halamines: Characterization of surface chemistry and N-halamine chlorination. *Journal of Applied Polymer Science, 127*(1), 821–831. https://doi.org/10.1002/app.37806.

Batmaz, R., Mohammed, N., Zaman, M., Minhas, G., Berry, R. M., & Tam, K. C. (2014). Cellulose nanocrystals as promising adsorbents for the removal of cationic dyes. *Cellulose, 21*(3), 1655–1665. https://doi.org/10.1007/s10570-014-0168-8.

Bayramoglu, G., Akbulut, A., & Arica, M. Y. (2015). Study of polyethyleneimine- and amidoxime-functionalized hybrid biomass of *Spirulina (Arthrospira) platensis* for adsorption of uranium (VI) ion. *Environmental Science and Pollution Research, 22*(22), 17998–18010. https://doi.org/10.1007/s11356-015-4990-9.

Bracone, M., Merino, D., González, J., Alvarez, V. A., & Gutiérrez, T. J. (2016). Chapter 6. Nanopackaging from natural fillers and biopolymers for the development of active and intelligent films. In S. Ikram & S. Ahmed (Eds.), *Natural polymers: Derivatives, blends and composites* (pp. 119–155). New York. EE.UU. ISBN: 978-1-63485-831-1: Editorial Nova Science.

Chaker, A., & Boufi, S. (2015). Cationic nanofibrillar cellulose with high antibacterial properties. *Carbohydrate Polymers, 131*, 224–232. https://doi.org/10.1016/j.carbpol.2015.06.003.

Chen, S. H., Fukazawa, K., Inoue, Y., & Ishihara, K. (2018). Photoinduced surface zwitterionization for antifouling of porous polymer substrates. *Langmuir, 35*(5), 1312–1319. https://doi.org/10.1021/acs.langmuir.8b01089.

Choi, S. W., Kim, W. S., & Kim, J. H. (2003). Surface modification of functional nanoparticles for controlled drug delivery. *Journal of Dispersion Science and Technology, 24*(3–4), 475–487. https://doi.org/10.1081/dis-120021803.

Cu, Y., & Saltzman, W. M. (2008). Controlled surface modification with poly(ethylene)glycol enhances diffusion of PLGA nanoparticles in human cervical mucus. *Molecular Pharmaceutics, 6*(1), 173–181. https://doi.org/10.1021/mp8001254.

Delfi, M., Ghomi, M., Zarrabi, A., Mohammadinejad, R., Taraghdari, Z. B., Ashrafizadeh, M., Zare, E. N., Agarwal, T., Padil, V. V. T., Mokhtari, B., Rossi, F., Perale, G., Sillanpaa, M., Borzacchiello, A., Maiti, T. K., & Makvandi, P. (2020). Functionalization of polymers and nanomaterials for biomedical applications: Antimicrobial platforms and drug carriers. *Prosthesis, 2*(2), 117–139. https://doi.org/10.3390/prosthesis2020012

De Bruycker, K., Delahaye, M., Cools, P., Winne, J., & Prez, F. E. D. (2017). Covalent fluorination strategies for the surface modification of polydienes. *Macromolecular Rapid Communications, 38*(11), 1700122. https://doi.org/10.1002/marc.201700122.

El-Saftawy, A. A., Ragheb, M. S., & Zakhary, S. G. (2018). Electron beam irradiation impact on surface structure and wettability of ethylene-vinyl alcohol copolymer. *Radiation Physics and Chemistry, 147*, 106–113. https://doi.org/10.1016/j.radphyschem.2018.02.001.

Fadida, T., Kroupitski, Y., Peiper, U. M., Bendikov, T., Sela, S., & Poverenov, E. (2014). Air-ozonolysis to generate contact active antimicrobial surfaces: Activation of polyethylene and polystyrene followed by covalent graft of quaternary ammonium salts. *Colloids and Surfaces B: Biointerfaces, 122*, 294–300. https://doi.org/10.1016/j.colsurfb.2014.07.003.

Fu, X., Shen, Y., Jiang, X., Huang, D., & Yan, Y. (2011). Chitosan derivatives with dual-antibacterial functional groups for antimicrobial finishing of cotton fabrics. *Carbohydrate Polymers, 85*(1), 221–227. https://doi.org/10.1016/j.carbpol.2011.02.019.

Gao, H., & Matyjaszewski, K. (2007). Synthesis of molecular brushes by “grafting onto” method: Combination of ATRP and click reactions. *Journal of the American Chemical Society, 129*(20), 6633–6639. https://doi.org/10.1021/ja0711617.

Gu, H., Ho, P. L., Tsang, K. W., Wang, L., & Xu, B. (2003). Using biofunctional magnetic nanoparticles to capture vancomycin-resistant enterococci and other Gram-positive bacteria at ultralow concentration. *Journal of the American Chemical Society, 125*(51), 15702–15703. https://doi.org/10.1021/ja0359310.

Gutiérrez, T. J., & Alvarez, V. A. (2017). Cellulosic materials as natural fillers in starch-containing matrix-based films: A review. *Polymer Bulletin, 74*(6), 2401–2430. https://doi.org/10.1007/s00289-016-1814-0.

Hasani, M., Cranston, E. D., Westman, G., & Gray, D. G. (2008). Cationic surface functionalization of cellulose nanocrystals. *Soft Matter, 4*(11), 2238–2244. https://doi.org/10.1039/b806789a.

He, X. M., Zhu, G. T., Zhu, Y. Y., Chen, X., Zhang, Z., Wang, S. T., Yuan, B. F., & Feng, Y. Q. (2014). Facile preparation of biocompatible sulfhydryl cotton fiber-based sorbents by “thiol-ene” click chemistry for biological analysis. *ACS Applied Materials & Interfaces, 6*(20), 17857–17864. https://doi.org/10.1021/am505876b.

He, X. M., Chen, X., Yuan, B. F., & Feng, Y. Q. (2017). Graft modification of cotton with phosphate group and its application to the enrichment of phosphopeptides. *Journal of Chromatography A, 1484*, 49–57. https://doi.org/10.1016/j.chroma.2017.01.020.

Herniou--Julien, C., Mendieta, J. R., & Gutiérrez, T. J. (2019). Characterization of biodegradable/non-compostable films made from cellulose acetate/corn starch blends processed under reactive extrusion conditions. *Food Hydrocolloids, 89*, 67–79. https://doi.org/10.1016/j.foodhyd.2018.10.024.

Hong, H. J., Lim, J. S., Hwang, J. Y., Kim, M., Jeong, H. S., & Park, M. S. (2018). Carboxymethlyated cellulose nanofibrils (CMCNFs) embedded in polyurethane foam as a modular adsorbent of heavy metal ions. *Carbohydrate Polymers, 195*, 136–142. https://doi.org/10.1016/j.carbpol.2018.04.081.

Jackson, J. K., Letchford, K., Wasserman, B. Z., Ye, L., Hamad, W. Y., & Burt, H. M. (2011). The use of nanocrystalline cellulose for the binding and controlled release of drugs. *International Journal of Nanomedicine, 6*, 321–330. https://doi.org/10.2147/ijn.s16749.

Jin, L., Li, W., Xu, Q., & Sun, Q. (2015). Amino-functionalized nanocrystalline cellulose as an adsorbent for anionic dyes. *Cellulose, 22*(4), 2443–2456. https://doi.org/10.1007/s10570-015-0649-4.

Kayaci, F., Aytac, Z., & Uyar, T. (2013). Surface modification of electrospun polyester nanofibers with cyclodextrin polymer for the removal of phenanthrene from aqueous solution. *Journal of Hazardous Materials, 261*, 286–294. https://doi.org/10.1016/j.jhazmat.2013.07.041.

Kim, Y. H., & Sun, G. (2001). Durable antimicrobial finishing of nylon fabrics with acid dyes and a quaternary ammonium salt. *Textile Research Journal, 71*(4), 318–323. https://doi.org/10.1177/004051750107100407.

Kim, Y. H., Choi, H. M., & Yoon, J. H. (1998). Synthesis of a quaternary ammonium derivative of chitosan and its application to a cotton antimicrobial finish. *Textile Research Journal, 68*(6), 428–434. https://doi.org/10.1177/004051759806800607.

Kobayashi, S., & Uyama, H. (2003). Biomacromolecules and bio-related macromolecules. *Macromolecular Chemistry and Physics, 204*(2), 235–256. https://doi.org/10.1002/macp.200290084.

Kwak, H. W., & Lee, K. H. (2018). Polyethylenimine-functionalized silk sericin beads for high-performance remediation of hexavalent chromium from aqueous solution. *Chemosphere, 207*, 507–516. https://doi.org/10.1016/j.chemosphere.2018.04.158.

Lee, M. Y., Yang, J. A., Jung, H. S., Beack, S., Choi, J. E., Hur, W., Koo, H., Kim, K., Yoon, S. K., & Hahn, S. K. (2012). Hyaluronic acid-gold nanoparticle/interferon α complex for targeted treatment of hepatitis C virus infection. *ACS Nano, 6*(11), 9522–9531. https://doi.org/10.1021/nn302538y.

Liu, C. Y., & Huang, C. J. (2016). Functionalization of polydopamine via the aza-michael reaction for antimicrobial interfaces. *Langmuir, 32*(19), 5019–5028. https://doi.org/10.1021/acs.langmuir.6b00990.

Makvandi, P., Ghaemy, M., Ghadiri, A. A., & Mohseni, M. (2015). Photocurable, antimicrobial quaternary ammonium-modified nanosilica. *Journal of Dental Research, 94*(10), 1401–1407. https://doi.org/10.1177/0022034515599973.

Makvandi, P., Ghaemy, M., & Mohseni, M. (2016). Synthesis and characterization of photo-curable bis-quaternary ammonium dimethacrylate with antimicrobial activity for dental restoration materials. *European Polymer Journal, 74*, 81–90. https://doi.org/10.1016/j.eurpolymj.2015.11.011.

Makvandi, P., Esposito Corcione, C., Paladini, F., Gallo, A. L., Montagna, F., Jamaledin, R., Pollini, M., & Maffezzoli, A. (2018a). Antimicrobial modified hydroxyapatite composite dental bite by stereolithography. *Polymers for Advanced Technologies, 29*(1), 364–371. https://doi.org/10.1002/pat.4123.

Makvandi, P., Jamaledin, R., Jabbari, M., Nikfarjam, N., & Borzacchiello, A. (2018b). Antibacterial quaternary ammonium compounds in dental materials: A systematic review. *Dental Materials, 34*(6), 851–867. https://doi.org/10.1016/j.dental.2018.03.014.

Makvandi, P., Ali, G. W., Della Sala, F., Abdel-Fattah, W. I., & Borzacchiello, A. (2019a). Biosynthesis and characterization of antibacterial thermosensitive hydrogels based on corn silk extract, hyaluronic acid and nanosilver for potential wound healing. *Carbohydrate Polymers, 223*, 115023. https://doi.org/10.1016/j.carbpol.2019.115023.

Makvandi, P., Ali, G. W., Della Sala, F., Abdel-Fattah, W. I., & Borzacchiello, A. (2019b). Hyaluronic acid/corn silk extract based injectable nanocomposite: A biomimetic antibacterial scaffold for bone tissue regeneration. *Materials Science and Engineering: C, 107*, 110195. https://doi.org/10.1016/j.msec.2019.110195.

Makvandi, P., Ting Gu, J., Zare, E. N., Ashtari, K., Moeini, A., Tay, F. R., & Niu, L.-N. (2019c). Polymeric and inorganic nanoscopical antimicrobial fillers in dentistry. *Acta Biomaterialia, 101*, 69–101. https://doi.org/10.1016/j.actbio.2019.09.025.

Mayol, L., Biondi, M., Russo, L., Malle, B. M., Schwach-Abdellaoui, K., & Borzacchiello, A. (2014). Amphiphilic hyaluronic acid derivatives toward the design of micelles for the sustained delivery of hydrophobic drugs. *Carbohydrate Polymers, 102*, 110–116. https://doi.org/10.1016/j.carbpol.2013.11.003.

Monier, M., & Abdel-Latif, D. A. (2013). Modification and characterization of PET fibers for fast removal of Hg(II), Cu(II) and Co(II) metal ions from aqueous solutions. *Journal of Hazardous Materials, 250*, 122–130. https://doi.org/10.1016/j.jhazmat.2013.01.056.

Nafee, N., Taetz, S., Schneider, M., Schaefer, U. F., & Lehr, C. M. (2007). Chitosan-coated PLGA nanoparticles for DNA/RNA delivery: Effect of the formulation parameters on complexation and transfection of antisense oligonucleotides. *Nanomedicine: Nanotechnology, Biology and Medicine, 3*(3), 173–183. https://doi.org/10.1016/j.nano.2007.03.006.

Park, J., Fong, P. M., Lu, J., Russell, K. S., Booth, C. J., Saltzman, W. M., & Fahmy, T. M. (2009). PEGylated PLGA nanoparticles for the improved delivery of doxorubicin. *Nanomedicine: Nanotechnology, Biology and Medicine, 5*(4), 410–418. https://doi.org/10.1016/j.nano.2009.02.002.

Pearson, H. A., & Urban, M. W. (2014). Simple click reactions on polymer surfaces leading to antimicrobial behavior. *Journal of Materials Chemistry B, 2*(15), 2084–2087. https://doi.org/10.1039/c3tb21865a.

Pei, A., Butchosa, N., Berglund, L. A., & Zhou, Q. (2013). Surface quaternized cellulose nanofibrils with high water absorbency and adsorption capacity for anionic dyes. *Soft Matter, 9*(6), 2047–2055. https://doi.org/10.1039/c2sm27344f.

Pour, Z. S., Makvandi, P., & Ghaemy, M. (2015). Performance properties and antibacterial activity of crosslinked films of quaternary ammonium modified starch and poly(vinyl alcohol). *International Journal of Biological Macromolecules, 80*, 596–604. https://doi.org/10.1016/j.ijbiomac.2015.07.008.

Qiao, H., Zhou, Y., Yu, F., Wang, E., Min, Y., Huang, Q., Pang, L., & Ma, T. (2015). Effective removal of cationic dyes using carboxylate-functionalized cellulose nanocrystals. *Chemosphere, 141*, 297–303. https://doi.org/10.1016/j.chemosphere.2015.07.078.

Ram, B., & Chauhan, G. S. (2018). New spherical nanocellulose and thiol-based adsorbent for rapid and selective removal of mercuric ions. *Chemical Engineering Journal, 331*, 587–596. https://doi.org/10.1016/j.cej.2017.08.128.

Richey, T., Iwata, H., Oowaki, H., Uchida, E., Matsuda, S., & Ikada, Y. (2000). Surface modification of polyethylene balloon catheters for local drug delivery. *Biomaterials, 21*(10), 1057–1065. https://doi.org/10.1016/s0142-9612(99)00281-1.

Selkälä, T., Suopajärvi, T., Sirviö, J. A., Luukkonen, T., Lorite, G. S., Kalliola, S., Sillanpää, M., & Liimatainen, H. (2018). Rapid uptake of pharmaceutical salbutamol from aqueous solutions with anionic cellulose nanofibrils: The importance of pH and colloidal stability in the interaction with ionizable pollutants. *Chemical Engineering Journal, 350*, 378–385. https://doi.org/10.1016/j.cej.2018.05.163.

Sheikhi, A., Safari, S., Yang, H., & van de Ven, T. G. (2015). Copper removal using electrosterically stabilized nanocrystalline cellulose. *ACS Applied Materials & Interfaces, 7*(21), 11301–11308. https://doi.org/10.1021/acsami.5b01619.

Sirviö, J. A., Hasa, T., Leiviskä, T., Liimatainen, H., & Hormi, O. (2016). Bisphosphonate nanocellulose in the removal of vanadium (V) from water. *Cellulose, 23*(1), 689–697. https://doi.org/10.1007/s10570-015-0819-4.

Srivastava, S., Kardam, A., & Raj, K. R. (2012). Nanotech reinforcement onto cellulosic fibers: Green remediation of toxic metals. *International Journal of Green Nanotechnology, 4*(1), 46–53. https://doi.org/10.1080/19430892.2012.654744.

Sumerlin, B. S., Tsarevsky, N. V., Louche, G., Lee, R. Y., & Matyjaszewski, K. (2005). Highly efficient "click" functionalization of poly (3-azidopropyl methacrylate) prepared by ATRP. *Macromolecules, 38*(18), 7540–7545. https://doi.org/10.1021/ma0511245.

Sun, G., Xu, X., Bickett, J. R., & Williams, J. F. (2001). Durable and regenerable antibacterial finishing of fabrics with a new hydantoin derivative. *Industrial & Engineering Chemistry Research, 40*(4), 1016–1021. https://doi.org/10.1021/ie000657t.

Tountas, M., Georgiadou, D. G., Zeniou, A., Seintis, K., Soultati, A., Polydorou, E., Gardelis, S., Douvas, A. M., Speliotis, T., Tsikritzis, D., Kennou, S., Fakis, M., Gogolides, E., Tsoukalas, D., Argitis, P., & Vasilopoulou, M. (2018). Plasma induced degradation and surface electronic structure modification of poly(3-hexylthiophene) films. *Polymer Degradation and Stability, 149*, 162–172. https://doi.org/10.1016/j.polymdegradstab.2017.12.010.

Tripathi, B. P., Dubey, N. C., & Stamm, M. (2013). Functional polyelectrolyte multilayer membranes for water purification applications. *Journal of Hazardous Materials, 252*, 401–412. https://doi.org/10.1016/j.jhazmat.2013.02.052.

Tsarevsky, N. V., Bencherif, S. A., & Matyjaszewski, K. (2007). Graft copolymers by a combination of ATRP and two different consecutive click reactions. *Macromolecules, 40*(13), 4439–4445. https://doi.org/10.1021/ma070705m.

Van Camp, W., Germonpré, V., Mespouille, L., Dubois, P., Goethals, E. J., & Du Prez, F. E. (2007). New poly (acrylic acid) containing segmented copolymer structures by combination of "click" chemistry and atom transfer radical polymerization. *Reactive and Functional Polymers, 67*(11), 1168–1180. https://doi.org/10.1016/j.reactfunctpolym.2007.07.004.

Wang, D. (2019). A critical review of cellulose-based nanomaterials for water purification in industrial processes. *Cellulose, 26*(2), 687–701. https://doi.org/10.1007/s10570-018-2143-2.

Yang, J. S., Xie, Y. J., & He, W. (2011). Research progress on chemical modification of alginate: A review. *Carbohydrate Polymers, 84*(1), 33–39. https://doi.org/10.1016/j.carbpol.2010.11.048.

Yang, H., Alam, M. N., & van de Ven, T. G. (2013). Highly charged nanocrystalline cellulose and dicarboxylated cellulose from periodate and chlorite oxidized cellulose fibers. *Cellulose, 20*(4), 1865–1875. https://doi.org/10.1007/s10570-013-9966-7.

Ye, S., Jiang, L., Wu, J., Su, C., Huang, C., Liu, X., & Shao, W. (2018). Flexible amoxicillin-grafted bacterial cellulose sponges for wound dressing: In vitro and in vivo evaluation. *ACS Applied Materials & Interfaces, 10*(6), 5862–5870. https://doi.org/10.1021/acsami.7b16680.

Yu, X., Tong, S., Ge, M., Wu, L., Zuo, J., Cao, C., & Song, W. (2013). Adsorption of heavy metal ions from aqueous solution by carboxylated cellulose nanocrystals. *Journal of Environmental Sciences, 25*(5), 933–943. https://doi.org/10.1016/S1001-0742(12)60145-4.

Zare, E. N., Makvandi, P., Ashtari, B., Rossi, F., Motahari, A., & Perale, G. (2019a). Progress in conductive polyaniline-based nanocomposites for biomedical applications: A review. *Journal of Medicinal Chemistry, 63*, 1–22. https://doi.org/10.1021/acs.jmedchem.9b00803.

Zare, E. N., Makvandi, P., & Tay, F. R. (2019b). Recent progress in the industrial and biomedical applications of tragacanth gum. *Carbohydrate Polymers, 212*, 450–467. https://doi.org/10.1016/j.carbpol.2019.02.076.

Zarrintaj, P., Jouyandeh, M., Ganjali, M. R., Hadavand, B. S., Mozafari, M., Sheiko, S. S., Vatankhah-Varnoosfaderani, M., Gutiérrez, T. J., & Saeb, M. R. (2019). Thermo-sensitive polymers in medicine: A review. *European Polymer Journal, 117*, 402–423. https://doi.org/10.1016/j.eurpolymj.2019.05.024.

Zhan, J., Wang, L., Zhu, Y., Gao, H., Chen, Y., Chen, J., Jia, Y., He, J., Fang, Z., Zhu, Y., Mao, C., Ren, L., & Wang, Y. (2018). Temperature-controlled reversible exposure and hiding of antimicrobial peptides on an implant for killing bacteria at room temperature and improving biocompatibility in vivo. *ACS Applied Materials & Interfaces, 10*(42), 35830–35837. https://doi.org/10.1021/acsami.8b14534.

Zhang, X., Zhao, J., Cheng, L., Lu, C., Wang, Y., He, X., & Zhang, W. (2014). Acrylic acid grafted and acrylic acid/sodium humate grafted bamboo cellulose nanofibers for Cu^{2+} adsorption. *RSC Advances, 4*(98), 55195–55201. https://doi.org/10.1039/c4ra08307e.

Chapter 4
Polymer Interface Reactions

Michael Cordin, Judith R. Büttler, Thomas Bechtold, and Tung Pham

Abstract In recent decades, the functionalization and modification of polymers has been extensively investigated in order to improve the compatibilization of immiscible polymers in multiphase systems. Strengthening the interface increases the phase stability, reduces coalescence and phase separation. The underlying mechanisms play a crucial role in the control of the polymer interfaces, e.g. *in-situ* formation of copolymers acting as phase compatibilizer, reduction of interfacial tension, thus favoring the diffusion of a polymer into the other phase. Among others, the interface reaction is an efficient method to tailor the polymer interface, as well as to improve the phase bonding between polymer matrixes and reinforcing fibers, typically in polymer composites. The objective of this chapter was to review the recent advances in polymer interface reactions and the characterization of polymer interfaces. In a selected polymer system, traditional techniques such as shear lab test and rheological investigation, but also most advanced techniques, such as high-lateral resolved infrared spectroscopy coupled with atomic force microscopy (nanoIR-AFM) to characterize the polymer interface, were discussed.

Keywords Compatibilization · Functionalization · Interface reaction · Nano-scale analysis

4.1 Introduction

The development of high-performance polymeric materials in recent decades has been driven by a new design, synthesis and functionalization to create new polymer structures, but also very strongly by the combination of the desired properties of constituents in the multiphase system, such as polymer blends and composites. One

---

M. Cordin · J. R. Büttler · T. Bechtold · T. Pham (✉)
Research Institute of Textile Chemistry and Textile Physics, University of Innsbruck, Dornbirn, Austria
e-mail: tung.pham@uibk.ac.at

T. J. Gutiérrez (ed.), *Reactive and Functional Polymers Volume Four*,
https://doi.org/10.1007/978-3-030-52052-6_4

of the advantages of blends and composites is the flexibility in the design of the combination of an almost unlimited number of constituents with respect to the compositions and properties of the single components. Properties such as permeability, stiffness, surface hardness, toughness, are just a few of those mentioned here.

One of the most critical aspects in the design of multiphase polymeric systems is the interaction at the interface of the components, e.g. polymer/polymer interface, polymer/reinforcement material interface, etc. Since most polymers are thermodynamically immiscible, the research field in functionalization and modification of polymers has been extensively investigated in order to improve the compatibility of immiscible polymers in multiphase systems. Strengthening the interface increases the phase stability, reduces coalescence and phase separation. The underlying mechanisms play a crucial role in the control of the polymer interfaces, e.g. *in-situ* formation of copolymers acting as phase compatibilizer, reduction of interfacial tension, thus favoring the diffusion of a polymer into the other phase. Among others, the interface reaction is an efficient method to tailor the polymer interface, as well as to improve the phase bonding between polymer matrices and reinforcing fibers, typically in polymer composites.

In general, the miscibility of polymers depends on the free energy of mixture (ΔG_m) (Gibbs-Helmholtz equation – $\Delta G_m = \Delta H_m - T.\ \Delta S_m$) (Zarrintaj et al. 2019). Polymers are miscible if the ΔG_m is negative and the second derivation of the ΔG_m (in terms of the volume fraction of one of the components) has to be greater than zero. From the point of view of entropy, the polymer blend is always preferred, because this increases the disorder or randomness of the distribution of components in the new material formed, but because of the high molecular weight (Mw) of the polymers, the entropy contribution to ΔG_m is small and the question whether polymers are miscible or not is decided by the enthalpy of mixture (ΔH_m). The exact ΔH_m value is determined by the intermolecular forces between the different polymer molecules. If there are strong interactions between the components of the blend, then ΔH_m is negative, which means that the energy is released during the mixing due to an exothermic reaction. The energy released increases the entropy in the environment, and consequently, the mixing of the components occurs spontaneously. It is thus very important to improve the interaction between the polymer components, which occurs at the polymer/polymer interface (Fig. 4.1).

The interphase is the area between the two phases, and may have different properties compared to the bulk of the separated phases. The chemical interactions, the crystallinity, the melting temperature (T_m), the viscosity and other properties may be altered at the interphase.

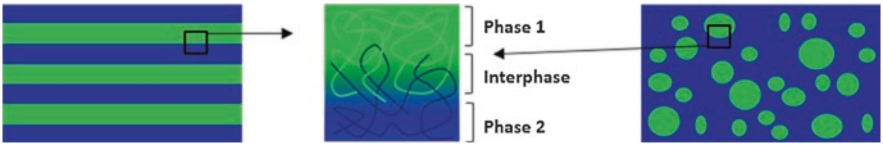

Fig. 4.1 Model of the interphase in a multilayer polymer system (left) and polymer blend (right)

If the interaction between the polymer components is low, miscibility is not possible. If there is a low interaction between the components, then more energy is needed to decrease the size of the phase separated particles, because the surface/volume ratio increases as the particle size decreases. Poorly mixed polymers have large phase separated polymer particles, and consequently, show poor mechanical properties. There are few polymers pairs with strong intermolecular interactions, which can form a homogenous single phase, but such polymer combinations are normally the exception and the most polymer combination need special strategies to form blends with good mechanical properties to be attractive for commercial applications.

In general, the following general strategies are applied to strengthen the interface:

- Chemical interface reactions,
- Reduction of the interface tension by modifying the surfaces of the components,
- Adding a small amount of copolymers consisting of segments of both components, such as block copolymers.

All these techniques are often summarized under the term ‘compatibilization’ between phases in multiphase systems.

4.2 Chemical Interface Reactions

An effective method to improve the interface adhesion is reactive mixture, i.e. the combination of the physical mixture and the chemical interface reaction. The prerequisite for a reaction between the components is only possible, if the polymer molecules contain appropriate functional groups. These functional groups can already be present into the polymer molecule, such as alcohol, amine or carboxylic groups. Alternatively, the functional groups can be subsequently linked at the polymer molecule by specific reactions, often called grafting reactions onto polymers. The best-known grafting reaction is the attachment of maleic anhydride (MA) in the poly(propylene) (PP). Such modification not only improves the miscibility of polymer components, but can also improve the adhesion to other solid materials, e.g. to reinforcing fibers in composites to improve the mechanical properties. The chemical interface reaction during mixing is often called reactive compatibilization.

Reactive compatibilization is based on the reaction between functional groups, e.g. as end groups in polymers, synthesized by polycondensation or as grafted side groups. There are several typical compatibilization reactions which form covalent bonds across the polymer phase boundaries. The following functional groups can be used for the formation of covalent bonds:

Acyllactam and amine:

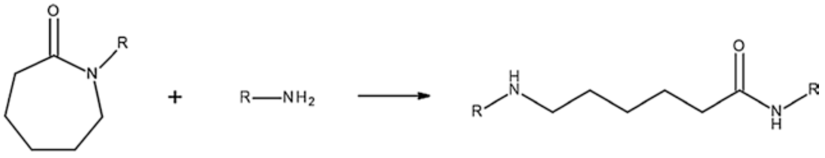

(4.1)

Amine and anhydride:

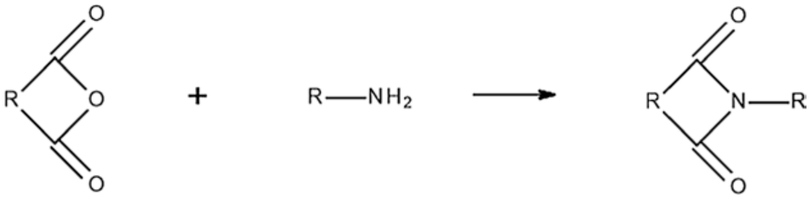

(4.2)

Anhydride and epoxy:

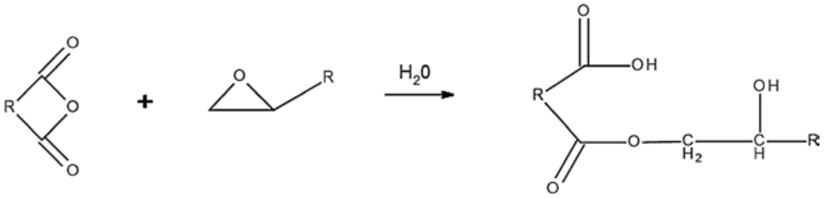

(4.3)

Carbodiimide and carboxylic acid:

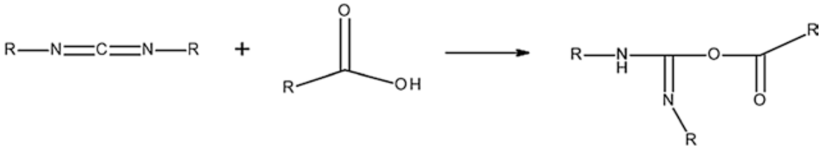

(4.4)

Carboxylic acid and isocyanate:

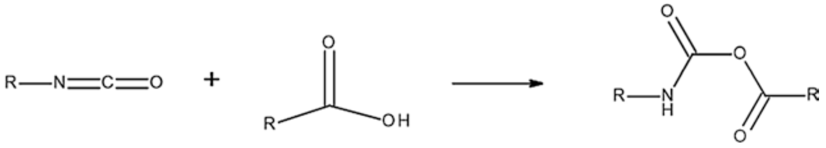

(4.5)

Carboxylic acid and oxazoline:

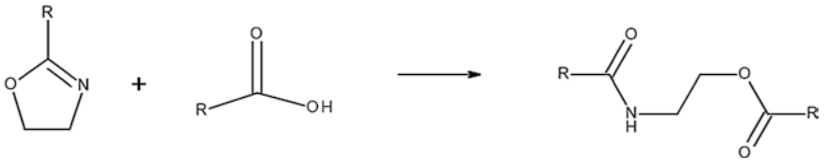

(4.6)

Among others, interface reactions based on glycidyl methacrylate (GMA) and MA have been investigated and used most in the literature. In flowing sections, these main interface reactions will be discussed in more details.

4.2.1 MA Based Reactions

4.2.1.1 Grafting of MA onto Polymers

In order to realize the interface reaction on MA base, the grafting step of MA onto polymer (often referred as functionalization) is often required, since the direct synthesis of MA as a comonomer is only possible under very special conditions and not yet is commercialized. If the other polymer component in the multiphase system has suitable functional groups, the formation of covalent bonds through the polymer/polymer interface is possible through the interface reaction by reacting with MA.

The functionalization of PP with MA can be done in solution, solid or molten state (Ko and Ning 2000; Shi et al. 2001; Garcia-Martinez et al. 2002). The MA grafting reactions are usually initiated by peroxide radicals under alkaline pH conditions. Peroxides form radicals by the cleavage of the oxygen-oxygen bond. These radicals then extract hydrogen from the polymer chain, which can react with MA (Eq. 4.7).

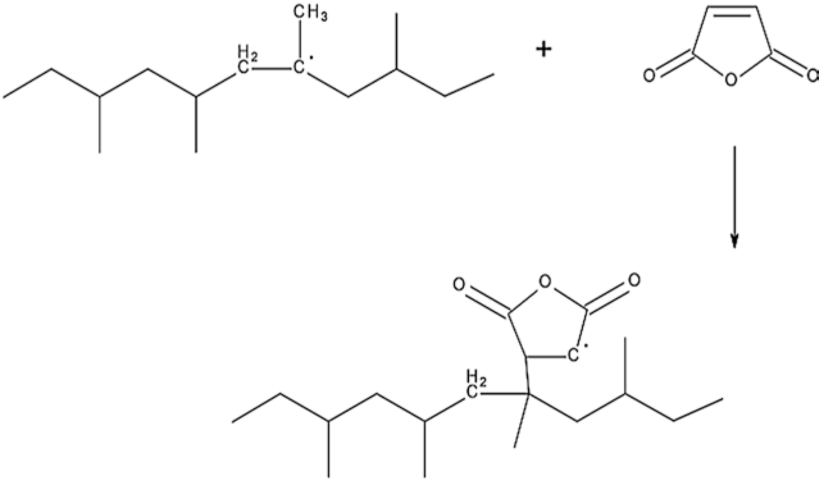

(4.7)

The MA grafting onto polyolefins was already explored in the 1950s (Van Duin 2003). The MA grafting onto PP is one of the most common systems for polymer modification (Sathe et al. 1994; Machado et al. 2000). Several studies can be found in the literature which discuss the reaction process and the mechanism for the MA grafting onto PP (Gaylord and Mishra 1983; Shi et al. 2001; Li et al. 2003).

The solvent used also has a significant influence on the reaction conversion. The stereospecificity of the polymer molecules and process conditions also influences the reaction conversion. A quantitative analysis on the number of functional carboxylic groups linked to the polymer molecule during the MA grafting reaction can be determined by titration. Often for these tests it is necessary to purify the grafted polymer to remove the residual MA (Bettini and Agnelli 2000). The higher the peroxide concentration, the more grafting occur (Garcia-Martinez et al. 2002). This relation is valid for low initial concentrations of MA. The conversion rate is optimal for low concentrations of MA in the media. For a high peroxide concentration in solution, a radical transfer to the solvent molecules can occur so that a part of the active grafting species can react with the solvent. So, a part of the MA reacts with the polymer and another part can react with the solvent. A higher level of grafting and conversion is produced by the reaction in the molten state without solvent. In addition, the grafting of atactic PP is higher than that of isotactic PP. The influence of the initial MA concentration on the grafting reaction yield depends on the peroxide concentration (Bettini and Agnelli 1999). The reaction conditions for the grafting are difficult to optimize, because the MA concentration, the reaction time and temperature, the reagent addition, the rotor speed and the type and concentration of peroxide sequence show an influence on the grafting efficiency. The reactive extrusion for grafting of MA onto PP, e.g. was investigated by Bettini and Agnelli (2002) using single extruder, twin-screw extruders and torque rheometer.

The solid-state MA grafting onto PP can also be carried out in a ball mill, which provides a higher degree of grafting and alleviates the degradation of the PP (Qiu et al. 2005; Qiu and Hirotsu 2005). The amount of reacted MA can be increased by the presence of styrene during the grafting reaction (Bettini and Ruvolo Filho 2007). A possible explanation is the activation of the MA double bond, which increases the grafting efficiency and reduces chain cleavage, because styrene is an electron donating substance. A similar effect was also reported by Li et al. (2001) for styrene on the reactivity of MA in the melt free radical-grafting reaction. The photoinitiated MA grafting onto PP can also be carried out in the presence of benzophenone as initiator (Pan et al. 2004). In this sense, Pan et al. (2004) observed a high level of grafting. Unlike the peroxide-initiated grafting, the photo-assisted grafting is produced without a decrease in the conversion as the monomer concentration increases. There are many different possible reaction pathways between peroxide radicals, polymer and MA as reported in the literature. A good summary and overview was provided by Oromiehie et al. (2014).

The grafting is always associated with a decrease in Mw of the polymer caused by side reactions (De Roover et al. 1995). De Roover et al. (1995) also demonstrated that the grafting reaction is limited by diffusion, while the crosslinking reactions is limited the amount of initiator that can be used (Ganzeveld and Janssen 1992). Typical side reaction are ß-chain scission and termination by combination and disproportionation (Abacha and Fellahi 2005). The grafting mechanism of MA onto PP was also investigated by Zhu et al. (2003) *via* Monte Carlo Simulation. These authors found that at a lower monomer concentration, the MA is grafted mainly onto the radical chain ends arising from ß-chain scission, while at a higher monomer concentration, the MA is grafted mainly onto the tertiary carbons of the polymer.

The success of the grafting reaction can be confirmed by Fourier transform infrared (FTIR) spectroscopy or titration. An investigation by ^{13}C-nuclear magnetic resonance (NMR) spectroscopy can also be carried out to test the presence of MA after grafting (Heinen et al. 1996). The presence of grafted MA also influences the crystallization behavior (Seo et al. 2000). Following Seo et al. (2000) the half-crystallization times of PP-*g*-MA increases with the crystallization temperature, but increases more rapidly for pure PP than for PP-*g*-MA, while Zhang et al. (2005) investigated the influence of the initial MA content on the grafting efficiency onto PP, and found that the Mw decreased with increasing MA content, because ß-scission occurred more widely after MA is attached to the tertiary carbon (Eq. 4.8). The MA grafting onto PP *via* an ene reaction can be promoted by $SnCl_2.2H_2O$ and Lewis acids, which are efficient catalysts for ene reactions (Sclavons et al. 2005).

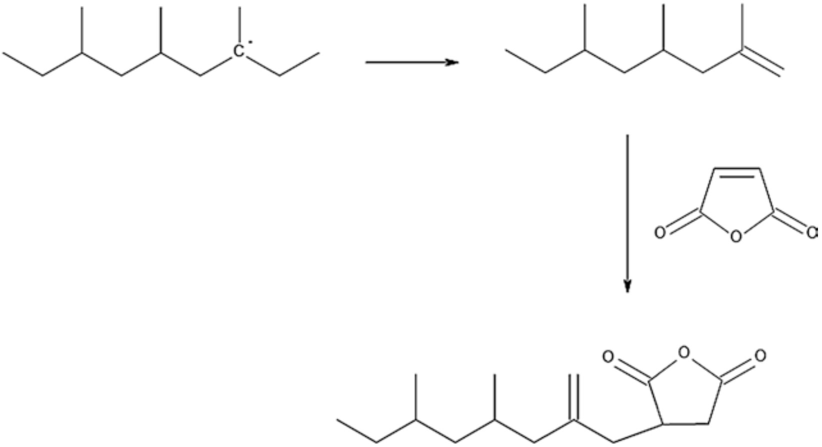

(4.8)

In addition to the MA grafting onto PP, many other studies have studied grafting onto (PE) poly(ethylene) (PE) (Gabara and Porejko 1967; Porejko et al. 1967a). A similar reaction mechanism was proposed by Gabara and Porejko (1967), Porejko et al. (1967b) and Li et al. (2003) for the MA grafting onto PE and PP. In order to minimize the crosslinking reaction of PE (different compared to PP) caused by free radicals, Gaylord and Mehta (1988) and Gaylord et al. (1989) added an electron donor. For example, Samay et al. (1995) investigated the influence of different comonomers (styrene) to increase the MA grafting efficiency onto PE. In contrast, Clark et al. (2001) reported that the grafting of MA onto PE cannot be improved by the presence of styrene, at least for the concentration used of the reagents in the described experiments. Martínez et al. (2004) also investigated the grafting reaction of MA initiated by ultraviolet (UV) radiation in the solid state. The irradiation of PE in the presence of oxygen formed hydroperoxide groups, which can then react further with a polymer radical to form organic peroxides. Finally, these peroxides form polymer radicals, which can induce grafting reactions with MA. The influence of solvent on the reaction was also investigated by Priola et al. (1994) for low-density PE (LDPE).

In the case of the copolymers, the structure of copolyolefin has influenced the MA grafting reaction (Machado et al. 2001). Grigoryeva and Karger-Kocsis (2000) showed that in ethylene-propylene copolymer, the MA graft content is higher, when the propene content less than 50%. A similar polymer system was investigated Grigoryeva and Karger-Kocsis (2000) with ethylene-propylene-diene terpolymer (EPDM). MA can also be grafted onto poly(L-lactic acid) (PLLA). In this type of system, Hwang et al. (2012) found a slight increase in Mw, possibly due to the crosslinking reaction. The crosslinking can even be improved by adding a certain amount of styrene (Ma et al. 2014). Polystyrene (PS) can also be grafted by MA (Li et al. 2002) and if poly(ethylene-*co*-*p*-methylstyrene) and poly(propylene-*co*-*p*-methylstyrene) are used (Lu and Chung 2000), then the grafting is performed selectively at the *p*-methyl group of the methylstyrene. In addition, Wu et al. (1993) successfully grafted MA onto (styrene-*b*-(ethylene-*co*-butylene)-*b*-styrene) (SEBS) triblock copolymer using xylene as solvent, as well as acrylonitrile-butadiene-styrene (ABS) terpolymer has been grafted (Qi et al. 2003; Rao et al. 2008). Different types of rubber can also be used for MA grafting. Some examples are EPDM rubber (Oostenbrink and Gaymans 1992) and natural rubber (NR) (Nakason et al. 2004; Saelao and Phinyocheep 2005). The grafting onto aromatic/aliphatic copolyester was also investigated by Mani et al. (1999) using ^{1}H-NMR, which indicates that the MA grafting is produced at the aliphatic dicarboxylic acid unit in the polymer molecule.

4.2.1.2 Interface Reaction with MA Grafted Polymers

The classic example for the interface reaction with the MA grafted polymer is the reactive compatibilization reaction between MA grafted PP and polyamide-6 (PA6). The *in-situ* reaction occurs between the terminated amine group of PA6 with the anhydride group of the functionalized PP (Eq. 4.9) (Mülhaupt et al. 1993). The reaction product is PP-*g*-PA6, which is an effective dispersing agent. The reaction between amino groups of poly(amide) (PA) and the anhydride group of MA grafted polymers can be quite complex (Van Duin et al. 1998).

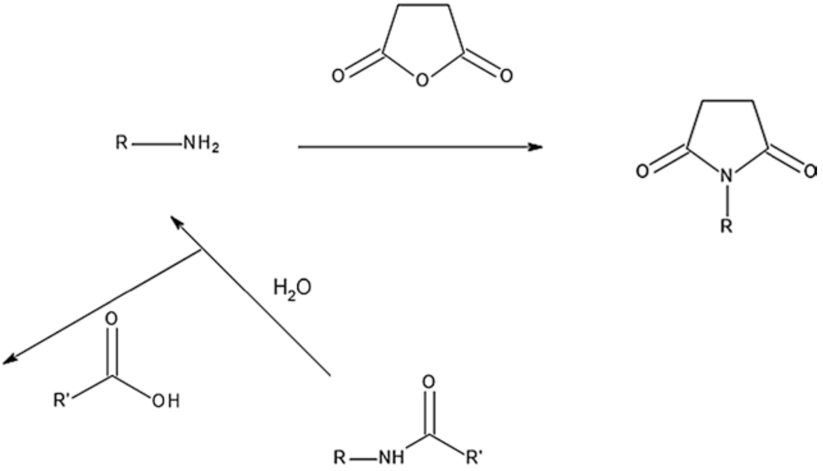

(4.9)

The amine end group of PA reacts with the anhydride group, thus forming an imide bond. The amide group in the PA chain can also react if there is an excess of anhydride available, but probably only after a hydrolysis by water to an amine and carboxylic acid, finally resulting in a chain scission of the PA and the formation of imide.

According to Mülhaupt et al. (1993), the increase in the volume fraction of the *in-situ* synthesized compatibilizer leads to a decrease in the average domain size of the minor phase of PA6 in the PP phase. The blend shows improved properties in terms of moisture absorption compared to pure PP. In addition, the addition of PA6 improved the dyeability, stiffness and toughness of the blend. Datta et al. (1995) also reported an increase in the dispersibility of PA6 in PP with the use of MA-*g*-PP due to the fact that the grafted copolymer has segments similar to the components of the polymers in the blend. MA-*g*-PP increased the interactions between the phases and influenced the viscosity of the PP/PA6 blend depending on the composition. In addition, there is an increase of the impact strength, maximum stress (σ_m) and strain at break (ε_b). The compatibilized blend shows a decrease of the melt flow rate, probably due to an increase in Mw by the formation of intermolecular bonds between the anhydride and amine groups. However, the formation of covalent bonds was also supported by the observation, that formic acid extract was very turbid for the compatibilized blend, in contrast to the non-treated blend. The decrease in solubility can be explained by the binding of non-polar PP onto the PA6 molecules. The successful formation of an imide bond between the MA-*g*-PP and the amino group of PA6 was evidenced by Roeder et al. (2002) using FTIR spectroscopy. These authors assigned three additional FTIR peaks to the formation of imide, which can be distinguished between the carbonyl vibration of an unreacted MA-*g*-PP molecule and that of an imide group, the first one was found at 1710 cm^{-1} and the second at 1764 cm^{-1}. The uncompatibilized blends absorbed more water, even more than expected due to the presence of PA6. A possible reason is the filling of voids in the interface with water. The compatibilized blends absorbed less water, probably due to the decrease in the concentration of free NH-groups. In addition, the interfacial adhesion was improved and reduced the formation of voids. In principle, the grafting of MA improved the adhesion between olefins to polar phases (Lin 1993). On the other hand, the grafting of too much polar groups can have a negative influence on the properties of the blend due to a greater moisture absorption capacity in the interface, which can cause more swelling of the material.

In the course of the reactive compatibilization with MA, the chemical kinetics and conversion, the interface adhesion and the viscosity are strongly influenced by the processing equipment and conditions. After reactive blending, PA shows a lower Mw due to the PA6 chain scission by reaction with MA, preferentially on the grafted PA6 chain (Van Duin et al. 1998).

The influence of MA-*g*-PP on the morphology of the PP/PA6 blend was observed by Kyu Kim et al. (1991). During the fracture process, pull-out of domains was observed, indicating a poor adhesion between the two components and scanning electron microscopy (SEM) micrographs show the disappearance of spherical particles in the PP/PA6-6/MA-*g*-PP blend due to the addition of the compatibilizer. Differential scanning calorimetry (DSC) measurements showed that the T_m of PP in a compatibilized PP/PA6 blends increased with the increase in PA6 content, probably due to the dissolution of grafted PP molecules. A positive deviation of the blend viscosity from the additive rule was explained by the stronger interactions between the components through the interface reaction. Another method to visualize the distribution of PA6 in the PP matrix was developed by Zhou et al. (2009) based on chemical mapping using attenuated total reflectance (ATR)-FTIR spectroscopy. In this regard, Zhou et al. (2009) was confirmed that the addition of PP-*g*-MA significantly improved the miscibility, while Seo and Ninh (2004) reported that the fracture toughness of the PP/PA6/PA6-*g*-PP blends depended on bonding temperature and time. The fracture toughness increased as the bonding time increased and finally shows a plateau for longer times for all tested bonding temperatures. The fracture toughness was investigated for temperature between 180 and 240 °C and the highest value for an annealing temperature of 220 °C was observed. Following Seo and Ninh (2004) there is an early increase in interfacial adhesion with the bonding time, probably due to a greater number of intermolecular reactions at the interface. The adhesion at the interface increased more rapidly with a higher bonding temperature due to a higher density of graft copolymer at the interface. For longer bonding times, the reaction rate decreased due to the low concentration of functional groups at the interface. The reason for the highest fracture toughness at the temperature of 220 °C was the interaction of the adhesion fracture at the interface and the cohesive failure between the polymer chains. The cohesive strength decreased with temperature due to a lower entanglement of the polymer chain.

The influence of MA-*g*-PP on the crystallization behavior of PP/PA6 blends was also investigated by Moon et al. (1994) using a blend composition of 70% PP and 30% PA6. These authors observed an increase in the crystallization temperature of the minor phase of PA6 compared to pure PA6 due to the molecular arrangement more ordered by the extrusion process as a possible explanation. By adding MA-*g*-PP to the blend system, the crystallization temperature of PA6 was degreased with a higher content of MA-*g*-PP. Through interface reaction between MA-*g*-PP and PA6, PA6-*g*-PP was formed *in-situ*, which can act as a polymeric diluent in the PA6 phase and reduce the crystallization temperature of PA6. Moon et al. (1994) also reported that the magnitude of the PP crystallization peak increased and that of the PA6 peak decreased up to an amount of MA-*g*-PP of 1.5%. Beyond the amount of MA-*g*-PP of 1.5%, there was even a disappearance of the crystallization peak of PA6 (at the crystallization temperature of pure PA6). This phenomenon could be explained by the concurrent crystallization of PA6 with PP due to the reduced particle size of PA6 in the PP matrix, since a larger particle has a higher probability to contain units of certain heterogeneity. The effect of reducing the particle size of the minor PA6 phase in PP was confirmed by our own research using atomic force microscopy (AFM) (Fig. 4.2).

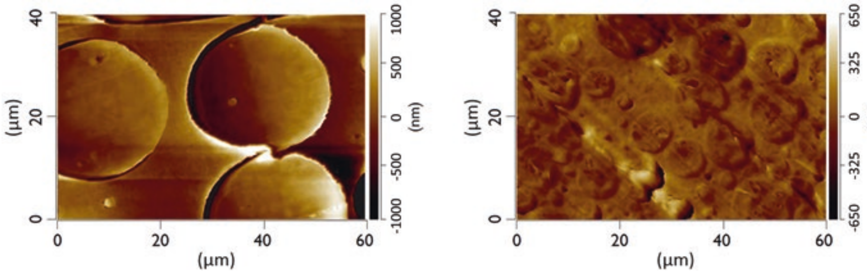

Fig. 4.2 AFM micrographs of PA6/PP (40:60) blends: without modification (left) and with modification with 0.13 wt.% MA based on total polymer content (right)

The preparation of bi-component fibers, consisting of PP shell and PA6 core was reported by Godshall et al. (2001) in order to combine the surface properties of PP with the mechanical properties of PA6. To improve the interface interaction, the *in-situ* reactive compatibilization was performed with MA-*g*-PP. Here, the compatibilization took place during the fiber spinning process. Most likely, the amide bond formed *in-situ* was transformed into an imide bond by cyclodehydration due to the high temperature during the melt spinning process. Abacha and Fellahi (2005) suggested that the performance of glass fiber-reinforced PP/PA6 composites can also be improved by the addition of MA-*g*-PP. Abacha and Fellahi (2005) made observations using SEM to test the hypothesis of improved interfacial adhesion as a reason for the improved mechanical properties.

Another approach was used by Teng et al. (2004) to synthesize PA6 *in-situ* during the PP/MA-*g*-PP reactive blend processing. The amino groups of PA6 formed *in-situ* can then react with MA-*g*-PP to yield PP-*g*-PA6, which suppress particle coalescence. Reactive compatibilization of PAs (PA6, PA6.6) with PP was also possible with MA-*g*-SEBS (Ohlsson et al. 1998).

According to Jiang et al. (2003) the reactive blending of PE with PA6 is possible by using MA-*g*-PE. In addition, Filippi et al. (2005) reported that the compatibilization efficiency of MA-*g*-PE depends on the structure and the molar mass of the used PE. These authors also found that MA-*g*-LDPE was not very effective compared to MA-*g*-high-density PE (MA-*g*-HDPE) in LDPE/PA6 systems. The reason could be in the miscibility of different PEs. While MA-*g*-LDPE does not accumulate much at the interface, a higher concentration of MA-*g*-HDPE was observed at the interface, which led to greater compatibilization effectiveness, and the compatibilization was also improved by a lower molar mass of the MA-*g*-HDPE substrate and when the succinic groups are distributed rather uniform along the HDPE chain (Eq. 4.10).

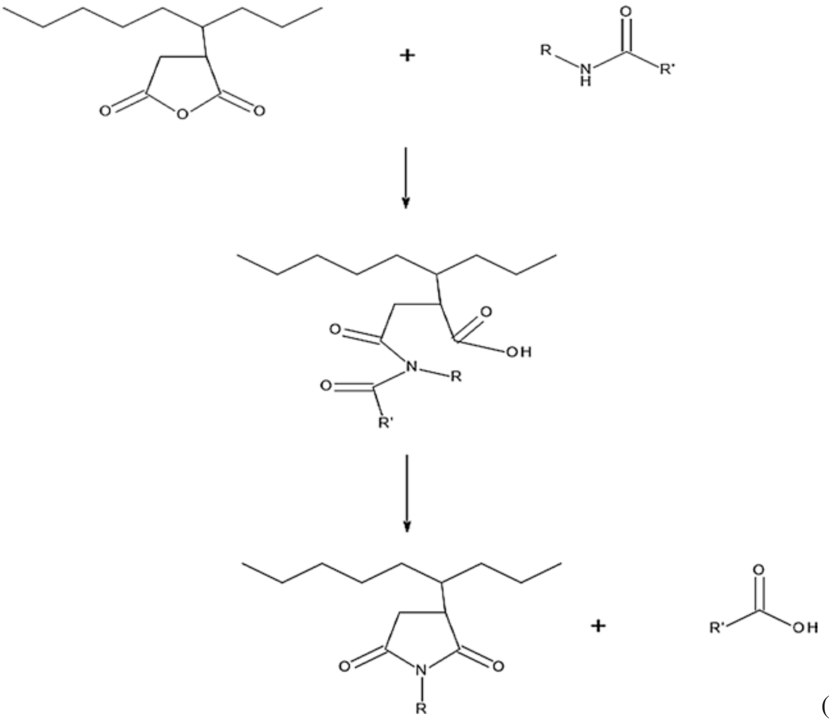

(4.10)

In another study, Kyu Kim et al. (1991) investigated the interface reaction between MA-*g*-PE and PA6 with respects to fracture morphology. SEM micrographs of fractured HDPE/PA6 surfaces showed a poor adhesion at the interface, indicated by the pull-out of the dispersed phase, while PE/PA6/MA-*g*-PE clearly showed a compatibilization effect, which was reflected by a reduced size of dispersed PA6 particles. Similar to the reported works on PP/PA6 systems, the compatibilization also influenced the T_m of the components in the blends due to the selective dissolution of the defective PA6 molecules. In addition, an increase in the steady shear viscosity was also observed, probably due to the increased adhesion at the interface between PE and PA6. A comparison of mechanical and tribological properties of HDPE/PA6 blends with and without interface reaction on MA base was conducted by Palabiyik and Bahadur (2000). Interestingly, although the compatibilizer improved the adhesion between the two phases, a weak boundary layer can also be introduced, which could explain the decrease in the σ_m in the investigated system.

Apart from vast studies with PAs in polyolefins (PP/PA and PE/PA), there are also other polymer systems which have been successfully compatibilized using MA interface reactions. Keeping this in view, Lim et al. (2002) investigated the compatibilization of MA-grafted syndiotactic PS (sPS) with PA6. The poor interfacial adhesion in a non-compatibilized system can be linked to the smooth and clear surface of the distributed domains of PA6 as observed by SEM. The addition of MA-*g*-sPS decreased the domain size and improved the Izod impact strength due to the improved interface adhesion.

The compatibilization effect by adding styrene-maleic anhydride (S-MA) and styrene-GMA (S-GMA) copolymers to a PS/PA6.6 blend due to the intermolecular reaction was reported by Chang and Hwu (1991). Here, S-GMA seemed to be more reactive than S-MA. The compatibilizer formed *in-situ* was not located exclusively in the interface, but was also distributed in both phases. The compatibilized blends showed a higher viscosity due to better miscibility and an increase in Mw due to the *in-situ* formation of the copolymer. The distribution of the compatibilizer in the two polymer components also altered the mechanical properties of these components, which led to a decreased toughness, although the interfacial adhesion was improved. Especially, the distribution of the brittle S-MA in the PA6.6 phase caused losses in toughness. Compatibility of PS with poly(urethane) (PU) is possible, e.g. with the use of S-MA as investigated by Cassu and Felisberti (2001). In case of the poly(methyl methacrylate) (PMMA)/PA6 blend, MA-PMMA copolymer was synthesized. The interface reaction with PA6 was confirmed by rheological measurements. An increase of the torque level of the rheometer was also observed by increasing the MA concentration in the copolymer, which was added to the PA6 blend.

The reactive compatibilization of HDPE with poly(ethylene terephthalate) (PET) was done by Lusinchi et al. (2001), starting from MA-grafting reaction onto HDPE in refluxing toluene without free-radical initiator in order to avoid crosslinking. Mechanical properties, such as σ_m and the ε_b were improved for a 60/40 blend of HDPE/PET with low amounts of MA. The compatibilized blends showed a better dispersion of the minor phase with a smaller domain size due to the improved interfacial adhesion.

Chiu and Hsiao (2006) carried out a successful compatibilization of PET/PP blends by using MA-grafted poly(ethylene-*co*-octene), meanwhile Carone et al. (2000) investigated the reactive compatibilization of the NR/PA6 system, finding that the non-maleated PA6/NR blend showed phase separation in the Molau test after 30 days, the MA-based interface reaction indicated the improved adhesion, which was also supported by the deceased particle size through investigation by transmission electron microscopy (TEM).

Interface reaction of poly(butylene terephthalate) (PBT) and ethylene-vinylacetate (EVA) copolymers was also realized by Kim et al. (2001b) using MA reaction. Before blending, EVA was modified by free radical MA grafting. PBT was then blended with the MA-*g*-EVA and the formation of PBT-*g*-EVA copolymer was produced by *in-situ* interfacial reaction. The reaction of MA-*g*-EVA with carboxylic and hydroxyl groups of PBT was confirmed by FTIR spectroscopy. Here, the PBT extracted from the compatibilized blend showed two peaks at 2923 and 2852 cm^{-1} due to the C-H stretch of the ethylene group of EVA. This demonstrated the *in-situ* reaction of MA-grafted EVA with the carboxyl and hydroxyl groups of PBT by the formation of PBT-*g*-EVA copolymer. Kim et al. (2001b) also observed that a higher dicumyl peroxide (DCP) concentration by MA grafting lead to a smaller particle size of EVA and the phase boundaries between PBT and EVA matrices become less clear, which indicated a better interfacial adhesion. This also resulted in higher impact fracture energy compared to the PBT/EVA blend. In a later study, Kim et al. (2003) reported on the lowest limit of EVA particle size of approx. 1.7 μm, regardless of the additional increase in the MA content. A possible explanation was the existence of an optimum concentration of PBT-*g*-EVA copolymer due to the limitation by the carboxyl and hydroxyl end groups of PBT.

The application of the classical MA-based interface reaction in biobased polymers was investigate by Rubino et al. (2012) for PLLA/starch blends. The PLLA/starch blend was melted and the grafting reaction with MA was initiated by dicumyl peroxide, which led to a covalent C-C bond between PLLA and MA. The reactive compatibilization occurred by the reaction between the anhydride group and a hydroxyl group of starch. Due to the reactive compatibilization effect, a reduction of the glass transition temperature (T_g) and T_m was also observed, as well as an improvement in the mechanical properties for blends with different PLLA contents, e.g. 90, 80 and 70%. A similar study was carried out by Zhang and Sun (2004) who investigated the influence of MA/initiator on the compatibilization effect in PLLA/starch blends. These authors found that the optimal MA/initiator ratio of 100:10 significantly improved the mechanical performance of the PLLA/starch blend.

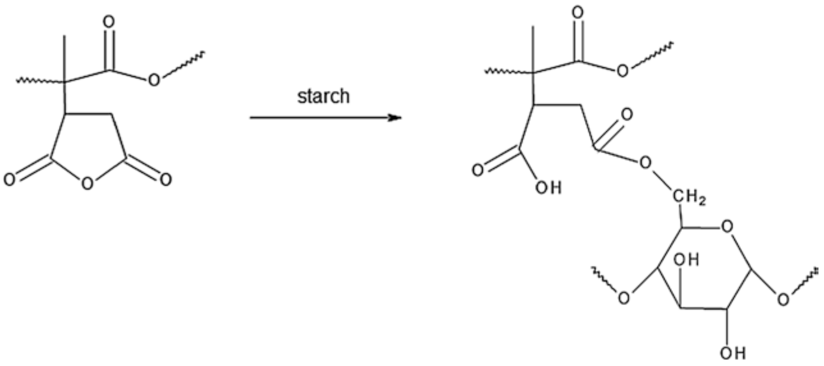

(4.11)

4.2.2 GMA Based Reactions

The second largest and most well investigated interface reaction is based on GMA. Similar to MA, GMA is often first grafted onto non-functionalized polymers before the interface reaction in multiphase polymer systems.

4.2.2.1 Grafting of GMA onto Polymers

GMA can be grafted by the melt free radical method onto ethylene-propylene-rubber (EPR) (Hu and Cartier 1999), PE (Cartier and Hu 1998b; Torres et al. 2001) and PP (Cartier and Hu 1998a). The grafting yield of GMA can be significantly increased by the addition of styrene (Eq. 4.12). The grafting mechanisms in different polymer systems are the same as reported for the reaction with PP. In these cases, the reaction rate and yield were lower, but can be increased by the addition of a second suitable monomer, such as styrene.

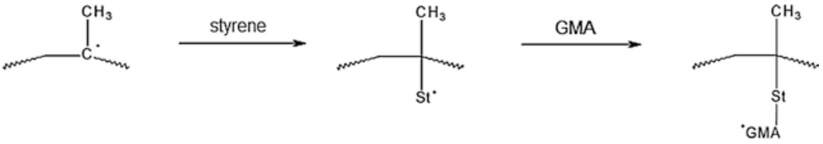

(4.12)

Cartier and Hu (1998a) suggested that the styrene molecule reacts more rapidly with the PP radical and then, in a second step, the GMA reacts with the new formed PP-styrene radical. The styryl macroradical is more stable than the PP radical, which probably increases the grafting yield of GMA and reduces the degradation of PP at the same time.

A similar effect was also reported by Sun et al. (1995) and Chen et al. (1996) who indicated that the extent of GMA grafting onto PP can be influenced by the monomer and initiator concentration and the reaction time, but is often accompanied by a ß-scission of the PP molecule. Alternatively, a higher degree in GMA grafting onto PP could be realized using acrylamide as initiator (Huang and Liu 1998). The thermally decomposed free radicals react preferentially with the GMA molecules instead of PP.

The GMA grafting onto powdered PP has also been possible by solid-phase reaction as follows: A liquid mixture of GMA, benzoyl peroxide and toluene were first absorbed by the PP powder and then the reaction was carried out in a preheated Haake mixer (Pan et al. 1997). Poly(lactic acid) (PLA) can also be grafted by GMA, using benzoyl peroxide as an initiator using the following methodology: in the first step, the radical captures a hydrogen atom in α position next to the ester group of the PLA molecule, and then the macroradical react with GMA to form GMA-*g*-PLA (Eq. 4.13) (Liu et al. 2012).

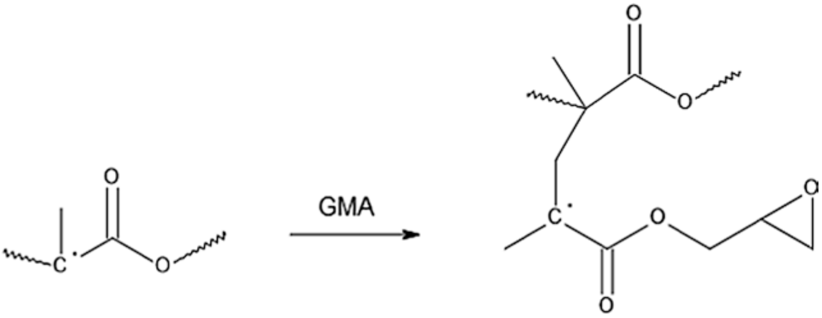

(4.13)

4.2.2.2 Interface Reaction with GMA Grafted Polymers

An interface reaction with GMA is based on the fact that the epoxy group of GMA can form covalent bonds with a series of functional groups, such as amine, carboxyl or hydroxyl groups. With this in mind, Wei et al. (2003, 2005) reported on the reactive compatibilization of GMA-*g*-LDPE with PA6. The epoxy group can react with the amine and carboxyl end groups of PA6 and the intermolecular reactions between the polymer molecules were detected indirectly by the increase in the mixing torque compared to the non-compatibilized blend. These authors also observed that the torque of PA6/GMA-*g*-LDPE blend (80:20) was five times greater than of the PA6/LDPE blend (80:20). If the amount of GMA-*g*-LDPE is increased further, a decrease of the torque was then observed indicating the completed reaction between the epoxy groups of GMA-*g*-LDPE and the amine and carboxyl groups of PA6 for a composition ratio close to 80:20. In addition, the compatibilized blends showed a better phase dispersion and the GMA-*g*-LDPE bonds with PA6 were confirmed by the Molau test, because the dissolution of the blend in formic acid led to a colloidal suspension of GMA-*g*-LDPE-*g*-PA6.

The immiscible PA6/poly(phenylene oxide) (PPO) system can be compatibilized using grafting and interface reaction with styrene-GMA (S-GMA) (Chiang and Chang 1996). In this sense, the epoxy group of the S-GMA molecule can react with the amino and carboxyl end group of PA6, but also with the hydroxyl group of PPO (Eq. 4.14). The *in-situ* formed S-GMA-*g*-PA6 was accumulated at the interface between the two polymers and had a strong compatibilization effect and it was also considered that a certain amount of S-GMA-*g*-PPO-*g*-PA6 was formed. The compatibility increased the interfacial adhesion, thus reducing the domain size. The mechanical properties of the blend, such as σ_m and Izod impact strength, were also significantly improved.

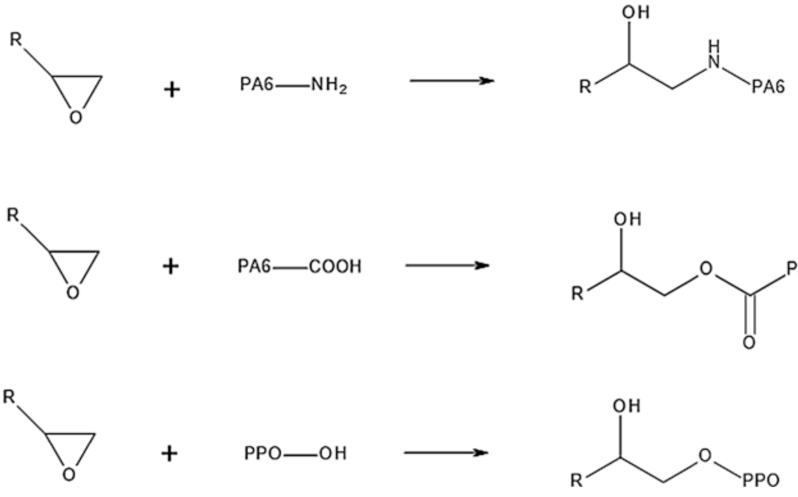

(4.14)

Reactive blending of PET with GMA-*g*-HDPE was investigated by Pazzagli and Pracella (2000). The end groups of the PET molecule could react with the epoxy group of GMA-*g*-PE, which was confirmed by the disappearance of a characteristic peak (910 cm^{-1}) in the FTIR spectrum. Due to the reactive blending, the phase dispersion and interfacial adhesion were significantly improved.

The compatibilization of PBT with GMA-modified PP was successfully carried out by Sun et al. (1996). Compared to other reactive species such as acrylic acid, GMA and MA, the best results were reported. The epoxy group of GMA can react with the carboxyl and hydroxyl groups of PBT. After the optimization of the processing conditions for the GMA grafting, the resulting PP/PBT blend (70:30) shows a 15- to 20-fold improvement in impact strength and ε_b compared to the non-compatibilized blend.

Blends of PET with GMA-grafted SEBS and styrene-*b*-(ethylene-*co*-propylene (SEPSEP) with different styrene content and different number of blocks in the polymer chain were investigated by Pracella and Chionna (2004). In the blends of PET with the grafted copolymers a better dispersion and an improved adhesion between the two phases were observed, resulting in a significant improvement in the ε_b values.

In another study, the interface reaction with GMA was applied by Kim et al. (2004) for PLA/LDPE system. The reactive compatibilization was produced by the interface reaction of epoxy groups in the GMA-*g*-PE molecule with carboxyl and hydroxyl groups at the chain ends of the PLA molecule. Additional peaks in the ^{1}H-NMR spectrum were a strong indication of a chemical reaction between PLA and the epoxy group of the GMA-*g*-PE molecule. Similarly, the compatibilization of PLA can also be achieved with poly(ethylene-*co*-octene) after GMA grafting. The possible interface reaction significantly improved the compatibility (Su et al. 2009).

In addition, PLA can also be blended with NR after GMA grafting (Juntuek et al. 2012). The polymer/polymer interface reaction was confirmed by FTIR measurements, thus showing that a characteristic IR band for carboxyl end groups of PLA at 3500 cm^{-1} disappears after the reaction with GMA-*g*-NR. SEM micrographs confirmed a better dispersion of NR in the PLA matrix due to the reactive blending, which led to improved ε_b and impact strength values.

Using the interface reaction between hydroxyl end group of the starch molecule and the epoxide group of GMA, the poly(caprolactone) (PCL) and the gelatinized starch was also compatibilized by reactive blending with GMA-*g*-PCL (Kim et al. 2001a).

4.3 Physical Interactions at Polymer Interface

Apart from the basic chemical interface reactions discussed in the previous section, physical interactions also strongly influence the polymer/polymer interface. Basically, if the interface adhesion (physical term) is strong, then the stress transfer between the two phases through the interface is effectively possible and results in good mechanical properties of the multiphase polymer systems. In addition to

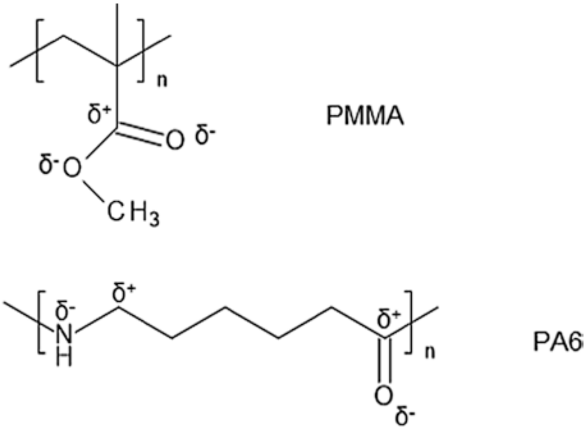

Fig. 4.3 General scheme of dipoles in PMMA and PA6. δ^+: positive partial charge and δ^-: negative partial charge

covalent bonds, the interface adhesion is strong, when the polymers are similar in interface adhesion and polarity often takes place through the acid-base reactions, the dipoles, donor-acceptor and ions interactions, or hydrogen bonding. Figure 4.3 shows relevant dipoles in the formulas of some polymers.

By extending multiphase systems beyond polymer/reinforcement (filler, fibers etc.) systems, the surface structure and the geometries of the reinforcements also show a strong contribution to the stability of the interface. Processing conditions such as pressure, shear forces, temperature, etc. also have an impact on the phase adhesion.

Physical interactions between the polymers are mainly based on the chain diffusion and entanglement and depend largely on the surface energy of the constituents. If the surface tensions are not adequate, the chain diffusion and entanglement of the polymer chains in the melted and solvated state is almost possible. If the surface energies are adequate with each other, the wetting occurs and then chain diffusion, entanglements and chemical reactions can take place (Bechtold and Pham 2019). The interfacial energy, chain diffusion and entanglement will be described below in more details:

4.3.1 Surface Energy

In multiphase systems, the surface energy is an important measure for the wettability of solid phases, such as fibers, films or textiles, by liquid phases such as polymers or sizing agents. Basically, molecules on the surface of the polymer have a higher energetic potential compared to the molecules in the bulk. Thermodynamically, molecules favor low energetic levels that can be achieved by interacting with adjacent molecules. However, on the surface, the molecules do not have similar molecules on one side for interactions, and therefore have a higher energetic level. This excess of energy is the surface energy (solids) or surface tension (fluids). Thus, for

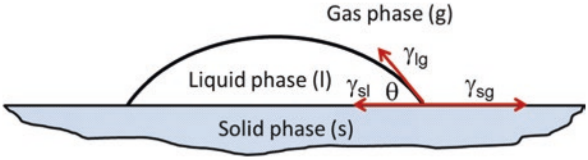

Fig. 4.4 Equilibrium state of wetting: compensation of the different surface tensions between solid/liquid/gas phase

the material it is energetically more favorable to have the smallest possible surface area with the surrounding phases. The energetic potential of the molecules on the surface results in an ability to interact with adjacent phases. There are different interaction forces contributing to the surface energy. Dispersion forces, on the one hand, are based on electrochemical interactions of weak van der Waals interactions between apolar molecules, resulting in weak attraction forces on the surface. Polar forces at the phase boundary, on the other hand, are caused by permanent electronegativity of covalent or ionic interactions in the molecules. These stronger forces ensure a higher polarity on the surface of the phase (Cherif 2011; Gutiérrez et al. 2018, 2019; Herniou-Julien et al. 2019).

The easiest way to obtain information about the surface energy of a solid polymer is to determine the contact angle of a liquid (e.g. water) on the surface. The amount of wetting taking place depends on the surface energies of the polymers. If the water contact angle (WCA – θ) is 180°, the solid is not moistened and the surface tension is high (Fig. 4.4). A WCA greater than 90° indicates that the solid is relatively hydrophobic and apolar, the wetting is low. The wetting is better if the WCA is less than 90°. This is the case with relatively hydrophilic and polar materials having a low surface energy. If the WCA is 0°, then the liquid wets the material completely (Elias 1997).

The precise determination of the surface energy of a solid is more complex. In fact, the surface energy is calculated by the interfacial energy between a solid and a liquid (γ_{sl}). In case the liquid resides as a drop on the solid surface, there is also interfacial tension between solid and gas (γ_{sg}) and between liquid and gas (γ_{lg}) (Elias 1997). The Young's equation describes the relationship of the contact angle (θ) with those interfacial tensions as follows (Bechtold and Pham 2019):

$$\gamma_{sg} = \gamma_{sl} + \gamma_{lg} \cos(\theta) \tag{4.15}$$

Experiments show that the contact angle is related to γ_{lg} by a straight-line equation (Eq. 4.16). This counts for values $\gamma_{lg} > \gamma_c$ (Zisman 1964).

$$\cos(\theta) = a - b\gamma_{lg} \tag{4.16}$$

γ_{lg} approaches γ_c when the contact angle approaches zero ($\cos(\theta) = 1$), the equation can be written as follows:

$$\cos(\theta) = 1 + b(\gamma_c - \gamma_{lv}) \tag{4.17}$$

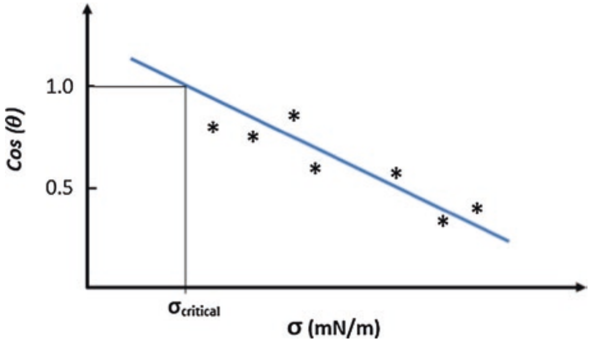

Fig. 4.5 Determination of the critical surface energy according to Zisman (1964)

The critical surface energy is the surface energy at which a liquid wets a solid totally. The critical surface energy (σ_{cr}) of a polymer is determined by the contact angles of different liquids (Elias 1997). Graphically, the surface tensions of different liquids can be plotted against the cosine of the contact angle. The solid is totally wetted if the WCA = 0°, giving cos(θ) = 1. The surface energy value at cos(θ) = 1, is the critical surface tension of a solid (Fig. 4.5).

The general formula for calculating the surface energy is as follows:

$$\sigma_{ls} = \sigma_l + \sigma_s - \left(interaction\,between\,phases\right) \tag{4.18}$$

σ_s is the surface energy of a solid and σ_l is the surface tension of a liquid. The difference between the models is the interpretation of the interactions responsible for the surface tensions of the separated phases and the components used for the calculation. The surface energy can be calculated by combining contact angle derived from a polar and an apolar liquid, e.g. water and diiodomethane.

4.3.2 *Interfacial Energy*

Work of adhesion (W_A) between two phases (solid/solid, solid/liquid, liquid/liquid) can be described by the Dupré's equation (Eq. 4.19). If one phase wets the other, the surface energies of both phases are released as follows: $\sigma_1 + \sigma_2$. For the formation of the interphase energy is used, called interfacial energy (σ_{12}) (Cherif 2011):

$$W_A = \sigma_1 + \sigma_2 - \sigma_{12} \tag{4.19}$$

The W_A is a measure of the strength of adhesion between two phases. This information is useful for adhesives, cleaning products, coatings and sizing agents. The W_A is necessary to separate phase 1 from phase 2. If a liquid wet a solid, the W_A can be determined by using the contact angle. Young related the W_A to the contact angle (derived from $\gamma_{sg} = \gamma_{sl} + \gamma_{lg}\cos(\theta)$ and $W_A = \sigma_1 + \sigma_2 - \sigma_{12}$), which leads to the Young-Dupré's equation (Habenicht 2009):

$$W_A = W_{ls} = \sigma_l \left(1 + \cos\theta\right) \tag{4.20}$$

However, the Young-Dupré's equation does not take into account the disperse and polar force fractions of the materials. Owens and Wendt (Cherif 2011) included those forces in the equation for interfacial energy (Eq. 4.21). Thus, the total surface energy is the sum of the disperse and the polar fractions.

$$\sigma = \sigma^P + \sigma^D \tag{4.21}$$

As for a second phase, the interfacial energy depends on disperse and polar fractions of the two phases. Owens and Wendt (Cherif 2011) described the interfacial energy for two immiscible phases that are in contact with each other: solid/solid, solid/liquid or liquid/liquid as follows:

$$\sigma_{12} = \sigma_1 + \sigma_2 - 2\left(\sqrt{\sigma_1^D \cdot \sigma_2^D} + \sqrt{\sigma_1^P \cdot \sigma_2^P}\right) \tag{4.22}$$

σ_{12}: Interfacial energy between phases 1 and 2.
σ_1: Surface energy of phase 1.
σ_2: Surface energy of phase 2.
σ_1^D : Dispersive proportion of surface energy of phase 1.
σ_2^D : Dispersive proportion of surface energy of phase 2.
σ_1^P : Polar proportion of surface energy of phase 1.
σ_2^P : Polar proportion of surface energy of phase 2.

Since there is disperse and polar interactions in surface energy, the adhesive strength (W_A) depends on whether there are similar adhesive forces (disperse or polar) in both phases. Including the disperse and polar forces of the interfacial energy of the Owens and Wendt's equation to Dupré's formula, then the following equation emerges (Eq. 4.23).

$$W_a = \sigma_1 + \sigma_2 - \sigma_1 - \sigma_2 + 2\left(\sqrt{\sigma_1^D \cdot \sigma_2^D} + \sqrt{\sigma_1^P \cdot \sigma_2^P}\right) = 2\left(\sqrt{\sigma_1^D \cdot \sigma_2^D} + \sqrt{\sigma_1^P \cdot \sigma_2^P}\right) \tag{4.23}$$

Taking the polymer/reinforcement system as an example. Figure 4.6 describes the correlation between adhesion behavior, surface energy and wetting.

Polar solids are easier to wet compared to apolar materials because the latter have more surface energy. The wetting increases if the solid has a lower surface energy than the liquid. Most polymers have a surface energy greater than water, thus water does not have a good wettability on polymers. In contrast, fats and oils have a higher surface energy than most polymers, and can wet the polymers (Elias 1997; Cherif 2011).

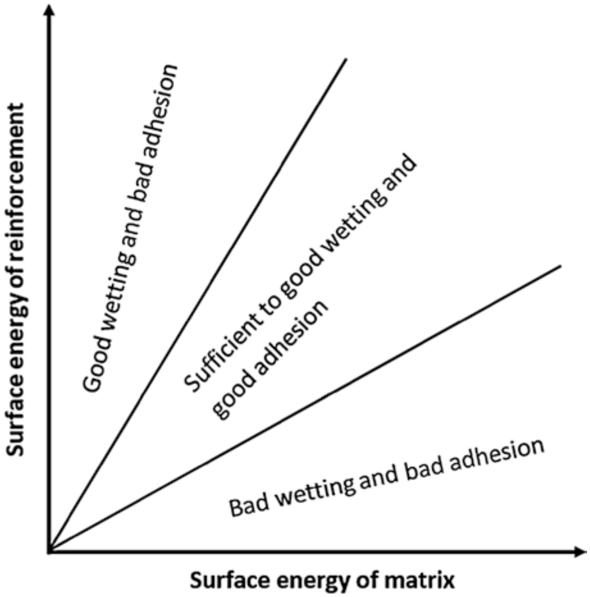

Fig. 4.6 Correlation between adhesion behavior, surface energy and wetting of composites. Data according to Cherif (2011)

4.3.3 Interfacial Diffusion and Entanglement of the Polymer Chain

At the interphase of two different melted or solvated polymers, diffusion and chain entanglements of the polymer molecules can take place, depending on the chemical and physical properties of the polymers and the processing conditions. Good diffusion and entanglements are favorable for good adhesion between the polymers.

The mobility of the polymer chains depends on the physical conditions of the environment. At temperatures beyond the T_g, the molecular motion is frozen. Above the T_g, the polymeric material softens or becomes rubbery due to the fact that the electrostatic interactions become less stable and the mobility of the polymer chain increases. The molecular mobility is greater above the T_m, where the thermoplastic polymers are in a viscous fluid state. The movement of the chain in a polymer melt or solution depends largely on the forces, such as extension, pressure and shear, under which the polymer is found. In general, the chains are oriented in the direction of the force (Elias 1997).

4.3.3.1 Brownian Motion

The development of the polymer diffusion theory began with the diffusion theory of small colloidal particles in a fluid. The diffusion of small colloidal particles (1 nm–10 μm) is caused by fast fluctuations of the surrounding molecules, which hit the particles randomly. This diffusion is diffusive motion, it is also known as

Brownian motion. The Einstein's relationship describes the Brownian motion (diffusion coefficient D—Eq. 4.24) as a constant force applied to a particle resulting in a constant velocity, counteracted by a frictional force caused by the fluid on the particle (frictional coefficient ζ), depending of the Boltzmann constant (k) and the temperature (T) (Rubinstein and Colby 2003):

$$D = \frac{kT}{\zeta} \tag{4.24}$$

The time (τ) a particle needs to diffuse the distance of its own size (R) is given by Eq. 4.25:

$$\tau \approx \frac{R^2}{D} \approx \frac{R^2 \zeta}{kT} \tag{4.25}$$

In this equation, the diffusion time (τ) is proportional to the friction coefficient (ζ).

4.3.3.2 Dynamics of Short Chain Polymers

For polymer melts and concentrated solutions made of short chain polymers (N < 200 monomeric units) having no entanglements, the Einstein's relationship about the Brownian motion is expanded by Rouse model. The Rouse model describes the melting dynamics of the polymer for short chain polymer. The polymer chains are represented as a linear series of spring-connected beads, schematically represented in Figure 4.7 (Kausch and Tirrell 1989; Lee 1991; Rubinstein and Colby 2003).

The Rouse diffusion coefficient (D_R) depends on the Rouse friction coefficient (ζ_R) and the number of beads (monomeric units, N). Using the Einstein's relationship, the D_R is determined by Eq. 4.26.

$$D_R = \frac{kT}{\zeta_R} = \frac{kT}{N\zeta} \tag{4.26}$$

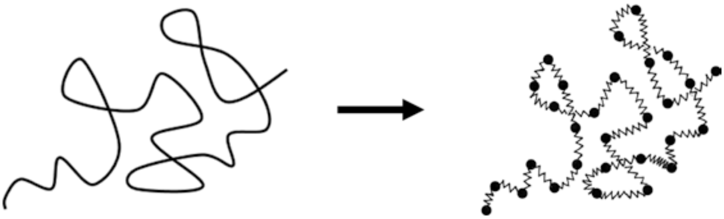

Fig. 4.7 The Rouse model describing the dynamics of the short chain polymer

The Rouse relaxation time (τ_R) of the chains can be calculated using Eq. 4.27, where the friction of the beads with the surrounding medium or chains (friction coefficient, ζ) and the motion of each bead caused by the oscillating springs (Rubinstein and Colby 2003).

$$\tau_R \approx \frac{R^2}{D_R} \approx \frac{R^2}{kT/(N\zeta)} = \frac{\zeta}{kT} NR^2 \tag{4.27}$$

Another model that describes the diffusion of short chain polymers is the Zimm model. In addition to the Rouse model, this model includes the hydrodynamic interactions (Doi and Edwards 1986).

4.3.3.3 Entangled Polymer Chain Dynamics

For long polymer chains (N > 200 monomeric units) the Rouse model is no longer valid, since additional interactions between the chains occur, namely entanglements. Because of these entanglements, the motions, such as relaxation times and self-diffusion, in a polymer melt or concentrated solution, are slower compared to the dynamics of the short chain polymer and depend on the Mw of the polymer (Kausch and Tirrell 1989). Several models considering the entanglement of the chains were developed in history. The reptation theory developed by de Gennes (1971) and later adapted by Doi and Edwards (1986) to the tube model prevailed in science. The tube model describes the snake-like motion of the polymer chains along its own line in a 'tube', surrounded by entangled chains (Fig. 4.8). The motion area is limited by the neighboring chains, which contribute to the tube topography, although they are mobile. This reptation mechanism explains the viscous flow in polymer melts. The assumptions of this model are that the movement of the chains is independent of the motion of the surrounding chains and that the lateral movement outside the tube is insignificant (Kausch and Tirrell 1989).

The diffusive motion of the chain along the tube is the diffusion coefficient (D_{Rouse}). The time required to escape the tube is the longest relaxation time (τ_{rep}—Eq. 4.28). The parts of the chain leaving the tube adopt random configurations.

Fig. 4.8 The tube model

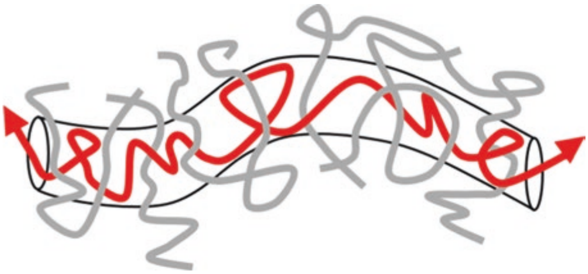

$$\tau_{rep} = \frac{(1/2)L^2}{D_R} \approx M^3 \tag{4.28}$$

The entangled polymers are melted at zero shear rate viscosity, where the τ_{rep} is approx. $M^3 - M^{3.4}$. M refers to the Mw of the polymer. The reptation diffusion coefficient (D_{rep}—Eq. 4.29) is derived from the gyrus radius of the chain (R_g) and the τ_{rep} (Kausch and Tirrell 1989):

$$D_{rep} = \frac{(1/6)R_g^2}{\tau_{rep}} \approx M^{-2} \tag{4.29}$$

The reptation diffusion coefficient describes the diffusion of the chain through the tube and is approximately equal to $M^{-2} - M^{-2.3}$. The radius of gyration is a measure for the random shape of the coil and the polymer chain in the amorphous state. The radius of gyration of polymers in solutions and melts depends on the Mw and chemical structure, and can be determined by light scattering and neutron scattering for polymer solutions and melts, respectively (Rubinstein and Colby 2003).

4.3.3.4 Interfacial Diffusion Dynamics of Polymers

The intermolecular interactions between polymer chains depend on the distance between the chains. A solid body is formed when the chains approach a distance less than 3 Å at which van der Waal forces may be operating. This also counts for adhesion between two different polymers. A proper adhesion between two distinct polymers depends on the diffusion and wetting the between the two phases at the interphase. Wetting of one polymer by the other is achieved when the distance is close enough, depending on the surface energies of the materials (Lee 1991). Once wetting occurs, diffusion can take place. The degree of diffusion depends on the functional groups present in both polymers, entanglements, molecular structure and Mw. The diffusion of polymers at the interphase is an important process during the entanglement of the chain at the interphase of polymer melts. Generally, the interfacial adhesion process includes (1) interfacial wetting (weak adhesion depending on van der Waals forces), (2) low level diffusion between the surfaces and (3) diffusion (equilibration, chain entanglement and randomisation). Polymer/polymer interdiffusion is mainly controlled by the mutual diffusion coefficient (D_M), which is also known as the interdiffusion coefficient. However, the diffusion process also depends on the self-diffusion of the polymer molecules. Self-diffusion is the diffusion of the polymer molecule trough identical molecules. The self-diffusion coefficient (D_S) can be defined as the movement along the distance (x—Eq. 4.30) (evolution of the position of the center of mass) during time (t) (Lee 1991):

$$x^2 = 2D_S t \tag{4.30}$$

D_S depends on the Mw and the presence of branches. Self-diffusion is driven by entropy and then towards maximum randomisation of the system. Mutual diffusion is the movement of the polymer chains through the interface, the rate of disappearance (J) of a inhomogeneous system to a homogeneous system is given by Eq. 4.31:

$$-J_A = D_M \nabla c_A \quad or \quad -J = D_M \nabla \phi \tag{4.31}$$

The flux of molecule A (J_A) is related to the gradient in its concentration (∇c_A—moles of molecules *per* unit volume) and the D_M. Instead of the gradient, the volume fraction ($\phi = cA^3$, where c is the concentration and A^3 the volume *per* monomer of A) can be used. Thus, the D_M depends on the thermodynamic interactions between the molecules of polymer A and polymer B (Lee 1991). In a blend of two polymers, one A and one B, there are 3 diffusion coefficients: D_{Sa}, D_{Sb} and D_M. If there is no diffusion, $J_A = 0$ ($\phi = 0$), then $D_M = D_{Sa}$ and if $J_A = 1$ ($\phi = 1$) then DM = D_{Sb}.

There are several methods to investigate the diffusion dynamics of polymers:

- Donor-acceptor fluorescence labeling.
- Electron induced X-ray fluorescence radioactive tracing.
- Forced Rayleigh scattering.
- Forward recoil spectrometry.
- Infrared spectroscopy with labeled polymers.
- NMR field gradient technique.
- Photo beaching with fluorescent labeling.
- Photon correlation spectroscopy.
- Rutherford back scattering.
- Small angle neutron scattering.

The disadvantage of these methods is that they are laborious and labeling of the polymers is required, except for NMR. In addition, the results obtained with these techniques are not totally reliable, since the marker molecule influences the diffusion of the polymer (Lee 1991).

4.3.3.5 Surface Activation by Plasma

As an alternative to the chemical modification of inert polymers (e.g. PE and PP), plasma treatment is a technique to activate the surface of materials. In addition to surface activation, plasma technology can also be used for coating, grafting and polymerization of surfaces, called surface functionalization (Rauscher et al. 2010). For example, Gao (2011) and Büttler and Pham (2019) showed that the interfacial adhesion is stronger between PA and PP when PP is treated with plasma.

Surface activation by plasma treatment causes a temporary increase in surface energy by addition of functional groups on the polymer surface. The electrons, ions, photons and radicals of the plasma irradiate the polymer surface, which leads to hydrogen abstraction, generation of free radicals and chemical interactions (Wolf 2013). The chemical interactions with the polymer depend on the type of gas used

Table 4.1 WCAs on PE after plasma treatments with different gases

Gas used for plasma treatment	WCA (°)
Untreated	102
CO_2	8
CO	16
NO	25
O_2	35
NO_2	37

Reproduced with permission from Paracchini (2003)

for the treatment. In general, surface activation by plasma treatment is performed with reactive gases such as air, nitrogen, oxygen (O_2) or mixed gases. In case of treatment with helium or argon, the radicals on the activated surface can react with O_2, nitrogen, carbon dioxide (CO_2) and water in the air after the treatment. A short treatment time and bombardment with electrons having less than 10 eV keeps the side reactions, such as chain scission, oxidative degradation and deterioration of functional groups formed on the polymer surface, at a low level (Thomas and Mittal 2013). Table 4.1 describes the WCAs of PE after treatment with plasma in the presence of different gases. CO_2 an O_2 are main components in the air. The presence of O_2 during the treatment results in a less polar activated surface compared to CO_2. In presence of –OH, =O or –COOH groups arise on the polymer surface (Rauscher et al. 2010).

Morent et al. (2008) described the presence of carbonyl groups and OH stretching vibrations by the ATR-FTIR spectra of dielectric barrier discharge (DBD)-treated PP films in air. It should be noted that moisture can also contribute to OH vibrations (Günzler and Gremlich 2003). If PP is more hydrophilic, it can adsorb moisture from the environment. The X-ray photoelectron spectroscopy (XPS) analysis has also shown an increase in oxygen content in PP after plasma treatment indicated by peaks for carbonyl and carboxyl groups. Morent et al. (2008) also showed that WCA values had a 40% decrease in the plasma-treated PP materials. The longer the treatment, the greater the decrease in WCA values (Morent et al. 2008).

The functional groups formed on the polymer surface are similar for low pressure and atmospheric pressure plasma treatment. In low pressure plasma, the ionized gas species are too energetic to control the chemical interactions at the polymer surface. In high-energy plasma, a variation of functional groups appears on the surface. For a smaller variation of the functionalized groups, the plasma energy level must be reduced. In contrast, atmospheric pressure plasma is more appropriate for grafting monotype functional groups (Thomas and Mittal 2013). However, the functional groups formed by the reaction between the ionized gas and the polymer surface are not permanent. The groups tend to be reoriented after treatment and the surface activation effect is reduced. This phenomenon is known as plasma aging (Rauscher et al. 2010). However, a precise chemical mechanism behind is still unclear.

4.4 Advances in the Characterization of Interfaces

Generally, the following classical methods to characterize the polymer/polymer and polymer/reinforcement are often applied in the literature with a series of examples given in Sect. 4.2.

- Electron microscopy techniques such as SEM and TEM to determine the particle size of the dispersed phase in blends as a result of phase stabilization and reduced interface tension.
- Rheological measurement as an indicator of a better phase bonding, such as melt viscosity, torque level, etc.
- Mechanical testing, e.g. σ_m and impact testing to evaluate the mechanical performance as a result of better phase adhesion.

Such classical analytical methods mainly provide information on the bond strength and quality, but the information about the chemical and physical interfacial behavior is limited. Thus, more advanced characterization techniques are needed to obtain more detailed information about the interfacial interaction.

Another aspect is the model system for the investigation of polymer interfaces. In the literature reported in Sect. 4.2 above, polymer blends are mainly investigated. As a good alternative, multilayer systems or laminates could be used for characterizing interfacial interactions and diffusion processes. A layered system would eliminate the influence of the dispersed phase morphology present in blends on the rheological measurement. With this in mind, Valenza et al. (2000) demonstrated with plate-plate rheology measurements that PA/PE laminates (4–12 layers systems) have a significantly changed viscoelastic behavior after compatibilization using ethylene/*tert*-butyl acrylate/acrylic acid terpolymers. This study also showed that the viscosities of the blends with modified PE are higher compared to that of unmodified PE. In addition, Valenza et al. (2000) demonstrated that the more layers of PA and modified PE the system has, the higher the viscosity is. Since the multilayer system containing unmodified PE showed the opposite effect, it is likely that the higher viscosity observed by Valenza et al. (2000) was due to the improved interactions between PA and modified PE. The analysis of multilayer systems containing different proportions of PE has also shown that the viscosity of the laminates is between the viscosity of PA and PE. Therefore, both polymers contribute to the flow behavior of the laminate, but the data did not give indications of interfacial interactions. However, the investigation of multilayer systems containing different proportions PE modified by γ-ray irradiation was interestingly. The viscosity of the laminates was greater than the viscosity of PA or PE irradiated at low frequencies. This clearly demonstrated an interfacial strengthening effect.

In the next section, we report on different techniques compared to our own study on the classical PP/PA polymer system. Unlike the literature reported in the previous section, our experimental investigation was performed on laminates on PA6.6 fabrics and PP/PA6 films as a model for multilayer systems (Büttler and Pham 2018, 2019).

The objective of our research was to provide a better view of the interface phenomenon. Apart from the classical method such as rheology on film laminate, we have also applied modifies T-peel test on fabric laminate and the most advanced nano-infrared (nano-IR) technique (nano-scale infrared spectroscopy) to investigate the interface.

4.4.1 Interface Characterization by Melt Rheology

Basically, the melt flow behavior of a polymer depends on their structure, the presence of reactive groups, the Mw, the Mw distribution (MWD or polydispersity index − PDI = weight-average apparent molecular weight (M_w)/number-average apparent molecular weight (M_n)), pressure, temperature, etc. (Osswald and Rudolph 2015). Changes in the melt flow are due to chemical interactions and degradation due to the exposure to high temperatures or addition of another material. For blends made from two or more polymers forming a continuous matrix and a disperse phase, the blend morphology and the interfacial mechanisms also play an important role. Depending on the characteristics of the polymers and their miscibility, the disperse phase may have large or small structures (see examples in Sect. 4.2). In case of immiscible systems, there are shear interphases. The better the compatibilization, the smaller the structures of the disperse phase and, due to interdiffusion, the interphase is less clear (Shi et al. 2002).

During the melt flow analysis, the morphology of the blend and the microstructure at the interphase play an important role. The shear deformation increases the interfacial tension, also known as Gibbs elasticity. The effect of interfacial diffusion on the interfacial shear modulus and viscosity is still unclear, but interfacial viscoelasticity is likely to be related to the interfacial tension. However, the experimental demonstration of this is very complicated (van Puyvelde et al. 2001).

Several studies have investigated the compatibility of immiscible polymer blends and have shown that the melt flow behavior changes after the addition of compatibilizer. Figure 4.9 shows an example on the effect of compatibilization of the PP/PA6 blend by MA-*g*-PP (Büttler and Pham 2019). The left shift of the storage and loss modulus causes a left shift of the gelation point, indicating that chemical interactions occur between the amine end groups of PA and MA of MA-*g*-PP.

The presence of MA-*g*-PP in the blend also causes an increase of the viscosity, thus suggesting a greater strength of the interface. This behavior is caused by strong chemical interactions or the increase in Mw (Osswald and Rudolph 2015; Hernandez-Alamilla and Valadez-Gonzalez 2016). These data were obtained for PA/PP blends with a 40%/60% ratio, but similar results were also obtained by Chow et al. (2005) for a 70%/30% ratio. In this sense, at lower PA proportions, the storage module is even diminished in the presence of MA-*g*-PP (Shi et al. 2002). For a precise analysis of the influence of the polymer proportions on the viscoelastic behavior of the blend, the composition process should be considered, since this determines the morphology of the blend (Pham and Gahleitner 2005).

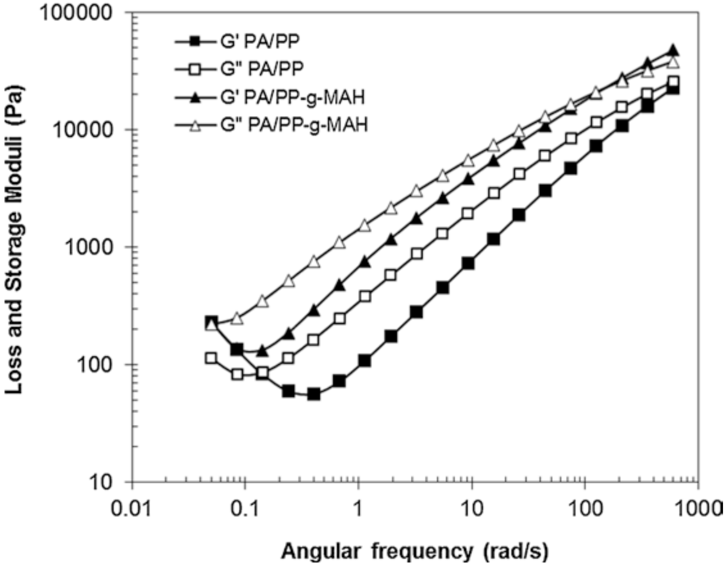

Fig. 4.9 Storage and loss modules for PA/PP and PA/PP-*g*-MA blends. The gelation point ($G' = G''$) shifts to the left, indicating interfacial strengthening. Reproduced with permission from Büttler and Pham (2019)

It is worthwhile, however, to point out that the diffusion of polymers is different in laminated structures. During the shear in the parallel plate/plate setting, the polymer chains are arranged in the direction of the shear, which possibly hinders the diffusion of the polymers from one phase to the other. An increase in viscosity and viscoelastic modules were further increased at the end of the measurement at low frequencies (Valenza et al. 2000; Büttler and Pham 2019). The longer the laminate is in molten state, the more interactions and diffusion take place, which contributes to greater interfacial strength. However, interfacial strengthening does not always have the same effect on the melt flow behavior of the blend. According to Carvalho and Sirqueira (2016), the interfacial strengthening of PA/SEBS by adding MA-*g*-SEBS caused an increase in the storage module, but a decrease in the loss modulus, thus suggesting that the elastic portion becomes more dominant due to the high elasticity of SEBS. The elastic portion prevails over the effect of chemical interactions which occur at the interface. Nevertheless, the viscosity increases and the blends showed more solid properties after modification, indicating that there is less interfacial slippage.

4.4.2 Characterization of the Interface by Advanced Mechanical Testing

Apart from classical mechanical testing, such as σ_m or bending test, the direct bond strength between the reinforcement and the matrix is mainly tested by lap-shear and T-Peel testing. These methods have advantages that are simple, easy to handle,

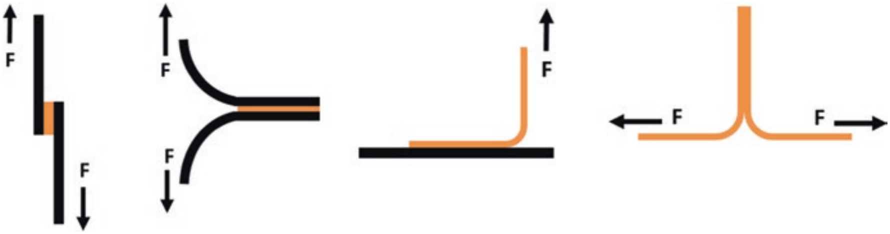

Fig. 4.10 Shear- and peel tests for adhesive testing of films and fabrics: from left to right: single lap joint shear test, T-peel test, 90° and 180° peel test. The arrows indicate the applied force on the materials. Reproduced with permission from Heinzmann et al. (2016)

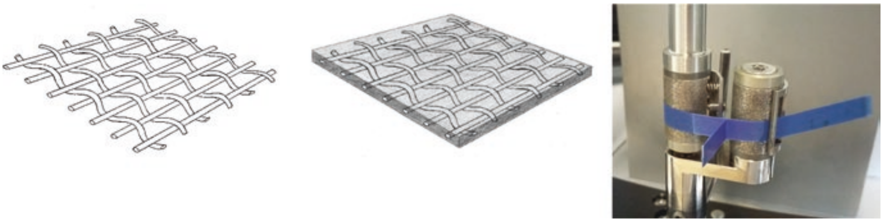

Fig. 4.11 Scheme of a textile polymer composite. The textile structure (left) and the textile embedded into polymer matrix (center). The universal extensional fixture (UXF) setting of the rheometer for advanced adhesive T-peel strength testing at variable temperatures (right)

provide direct information about the adhesive forces and modules. The type of mechanical test depends on the composite. For adhesive bonds with films or fabrics, shear- or peel tests are suitable (Fig. 4.10) (Heinzmann et al. 2016).

In case of the adhesive determination between a matrix and fibers, micro-bond tests are more suitable (Zhandarov and Maeder 2005; Deng et al. 2012). However, these experiments are laborious and micro testing machinery is required. In addition, the break surface of the composite can be analyzed optically. For the visualization of adhesion quality light, polarized light, stereo-, 3D- microscopy, as well as AFM, SEM and TEM can be used for the analysis of the surface, the break surface and the cross-section (Botelho et al. 2003; Yang and Thomason 2012; Heinzmann et al. 2016).

In our study, PP and PA6.6 fabric laminates were used. It served as a model system to simulate the adhesion between the woven reinforcing structure of PA6.6 and the PP matrix in polymer-based textile composites (Fig. 4.11).

The T-peel was performed using a modified setup of the UXF of the rheometer MCR302 (Anton Paar Modular Compact Rheometer). This advanced T-peel test using extensional rheology has the advantage of a more sensitive detection level (1–50 nM*m), which measures a variation of set temperatures and allows obtaining information about the viscoelastic behavior during extensional peeling, as well as changes in the adhesional strength between the polymers can be observed after interfacial modification as a consequence of the interfacial diffusion changes and the interphase interactions at different temperatures.

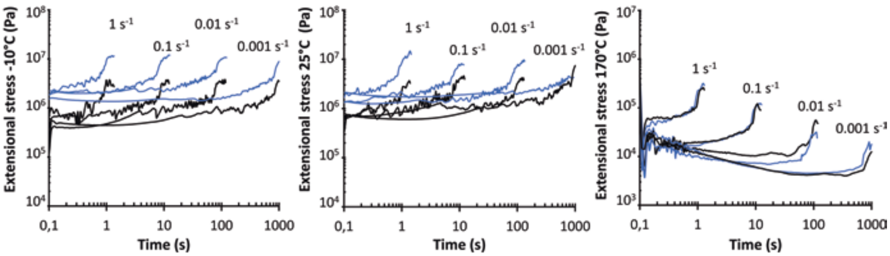

Fig. 4.12 Advanced extensional T-peel testing at −10 °C, 25 °C and 170 °C (from left to right). PA66 textile composites with non-treated PP (black) and with PP-*g*-MA (blue). The rates of extensional strain are those indicated in the graph. Reproduced with permission from Büttler and Pham (2018)

As shown in Fig. 4.12, the peel stress increases after interphase modification by MA grafting onto PP. However, above the T_m of PP matrix, the PP modification no longer plays any significant role in interfacial strengthening. For both matrices, with or without modification, the peel stress decreases with increasing temperature, which indicates that the viscosity of the matrix itself influences the peel stress (Büttler and Pham 2018).

4.4.3 Interfacial Characterization by Nano-IR Technique

Interfacial diffusion between PA and PP is a measure for interfacial adhesion. The main disadvantage of the research methods with the labelling technique as mentioned above is that label molecules influence the diffusion. A more advanced technique for visualizing the diffusion, where no labelling is needed, is AFM in combination with IR at nano-scale, which has a higher resolution than ATR-FTIR imaging (Zhou et al. 2009). AFM is a known technique to visualize the surface morphology of materials (Binning and Quate 1986; Gutiérrez et al. 2016; Gutiérrez and González 2016, 2017; Gutiérrez 2017). This technique is based on a cantilever scanning the surface area. A laser diode is focused on the cantilever and is reflected in a photodetector to register each configurational change of the cantilever due to the surface morphology and a height image with very high resolution is obtained. The use of the same cantilever for IR analysis gives the possibility for chemical mapping of the sample surface at nano-scale. This overcomes the problem of the low resolution obtained by IR spectroscopy (Dazzi et al. 2010, 2012). During nano-IR characterization, an infrared laser pulse irradiates the sample at different wavelengths. The different wavelengths bring a specific molecular structure in resonance. The light adsorbed at that wavelength causes a local increase in the temperature of the sample, resulting in a thermal expansion of the sample. This thermal expansion again causes a change in the cantilever of laser diode reflection on the photodetector. The amplitude detected is proportional to the absorption, and therefore, the

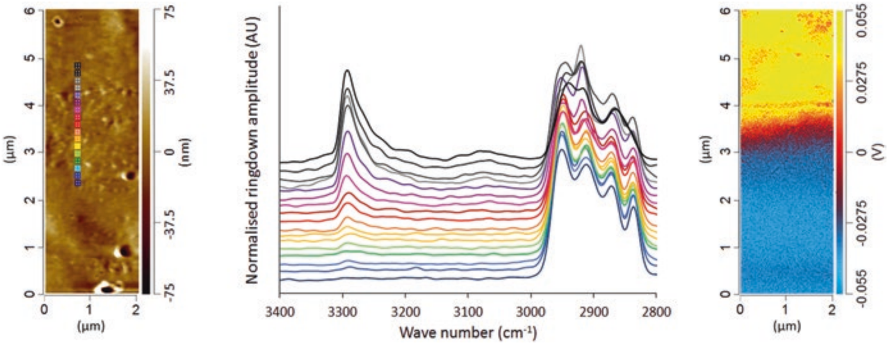

Fig. 4.13 AFM height image, nano-IR spectra and nano-IR image taken at 3300 cm^{-1} of the PA/PP-*g*-MA laminar interphase (from left to right). The colored markers (150 nm spacing) correspond to the color of the spectra

nano-IR spectra can be correlated with the FTIR spectra. It is possible with this technique to scan at a desired spot in the spectrum, or to map the surface of a sample at a specific wavelength in contact mode (Dazzi et al. 2010). Nano-IR is a useful tool for the characterization of composite blends (Marcott et al. 2014; Ghosh et al. 2015; Tang et al. 2016), fiber cross-sections (Rietzler et al. 2019), multi-layer laminates (Kelchtermans et al. 2016) and polymer composites (Ye et al. 2012).

The application of this advanced technique on our PA6/PP laminate system allowed us to observe the diffusion from polymer to the other, forming an interphase. Figure 4.13 shows an AFM image and nano-IR spectra across the interphase between PA and PP-*g*-MA. In the presence of MA-*g*-PP, diffusion takes place between the PA6 phase and the PP phase. If there is no modification, diffusion does not occur.

In case of PA6/MA-*g*-PP laminate system, the interface between PA6 and PP is quite diffuse (Fig. 4.13, left). In addition, by observing at N-H stretching absorbance band at 3300 cm^{-1} in different nano-IR spectra in a 15 nm spacing (Fig. 4.13, middle), the high increase of the absorbance peaks indicates the increased amount of PA6 molecules, when moving from PP phase to PA6 phase. The chemical image taken at 3300 cm^{-1} at the interface demonstrated the interdiffusion (Fig. 4.13, right).

4.5 Conclusions and Remarks

The subject of polymer interface reactions is an interdisciplinary field of research including pure chemistry, chemistry and physics of polymers, and materials science, also covering adhesion of the physical phase, chemical reactions and interdiffusion phenomena of polymers. Using polymer interface reactions in multiphase polymer systems, the interface could be tailored. Strengthening the interface increases the phase stability, reduces coalescence and phase separation. The underlying mechanisms play a crucial role in the control of the polymer interfaces, e.g. *in-situ* formation of copolymers acting as phase compatibilizer and reduction of interfacial tension, thus favoring the diffusion of a polymer into the other phase. This technique also often used to improve the phase bonding between polymer matrices and reinforcing fibers, typically in polymer composites.

Despite a large number of papers published on the subject in the last decades and well-understood basic chemical reactions, deep and throughout understanding of the chemical and physical formation of the interface by interface reaction is still an interesting field to be explored. Additional potential research on the more advanced chemical modification of the polymer surface and interface, as well as modern (direct) characterization techniques of the polymer/polymer interface, can be carried out.

Acknowledgments The authors gratefully acknowledge the financial support from the Austrian Federal Ministry for Climate Action, Environment, Energy, Mobility, Innovation and Technology (BMK) to the Endowed Professorship Advanced Manufacturing FFG-846932.

Conflicts of Interest The authors declare no conflict of interest.

References

Abacha, N., & Fellahi, S. (2005). Synthesis of polypropylene-graft-maleic anhydride compatibilizer and evaluation of nylon 6/polypropylene blend properties. *Polymer International, 54*(6), 909–916. https://doi.org/10.1002/pi.1788.

Bechtold, T., & Pham, T. (2019). *Textile chemistry*. Berlin/Boston: de Gruyter STEM.

Bettini, S. H. P., & Agnelli, J. A. M. (1999). Grafting of maleic anhydride onto polypropylene by reactive processing. I. Effect of maleic anhydride and peroxide concentrations on the reaction. *Journal of Applied Polymer Science, 74*(2), 247–255. https://doi.org/10.1002/(sici)1097-4628(19991010)74:2%3c247::aid-app2%3e3.0.co;2-a.

Bettini, S. H. P., & Agnelli, J. A. M. (2000). Evaluation of methods used for analyzing maleic anhydride grafted onto polypropylene by reactive processing. *Polymer Testing, 19*(1), 3–15. https://doi.org/10.1016/s0142-9418(98)00066-x.

Bettini, S. H. P., & Agnelli, J. A. M. (2002). Grafting of maleic anhydride onto polypropylene by reactive extrusion. *Journal of Applied Polymer Science, 85*(13), 2706–2717. https://doi.org/10.1002/app.10705.

Bettini, S. H. P., & Ruvolo Filho, A. C. (2007). Styrene-assisted grafting of maleic anhydride onto polypropylene by reactive processing. *Journal of Applied Polymer Science, 107*(3), 1430–1438. https://doi.org/10.1002/app.27201.

Binning, G., & Quate, C. F. (1986). Atomic force microscope. *Physical Review Letters, 56*(9), 930–935. https://doi.org/10.1103/physrevlett.56.930.

Botelho, E. C., Figiel, L., Rezende, M. C., & Lauke, B. (2003). Mechanical behavior of carbon fiber reinforced polyamide composites. *Composites Science and Technology, 63*(13), 1843–1855. https://doi.org/10.1016/s0266-3538(03)00119-2.

Büttler, J. R., & Pham, T. (2018). A dynamic mechanical thermal T-Peel test approach to characterize interfacial behavior of polymeric textile composites. *International Journal of Materials and Metallurgical Engineering, 12*(8), 389–395. https://doi.org/10.5281/zenodo.1474269.

Büttler, J. R., & Pham, T. (2019). Characterization of polyamide 6—polypropylene laminates. *AIP Conference Proceedings, 2055*, 050008. https://doi.org/10.1063/1.5084827.

Carone, E., Kopcak, U., Gonçalves, M. C., & Nunes, S. P. (2000). In situ compatibilization of polyamide 6/natural rubber blends with maleic anhydride. *Polymer, 41*(15), 5929–5935. https://doi.org/10.1016/S0032-3861(99)00800-9.

Cartier, H., & Hu, G. (1998a). Styrene-assisted melt free radical grafting of glycidyl methacrylate onto polypropylene. *Journal of Polymer Science: Part A: Polymer Chemistry, 36*(7), 1053–1063. https://doi.org/10.1002/(sici)1099-0518(199805)36:7%3c1053::aid-pola3%3e3.0.co;2-3.

Cartier, H., & Hu, G. H. (1998b). Styrene-assisted free radical grafting of glycidyl methacrylate onto polyethylene in the melt. *Journal of Polymer Science, Part A: Polymer Chemistry, 36*(15), 2763–2774. https://doi.org/10.1002/(sici)1099-0518(19981115)36:15<2763::aid-pola13>3.0.co;2-y.

Carvalho, A., & Sirqueira, S. (2016). Effect of compatibilization in situ on PA/SEBS blends. *Polimeros, 26*(2), 123–128. https://doi.org/10.1590/0104-1428.2195

Cassu, S. N., & Felisberti, M. I. (2001). *In situ* compatibilization of polystyrene and polyurethane blends by using poly(styrene-*co*-maleic anhydride) as reactive compatibilizer. *Journal of Applied Polymer Science, 82*(10), 2514–2524. https://doi.org/10.1002/app.2102.

Chang, F.-C., & Hwu, Y.-C. (1991). Styrene maleic anhydride and styrene glycidyl methacrylate copolymers as *in situ* reactive compatibilizers of polystyrene/nylon 6,6 blends. *Polymer Engineering and Science, 31*(21), 1509–1519. https://doi.org/10.1002/pen.760312102.

Chen, L. F., Wong, B., & Baker, W. E. (1996). Melt grafting of glycidyl methacrylate onto polypropylene and reactive compatibilization of rubber toughened polypropylene. *Polymer Engineering and Science, 36*(12), 1594–1607. https://doi.org/10.1002/pen.10556.

Cherif, C. (2011). *Textile Werkstoffe für den Leichtbau*. Heidelberg: Springer. https://doi.org/10.1007/978-3-642-17992-1.

Chiang, C., & Chang, F. (1996). Polymer blends of polyamide-6 and poly(phenylene oxide) compatibilized by styrene-co-glycidyl methacrylate. *Journal of Applied Polymer Science, 61*(13), 2411–2421. https://doi.org/10.1002/(sici)1097-4628(19960926)61:13<2411::aid-app21>3.3.co;2-v.

Chiu, H. T., & Hsiao, Y. K. (2006). Compatibilization of poly(ethylene terephthalate)/polypropylene blends with maleic anhydride grafted polyethylene-octene elastomer. *Journal of Polymer Research, 13*(2), 153–160. https://doi.org/10.1007/s10965-005-9020-z.

Chow, W. S., Ishak, Z., & Karger-Kocsis, J. (2005). Morphological and rheological properties of polyamide 6/poly (propylene)/organoclay nanocomposites. *Macromolecular Materials and Engineering, 290*(2), 122–127. https://doi.org/10.1002/mame.200400269.

Clark, D. C., Baker, W. E., & Whitney, R. A. (2001). Peroxide-initiated comonomer grafting of styrene and maleic anhydride onto polyethylene: Effect of polyethylene microstructure. *Journal of Applied Polymer Science, 79*(1), 96–107. https://doi.org/10.1002/1097-4628(20010103)79:1<96::aid-app120>3.0.co;2-x.

Datta, R. K., Polk, M. B., & Kumar, S. (1995). Reactive compatibilization of polypropylene and nylon. *Polymer-Plastics Technology and Engineering, 34*(4), 551–560. https://doi.org/10.1080/03602559508012204.

Dazzi, A., Glotin, F., & Carminati, R. (2010). Theory of infrared nanospectroscopy by photothermal induced resonance. *Journal of Applied Physics, 107*(12), 124519. https://doi.org/10.1063/1.3429214.

Dazzi, A., Prater, C. B., Hu, Q., Chase, D. B., Rabolt, J. F., & Marcott, C. (2012). AFM—IR: Combining atomic force microscopy and infrared spectroscopy for nanoscale chemical characterization. *Applied Spectroscopy, 66*(12), 1365–1384. https://doi.org/10.1366/12-06804.

de Gennes, P. G. (1971). Reptation of a polymer chain in the presence of fixed obstacles. *The Journal of Chemical Physics, 55*(2), 572–579. https://doi.org/10.1063/1.1675789.

De Roover, B., Scalvons, M., Carlier, V., Devaux, J., Legras, R., & Momtaz, A. (1995). Molecular characterization of maleic anhydride-functionalized polypropylene. *Journal of Polymer Science: Part A: Polymer Chemistry, 33*(5), 829–842. https://doi.org/10.1002/pola.1995.080330509.

Deng, S., Ma, W., Zhou, X., & Fan, C. (2012). Maintenance of highly interfacial shear strength by diblock copolymer between carbon fiber and epoxy resin in hostile environment. *Composite Interfaces, 19*(8), 499–509. https://doi.org/10.1080/15685543.2012.761810.

Doi, M., & Edwards, S. F. (1986). *The theory of polymer dynamics*. Oxford: Oxford University Press.

Elias, H. G. (1997). *An introduction to polymer science*. VCH Verlagsgesellschaft mbH: Weinheim.

Filippi, S., Minkova, L., Dintcheva, N., Narducci, P., & Magagnini, P. (2005). Comparative study of different maleic anhydride grafted compatibilizer precursors towards LDPE/PA6 blends: Morphology and mechanical properties. *Polymer, 46*(19), 8054–8061. https://doi.org/10.1016/j.polymer.2005.06.090.

Gabara, W., & Porejko, A. W. (1967). Grafting in reaction of polyethylene and poly (maleic anhydride) properties. *Journal of Polymer Science: Part A-1, 5*(7), 1539–1545. https://doi.org/10.1002/pol.1967.150050705.

Ganzeveld, K. J., & Janssen, L. P. B. M. (1992). The grafting of maleic anhydride on high density polyethylene in an extruder. *Polymer Engineering and Science, 32*(7), 467–474. https://doi.org/10.1002/pen.760320703.

Gao, Z. (2011). Applied surface science modification of surface properties of polyamide 6 films with atmospheric pressure plasma. *Applied Surface Science, 257*(14), 6068–6072. https://doi.org/10.1016/j.apsusc.2011.01.132.

Garcia-Martinez, J. M., Laguna, O., & Collar, E. P. (2002). Chemical modification of polypropylenes by maleic anhydride: Influence of stereospecificity and process conditions. *Journal of Applied Polymer Science, 68*(3), 483–495. https://doi.org/10.1002/(sici)1097-4628(19980418)68:3<483::aid-app14>3.0.co;2-w.

Gaylord, N. G., & Mehta, R. (1988). Peroxide-catalyzed grafting of maleic anhydride onto molten polyethylene in the presence of polar organic compounds. *Journal of Polymer Science Part A: Polymer Chemistry, 26*(4), 1189–1198. https://doi.org/10.1002/pola.1988.080260419.

Gaylord, N. G., & Mishra, M. K. (1983). Nondegradative reaction of maleic anhydride and molten polypropylene in the presence of peroxides. *Journal of Polymer Science Part C: Polymer Letters, 21*(1), 23–30. https://doi.org/10.1002/pol.1983.130210104.

Gaylord, N. G., Mehta, R., Kumar, V., & Tazi, M. (1989). High density polyethylene-g-maleic anhydride preparation in presence of electron donors. *Journal of Applied Polymer Science, 38*(2), 359–371. https://doi.org/10.1002/app.1989.070380217.

Ghosh, S., Ramos, L., Remita, S., Dazzi, A., Deniset-Besseau, A., Beaunier, P., & Remita, H. (2015). Conducting polymer nanofibers with controlled diameters synthesized in hexagonal mesophases. *New Journal of Chemistry, 39*(11), 8311–8320. https://doi.org/10.1039/c5nj00826c.

Godshall, D., White, C., & Wilkes, G. L. (2001). Effect of compatibilizer molecular weight and maleic anhydride content on interfacial adhesion of polypropylene-PA6 bicomponent fibers. *Journal of Applied Polymer Science, 80*(2), 130–141. https://doi.org/10.1002/1097-4628(20010411)80:2<130::aid-app1081>3.0.co;2-c.

Grigoryeva, O., & Karger-Kocsis, J. (2000). Melt grafting of maleic anhydride onto an ethylene-propylene-diene terpolymer (EPDM). *European Polymer Journal, 36*(7), 1419–1429. https://doi.org/10.1016/s0014-3057(99)00205-0.

Günzler, H., & Gremlich, H. (2003). *IR-Spektroskopie: Eine Einführung*. Weinheim: Wiley.

Gutiérrez, T. J. (2017). Surface and nutraceutical properties of edible films made from starchy sources with and without added blackberry pulp. *Carbohydrate Polymers, 165*, 169–179. https://doi.org/10.1016/j.carbpol.2017.02.016.

Gutiérrez, T. J., & González, G. (2016). Effects of exposure to pulsed light on surface and structural properties of edible films made from cassava and taro starch. *Food and Bioprocess Technology, 9*(11), 1812–1824. https://doi.org/10.1007/s11947-016-1765-3.

Gutiérrez, T. J., & González, G. (2017). Effect of cross-linking with *Aloe vera* gel on surface and physicochemical properties of edible films made from plantain flour. *Food Biophysics, 12*(1), 11–22. https://doi.org/10.1007/s11483-016-9458-z.

Gutiérrez, T. J., Suniaga, J., Monsalve, A., & García, N. L. (2016). Influence of beet flour on the relationship surface-properties of edible and intelligent films made from native and modified plantain flour. *Food Hydrocolloids, 54*, 234–244. https://doi.org/10.1016/j.foodhyd.2015.10.012.

Gutiérrez, T. J., Ollier, R., & Alvarez, V. A. (2018). Chapter 5. Surface properties of thermoplastic starch materials reinforced with natural fillers. In V. K. Thakur & M. K. Thakur (Eds.), *Functional biopolymers* (pp. 131–158). Cham: Editorial Springer International.. EE.UU. ISBN: 978-3-319-66416-3. eISBN: 978-3-319-66417-0. https://doi.org/10.1007/978-3-319-66417-0_5.

Gutiérrez, T. J., Toro-Márquez, L. A., Merino, D., & Mendieta, J. R. (2019). Hydrogen-bonding interactions and compostability of bionanocomposite films prepared from corn starch and nano-fillers with and without added Jamaica flower extract. *Food Hydrocolloids, 89*, 283–293. https://doi.org/10.1016/j.foodhyd.2018.10.058.

Habenicht, G. (2009). *Kleben: Grundlagen, Technologie, Anwendungen*. Berlin: Springer.

Heinen, W., Rosenmöller, C. H., Wenzel, C. B., de Groot, H. J. M., Lugtenburg, J., & van Duin, M. (1996). ^{13}C NMR study of the grafting of maleic anhydride onto polyethene, polypropene, and ethene−propene copolymers. *Macromolecules, 29*(4), 1151–1157. https://doi.org/10.1021/ma951015y.

Heinzmann, C., Weder, C., & De Espinosa, L. M. (2016). Supramolecular polymer adhesives: Advanced materials inspired by nature. *Chemical Society Reviews, 45*(2), 342–358. https://doi.org/10.1039/c5cs00477b.

Hernandez-Alamilla, M., & Valadez-Gonzalez, A. (2016). The effect of two commercial melt strength enhancer additives on the thermal, rheological and morphological properties of polylactide. *Journal of Polymer Engineering, 36*(43), 31–41. https://doi.org/10.1515/polyeng-2014-0322.

Herniou-Julien, C., Mendieta, J. R., & Gutiérrez, T. J. (2019). Characterization of biodegradable/non-compostable films made from cellulose acetate/corn starch blends processed under reactive extrusion conditions. *Food Hydrocolloids, 89*, 67–79. https://doi.org/10.1016/j.foodhyd.2018.10.024.

Hu, G., & Cartier, H. (1999). Styrene-assisted melt free radical grafting of glycidyl methacrylate onto an ethylene and propylene rubber. *Journal of Applied Polymer Science, 71*(1), 125–133. https://doi.org/10.1002/(sici)1097-4628(19990103)71:1<125::aid-app15>3.0.co;2-s.

Huang, H., & Liu, N. C. (1998). Nondegradative melt functionalization of polypropylene with glycidyl methacrylate. *Journal of Applied Polymer Science, 67*(12), 1957–1963. https://doi.org/10.1002/(sici)1097-4628(19980321)67:12<1957::aid-app1>3.3.co;2-a.

Hwang, S. W., Lee, S. B., Lee, C. K., Lee, J. Y., Shim, J. K., Selke, S. E. M., Soto-Valdez, H., Matuana, L., Rubino, M., & Auras, R. (2012). Grafting of maleic anhydride on poly(L-lactic acid). Effects on physical and mechanical properties. *Polymer Testing, 31*(2), 333–344. https://doi.org/10.1016/j.polymertesting.2011.12.005.

Jiang, C., Filippi, S., & Magagnini, P. (2003). Reactive compatibilizer precursors for LDPE/PA6 blends. II: Maleic anhydride grafted polyethylenes. *Polymer, 44*(8), 2411–2422. https://doi.org/10.1016/s0032-3861(03)00133-2.

Juntuek, P., Ruksakulpiwat, C., Chumsamrong, P., & Ruksakulpiwat, Y. (2012). Effect of glycidyl methacrylate-grafted natural rubber on physical properties of polylactic acid and natural rubber blends. *Journal of Applied Polymer Science, 125*(1), 745–754. https://doi.org/10.1002/app.36263.

Kausch, H. H., & Tirrell, M. (1989). Polymer interdiffusion. *Annual Review of Materials Science, 19*(1), 341–377. https://doi.org/10.1146/annurev.ms.19.080189.002013?journalCode=matsci.1.

Kelchtermans, M., Lo, M., Dillon, E., Kjoller, K., & Marcott, C. (2016). Characterization of a polyethylene–polyamide multilayer film using nanoscale infrared spectroscopy and imaging. *Vibrational Spectroscopy, 82*, 10–15. https://doi.org/10.1016/j.vibspec.2015.11.004.

Kim, C. H., Cho, K. Y., & Park, J. K. (2001a). Reactive blends of gelatinized starch and polycaprolactone-*g*-glycidyl methacrylate. *Journal of Applied Polymer Science, 81*(6), 1507–1516. https://doi.org/10.1002/app.1579.

Kim, S., Shin, B., Hong, J., Cho, W., & Ha, C. (2001b). Reactive compatibilization of the PBT/EVA blend by maleic anhydride. *Polymer, 42*(9), 4073–4080. https://doi.org/10.1016/s0032-3861(00)00810-7.

Kim, S. J., Kang, C. J., Chowdhury, S. R., Cho, W. J., & Ha, C. S. (2003). Reactive compatibilization of the poly(butylene terephthalate)-EVA blend by maleic anhydride. II. Correlations among gel contents, grafting yields, and mechanical properties. *Journal of Applied Polymer Science, 89*(5), 1305–1310. https://doi.org/10.1002/app.12245.

Kim, Y. F., Choi, C. N., Kim, Y. D., Lee, K. Y., & Lee, M. S. (2004). Compatibilization of immiscible poly(l-lactide) and low density polyethylene blends. *Fibers and Polymers, 5*(4), 270–274. https://doi.org/10.1007/bf02875524.

Ko, T. M., & Ning, P. (2000). Peroxide-catalyzed swell grafting of maleic anhydride onto polypropylene. *Polymer Engineering and Science, 40*(7), 1589–1595. https://doi.org/10.1002/pen.11289.

Kyu Kim, B., Yun Park, S., & Jin Park, S. (1991). Morphological, thermal and rheological properties of blends: Polyethylene/nylon-6, polyethylene/nylon-6/(maleic anhydride-g-polyethylene) and (maleic anhydride-g-polyethylene)/nylon-6. *European Polymer Journal, 27*(4–5), 349–354. https://doi.org/10.1016/0014-3057(91)90186-r.

Lee, L.-H. (Ed.). (1991). *Fundamentals of adhesion*. New York: Springer Science & Business Media. https://doi.org/10.1007/978-1-4899-2073-7.

Li, Y., Xie, X. M., & Guo, B. H. (2001). Study on styrene-assisted melt free-radical grafting of maleic anhydride onto polypropylene. *Polymer, 42*(8), 3419–3425. https://doi.org/10.1016/s0032-3861(00)00767-9.

Li, H., Chen, H., Shen, Z., & Lin, S. (2002). Preparation and characterization of maleic anhydride modified syndiotactic polystyrene. *Polymer, 43*(20), 5455–5461. https://doi.org/10.1016/s0032-3861(02)00369-5.

Li, C., Zhang, Y., & Zhang, Y. (2003). Melt grafting of maleic anhydride onto low-density polyethylene/polypropylene blends. *Polymer Testing, 22*(2), 191–195. https://doi.org/10.1016/s0142-9418(02)00079-x.

Lim, J. G., Baïk, J. H., Zhang, X. Q., Son, Y., Choi, W. M., & Park, O. O. (2002). A novel preparation method of maleic anhydride grafted syndiotactic polystyrene and its blend performance with nylon6. *Polymer Bulletin, 48*(4–5), 397–405. https://doi.org/10.1007/s00289-002-0046-7.

Lin, C. (1993). Modification of polypropylene by peroxide-catalysed grafting of maleic anhydride for adhesive bonding: Surface and interface. *Journal of Materials Science Letters, 12*(8), 612–614. https://doi.org/10.1007/bf00278342.

Liu, J., Jiang, H., & Chen, L. (2012). Grafting of glycidyl methacrylate onto poly(lactide) and properties of pla/starch blends compatibilized by the grafted copolymer. *Journal of Polymers and the Environment, 20*(3), 810–816. https://doi.org/10.1007/s10924-012-0438-1.

Lu, B., & Chung, T. C. (2000). Synthesis of maleic anhydride grafted polyethylene and polypropylene, with controlled molecular structures. *Journal of Polymer Science, Part A: Polymer Chemistry, 38*(8), 1337–1343. https://doi.org/10.1002/(sici)1099-0518(20000415)38:8<1337::aid-pola18>3.0.co;2-8.

Lusinchi, J. M., Boutevin, B., Torres, N., & Robin, J. J. (2001). *In situ* compatibilization of HDPE/PET blends. *Journal of Applied Polymer Science, 79*(5), 874–880. https://doi.org/10.1002/1097-4628(20010131)79:5<874::aid-app120>3.0.co;2-b.

Ma, P., Jiang, L., Ye, T., Dong, W., & Chen, M. (2014). Melt free-radical grafting of maleic anhydride onto biodegradable poly(lactic acid) by using styrene as a comonomer. *Polymers, 6*(5), 1528–1543. https://doi.org/10.3390/polym6051528.

Machado, A. V., van Duin, M., & Covas, J. A. (2000). Monitoring polyolefin modification along the axis of a twin-screw extruder. II. Maleic anhydride grafting. *Journal of Polymer Science: Part A: Polymer Chemistry, 38*(21), 3919–3932. https://doi.org/10.1002/1099-0518(20001101)38:21%3c3919::aid-pola90%3e3.0.co;2-l.

Machado, A. V., Covas, J. A., & Van Duin, M. (2001). Effect of polyolefin structure on maleic anhydride grafting. *Polymer, 42*(8), 3649–3655. https://doi.org/10.1016/s0032-3861(00)00692-3.

Mani, R., Bhattacharya, M., & Tang, J. (1999). Functionalization of polyesters with maleic anhydride by reactive extrusion. *Journal of Polymer Science: Part A: Polymer Chemistry, 37*(11), 1693–1702. https://doi.org/10.1002/(sici)1099-0518(19990601)37:11%3c1693::aid-pola15%3e3.0.co;2-y.

Marcott, C., Lo, M., Hu, Q., Dillon, E., Kjoller, K., & Prater, C. (2014). Nanoscale infrared spectroscopy of polymer composites. *American Laboratory, 46*(3), 23–25.

Martínez, J. G., Benavides, R., Guerrero, C., & Reyes, B. E. (2004). UV sensitisation of polyethylenes for grafting of maleic anhydride. *Polymer Degradation and Stability, 86*(1), 129–134. https://doi.org/10.1016/j.polymdegradstab.2004.02.016.

Moon, H., Ryoo, B., & Park, J. (1994). Concurrent crystallization in polypropylene/nylon-6 blends using maleic anhydride grafted polypropylene as a compatibilizing agent. *Journal of Polymer Science Part B: Polymer Physics, 32*(8), 1427–1435. https://doi.org/10.1002/polb.1994.090320814.

Morent, R., De Geyter, N., Leys, C., Gengembre, L., & Payen, E. (2008). Comparison between XPS- and FTIR-analysis of plasma-treated polypropylene film surfaces. *Surface and Interface Analysis, 40*(3–4), 597–600. https://doi.org/10.1002/sia.2619.

Mülhaupt, R., Duschek, T., & Rösch, J. (1993). Reactive blending of polypropylene/polyamide-6 in the presence of tailor-made succinic anhydride-terminated oligopropene compatibilizers. *Polymers for Advanced Technologies, 4*(7), 465–474. https://doi.org/10.1002/pat.1993.220040710.

Nakason, C., Kaesaman, A., & Supasanthitikul, P. (2004). The grafting of maleic anhydride onto natural rubber. *Polymer Testing, 23*(1), 35–41. https://doi.org/10.1016/s0142-9418(03)00059-x.

Ohlsson, B., Hassander, H., & Törnell, B. (1998). Improved compatibility between polyamide and polypropylene by the use of maleic anhydride grafted SEBS. *Polymer, 39*(26), 6705–6714. https://doi.org/10.1016/S0032-3861(97)10290-7.

Oostenbrink, A. J., & Gaymans, R. J. (1992). Maleic anhydride grafting on EPDM rubber in the melt. *Polymer, 33*(14), 3086–3088. https://doi.org/10.1016/0032-3861(92)90102-3.

Oromiehie, A., Ebadi-Dehaghani, H., & Mirbagheri, S. (2014). Chemical modification of polypropylene by maleic anhydride: Melt grafting, characterization and mechanism. *International Journal of Chemical Engineering and Applications, 5*(2), 117–122. https://doi.org/10.7763/ijcea.2014.v5.363.

Osswald, T., & Rudolph, N. (2015). *Polymer rheology*. Munich: Carl Hanser.

Palabiyik, M., & Bahadur, S. (2000). Mechanical and tribological properties of polyamide 6 and high density polyethylene polyblends with and without compatibilizer. *Wear, 246*(1–2), 149–158. https://doi.org/10.1016/S0043-1648(00)00501-9.

Pan, Y., Ruan, J., & Zhou, D. (1997). Solid-phase grafting of glycidyl methacrylate onto polypropylene. *Journal of Applied Polymer Science, 65*(10), 1905–1912. https://doi.org/10.1002/(sici)1097-4628(19970906)65:10%3c1905::aid-app7%3e3.0.co;2-j.

Pan, B., Viswanathan, K., Hoyle, C. E., & Moore, R. B. (2004). Photoinitiated grafting of maleic anhydride onto polypropylene. *Journal of Polymer Science, Part A: Polymer Chemistry, 42*(8), 1953–1962. https://doi.org/10.1002/pola.20038.

Paracchini, L. (2003). *Manuale di trattamenti e finiture*. Milan: Tecniche Nuove.

Pazzagli, F., & Pracella, M. (2000). Reactive compatibilization of polyolefin/pet blends by melt grafting with glycidyl methacrylate. *Macromolecular Symposia, 149*(1), 225–230. https://doi.org/10.1002/1521-3900(200001)149:1%3c225::aid-masy225%3e3.0.co;2-8.

Pham, T., & Gahleitner, M. (2005). Interfacial strengthening of high-impact polypropylene compounds by reactive modification. *Composite Interfaces, 12*(8–9), 707–723. https://doi.org/10.1163/156855405774984129.

Porejko, S., Gabara, W., & Kulesza, J. (1967a). Grafting of maleic anhydride on polyethylene. I. Mechanism of grafting in a heterogeneous medium in the presence of radical initiators. *Journal of Polymer Science Part A-1: Polymer Chemistry, 5*(7), 1547–1562. https://doi.org/10.1002/pol.1967.150050706.

Porejko, S., Gabara, W., & Kulesza, J. (1967b). Grafting of maleic anhydride on polyethylene. II. Mechanism of grafting in a homogeneous medium in the presence of radical initiators. *Journal of Polymer Science Part A-1: Polymer Chemistry, 5*(7), 1563–1571. https://doi.org/10.1002/pol.1967.150050707.

Pracella, M., & Chionna, D. (2004). Functionalization of styrene-olefin block copolymers by melt radical grafting of glycidyl methacrylate and reactive blending with PET. *Macromolecular Symposia, 218*(1), 173–182. https://doi.org/10.1002/masy.200451418.

Priola, A., Bongiovanni, R., & Gozzelino, G. (1994). Solvent influence on the radical grafting of maleic anhydride on low density polyethylene. *European Polymer Journal, 30*(9), 1047–1050. https://doi.org/10.1016/0014-3057(94)90197-x.

Qi, R., Qian, J., & Zhou, C. (2003). Modification of acrylonitrile-butadiene-styrene terpolymer by grafting with maleic anhydride in the melt. I. Preparation and characterization. *Journal of Applied Polymer Science, 90*(5), 1249–1254. https://doi.org/10.1002/app.12679.

Qiu, W., & Hirotsu, T. (2005). A new method to prepare maleic anhydride grafted poly(propylene). *Macromolecular Chemistry and Physics, 206*(24), 2470–2482. https://doi.org/10.1002/macp.200500375.

Qiu, W., Endo, T., & Hirotsu, T. (2005). A novel technique for preparing of maleic anhydride grafted polyolefins. *European Polymer Journal, 41*(9), 1979–1984. https://doi.org/10.1016/j.eurpolymj.2005.03.016.

Rao, B. M., Rao, P. R., & Sreenivasulu, B. (2008). Grafting of maleic anhydride onto acrylonitrile-butadiene-styrene terpolymer: Synthesis and characterization. *Polymer-Plastics Technology and Engineering, 38*(5), 967–977. https://doi.org/10.1080/03602559909351625.

Rauscher, H., Perucca, M., & Buyle, G. (Eds.). (2010). *Plasma spray coating plasma processes and plasma kinetics low temperature plasmas*. Weinheim: Wiley.

Rietzler, B., Bechtold, T., & Pham, T. (2019). Spatial structure investigation of porous shell layer formed by swelling of PA66 fibers in $CaCl_2/H_2O/EtOH$ mixtures. *Langmuir, 35*(14), 4902–4908. https://doi.org/10.1021/acs.langmuir.8b03741.

Roeder, J., Oliveira, R. V. B., Gonçalves, M. C., Soldi, V., & Pires, A. T. N. (2002). Polypropylene/polyamide-6 blends: Influence of compatibilizing agent on interface domains. *Polymer Testing, 21*(7), 815–821. https://doi.org/10.1016/S0142-9418(02)00016-8.

Rubino, M., Hwang, S. W., Shim, J. K., Selke, S., Soto-Valdez, H., & Auras, R. (2012). Effect of maleic-anhydride grafting on the physical and mechanical properties of poly(L-lactic acid)/starch blends. *Macromolecular Materials and Engineering, 298*(6), 624–633. https://doi.org/10.1002/mame.201200111.

Rubinstein, M., & Colby, R. H. (Eds.). (2003). *Polymer physics*. Oxford: Oxford University Press.

Saelao, J., & Phinyocheep, P. (2005). Influence of styrene on grafting efficiency of maleic anhydride onto natural rubber. *Journal of Applied Polymer Science, 95*(1), 28–38. https://doi.org/10.1002/app.20810.

Samay, G., Nagy, T., & White, J. L. (1995). Grafting maleic anhydride and comonomers onto polyethylene. *Journal of Applied Polymer Science, 56*(11), 1423–1433. https://doi.org/10.1002/app.1995.070561105.

Sathe, S. N., Rao, S. G. S., & Devi, S. (1994). Grafting of maleic anhydride onto polypropylene: Synthesis and characterization. *Journal of Applied Polymer Science, 53*(2), 239–245. https://doi.org/10.1002/app.1994.070530212.

Sclavons, M., Laurent, M., Devaux, J., & Carlier, V. (2005). Maleic anhydride-grafted polypropylene: FTIR study of a model polymer grafted by ene-reaction. *Polymer, 46*(19), 8062–8067. https://doi.org/10.1016/j.polymer.2005.06.115.

Seo, Y., & Ninh, T. H. (2004). Enhanced interfacial adhesion between polypropylene and nylon 6 by in situ reactive compatibilization. *Polymer, 45*(25), 8573–8581. https://doi.org/10.1016/j.polymer.2004.10.006.

Seo, Y., Kim, J., Kim, K. U., & Kim, Y. C. (2000). Study of the crystallization behaviors of polypropylene and maleic anhydride grafted polypropylene. *Polymer, 41*(7), 2639–2646. https://doi.org/10.1016/S0032-3861(99)00425-5.

Shi, D., Yang, J., Yao, Z., Wang, Y., Huang, H., Jing, W., Yin, J., & Costa, G. (2001). Functionalization of isotactic polypropylene with maleic anhydride by reactive extrusion: Mechanism of melt grafting. *Polymer, 42*(13), 5549–5557. https://doi.org/10.1016/s0032-3861(01)00069-6.

Shi, D., Ke, Z., Yang, J., Gao, Y., Wu, J., & Yin, J. (2002). Rheology and morphology of reactively compatibilized PP/PA6 blends. *Macromolecules, 35*(21), 8005–8012. https://doi.org/10.1021/ma020595d.

Su, Z., Li, Q., Liu, Y., Hu, G. H., & Wu, C. (2009). Compatibility and phase structure of binary blends of poly(lactic acid) and glycidyl methacrylate grafted poly(ethylene octane). *European Polymer Journal, 45*(8), 2428–2433. https://doi.org/10.1016/j.eurpolymj.2009.04.028.

Sun, Y. J., Hu, G. H., & Lambla, M. (1995). Melt free-radical grafting of glycidyl methacrylate onto polypropylene. *Die Angewandte Makromolekulare Chemie, 229*(1), 1–13. https://doi.org/10.1002/apmc.1995.052290101.

Sun, Y. J., Hu, G. H., Lambla, M., & Kotlar, H. K. (1996). In situ compatibilization of polypropylene and poly(butylene terephthalate) polymer blends by one-step reactive extrusion. *Polymer, 37*(18), 4119–4127. https://doi.org/10.1016/0032-3861(96)00229-7.

Tang, F., Bao, P., & Su, Z. (2016). Analysis of nanodomain composition in high-impact polypropylene by atomic force microscopy-infrared. *Analytical Chemistry, 88*(9), 4926–4930. https://doi.org/10.1021/acs.analchem.6b00798.

Teng, J., Otaigbe, J. U., & Taylor, E. P. (2004). Reactive blending of functionalized polypropylene and polyamide 6: *In situ* polymerization and in situ compatibilization. *Polymer Engineering and Science, 44*(4), 648–659. https://doi.org/10.1002/pen.20059.

Thomas, M., & Mittal, K. L. (Eds.). (2013). *Atmospheric pressure plasma treatment of polymers*. Hoboken, NJ: Wiley. https://doi.org/10.1002/9781118747308.

Torres, N., Robin, J. J., & Boutevin, B. (2001). Functionalization of high-density polyethylene in the molten state by glycidyl methacrylate grafting. *Journal of Applied Polymer Science, 81*(3), 581–590. https://doi.org/10.1002/app.1473.

Valenza, A., Spadaro, G., & Acierno, D. (2000). Dynamic rheological characterization of polyamide/modified polyolefin laminates. *Colloid and Polymer Science, 278*(10), 986–992. https://doi.org/10.1007/s003960000357.

Van Duin, M. (2003). Grafting of Polyolefins with maleic anhydride: Alchemy or technology? *Macromolecular Symposia, 202*(1), 1–10. https://doi.org/10.1002/masy.200351201.

Van Duin, M., Aussems, M., & Borggreve, R. J. M. (1998). Graft formation and chain scission in blends of polyamide-6 and -6.6 with maleic anhydride containing polymers. *Journal of Polymer Science, Part A: Polymer Chemistry, 36*(1), 179–188. https://doi.org/10.1002/(sici)1099-0518(19980115)36:1<179::aid-pola22>3.0.co;2-f.

van Puyvelde, P., Velankar, S., & Moldenaers, P. (2001). Rheology and morphology of compatibilized polymer blends. *Current Opinion in Colloid & Interface Science, 6*(5–6), 457–463. https://doi.org/10.1016/s1359-0294(01)00113-3.

Wei, Q., Chionna, D., Galoppini, E., & Pracella, M. (2003). Functionalization of LDPE by melt grafting with glycidyl methacrylate and reactive blending with polyamide-6. *Macromolecular Chemistry and Physics, 204*(8), 1123–1133. https://doi.org/10.1002/macp.200390081.

Wei, Q., Chionna, D., & Pracella, M. (2005). Reactive compatibilization of PA6/LDPE blends with glycidyl methacrylate functionalized polyolefins. *Macromolecular Chemistry and Physics, 206*(7), 777–786. https://doi.org/10.1002/macp.200400362.

Wolf, R. A. (2013). *Atmospheric pressure plasma for surface modification*. Hoboken, NJ: Wiley. https://doi.org/10.1002/9781118547519.

Wu, C.-J., Chen, C.-Y., Woo, E., & Kuo, J.-F. (1993). A kinetic study on grafting of maleic anhydride onto a thermoplastic elastomer. *Journal of Polymer Science: Part A: Polymer Chemistry, 31*(13), 3405–3415. https://doi.org/10.1002/pola.1993.080311329.

Yang, L., & Thomason, J. L. (2012). Development and application of micromechanical techniques for characterising interfacial shear strength in fibre-thermoplastic composites. *Polymer Testing, 31*(7), 895–903. https://doi.org/10.1016/j.polymertesting.2012.07.001.

Ye, J., Midorikawa, H., Awatani, T., Marcott, C., Lo, M., Kjoller, K., & Shetty, R. (2012). Nanoscale infrared spectroscopy and AFM imaging of a polycarbonate/acrylonitrile-styrene/butadiene blend. *Microscopy and Analysis, 26*, 24–27. Retrieved from https://microscopy-analysis.com/sites/default/files/magazine_pdfs/magazine%202012_april_ye.pdf.

Zarrintaj, P., Jouyandeh, M., Ganjali, M. R., Hadavand, B. S., Mozafari, M., Sheiko, S. S., Vatankhah-Varnoosfaderani, M., Gutiérrez, T. J., & Saeb, M. R. (2019). Thermo-sensitive polymers in medicine: A review. *European Polymer Journal, 117*, 402–423. https://doi.org/10.1016/j.eurpolymj.2019.05.024.

Zhandarov, S., & Maeder, E. (2005). Characterization of fiber/matrix interface strength: Applicability of different tests, approaches and parameters. *Composites Science and Technology, 65*(1), 149–160. https://doi.org/10.1016/j.compscitech.2004.07.003.

Zhang, J., & Sun, X. (2004). Mechanical properties of poly(lactic acid)/starch composites compatibilized by maleic anhydride. *Biomacromolecules, 5*(4), 1446–1451. https://doi.org/10.1021/bm0400022.

Zhang, R., Zhu, Y., Zhang, J., Jiang, W., & Yin, J. (2005). Effect of the initial maleic anhydride content on the grafting of maleic anhydride onto isotactic polypropylene. *Journal of Polymer Science, Part A: Polymer Chemistry, 43*(22), 5529–5534. https://doi.org/10.1002/pola.21038.

Zhou, X., Zhang, P., Jiang, X., & Rao, G. (2009). Influence of maleic anhydride grafted polypropylene on the miscibility of polypropylene/polyamide-6 blends using ATR-FTIR mapping. *Vibrational Spectroscopy, 49*(1), 17–21. https://doi.org/10.1016/j.vibspec.2008.04.004.

Zhu, Y., An, L., & Jiang, W. (2003). Monte Carlo simulation of the grafting of maleic anhydride onto polypropylene at higher temperature. *Macromolecules, 36*(10), 3714–3720. https://doi.org/10.1021/ma0342168.

Zisman, W. A. (1964). Relation of the equilibrium contact angle to liquid and solid constitution. *Advances in Chemistry Series, 43*, 1–51. https://doi.org/10.1021/ba-1964-0043.ch001.

Chapter 5
Design of Switchable and Supramolecular Polymers for Biointerface Applications

Luanda Lins

Abstract An elegant combination of switchable and supramolecular polymers exhibiting linear and nonlinear topological structures results a new range of advanced materials. A good methodology for creating surface-based switchable structures is to use molecules capable of building an extended supramolecular network without the requirement to adding any additional agent. The supramolecular interactions are inspired by natural processes, thus providing complex systems from spontaneous assemblies of molecules. Switchable and supramolecular polymers are inherently dynamic, and their constituents are linked by reversible connections allowing assembly/disassembly processes under particular conditions. Due to this intrinsic capacity, these materials can select their constituents in response to external stimuli and have capacity for adaptability. As a consequence, these dynamic materials have new properties, such as self-repair, adaptability and response to stimuli (additives, heat, light, etc.). This leads to perfect control of the spatial (structural) and temporal (dynamic) characteristics of matter. This chapter highlights the advances in the use of switchable and supramolecular polymers to form extended self-assemble arrays that propagate in parallel to the plane of a surface substrate. The use of such supramolecular assemblies to trap bio-guest molecules and living cells, mimicking natural nanostructures, will also be discussed.

Keywords Responsive polymers · Supramolecular polymers · Surface-based self-assembly · Switchable molecules

---

L. Lins (✉)
Université de Lyon, INSA de LYON, MATEIS UMR CNRS 5510,
Villeurbanne Cedex, France

National Institute of Applied Sciences, Lyon, France

T. J. Gutiérrez (ed.), *Reactive and Functional Polymers Volume Four*,
https://doi.org/10.1007/978-3-030-52052-6_5

5.1 Introduction

Switchable bio-interfaces can change their properties in response to applied stimuli, such as electric/magnetic field, ionic, light, pH strength, solvent polarity, temperature or small biomolecules. Interfaces are particularly important at the nanoscale and often dominate the properties of biomaterials. Driven by the initial studies of interactions between biomaterials and living fluids, self-assembled monolayers on surfaces have clarified many aspects of nanotechnology, offering new strategies and methodologies to advance our understanding of biotechnology at the molecular scale. From the perspective of molecular science, interfaces serve as templates that facilitate the organization of cells, biomolecules, and proteins. Interfaces are particularly important at nanoscale and often dominate the properties of biomaterials. It is precisely at this scale that exactly where the interface interacts actively altering the properties of surface-arranged assemblies and organizing complex molecular arrangements (Goronzy et al. 2018). Since the material surface is the first to interact with the *in vivo* environment, interface interactions play a key role in the implantation of a biomaterial. In this sense, to achieve adequate surface functionality, a wide spectrum of different strategies can be used, such as supramolecular interactions, covalent modification and the incorporation of biomimetic signals (Chang et al. 2019).

In the biological environment, not only the functionalities as tunable mechanical properties, regulation of the degradability and the ease for bioactivity incorporation must be ideal, but the material must also mimic the natural environment where the materials are carried (Dankers Patricia and Meijer 2007). Keeping this in view, a modular self-assembly approach can be applied by using several supramolecular moieties. This is an exquisite way to produce ‘responsive’ biomaterials. Responsive switchable and supramolecular materials are a path to the guidance of living biomimetic molecules. Several strategies have been reported to obtain a surface that can undergo topographic changes and switchable interactions, including light-, pH- and thermo-responsive, which can control cell adhesion and detachment, control of self-propelled bacteria, release of active principles, or detection of bio-molecules (Goor et al. 2017a).

Supramolecular chemistry is an exciting multidisciplinary domain of science that can bring together different areas, from molecular medicine to nanotechnology (Dankers Patricia and Meijer 2007). The science of materials based on supramolecular interactions remains an emerging field, and has given great steps for the advancement of biotechnology. Supramolecular assemblies consist of molecules (or macromolecules) that are held together by non-covalent interactions such as hydrophobic interactions, hydrogen (H)-bonding, π-stacking, van der Waals forces, electrostatic interactions or combinations thereof in aqueous or organic solvent systems (Ulijn 2006). Figure 5.1 shows some supramolecular interactions that will be discussed in this chapter. Previously, in these systems, non-covalent interactions can usually be reversible by the application of stimuli such as addition/removal of

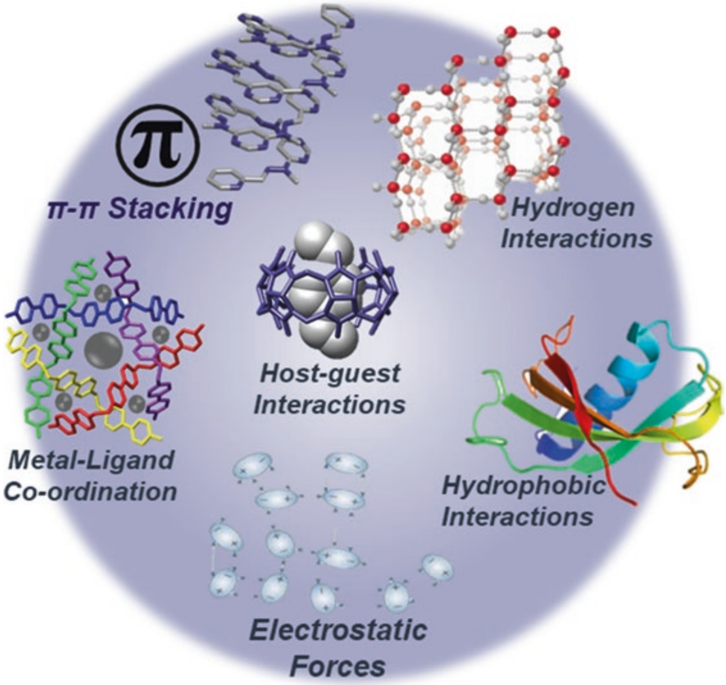

Fig. 5.1 Some supramolecular interactions

certain chemical entities, biochemical cues, ionic strength, pH changes, shear forces and temperature (Ulijn 2006).

Switchable and supramolecular polymers can be considered a new generation of biomaterials with special interactions for biotechnology applications. Supramolecular polymers can be defined as a monomeric network with reversible and dynamic interactions thought non-covalent bonds, resulting in specific polymeric properties. According to the theories of polymer physics, these systems are considered as supramolecular polymers due to their strength and directional interactions (Goor et al. 2017b). In summary, that switching of stimulus-sensitive polymer chains is expected to have specific characteristics given by secondary (or supramolecular) interactions between chains or for the construction of polymer chains.

In this chapter, the elementary features of the switchable and supramolecular polymers trailed by a profuse classification of responses to stimuli along with their applications in biointerfaces will be highlighted in terms of biotechnology, such as, antibacterial surface, biosensors, cell adhesion, drug delivery and smart biocoatings (Table 5.1).

Table 5.1 Stimulus-responsive supramolecular interfaces for biomaterial applications

Applications	Supramolecular functions	References
Antibacterial surface	Supramolecular self-assembled monolayer platform can capture and release bacteria through ultraviolet (UV) light irradiation or host-guest interactions.	Bian et al. (2018)
Biosensors	Supramolecular biosensor may be appropriately defined as a device capable to trigger an observable chemical or physical modulation in the presence of biomolecular species.	Tokarev and Minko (2009)
Cell adhesion	Supramolecular polymer on the surface allows specific localization and control over the cell interface and low interference with normal biological function.	Goulet-Hanssens et al. (2012)
Drug delivery	Modifications on surfaces of biomaterial carriers with supramolecular moieties is a new strategy to manufacture active principles (cells, drugs, proteins, etc.) that can release therapeutic agents through particular triggers.	Tran and Nguyen (2017)
Smart biocoatings	Smart coatings are referred as a surface coating layer which can exhibit a triggered macroscopic response by exposure to stimuli.	Zhao et al. (2019)

5.2 Supramolecular Polymer Interactions Building Switchable Biointerfaces

5.2.1 *Hydrogen Bonding*

DNA double helix formation is the best-known example of supramolecular systems with H-bonding interactions. The pairing of nucleic acid chains is perhaps the most elegant example of self-association in nature. Lehn (2005) defined this combination of self-assembly systems from electropositive or acidic hydrogen in association with electronegative or basic atoms (N, O, S, …) in polymer networks as dynamic dimers. These non-covalent bonds can provide directional interactions and selective force by homo- and heterocomplementarity. In view of the ability of the dimer to self-associate in response to external stimuli or environmental factors, they are widely used as switchable materials.

The combination of multiple H-bonds in dimers form more stable interactions, which makes these associative groups an optimal option for use on re-codable surfaces. Zeng et al. (2000) reported that the combination of dimers based on six linked H-bonds formed a stable molecular duplex with a dimerization constant of $1.3 \times 10^9\ M^{-1}$ in chloroform. Beijer et al. (1998a, b) and Söntjens et al. (2000) developed strongly self-complementary dimerizing quadruple H-bonding groups based on triazine and pyrimidine heterocycles.

The H-bonding energy is the sum of electrostatic energy, polarization and charge transfer, as well as repulsion and dispersion forces (Hiroshi 1954; Taylor et al. 1984). The supramolecular interactions depend on the sequence of the donors and acceptors. The result of energy exchanges occurs between a positively polarized hydrogen atom, covalently bound to a hetero atom with higher electronegativity

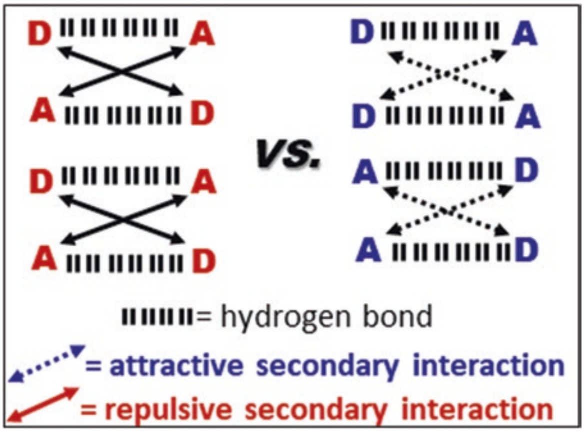

Fig. 5.2 Interactions in DADA and DDAA dimers. While both dimers have four primary attractive H-bonds, the DADA dimer has six repulsive secondary interactions, whereas the DDAA dimer has two repulsive and four attractive secondary interactions. Adapted with permission from Beijer et al. (1998b)

(N, O, F, P, S), called proton donors ‘D’, and a hetero atom with a pair of free electrons, called proton acceptor ‘A’ (Kollman and Allen 1972). As can be seen in Fig. 5.2, the interaction force of the dimers depends on the different arrangements between A and D, i.e. different repulsive and attractive interactions of the atoms.

The combinations between the intermolecular H-bonding sites provide an N number of different dimers. According to the example given by Zeng et al. (2000), these numbers of dimer sequences can be calculated from the following equation:

$$N = 2^{n-2} + 2^{(n-3)/2} \quad \text{when} \quad n = \text{odd number} \tag{5.1}$$

$$N = 2^{n-2} + 2^{(n-2)/2} \quad \text{when} \quad n = \text{even number} \tag{5.2}$$

when n is an odd number, only hetero-complementary dimers are formed. On the other hand, when n is an even number, self- and hetero-complementary dimers are made possible. In the second equation, the first term is the number of hetero-complementary dimers and the second term is number of self-complementary dimers. The increase in the number N is directly proportional to the number of intermolecular H-bonding. For example, for various applications of the supramolecular polymer domain, 2-ureido-4(1H)-pyrimidinone (UPy) is of particular interest because it endows reversible and self-commentary properties to oligomers or polymers. UPy is a self-complimentary quadruple H-bonding motif based on arrangement of AADD interactions. UPy’s tautomerized product with ADDA interactions or DAAD interactions shows a self-complementary homo-dimerization of $1.6 \times 10^7\ M^{-1}$ in chloroform (Fouquey et al. 1990). The UPy-units can be incorporated into sensitive polymers *via* a modular approach giving rise to a platform of material functionalization. For surface engineering, some researchers have been reported the incorporation of anti-fouling UPy-based polymers and additives for the development of functional biomaterials (van Almen et al. 2016; Pape et al. 2017). According to Goor et al. (2017a, b), this approach allows the surface modification

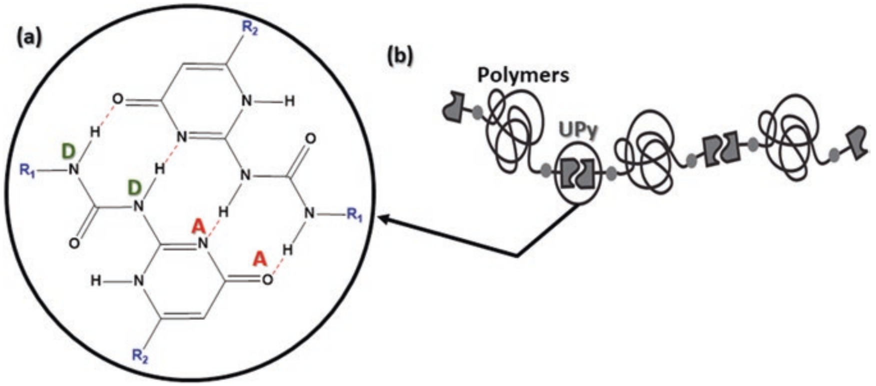

Fig. 5.3 (**a**) Combined sequences of H-bond donors and UPy acceptors, and (**b**) polymeric assembly of a bifunctional ureidopirimidinone derivative. (Adapted with permission from Ren et al. 2019)

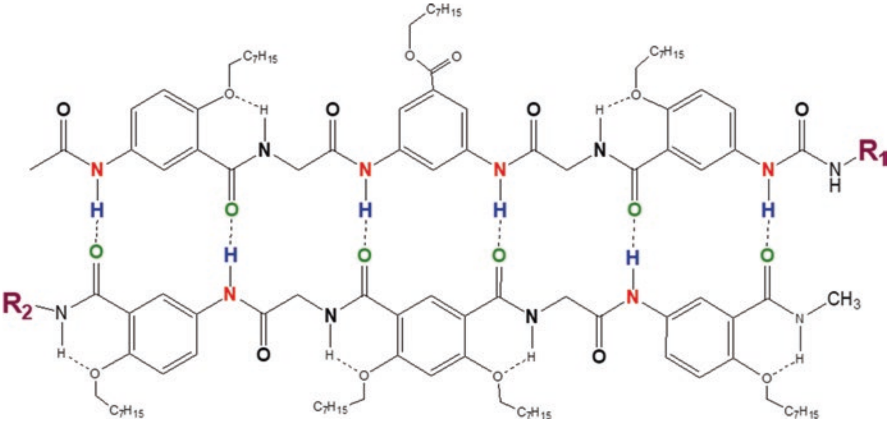

Fig. 5.4 Hetero-complementary H-bonding dimer of SOA and AOA. Adapted with permission from Zeng et al. (2000)

and can provide a method to decouple the material processing conditions and post-functionalization (Fig. 5.3).

Other polymer systems involving H-bonded hetero-complementary interactions for polymer science have also been speculated. Gong et al. (1999) were the pioneers to synthesize oligoamides with the self-complementary H-bonding sequences DADA and DDAA, which formed stable dimers *via* H-bonding interactions between donors of backbone amide hydrogens and carbonyl oxygen acceptors. Symmetric oligoamide (SOA) and the asymmetric oligoamide (AOA) represent the first example of a hetero-complementary H-bonding dimer with six H-bonding sites (Fig. 5.4). In another work Zeng et al. (2000) also demonstrated that the incorporation of alkoxy groups into self-complementary dimers leads to the formation of the highly favorable hetero-complementary H-bonded rings.

The stability of the dimers depends mainly on the number of intermolecular H-bonds, so increasing the number of H-bonding interactions in the complex should lead to an increase in dimer stability (Gong 2007). Henceforth, oligoamides are expected to exhibit a greater association constant than self-complementary UPy, as is the case of $Ka > 10^9$ M^{-1} in chloroform (Zeng et al. 2003). More recently, other authors have also demonstrated that oligoamides dimers show tunable affinity, programmable sequence specificity and convenient synthetic availability, thus offering an ideal class for the preparation of switchable polymers (Montarnal et al. 2015; Wedler-Jasinski et al. 2016).

Very few examples of rewritable surfaces from supramolecular interactions can be found from the literature. However, Wedler-Jasinski et al. (2016) inspired by surface-assisted DNA-directed immobilization have suggested the construction of recoverable surfaces from the SOA-AOA dimers. In summary, these authors immobilized AOA onto silicon surface *via* a photo-induced reaction. Onto the AOA layer, the SOA-polymer was immobilized and subsequently removed from the surface several times to underpin the system's switching.

In a parallel view, Montarnal et al. (2015) developed nanoimprinted surfaces from hetero-complementary supramolecular copolymers. AOA-polystyrene (PS) and SOA-poly(methyl methacrylate) (PMMA) were synthesized and fashioned on a surface, then the hydrophilic block was sacrificed forming well-ordered porous morphologies. The disassembled-on request by a solvent trigger of SOA-AOA motif-copolymer can be a good strategy for forming lithographic surfaces and could be very useful for selective cell-growth on the surface. Recoverable surfaces covered with AOA receptors can be a coded and re-encoded by their SOA-partner linked to biomolecules such as peptides and proteins.

5.2.2 *Macrocyclic Host-Guest Interactions*

The development of new approaches to the construction of micropatterned engineered surfaces is of great interest because they are frequently incorporated into biological sensors. With this in mind, the stimulus-sensitive supramolecular polymers based on the macrocyclic host-guest interactions, such as calix[n]arenes, cucurbit[n]urils (CB[n]), cyclodextrins (CDs) and pillar[n]arenes (PA[n]s), have been widely reported for the biological interface (Li et al. 2014, 2017; Lou and Yang 2018). In these examples, the assembly of guest molecules with a host-functionalized surface is achieved by the formation of binary complexes. The interactions between switchable polymers and host-guest macrocyclic can occur from functionalization of the polymer chains with the host molecules, guest molecules, or both (Lehn 2002; Korde and Kandasubramanian 2019).

Li et al. (2014) prepared hybrid nanocarriers from β-CD and star-shaped poly(glycidyl methacrylate)s, named PGMA (S5-PGMA-CD), to form a supramolecular gating machines for drug delivery systems. They reported that S5-PGMA-CD was anchored on the azobenzene-modified surface by driving the guest-host interactions (Li et al. 2014). These authors also reported that these supramolecular nanovalves exhibited competitive binding agents and temperature, and showed better performance in the load encapsulation and release compared to the traditional type of nanovalve system used by the β-CD itself (Li et al. 2014). Other similar research was conducted by Bian et al. (2018) for the manufacture of reusable platforms for biotechnological applications. In this work, visible-light-responsive polymers were produced, chemically linked to polyanionic and polycationic polymers and then reversibly bound to CD-terminated substrates by host-guest interactions. Polycations showed great antimicrobial properties, while the polyanions also showed good bioadhesive properties, since they could be switched through the host-guest interactions after visible light irradiation.

The host-guest complexes based on multivalent cucurbit[8]uril (CB[8]) have been based primarily on polymeric scaffolds (Valderrey et al. 2019). CB[8] can efficiently include a second electron-rich aromatic guest, thus showing an association constant of 10^5–10^6 M^{-1}, and the resulting methyl viologen⊂CB[8]. These host-guest complexes can be used to selectively adhere cells, bacteria or proteins to surfaces and controlled drug release (Bosmans et al. 2015). Valderrey et al. (2019) demonstrated that heteroternary complexes through CB[8] can be successfully formed on self-assembled surfaces providing complexes with bond strengths similar to those of the solution. Valderrey et al. (2019) grafted poly-L-lysine with oligo(ethylene glycol) on cyclic olefin polymer surfaces, then maleimide moieties were deposited and further modified with thiolated methyl viologen and CB[8] (Fig. 5.5b). In order to demonstrate the stability and switchable properties of complexes on CB[8] surfaces, the different valence and fluorescence of the guests were exploited to create surfaces of micrometer-sized patterns (Fig. 5.5c), and finally, the supramolecular exchange on surface-bound heterocomplexes was informed from empirical results, which allows cross-patterns to be created taking advantage of the molecular valence and also obtaining photoresponsive properties.

5.2.3 *Electrostatic Interactions*

Another biointerface strategy that takes advantage of supramolecular and switchable polymers is the deposition of multilayer polyelectrolytes, e.g. poly(styrene sulfonate)-poly(allylamine), hyaluronic acid-chitosan, among others. A simple method for surface deposition of these active layers is through layer-by-layer (LbL) method. In this technique, a charged surface is sequentially dipped into alternating aqueous solutions of polyelectrolytes of opposite charge to deposit thin multilayers of a polyelectrolyte complex (this technique will be discussed in Sect. 5.3.1). For example, an antibacterial surface was manufactured by Chua et al. (2008) using LbL self-assembly. The deposition alternating layers of hyaluronic acid (negatively charged) and chitosan (positively charged) were deposited on titanium, resulting in a reduced bacterial adhesion due to the antibacterial properties of chitosan.

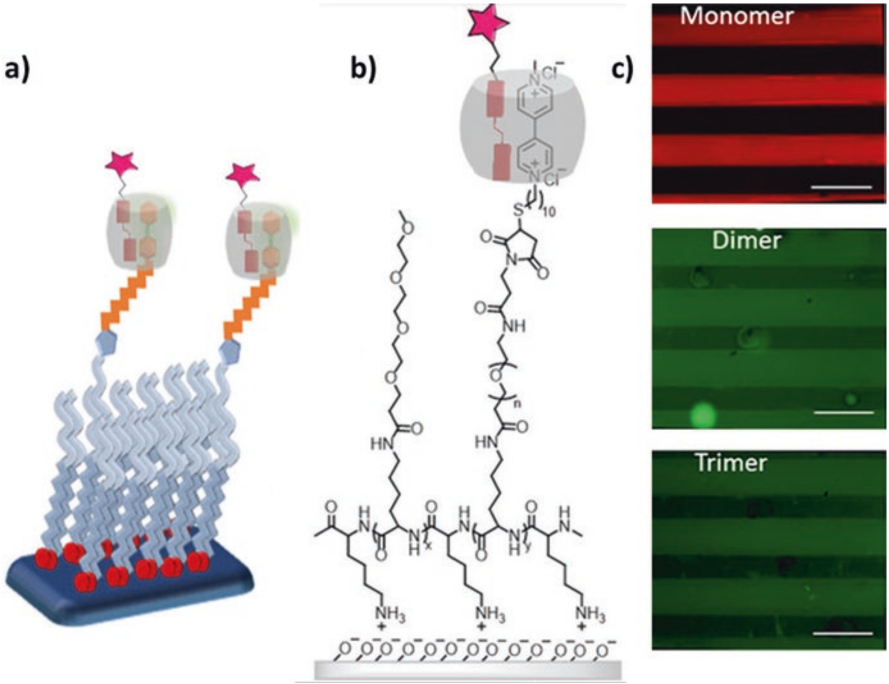

Fig. 5.5 (**a**) Schematic outline of the formation of the CB[8] layer on cyclic olefin polymer surfaces, (**b**) surfaces and formation of heteroternary complex, and (**c**) fluorescence microscopy images and their corresponding intensity profiles of 4b⊂CB[8]-functionalized cyclic olefin polymer surfaces, where monomer = rhodamine-labelled, dimer = dimeric azopyridine, and trimer = trimeric azopyridine. Adapted with permission from Valderrey et al. (2019)

Another approach is to create polyelectrolyte multilayers (PEMs) from a simple deposition or dip-coating. For example, Goulet-Hanssens et al. (2012) demonstrated the combination of cytophilicity of the photo-switched and tailored surfaces in order to create a surface capable of photoactivating. For this purpose, the surfaces were coated with poly(acrylic acid)-poly(allylamine hydrochloride) polyelectrolyte bilayer functionalized with a small fraction of an azobenzene-based photo-switchable endgroup, which included the cell-adhesive RGD peptide. According to Goulet-Hanssens et al. (2012) the use of PEMs with the combination of photo-switched surface provides a space of significant parameters for fine-tuning of tailored biosurfaces with ideal control.

In addition, the stimuli-responsive polyelectrolytes can be used as brushes on a switchable surface responding to triggers such as ionic strength, light, pH, temperature, etc. The interaction of the polyelectrolytes with the external stimulus, e.g. fluid with different pH or ionic strength causes swelling-shrinking of the polymer brush, thus affecting the permeability of the system (Fig. 5.6a–c) (Minko 2006; Tokarev and Minko 2009). An interface with mixtures of polyanionic and polycationic brushes can also respond to different stimuli forming nanoscopic domains (Fig. 5.6c).

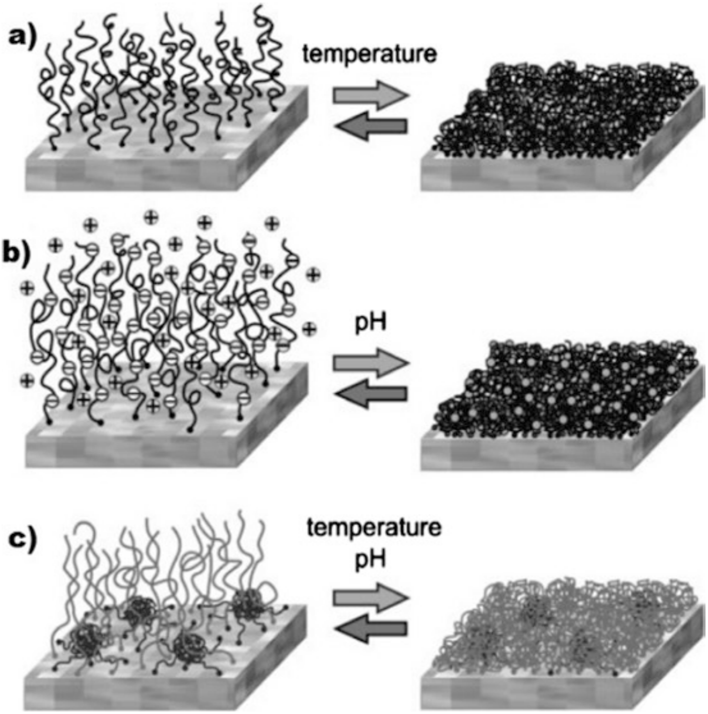

Fig. 5.6 (**a**) Swelling-shrinking transition of a thermo-responsive brush, (**b**) swelling-shrinking transition of a PE brush, and (**c**) swelling-shrinking transition of a mixed brush, all on external stimuli. Reproduced with permission from Tokarev and Minko (2009)

5.2.4 Metal-Ligand Coordination

Supramolecular structures are also represented by the great combination of inorganic metals and organic ligands. The inorganic component (polar) can be a metal, a transition metal or a group of metals, while the organic component (nonpolar) can be some polymer, biomolecule, ligand, among others (Barth 2007; Beg et al. 2017). Metal-organic coordination can produce a highly organized metal-organic network on surfaces from self-assembly strategies (Smith et al. 2004; Goronzy et al. 2018; Valencia et al. 2019). Metal organic frameworks are considered a new generation of hybrid material capable of producing sensitive and highly organized metallo-supramolecular grating for biomedical application (Fig. 5.7).

The metal-organic coupling scheme of carboxylate can, for example, be used to tailor coordination architectures in two dimensions. A series of investigations with polymeric coordination chains have allowed us to give an idea of the principles underlying the complexation of transition-metal centers on surfaces and illustrate their potential for rational 2-D (Barth 2007). Amino acids represent a class of biomolecules highly qualified for molecular recognition on surfaces (Schiffrin et al. 2007).

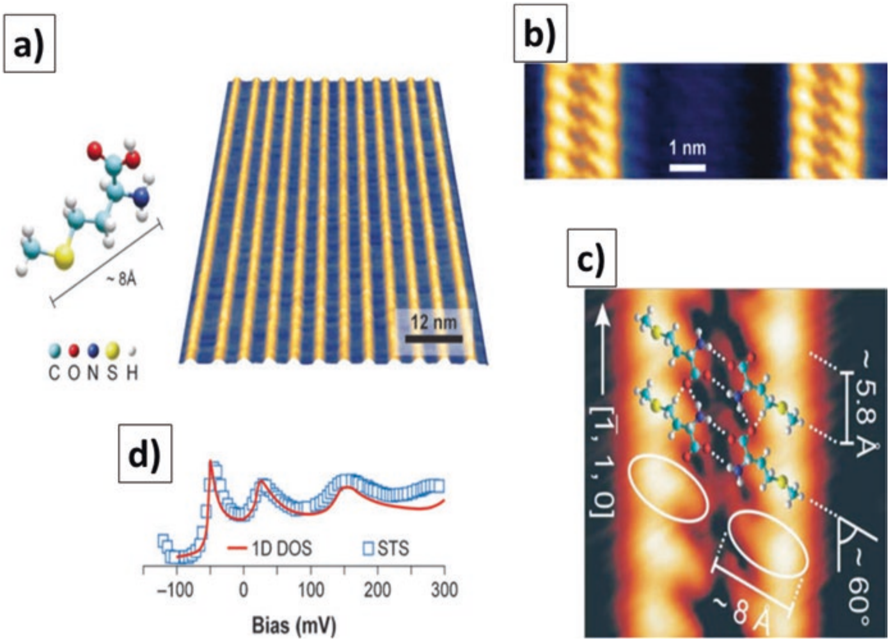

Fig. 5.7 (**a**) Periodicity in a nanograting of an amino acid on a metal surface, (**b**, **c**) high-resolution scanning tunneling microscopy image of twin amino acid chains, (**d**) scanning tunneling spectroscopy on undecorated substrate areas. Adapted with permission from Schiffrin et al. (2007)

In this sense, Pennec et al. (2007) and Schiffrin et al. (2007) underwent zwitterionic self-assembly of methionine on the substrate Ag(111), thus forming a highly regular 1D superlattices with a tunable periodicity. X-ray photoelectron spectroscopy (XPS) analysis showed that these nanogratings were formed by molecular quadruple or twin chains (see Fig. 5.7b, c).

Kumpfer et al. (2010) also produced stimulus-sensitive films from 4-oxy-2,6-bis-(1′-methylbenzimidazolyl)pyridine ditopic-endcapped poly(tetrahydrofuran) incorporating variable ratios of Eu^{3+} and Zn^{2+}. These authors reported that a possible biosensor was elucidated. For this purpose, a pronounced optical response was observed in exposure to chemicals, such as triethyl phosphate, which was used to mimic organophosphate pesticides and nerve gas agents (Kumpfer et al. 2010).

5.2.5 *π-π Staking*

The π-π stacking interaction is the result of the overlapping of p-orbitals present in conjugated systems. The π-conjugate interactions are non-covalent interfaces between aromatic parts in organic compounds, in which the interaction is strengthened with the increase of number of π-electrons (Korde and Kandasubramanian

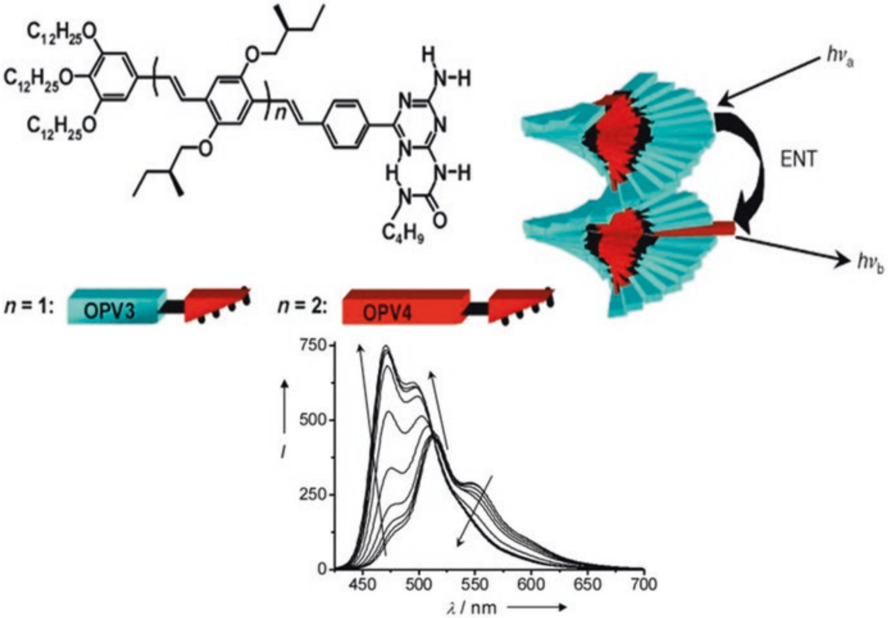

Fig. 5.8 Temperature-dependent fluorescence spectra of monofunctionalized oligo(*p*-phenylene vinylene)s MOPV4 and MOPV3 in dodecane solution (lexc = 412 nm). Extended columnar aggregates of MOPV3 incorporating MOPV4 show a very efficient extinction of MOPV3 fluorescence, indicating energy transfer within the supramolecular stacks from the shortest to the longest oligomer. Reproduced with permission from Hoeben et al. (2004)

2019). Despite the π-π stacking force is neither strong nor directional compared to H-bonding interactions. However, some studies have been reported on switchable biomaterials with π-conjugated systems (González-Rodríguez and Schenning 2011).

Another interesting supramolecular similar model is to create the self-assembly of small π-conjugated functional molecules into supramolecular polymers in solution or in solid state. With this in mind, considerable efforts are being focused on the modification of the structure of π-conjugated systems combined with biomolecules and responsive polymers. Jonkheijm et al. (2006) and Korevaar et al. (2012) have shown π-conjugated self-assembled structures ranging from micrometers to bridges top-down structures created by lithographic techniques. These authors reported the formation of helical columnar aggregates in dodecane by chiral π-conjugated oligo(*p*-phenylene vinylene) (OPV) linked in the hierarchical self-assembly of ureidotriazine units (Fig. 5.8). The well-defined structure of the molecular oligo(*p*-phenylene vinylene) (MOPV) column aggregates provides an attractive scaffold for studying energy transfer in these columns. When a small number of ureidotriazine units with a longer conjugation length (Fig. 5.8—MPOV4) is incorporate into a stack of columns, an energy transfer occurs, thus showing a temperature response (Hoeben et al. 2004).

The combination of other supramolecular interactions (e.g. H-bonding and host-guest interactions) and π-π stacking has also been beneficial for designing stimulus-sensitive polymeric materials with inherent properties of π-conjugated monomers. Supramolecular polymers were synthesized by Liu et al. (2011) from anthracene derivatives and CB[8] by using host-enhanced and π-π interactions in order to make water-soluble compounds. The main idea was to manufacture a ternary complex by encapsulating couple of anthracene molecules in a CB[8] cavity, but they also observed an increasing π-π interactions between the anthracene molecules after the distance was shortened. All these studies have generated a great deal of knowledge for the design of a variety of switchable materials with intriguing properties.

5.3 Preparation Techniques

5.3.1 Layer-by-Layer

A few decades ago, the classic realization of LbL assembly became passionate in materials science as an interesting alternative for switchable biointerfaces (Zhao et al. 2019). This technique involves the sequential assembly of the layers, followed by the washing step after the addition of each layer, in order to reduce the excess of unmounted materials or molecules. In the LBL technique, polycations and polyanions are deposited on the charged substrates *via* oppositely electrostatic forces (see Fig. 5.9) (Amani et al. 2019). In addition, other forces may also be involved in the assembly of multilayer films through the LBL technique such as, covalent, hydrophobic and H-bond interactions. The convenient tailoring the surface chemistry is due to a wide variety of materials from which layers can be formed.

An additional advantage of the LbL technique is the variability of each double layer in relation to chemical or physical properties, which allows the modular construction of multifunctional devices, thus enabling different combinations. The wide and independent variability of each double layer results in the control response capability of polyelectrolyte assemblies, making it an extremely versatile technology. Additionally, the LbL technology can mimic the physic-chemical properties of living organisms, which leads to the promising spectrum for biomaterial engineering.

For biointerface technology, the mild deposition conditions of the LbL provide a means to immobilize different biomolecules on the surfaces (El-khouri et al. 2011). The layer assemblies can integrate genetic material, plasmids, proteins (Jan et al. 2011), antibiotics, antibodies and growth factors (Crouzier et al. 2010) directly onto the layers or the components can be assembled as complexes (Romero et al. 2013). As a response mechanism of switchable polymer layers, e.g. growth factors, its action can be triggered by external stimuli or its controlled release can be regulated by barrier layers. The excellent material properties of the multilayer composite and the ease of technique approach makes possible the fabrication and implementation

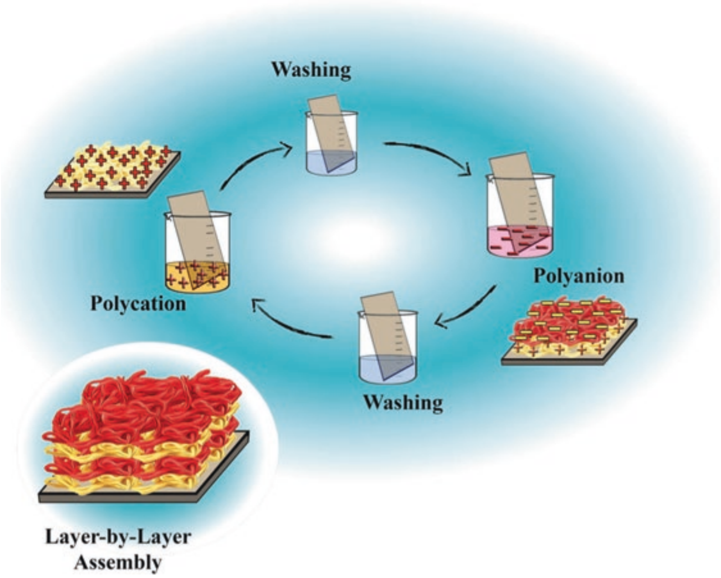

Fig. 5.9 The multilayer LbL assembly of polymers with opposite charges (polyanions and polycations) are deposited on the charged substrates *via* an electrostatic force, providing a surface coating on precisely controlled scales. Reproduced with permission from Amani et al. (2019)

of implantable devices (Kozai et al. 2012), antibacterial surfaces (Muzzio et al. 2017), biosensors (Montjoy et al. 2018), cells adhesion (Muzzio et al. 2019) and drug delivery vehicles (Tong et al. 2012).

5.3.2 Lithography

Lithography is a micro- and nano-fabrication printing on smooth surfaces of a plate or stone. This technique allows the formation of complex structures in two- or three-dimensional at extremely small scales. The lithography has been gaining ground for research in surface engineering, nanotechnology devices and especially in biomedical areas. The emergence of lithography-based techniques for designing surface-sensitive, defined-shape and highly-controlled systems offers a promising alternative in the field of biomedicine (Tran and Nguyen 2017). This fabrication approach has allowed the creation of nanopatterns of switchable responsive polymers, such as thermosensitive polymers (see Fig. 5.10) (He et al. 2007).

Different lithography techniques are being developed for the biomedical field. In this section, some lithography techniques that have been widely used in biointerfaces will be discussed. Photolithography is defined as a process that uses light to transfer patterns in selective areas using a photomask to a photoresist or using micro-scale features designed in a computer-aided design software (Hahn et al.

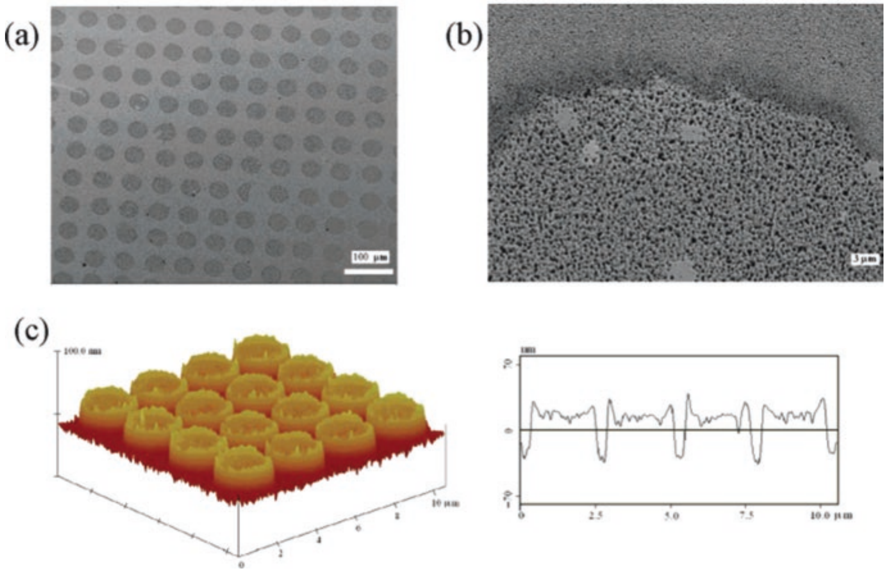

Fig. 5.10 (**a**) Manufacture of thermosensitive polymer nanopatterns by chemical lithography, (**b**) SEM micrographs of poly(*N*-isopropylacrylamide) (PNIPAM) brushes generated by chemical lithography, and (**c**) Tapping-mode AFM image of PNIPAM brushes with a 2.5-μm periodicity (1.8-μm diameter and 0.7-μm distance) in air and corresponding height profile. Reproduced with permission from He et al. (2007)

2006; del Campo and Arzt 2008). In this technique, a photoreactive material, typically a monomer, oligomer or polymer, is coated onto a substrate and then unused parts of the substrate are selectively removed. The photoreactive material is polymerized, crosslinked or degraded in the selective regions of exposure to UV light (Bae et al. 2014).

Soft lithography is a microfabrication technique in which ‘soft matter’ (complex biochemical, organic materials, polymers) is used to produce micron and submicron scale structures or molecules on a substrate. This method includes techniques for using elastomeric stamps, molds and photomasks to fabricate or replicate structures (Yamazoe et al. 2008).

Electron beam lithography is a high-resolution technique for manufacturing nanoscale features on the surface. This technique relies on electron beams to standardize electron sensitive resistors (Werts et al. 2002). For biointerface engineering, electron beam lithography can be used to fabricate nanopattern surfaces from inorganic materials, proteins, self-assembled monolayers and synthetic polymers (Bae et al. 2014). Finally, nanoimprint lithography is a thermal- or light-based process on a rigid mold. The technique is based on the pressure of a mold against a thermoplastic polymer whose temperature is above its glass transition temperature, then a cooling so the polymer returns to its glassy state (Chou et al. 1996).

5.3.3 Nanoimprint

The nanoimprint is an efficient technique which aligns the lamellar phases perpendicularly on surfaces. The nano- and microphase-separation of thin films from supramolecular block copolymers leads to tunable and perfect nanostructures on surfaces. Recently, supramolecular block copolymers have gained great attention, since they can tune the size and morphology of the nanophase-separated domains (Yang et al. 2014). The sacrifice of covalent bonds in diblock polymers to produce nanodomains on the imprinted surface can cause invasive degradation in the cleavage of the bonds (Montarnal et al. 2015). In fact, the microphase-separation domains designed by supramolecular block copolymers can have high stability and high non-self-complementary specificity, and at the same time the interactions are kinetically reversible (Yang et al. 2004a).

It should be noted that the amphiphilic supramolecular block copolymer could be formed into nanophase-separated patterns, e.g. with a solvent or by changing the temperature. Thereafter, the hydrophilic block can be removed from the nanopattern by a solvent-switchable disconnection (Barner and Barner-Kowollik 2015). The H-bonding motifs provide a bond between copolymer segments, such as SOA-AOA (see Sect. 5.2.1), which allow the disconnection of interactions through a well-defined change in the solvent system (see Fig. 5.11).

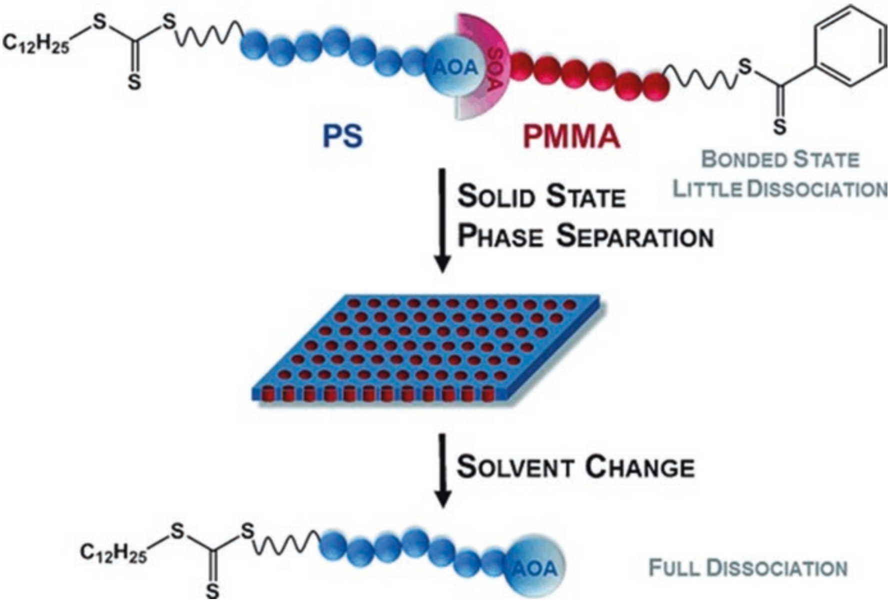

Fig. 5.11 Nanoprinting surface obtained from supramolecular amphiphilic block copolymers based on AOA and SOA motifs [co-PS-PMMA]. The release of the hydrophilic segment took place in response to a solvent trigger. Reproduced with permission from Barner and Barner-Kowollik (2015)

The inherent reversibility of these nanoporous membranes can be used to produce a new generation of switchable surfaces. The combination of supramolecular polymers with switchable nanoporous membranes allows tuning the permeability of functional chemicals, biomolecules and nanoparticles (Tokarev and Minko 2009). In addition, the supramolecular diblock copolymer on the surface can provide significant potential for use as templates and scaffolds.

5.3.4 Electrodeposition

The electrochemical deposition of polymer on surfaces makes use of electrolytic solutions, which contain monomeric starting materials or other polymeric materials. This technique can be easily controlled or automated and allows the coverage of various substrates with polymers of widely varying properties (Beck 1988). Electrodeposition can be done from different approaches: 'top-down' and 'bottom-up' are the most famous fabrication methods for obtaining structured surfaces.

The 'top-down' methods reduce their dimensions to form nanostructured materials, i.e. they are based on large scale patterns through the sculpture. Electrochemical polymerization is a method of 'top-down' modification, which consists of a rapid process of polymerization, deposition and structuration of the polymer film in one-step. In this method, the polymerization begins in an electrochemical cell, in which the monomer is oxidized by inducing the polymerization and deposition of the polymer film. For this, the monomer must be dissolved in a suitable solvent and a good electrolyte, so it is oxidized by applying an anodic potential that generates a radical (Li et al. 2009). Thereafter, the propagation and growth of the polymer chains are produced by oxidation of the dimer and sequential coupling with additional tuners (monomer, oligomer). Finally, when there is no more monomer in the medium, the polymerization is terminated, and then deposited (Sadki et al. 2000).

The 'bottom-up' methods are used to develop more complex structures through the integration of molecules to build up nanostructures. The electro-spinning process can be considered as a combination of 'bottom-up' approaches commonly used to form polymer micro- or nanofibers. It is based on the action of electrostatic forces under a polymeric solution to generate a jet with submicron scale diameters. The evaporation and solidification of this jet take place in the distance between the needle and the metallic collector. In typical electrospinning, the charges are induced on the liquid surface. The mutual charge repulsion causes a force directly opposite to the surface tension. When the electric field intensity increases, the solution at the needle outlet is elongated to form a conical shape known as Taylor cone. The charged jet undergoes a straight jet stage and/or a whipping motion before being collected as nonwoven fiber mats. At the same time, the jet solidifies rapidly due to the fast evaporation of the solvent or temperature gradient in the spinning region (Doshi and Reneker 1995; Haoyi and Yang 2016). Surface topography plays a crucial role in biointerfaces. It is thus possible through the electro-spinning technique

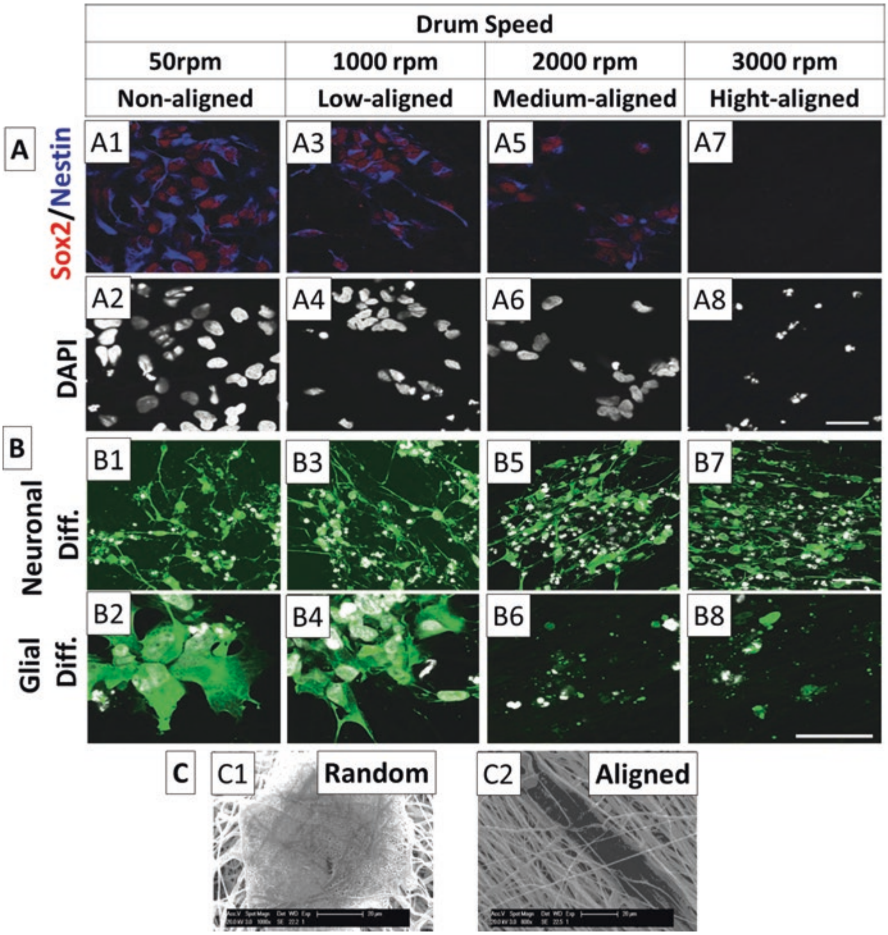

Fig. 5.12 Influence on cell behavior on the surface of the aligned electro-spun fiber (**a**) in comparison with aligned fibers, a greater expression of Sox2/Nestin was observed in the neuronal stem cells cultured on nonaligned fibers (scale bar = 20 μm), (**b**) neuronal and glial differentiation of stem neuronal cells on the surface of nonaligned and aligned poly(vinylidene fluoride) (PVDF) fibers (scale bar = 25 μm) and (**c**) SEM images of neuronal cells cultured on the aligned and non-aligned nanofibrous scaffolds. Reproduced with permission from Lins et al. (2017 and Amani et al. (2019)

to obtain a direction of the dominant patterns on the surface, which refers to the alignment of the surface. Alignment of fibers can be a determining factor in cell adhesion and differentiation (see Fig. 5.12) (Lins et al. 2017). In addition, the surface pattern can be designed from bioabsorbable and supramolecular networks (Lins et al. 2016a; Goor et al. 2017b).

5.4 Types of Stimulus-Response

Smart interfaces are increasingly being studied due to of their relevant properties for biotechnology research fields, such as artificial organs, biofunctional materials, drug delivery systems, regenerative medicine, separation of biomolecules and tissue engineering.

5.4.1 Thermosensitive

Thermosensitive polymer surfaces can modulate molecular interactions as a function of temperature for a wide application in materials science. The thermo-reversibility of a polymer solution is given at a specific temperature. The critical solution temperature is thermal value where a polymeric phase in suspension changes its structure. Typically, solutions whose polymer is soluble at low temperature but become insoluble at increasing temperatures are called as lower-critical solution temperature (LCST). In contrast, when the polymeric solution is insoluble below a specific temperature, then it is said to exhibit upper-critical solution temperature (UCST) (Zarrintaj et al. 2019). In polymers with adsorbed layers or brushes synthesized on the surface, this behavior is manifested by changes in layer adhesion, thickness or wettability (Fujii et al. 2018). For this intrinsic characteristic, thermosensitive polymers have been used particularly and widely for various biomedical applications (Vanparijs et al. 2017).

The most promising stimulus-responsive system for biomedical engineering is a thermo-responsive material based on PNIPAM attached on surfaces. PNIPAM is the most used polymer in tissue engineering because its LCST is around 32 °C in aqueous solutions, which is close to the natural temperature of the human body. In addition, it undergoes a sudden transition from a hydrophilic state to a hydrophobic state across the LCST, which allows cell attachment when the temperature is above 32 °C. Since the temperature is reduced below 32 °C, the cells can be easily separated from the surface (see Fig. 5.13) (Fujii et al. 2018).

It is worth noting that many other polymers exhibit temperature dependent solubility, i.e. they are thermosensitive. A wide range of polymers demonstrates temperature-sensitive such as poly(2-isopropyl 2-oxazoline) (PIOZ), poly(*N*,*N*-diethylacrylamide) (PDEAAM), poly(*N*-vinylcaprolactam) (PVCL) and poly(vinylmethylether) (PVME), which exhibit state conversion thermal values at 35 °C, 48 °C, 32 °C and 33 °C, respectively (Diab et al. 2004; Korde and Kandasubramanian 2019). It is also possible to tune the temperature value *via* copolymerization by hydrophobic or hydrophilic units. Currently, numerous thermosensitive polymers have been altered for the formation of block copolymers, thus increasing or decreasing LCST (Crespy and Rossi 2007).

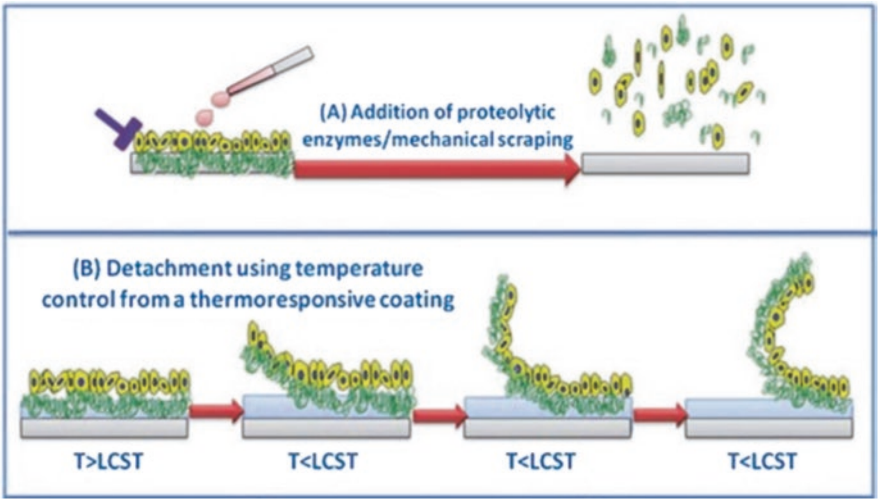

Fig. 5.13 Schematic representation of temperature-responsive culture dishes. (**a**) Conventional trypsinization to remove the cell sheet may have a possible adverse impact on the cell sheet for cell recovery and (**b**) cells harvested from temperature-responsive dishes are recovered as intact sheets by simple temperature reduction below LCST. Reproduced with permission from Nash et al. (2012)

5.4.2 *Photosensitive*

Although the investigation of photo-sensitive polymers began a long time ago, in recent years there has been progress in the areas of photo-complex macromolecular architectures. On photo-switching surfaces, the polymer backbone chains undergo changes in their characteristics which are typically produced because of physical modulations of definite functional assemblies (Korde and Kandasubramanian 2019). The photosensitivity in polymers is caused by chromophores that undergo structural isomerization, ring opening or cyclization by radiation at a specific wavelength, some of these photoinduced changes have the ability to reveal reversibility (Salonen et al. 2010).

Increasingly, investigations of light photosensitive polymers have been applied to several systems due to the interface response time and the precise site control on surfaces. Irradiation is a direct and non-invasive mechanism to induce responsive behavior, and is also an imperative attribute for application in biological interfaces. Light is a useful stimulus to provide a switchable cell attachment-detachment for sensitive surfaces. To sterilize biomaterials is used usually the UV irradiation, which is a relative mild and low energy sterilization method (Mollet et al. 2016). Photo-responsive molecules encompassing azobenzene and spiropyran are very well proven examples of light-induced cell attachment and detachment (Higuchi et al. 2004; Auernheimer et al. 2005). The azobenzene, e.g. is the distinguished chromophore showing light-prompted *cis*- to *trans*-isomerization. The incorporation of azobenzene derivatives can provide that the materials exhibit variable polarity, shape along with the self-assembly performance (Korde and Kandasubramanian 2019). Azobenzene and spiropyran groups can also be used for forming supramolecular assemblies of polymer associated with capacity to allow photo-switching of polymeric aggregates in solution, surface properties and bulk material properties (Natansohn and Rochon 2002; Yager and Barrett 2001, 2006).

5.4.3 pH-Sensitive

The pH switchable nature of polymer at the interfaces has been implemented for several bioapplications, such as acidic vapor sensing, encapsulation and release (Priya James et al. 2014), harvesting cells (Chen et al. 2012), sensors (FitzGerald et al. 2008), as well as pH-sensitive 'gates' in microfluidic devices (Tokarev and Minko 2009). pH-sensitive polymers have basic or acidic moieties that are able to accept or donate a proton in response triggered by environmental pH changes (Priya James et al. 2014). The charge induced electrostatic repulsions leads to swelling-shrinking of polymer chains which modify the hydrodynamic volumes at the biomaterial interfaces. The variation of the polymer chain in response to the cumulative charge on the suspended acid groups occurs at specific pHs, also known as 'pKa' (Chan et al. 2013).

As mentioned in the previous section, the polyelectrolytes are switchable polymers which comprise a multitude of ionizable functionalities, which can be branched into weak polybases and polyacids. Weaker polybases can accept protons and show swelling behavior under acidic conditions. Meanwhile, weak polyacids are proton donors at neutral or basic pH, which simultaneously can also accept protons at very low pH (Chan et al. 2013; Korde and Kandasubramanian 2019).

There are very few studies involving harvesting cells at the interface and the pH trigger, due to the limited range that the living system can be exposed (pH ~6.8 to 7.4) (Chen et al. 2012). However, a large number of scientific articles are devoted to the controlled release and modification of the interfaces caused by the pH change (Lins et al. 2014, 2016b; Priya James et al. 2014).

5.4.4 Electrosensitive

Electrosensitive polymers allow to shrink or swell in response to the electric field that transforms electrical energy into mechanical energy, such that these materials have potentials such as artificial muscle performance, biochemical separations, biosensors and controlled drug release (Priya James et al. 2014; Hu et al. 2019; Korde and Kandasubramanian 2019). The electrical stimulation is a fast and efficient way to control the interfacial properties and polymer morphologies. The modification of the structure of the polymer chain or the material distortion in the electrical field is influenced by various factors, such as applied voltage, changes in electrophoretic mobility, electrochemical reactions, pH of environmental media, salt concentration of the solution, thickness or shape of film, among others.

Polyelectrolytes are semi-conductive or electro-sensitive macromolecules, which are commonly used for switchable systems due to their electrochromic effect. In addition to polyelectrolytes, other polymers also establish sensitivity to the electric field, e.g. piezoelectric polymers, wherein such polymeric networks typically require the existence of a polarizable constituent capable to responding to the electrical field. Electrosensitive systems can be prepared from both synthetic and the natural polymers, where natural polymers include alginate (Kim et al. 2004a), chitosan (Jeong et al. 2002), chondroitin sulfate (Jensen et al. 2002) and hyaluronic acid (Sutani et al. 2001), while synthetic polymers include 2-hydroxyethyl methacrylate, 2-acrylamido-2-methylpropane sulfonic acid, acrylic acid, acrylonitrile, allylamine (Kim et al. 2004a), aniline, methacrylic acid (Kim et al. 2004b), vinyl alcohol and vinyl sulfonic acids (Kim et al. 2005).

5.4.5 Enzyme Sensitive

Enzyme sensitive polymers are stimulus sensitive materials that undergo macroscopic transitions as a result of changes in inter- or intramolecular interactions when activated by enzymes. The use of enzymes as triggers in interface materials was extended by a number of possible applications for diagnostics, drug delivery and regenerative medicine (Ulijn 2006). This new class of smart materials have been reported in recent years based on supramolecular assemblies, chemically cross-linked, surfaces and nanoparticles in which they respond to a range of different enzymes, such as acyl transferases, glycosidases, kinases, lipases, phosphatases, proteases and redox enzymes (McKimm-Breschkin et al. 2003; Guarise et al. 2006).

Understanding the role that enzymes play in biology and in polymer materials can be an important step in designing synthetic materials with dynamic process control between living systems and inanimate materials, such as cell differentiation and migration in the contexts of tissue formation and wound healing (Chen et al. 2003; Ulijn 2006). In addition, another new approach is to physically encapsulate the drug molecules and release them when an enzyme triggers supramolecular transitions in an exclusive location within the body where it is required (Langer 2001; Yang et al. 2004b).

5.4.6 Multiple Sensitive Stimuli

The join of numerous stimuli in polymers has been studied extensively in recent times to create smart and switchable materials revealing an additional stimulus in the same materials, i.e. dual or multiple stimuli responsive. Multiple responsive polymeric system is a combination of different responses to stimulation in a single material, in which they exhibit a triggered macroscopic response by exposure to different external stimuli. There are several kinds of polymers sensitive to different stimuli, such as redox- and temperature-sensitive, magnetic field and temperature-sensitive, pH- and temperature-sensitive (Gutiérrez and Alvarez 2018; Shen et al. 2019).

The response to two or more stimuli can occur in a combinatorial impact in parallel, serial or causal. In this sense, an orthogonal stimuli-responsive system does not affect the response of the other and vice versa (Schattling et al. 2014), i.e. only the specific reaction group in a macromolecule responds when the corresponding external stimulus is applied. The designated functional group generates a structural or environmental change, i.e. a conformational hydrophilic change. Thereafter, the second responsive group is subsequently stimulated and responds in a different way. Thus, a functional group can respond to a stimulus and another functional group is responsible for the response of a second stimulus.

Another alternative is the combination of supramolecular groups and functional surfaces. For example, Tokarev and Minko (2009) demonstrated that surfaces prepared with cationic polyelectrolyte (poly(2-vinylpyridine)—P2VP) gel on electroconductive support can operate as an electrochemical- and pH-controlled gate, being biomolecules responsive and pH dependent, *via* H-bonding and ionic interactions. Porous supramolecular membranes on the surface may swell and shrink their pore size in response to a stimulus or to various stimuli. The changes in pore size allow the control of the permeability of various solutions and biomolecules, e.g. pH and cholesterol, respectively, where it was observed that the pore size is a function of cholesterol concentration and pH variation (Fig. 5.14).

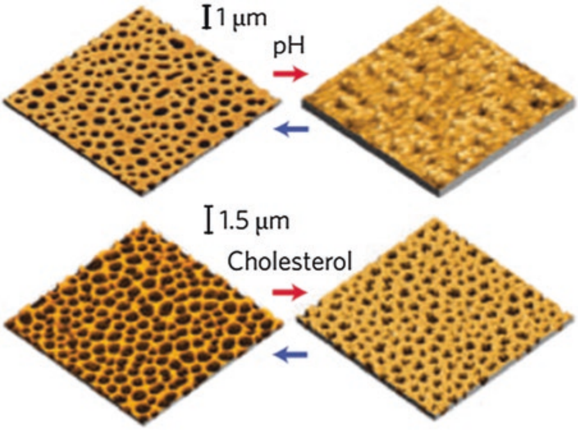

Fig. 5.14 Topography images showing the swelling of the P2VP gel in the pore diameter. Reproduced with permission from Tokarev and Minko (2009)

5.5 Conclusion

In summary, stimulus responsive interfaces represent one of the most emerging and active areas of scientific research for biotechnology. These interfaces are extraordinarily functional because they can provide additional tools to fine-tune their properties under a biological environment conditions in a cooperative manner. The supramolecular polymers combining various switchable features have proven to be good candidates for stimulus responsive interfaces. Interfaces showing supramolecular interactions have unique topological structures and specific functions, such as multifunctional groups with switchable flexibility for biomedical needs. Recent progress in switchable and supramolecular interfaces with a view to increasing the intake of systems based on stimulus-sensitive polymers for biomedical applications will definitely contribute to improving human life.

Acknowledgments The author acknowledge Institut National des Sciences Appliquées de Lyon for the financial support.

Conflicts of Interest The author declares no conflict of interest.

References

van Almen, G. C., Talacua, H., Ippel, B. D., Mollet, B. B., Ramaekers, M., Simonet, M., Smits, A. I. P. M., Bouten, C. V. C., Kluin, J., & Dankers, P. Y. W. (2016). Development of non-cell adhesive vascular grafts using supramolecular building blocks. *Macromolecular Bioscience, 16*(3), 350–362. https://doi.org/10.1002/mabi.201500278.

Amani, H., Arzaghi, H., Bayandori, M., Dezfuli, A. S., Pazoki-Toroudi, H., Shafiee, A., & Moradi, L. (2019). Controlling cell behavior through the design of biomaterial surfaces: A focus on surface modification techniques. *Advanced Materials Interfaces, 6*(13), 1900572. https://doi.org/10.1002/admi.201900572.

Auernheimer, J., Dahmen, C., Hersel, U., Bausch, A., & Kessler, H. (2005). Photoswitched cell adhesion on surfaces with RGD peptides. *Journal of the American Chemical Society, 127*(46), 16107–16110. https://doi.org/10.1021/ja053648q.

Bae, H., Chu, H., Edalat, F., Cha, J. M., Sant, S., Kashyap, A., Ahari, A. F., Kwon, C. H., Nichol, J. W., Manoucheri, S., Zamanian, B., Wang, Y., & Khademhosseini, A. (2014). Development of functional biomaterials with micro- and nanoscale technologies for tissue engineering and drug delivery applications. *Journal of Tissue Engineering and Regenerative Medicine, 8*(1), 1–14. https://doi.org/10.1002/term.1494.

Barner, L., & Barner-Kowollik, C. (2015). The link that lasts: A new frontier in supramolecular block copolymer design. *Angewandte Chemie International Edition, 54*(40), 11612–11614. https://doi.org/10.1002/anie.201506602.

Barth, J. V. (2007). Molecular architectonic on metal surfaces. *Annual Review of Physical Chemistry, 58*(1), 375–407. https://doi.org/10.1146/annurev.physchem.56.092503.141259.

Beck, F. (1988). Electrodeposition of polymer coatings. *Electrochimica Acta, 33*(7), 839–850. https://doi.org/10.1016/0013-4686(88)80080-x.

Beg, S., Rahman, M., Jain, A., Saini, S., Midoux, P., Pichon, C., Ahmad, F. J., & Akhter, S. (2017). Nanoporous metal organic frameworks as hybrid polymer-metal composites for drug delivery and biomedical applications. *Drug Discovery Today, 22*(4), 625–637. https://doi.org/10.1016/j.drudis.2016.10.001.

Beijer, F. H., Kooijman, H., Spek, A. L., Sijbesma, R. P., & Meijer, E. W. (1998a). Self-complementarity achieved through quadruple hydrogen bonding. *Angewandte Chemie International Edition, 37*(1-2), 75–78. https://doi.org/10.1002/(sici)1521-3773(19980202)37:1/2<75::aid-anie75>3.0.co;2-r.

Beijer, F. H., Sijbesma, R. P., Kooijman, H., Spek, A. L., & Meijer, E. W. (1998b). Strong dimerization of ureidopyrimidones via quadruple hydrogen bonding. *Journal of the American Chemical Society, 120*(27), 6761–6769. https://doi.org/10.1021/ja974112a.

Bian, Q., Chen, S., Xing, Y., Yuan, D., Lv, L., & Wang, G. (2018). Host-guest self-assembly toward reversible visible-light-responsive switching for bacterial adhesion. *Acta Biomaterialia, 76*, 39–45. https://doi.org/10.1016/j.actbio.2018.06.039.

Bosmans, R. P. G., Hendriksen, W. E., Verheijden, M., Eelkema, R., Jonkheijm, P., van Esch, J. H., & Brunsveld, L. (2015). Supramolecular protein immobilization on lipid bilayers. *Chemistry – A European Journal, 21*(50), 18466–18473. https://doi.org/10.1002/chem.201502461.

del Campo, A., & Arzt, E. (2008). Fabrication approaches for generating complex micro- and nanopatterns on polymeric surfaces. *Chemical Reviews, 108*(3), 911–945. https://doi.org/10.1021/cr050018y.

Chan, A., Orme, R. P., Fricker, R. A., & Roach, P. (2013). Remote and local control of stimuli responsive materials for therapeutic applications. *Advanced Drug Delivery Reviews, 65*(4), 497–514. https://doi.org/10.1016/j.addr.2012.07.007.

Chang, V. Y., Fedele, C., Priimagi, A., Shishido, A., & Barrett, C. J. (2019). Photoreversible soft azo dye materials: Toward optical control of bio-interfaces. *Advanced Optical Materials, 7*(16), 1900091. https://doi.org/10.1002/adom.201900091.

Chen, T., Small, D. A., McDermott, M. K., Bentley, W. E., & Payne, G. F. (2003). Enzymatic methods for in situ cell entrapment and cell release. *Biomacromolecules, 4*(6), 1558–1563. https://doi.org/10.1021/bm034145k.

Chen, Y.-H., Chung, Y.-C., Wang, I. J., & Young, T.-H. (2012). Control of cell attachment on pH-responsive chitosan surface by precise adjustment of medium pH. *Biomaterials, 33*(5), 1336–1342. https://doi.org/10.1016/j.biomaterials.2011.10.048.

Chou, S. Y., Krauss, P. R., & Renstrom, P. J. (1996). Imprint lithography with 25-nanometer resolution. *Science, 272*(5258), 85–87. https://doi.org/10.1126/science.272.5258.85.

Chua, P.-H., Neoh, K.-G., Kang, E.-T., & Wang, W. (2008). Surface functionalization of titanium with hyaluronic acid/chitosan polyelectrolyte multilayers and RGD for promoting osteoblast functions and inhibiting bacterial adhesion. *Biomaterials, 29*(10), 1412–1421. https://doi.org/10.1016/j.biomaterials.2007.12.019.

Crespy, D., & Rossi, R. M. (2007). Temperature-responsive polymers with LCST in the physiological range and their applications in textiles. *Polymer International, 56*(12), 1461–1468. https://doi.org/10.1002/pi.2277.

Crouzier, T., Boudou, T., & Picart, C. (2010). Polysaccharide-based polyelectrolyte multilayers. *Current Opinion in Colloid & Interface Science, 15*(6), 417–426. https://doi.org/10.1016/j.cocis.2010.05.007.

Dankers Patricia, Y. W., & Meijer, E. W. (2007). Supramolecular biomaterials. A modular approach towards tissue engineering. *Bulletin of the Chemical Society of Japan, 80*(11), 2047–2073. https://doi.org/10.1246/bcsj.80.2047.

Diab, C., Akiyama, Y., Kataoka, K., & Winnik, F. M. (2004). Microcalorimetric study of the temperature-induced phase separation in aqueous solutions of poly(2-isopropyl-2-oxazolines). *Macromolecules, 37*(7), 2556–2562. https://doi.org/10.1021/ma0358733.

Doshi, J., & Reneker, D. H. (1995). Electrospinning process and applications of electrospun fibers. *Journal of Electrostatics, 35*(2-3), 151–160. https://doi.org/10.1016/0304-3886(95)00041-8.

El-khouri, R. J., Szamocki, R., Sergeeva, Y., Felix, O., & Decher, G. (2011). Multifunctional layer-by-layer architectures for biological applications. In W. Knoll & R. C. Advincula (Eds.), *Functional polymer films: 2 Volume set*. New York: Wiley. https://doi.org/10.1002/9783527638482.ch2.

FitzGerald, P. A., Amalvy, J. I., Armes, S. P., & Wanless, E. J. (2008). Film-forming microgels for pH-triggered capture and release. *Langmuir, 24*(18), 10228–10234. https://doi.org/10.1021/la8017425.

Fouquey, C., Lehn, J.-M., & Levelut, A.-M. (1990). Molecular recognition directed self-assembly of supramolecular liquid crystalline polymers from complementary chiral components. *Advanced Materials, 2*(5), 254–257. https://doi.org/10.1002/adma.19900020506.

Fujii, S., Wanless, E. J., Yusa, S.-i., Webber, G. B., & Ishida, N. (2018). Stimulus-responsive soft surface/interface toward applications in adhesion, sensor and biomaterial. In A. Hozumi, L. Jiang, H. Lee, & M. Shimomura (Eds.), *Stimuli-responsive dewetting/wetting smart surfaces and interfaces* (pp. 287–397). Cham: Springer International Publishing. https://doi.org/10.1007/978-3-319-92654-4_12.

Gong, B. (2007). Engineering hydrogen-bonded duplexes. *Polymer International, 56*(4), 436–443. https://doi.org/10.1002/pi.2175.

Gong, B., Yan, Y., Zeng, H., Skrzypczak-Jankunn, E., Kim, Y. W., Zhu, J., & Ickes, H. (1999). A new approach for the design of supramolecular recognition units: Hydrogen-bonded molecular duplexes. *Journal of the American Chemical Society, 121*(23), 5607–5608. https://doi.org/10.1021/ja990904o.

González-Rodríguez, D., & Schenning, A. P. H. J. (2011). Hydrogen-bonded supramolecular π-functional materials. *Chemistry of Materials, 23*(3), 310–325. https://doi.org/10.1021/cm101817h.

Goor, O. J. G. M., Brouns, J. E. P., & Dankers, P. Y. W. (2017a). Introduction of anti-fouling coatings at the surface of supramolecular elastomeric materials via post-modification of reactive supramolecular additives. *Polymer Chemistry, 8*(34), 5228–5238. https://doi.org/10.1039/c7py00801e.

Goor, O. J. G. M., Keizer, H. M., Bruinen, A. L., Schmitz, M. G. J., Versteegen, R. M., Janssen, H. M., Heeren, R. M. A., & Dankers, P. Y. W. (2017b). Efficient functionalization of additives at supramolecular material surfaces. *Advanced Materials, 29*(5), 1604652. https://doi.org/10.1002/adma.201604652.

Goronzy, D. P., Ebrahimi, M., Rosei, F., Arramel, Fang, Y., De Feyter, S., Tait, S. L., Wang, C., Beton, P. H., Wee, A. T. S., Weiss, P. S., & Perepichka, D. F. (2018). Supramolecular assemblies on surfaces: Nanopatterning, functionality, and reactivity. *ACS Nano, 12*(8), 7445–7481. https://doi.org/10.1021/acsnano.8b03513.

Goulet-Hanssens, A., Lai Wing Sun, K., Kennedy, T. E., & Barrett, C. J. (2012). Photoreversible surfaces to regulate cell adhesion. *Biomacromolecules, 13*(9), 2958–2963. https://doi.org/10.1021/bm301037k.

Guarise, C., Pasquato, L., De Filippis, V., & Scrimin, P. (2006). Gold nanoparticles-based protease assay. *Proceedings of the National Academy of Sciences of the United States of America, 103*(11), 3978–3982. https://doi.org/10.1073/pnas.0509372103.

Gutiérrez, T. J., & Alvarez, V. A. (2018). Nanoparticles for hyperthermia applications. In C. M. Hussain (Ed.), *Handbook of nanomaterials for Industrial applications: Micro and nano technologies* (pp. 563–576). Amsterdam: Elsevier. https://doi.org/10.1016/b978-0-12-813351-4.00032-8.

Hahn, M. S., Miller, J. S., & West, J. L. (2006). Three-dimensional biochemical and biomechanical patterning of hydrogels for guiding cell behavior. *Advanced Materials, 18*(20), 2679–2684. https://doi.org/10.1002/adma.200600647.

Haoyi, L., & Yang, W. (2016). Electrospinning technology in non-woven fabric manufacturing. In J. Han-Yong (Ed.), *Non-woven fabrics* (Vol. 1, pp. 33–54). Rijeka: InTech.

He, Q., Küller, A., Grunze, M., & Li, J. (2007). Fabrication of thermosensitive polymer nanopatterns through chemical lithography and atom transfer radical polymerization. *Langmuir, 23*(7), 3981–3987. https://doi.org/10.1021/la062793u.

Higuchi, A., Hamamura, A., Shindo, Y., Kitamura, H., Yoon, B. O., Mori, T., Uyama, T., & Umezawa, A. (2004). Photon-modulated changes of cell attachments on poly(spiropyran-co-methyl methacrylate) membranes. *Biomacromolecules, 5*(5), 1770–1774. https://doi.org/10.1021/bm049737x.

Hiroshi, T. (1954). The nature of the hydrogen-bond. I. The delocalization energy in the hydrogen-bond as calculated by the atomic-orbital method. *Bulletin of the Chemical Society of Japan, 27*(7), 445–450. https://doi.org/10.1246/bcsj.27.445.

Hoeben, F. J. M., Herz, L. M., Daniel, C., Jonkheijm, P., Schenning, A. P. H. J., Silva, C., Meskers, S. C. J., Beljonne, D., Phillips, R. T., Friend, R. H., & Meijer, E. W. (2004). Efficient energy transfer in mixed columnar stacks of hydrogen-bonded oligo(*p*-phenylene vinylene)s in solution. *Angewandte Chemie International Edition, 43*(15), 1976–1979. https://doi.org/10.1002/anie.200353451.

Hu, L., Zhang, Q., Li, X., & Serpe, M. J. (2019). Stimuli-responsive polymers for sensing and actuation. *Materials Horizons, 6*(9), 1774–1793. https://doi.org/10.1039/c9mh00490d.

Jan, E., Pereira, F. N., Turner, D. L., & Kotov, N. A. (2011). *In situ* gene transfection and neuronal programming on electroconductive nanocomposite to reduce inflammatory response. *Journal of Materials Chemistry, 21*(4), 1109–1114. https://doi.org/10.1039/c0jm01895c.

Jensen, M., Birch Hansen, P., Murdan, S., Frokjaer, S., & Florence, A. T. (2002). Loading into and electro-stimulated release of peptides and proteins from chondroitin 4-sulphate hydrogels. *European Journal of Pharmaceutical Sciences, 15*(2), 139–148. https://doi.org/10.1016/s0928-0987(01)00193-2.

Jeong, S., Jun Park, S., Shin, M.-S., & Kim, S. I. (2002). Characteristics of electrical responsive chitosan/polyallylamine interpenetrating polymer network hydrogel. *Journal of Applied Polymer Science, 86*(9), 2290–2295. https://doi.org/10.1002/app.11217.

Jonkheijm, P., van der Schoot, P., Schenning, A. P. H. J., & Meijer, E. W. (2006). Probing the solvent-assisted nucleation pathway in chemical self-assembly. *Science, 313*(5783), 80–83. https://doi.org/10.1126/science.1127884.

Kim, S. J., Yoon, S. G., Lee, Y. H., & Kim, S. I. (2004a). Bending behavior of hydrogels composed of poly(methacrylic acid) and alginate by electrical stimulus. *Polymer International, 53*(10), 1456–1460. https://doi.org/10.1002/pi.1560.

Kim, S. J., Shin, S. R., Lee, S. M., Kim, I. Y., & Kim, S. I. (2004b). Electromechanical properties of hydrogels based on chitosan and poly(hydroxyethyl methacrylate) in NaCl solution. *Smart Materials and Structures, 13*(5), 1036–1039. https://doi.org/10.1088/0964-1726/13/5/008.

Kim, H. I., Gu, B. K., Shin, M. K., Park, S.-J., Yoon, S.-G., Kim, I.-Y., Kim, S. I., & Kim, S.-J. (2005). Electrical response characterization of interpenetrating polymer network hydrogels as an actuator. *Proceedings of SPIE, 5759*, 447. https://doi.org/10.1117/12.598404.

Kollman, P. A., & Allen, L. C. (1972). Theory of the hydrogen bond. *Chemical Reviews, 72*(3), 283–303. https://doi.org/10.1021/cr60277a004.

Korde, J. M., & Kandasubramanian, B. (2019). Fundamentals and effects of biomimicking stimuli-responsive polymers for engineering functions. *Industrial & Engineering Chemistry Research, 58*(23), 9709–9757. https://doi.org/10.1021/acs.iecr.9b00683.

Korevaar, P. A., George, S. J., Markvoort, A. J., Smulders, M. M. J., Hilbers, P. A. J., Schenning, A. P. H. J., De Greef, T. F. A., & Meijer, E. W. (2012). Pathway complexity in supramolecular polymerization. *Nature, 481*, 492–496. https://doi.org/10.1038/nature10720.

Kozai, T. D. Y., Langhals, N. B., Patel, P. R., Deng, X., Zhang, H., Smith, K. L., Lahann, J., Kotov, N. A., & Kipke, D. R. (2012). Ultrasmall implantable composite microelectrodes with bioactive surfaces for chronic neural interfaces. *Nature Materials, 11*, 1065–1073. https://doi.org/10.1038/nmat3468.

Kumpfer, J. R., Jin, J., & Rowan, S. J. (2010). Stimuli-responsive europium-containing metallo-supramolecular polymers. *Journal of Materials Chemistry, 20*(1), 145–151. https://doi.org/10.1039/b915490f.

Langer, R. (2001). Drugs on target. *Science, 293*(5527), 58–59.

Lehn, J.-M. (2002). Toward self-organization and complex matter. *Science, 295*(5564), 2400–2403. https://doi.org/10.1126/science.1071063.

Lehn, J.-M. (2005). Dynamers: Dynamic molecular and supramolecular polymers. *Progress in Polymer Science, 30*(8-9), 814–831. https://doi.org/10.1016/j.progpolymsci.2005.06.002.

Li, C., Bai, H., & Shi, G. (2009). Conducting polymer nanomaterials: Electrosynthesis and applications. *Chemical Society Reviews, 38*(8), 2397–2409. https://doi.org/10.1039/b816681c.

Li, Q.-L., Wang, L., Qiu, X.-L., Sun, Y.-L., Wang, P.-X., Liu, Y., Li, F., Qi, A.-D., Gao, H., & Yang, Y.-W. (2014). Stimuli-responsive biocompatible nanovalves based on β-cyclodextrin modified poly(glycidyl methacrylate). *Polymer Chemistry, 5*(10), 3389–3395. https://doi.org/10.1039/c4py00041b.

Li, Q., Wu, Y., Lu, H., Wu, X., Chen, S., Song, N., Yang, Y.-W., & Gao, H. (2017). Construction of supramolecular nanoassembly for responsive bacterial elimination and effective bacterial detection. *ACS Applied Materials & Interfaces, 9*(11), 10180–10189. https://doi.org/10.1021/acsami.7b00873.

Lins, L. C., Bazzo, G. C., Barreto, P. L. M., & Pires, A. T. N. (2014). Composite PHB/chitosan microparticles obtained by spray drying: Effect of chitosan concentration and crosslinking agents on drug release. *Journal of the Brazilian Chemical Society, 25*(8), 1462–1471. https://doi.org/10.5935/0103-5053.20140129.

Lins, L. C., Wianny, F., Livi, S., Hidalgo, I. A., Dehay, C., Duchet-Rumeau, J., & Gérard, J.-F. (2016a). Development of bioresorbable hydrophilic-hydrophobic electrospun scaffolds for neural tissue engineering. *Biomacromolecules, 17*(10), 3172–3187. https://doi.org/10.1021/acs.biomac.6b00820.

Lins, L. C., Padoin, N., Pires, A. T. N., & Soares, C. (2016b). Modeling ketoprofen release from PHB/chitosan composite microparticles. *Polymer Bulletin, 73*(6), 1515–1529. https://doi.org/10.1007/s00289-015-1559-1.

Lins, L. C., Wianny, F., Livi, S., Dehay, C., Duchet-Rumeau, J., & Gérard, J.-F. (2017). Effect of polyvinylidene fluoride electrospun fiber orientation on neural stem cell differentiation. *Journal of Biomedical Materials Research Part B: Applied Biomaterials, 105*(8), 2376–2393. https://doi.org/10.1002/jbm.b.33778.

Liu, Y., Liu, K., Wang, Z., & Zhang, X. (2011). Host-enhanced π–π interaction for water-soluble supramolecular polymerization. *Chemistry – A European Journal, 17*(36), 9930–9935. https://doi.org/10.1002/chem.201101611.

Lou, X.-Y., & Yang, Y.-W. (2018). Manipulating aggregation-induced emission with supramolecular macrocycles. *Advanced Optical Materials, 6*(22), 1800668. https://doi.org/10.1002/adom.201800668.

McKimm-Breschkin, J. L., Colman, P. M., Jin, B., Krippner, G. Y., McDonald, M., Reece, P. A., Tucker, S. P., Waddington, L., Watson, K. G., & Wu, W.-Y. (2003). Tethered neuraminidase inhibitors that bind an influenza virus: A first step towards a diagnostic method for influenza. *Angewandte Chemie International Edition, 42*(27), 3118–3121. https://doi.org/10.1002/anie.200250402.

Minko, S. (2006). Responsive polymer brushes. *Journal of Macromolecular Science, Part C, 46*(4), 397–420. https://doi.org/10.1080/15583720600945402.

Mollet, B. B., Nakano, Y., Magusin, P. C. M. M., Spiering, A. J. H., Vekemans, J. A. J. M., Dankers, P. Y. W., & Meijer, E. W. (2016). The effect of irradiation by ultraviolet light on ureido-pyrimidinone based biomaterials. *Journal of Polymer Science Part A: Polymer Chemistry, 54*(1), 81–90. https://doi.org/10.1002/pola.27887.

Montarnal, D., Delbosc, N., Chamignon, C., Virolleaud, M.-A., Luo, Y., Hawker, C. J., Drockenmuller, E., & Bernard, J. (2015). Highly ordered nanoporous films from supramolecular diblock copolymers with hydrogen-bonding junctions. *Angewandte Chemie International Edition, 54*(38), 11117–11121. https://doi.org/10.1002/anie.201504838.

Montjoy, D. G., Bahng, J. H., Eskafi, A., Hou, H., & Kotov, N. A. (2018). Omnidispersible hedgehog particles with multilayer coatings for multiplexed biosensing. *Journal of the American Chemical Society, 140*(25), 7835–7845. https://doi.org/10.1021/jacs.8b02666.

Muzzio, N. E., Pasquale, M. A., Diamanti, E., Gregurec, D., Moro, M. M., Azzaroni, O., & Moya, S. E. (2017). Enhanced antiadhesive properties of chitosan/hyaluronic acid polyelectrolyte multilayers driven by thermal annealing: Low adherence for mammalian cells and selective decrease in adhesion for Gram-positive bacteria. *Materials Science and Engineering: C, 80*, 677–687. https://doi.org/10.1016/j.msec.2017.07.016.

Muzzio, N. E., Pasquale, M. A., Rios, X., Azzaroni, O., Llop, J., & Moya, S. E. (2019). Adsorption and exchangeability of fibronectin and serum albumin protein corona on annealed polyelectrolyte multilayers and their consequences on cell adhesion. *Advanced Materials Interfaces, 6*(8), 1900008. https://doi.org/10.1002/admi.201900008.

Nash, M. E., Healy, D., Carroll, W. M., Elvira, C., & Rochev, Y. A. (2012). Cell and cell sheet recovery from pNIPAm coatings; motivation and history to present day approaches. *Journal of Materials Chemistry, 22*(37), 19376–19389. https://doi.org/10.1039/c2jm31748f.

Natansohn, A., & Rochon, P. (2002). Photoinduced motions in azo-containing polymers. *Chemical Reviews, 102*(11), 4139–4176. https://doi.org/10.1021/cr970155y.

Pape, A. C. H., Ippel, B. D., & Dankers, P. Y. W. (2017). Cell and protein fouling properties of polymeric mixtures containing supramolecular poly(ethylene glycol) additives. *Langmuir, 33*(16), 4076–4082. https://doi.org/10.1021/acs.langmuir.7b00467.

Pennec, Y., Auwärter, W., Schiffrin, A., Weber-Bargioni, A., Riemann, A., & Barth, J. V. (2007). Supramolecular gratings for tuneable confinement of electrons on metal surfaces. *Nature Nanotechnology, 2*(2), 99–103. https://doi.org/10.1038/nnano.2006.212.

Priya James, H., John, R., Alex, A., & Anoop, K. R. (2014). Smart polymers for the controlled delivery of drugs-A concise overview. *Acta Pharmaceutica Sinica B, 4*(2), 120–127. https://doi.org/10.1016/j.apsb.2014.02.005.

Ren, W., Li, Z., Chen, Y., Gao, H., Yang, W., Wang, Y., & Luo, Y. (2019). Facile Preparation of linear polyurethane from UPy-Capped poly(dl-lactic acid) macrodiol. *Macromolecular Materials and Engineering, 304*(1), 1800491. https://doi.org/10.1002/mame.201800491.

Romero, G., Ochoteco, O., Sanz, D. J., Estrela-Lopis, I., Donath, E., & Moya, S. E. (2013). Poly(lactide-*co*-glycolide) nanoparticles, layer by layer engineered for the sustainable delivery of antiTNF-α. *Macromolecular Bioscience, 13*(7), 903–912. https://doi.org/10.1002/mabi.201200478.

Sadki, S., Schottland, P., Brodie, N., & Sabouraud, G. (2000). The mechanisms of pyrrole electropolymerization. *Chemical Society Reviews, 29*(5), 283–293. https://doi.org/10.1039/a807124a.

Salonen, A., Langevin, D., & Perrin, P. (2010). Light and temperature bi-responsive emulsion foams. *Soft Matter, 6*(21), 5308–5311. https://doi.org/10.1039/c0sm00705f.

Schattling, P., Jochum, F. D., & Theato, P. (2014). Multi-stimuli responsive polymers – The all-in-one talents. *Polymer Chemistry, 5*(1), 25–36. https://doi.org/10.1039/c3py00880k.

Schiffrin, A., Riemann, A., Auwärter, W., Pennec, Y., Weber-Bargioni, A., Cvetko, D., Cossaro, A., Morgante, A., & Barth, J. V. (2007). Zwitterionic self-assembly of l-methionine nanogratings on the Ag(111) surface. *Proceedings of the National Academy of Sciences, 104*(13), 5279–5284. https://doi.org/10.1073/pnas.0607867104.

Shen, Y., Zhu, H., Wang, Y., Cui, H., & Sun, R. (2019). Applications and implications of environmental-responsive polymers toward agrochemicals. In T. J. Gutiérrez (Ed.), *Polymers for agri-food applications* (pp. 67–90). Cham: Springer. https://doi.org/10.1007/978-3-030-19416-1_5.

Smith, R. K., Lewis, P. A., & Weiss, P. S. (2004). Patterning self-assembled monolayers. *Progress in Surface Science, 75*(1-2), 1–68. https://doi.org/10.1016/j.progsurf.2003.12.001

Söntjens, S. H. M., Sijbesma, R. P., van Genderen, M. H. P., & Meijer, E. W. (2000). Stability and lifetime of quadruply hydrogen bonded 2-ureido-4[1H]-pyrimidinone dimers. *Journal of the American Chemical Society, 122*(31), 7487–7493. https://doi.org/10.1016/j.progsurf.2003.12.001.

Sutani, K., Kaetsu, I., & Uchida, K. (2001). The synthesis and the electric-responsiveness of hydrogels entrapping natural polyelectrolyte. *Radiation Physics and Chemistry, 61*(1), 49–54. https://doi.org/10.1016/s0969-806x(00)00381-9.

Taylor, R., Kennard, O., & Versichel, W. (1984). Geometry of the nitrogen-hydrogen…oxygen-carbon (N-H…O:C) hydrogen bond. 2. Three-center (bifurcated) and four-center (trifurcated) bonds. *Journal of the American Chemical Society, 106*(1), 244–248. https://doi.org/10.1021/ja00313a047.

Tokarev, I., & Minko, S. (2009). Multiresponsive, hierarchically structured membranes: New, challenging, biomimetic materials for biosensors, controlled release, biochemical gates, and nanoreactors. *Advanced Materials, 21*(2), 241–247. https://doi.org/10.1002/adma.200801408.

Tong, W., Song, X., & Gao, C. (2012). Layer-by-layer assembly of microcapsules and their biomedical applications. *Chemical Society Reviews, 41*(18), 6103–6124. https://doi.org/10.1039/c2cs35088b.

Tran, K. T. M., & Nguyen, T. D. (2017). Lithography-based methods to manufacture biomaterials at small scales. *Journal of Science: Advanced Materials and Devices, 2*(1), 1–14. https://doi.org/10.1016/j.jsamd.2016.12.001.

Ulijn, R. V. (2006). Enzyme-responsive materials: A new class of smart biomaterials. *Journal of Materials Chemistry, 16*(23), 2217–2225. https://doi.org/10.1039/b601776m.

Valderrey, V., Wiemann, M., Jonkheijm, P., Hecht, S., & Huskens, J. (2019). Multivalency in heteroternary complexes on cucurbit[8]uril-functionalized surfaces: Self-assembly, patterning, and exchange processes. *ChemPlusChem, 84*(9), 1324–1330. https://doi.org/10.1002/cplu.201900181.

Valencia, G. A., Zare, E. N., Makvandi, P., & Gutiérrez, T. J. (2019). Self-assembled carbohydrate polymers for food applications: A review. *Comprehensive Reviews in Food Science and Food Safety, 18*(6), 2009. https://doi.org/10.1111/1541-4337.12499.

Vanparijs, N., Nuhn, L., & De Geest, B. G. (2017). Transiently thermoresponsive polymers and their applications in biomedicine. *Chemical Society Reviews, 46*(4), 1193–1239. https://doi.org/10.1039/c6cs00748a.

Wedler-Jasinski, N., Delbosc, N., Virolleaud, M.-A., Montarnal, D., Welle, A., Barner, L., Walther, A., Bernard, J., & Barner-Kowollik, C. (2016). Recodable surfaces based on switchable hydrogen bonds. *Chemical Communications, 52*(56), 8753–8756. https://doi.org/10.1039/c6cc03612k.

Werts, M. H. V., Lambert, M., Bourgoin, J.-P., & Brust, M. (2002). Nanometer scale patterning of Langmuir-Blodgett films of gold nanoparticles by electron beam lithography. *Nano Letters, 2*(1), 43–47. https://doi.org/10.1021/nl015629u.

Yager, K. G., & Barrett, C. J. (2001). All-optical patterning of azo polymer films. *Current Opinion in Solid State and Materials Science, 5*(6), 487–494. https://doi.org/10.1016/s1359-0286(02)00020-7.

Yager, K. G., & Barrett, C. J. (2006). Novel photo-switching using azobenzene functional materials. *Journal of Photochemistry and Photobiology A: Chemistry, 182*(3), 250–261. https://doi.org/10.1016/j.jphotochem.2006.04.021.

Yamazoe, H., Uemura, T., & Tanabe, T. (2008). Facile cell patterning on an albumin-coated surface. *Langmuir, 24*(16), 8402–8404. https://doi.org/10.1021/la801221r.

Yang, X., Hua, F., Yamato, K., Ruckenstein, E., Gong, B., Kim, W., & Ryu, C. Y. (2004a). Supramolecular AB diblock copolymers. *Angewandte Chemie International Edition, 43*(47), 6471–6474. https://doi.org/10.1002/anie.200460472.

Yang, Z., Gu, H., Fu, D., Gao, P., Lam, J. K., & Xu, B. (2004b). Enzymatic formation of supramolecular hydrogels. *Advanced Materials, 16*(16), 1440–1444. https://doi.org/10.1002/adma.200400340.

Yang, X., Xiao, S., Hu, W., Hwu, J., van de Veerdonk, R., Wago, K., Lee, K., & Kuo, D. (2014). Integration of nanoimprint lithography with block copolymer directed self-assembly for fabrication of a sub-20 nm template for bit-patterned media. *Nanotechnology, 25*(39), 395301. https://doi.org/10.1088/0957-4484/25/39/395301.

Zarrintaj, P., Jouyandeh, M., Ganjali, M. R., Hadavand, B. S., Mozafari, M., Sheiko, S. S., Vatankhah-Varnoosfaderani, M., Gutiérrez, T. J., & Saeb, M. R. (2019). Thermo-sensitive polymers in medicine: A review. *European Polymer Journal, 117*, 402–423. https://doi.org/10.1016/j.eurpolymj.2019.05.024.

Zeng, H., Miller, R. S., Flowers, R. A., & Gong, B. (2000). A highly stable, six-hydrogen-bonded molecular duplex. *Journal of the American Chemical Society, 122*(11), 2635–2644. https://doi.org/10.1021/ja9942742.

Zeng, H., Yang, X., Brown, A. L., Martinovic, S., Smith, R. D., & Gong, B. (2003). An extremely stable, self-complementary hydrogen-bonded duplex. *Chemical Communications*, (13), 1556–1557. https://doi.org/10.1039/b301791e.

Zhao, S., Caruso, F., Dähne, L., Decher, G., De Geest, B. G., Fan, J., Feliu, N., Gogotsi, Y., Hammond, P. T., Hersam, M. C., Khademhosseini, A., Kotov, N., Leporatti, S., Li, Y., Lisdat, F., Liz-Marzán, L. M., Moya, S., Mulvaney, P., Rogach, A. L., Roy, S., Shchukin, D. G., Skirtach, A. G., Stevens, M. M., Sukhorukov, G. B., Weiss, P. S., Yue, Z., Zhu, D., & Parak, W. J. (2019). The future of layer-by-layer assembly: A tribute to ACS Nano Associate Editor Helmuth Möhwald. *ACS Nano, 13*(6), 6151–6169. https://doi.org/10.1021/acsnano.9b03326.

Chapter 6
Recycling of Reactive and Functional Polymers

A. M. M. Saleh and Reem K. Farag

Abstract The use of polymeric products such as reactive and functionalized polymers has become much greater than other materials such as metals for their superior properties such as corrosion resistance, high impact resistance, low density and light weight. Functional polymers are macromolecules that have unique properties based on the presence of chemical functional groups that are not similar to those of the pre-existing backbone chains. Chemical heterogeneity in the polymer chains increases the reactivity of the polymer and prevents phase separation of polymer mixtures. Polymer functionalization is used to impart new characteristics such as chemical, biophysical, physicochemical or optoelectronic properties to the desired polymer. With this in mind, the polymeric products can be classified into thermoset and thermoplastics. Crumb rubber is the most popular thermoset polymer, while thermoplastic polymers are represented by a wide range of plastic materials such as poly(ethylene terephthalate), low density poly(ethylene), high density poly(ethylene), poly(styrene), poly(propylene), poly(urethane), nylon, poly(carbonate), resins and phenolic compounds. In recent decades, concern about the problem of waste in the world and its effect on the environment has increased. The creation of non-decomposing waste, such as polymers combined with an ever-growing consumer population, has led to a waste disposal crisis. One of the solutions to this crisis lies in recycling waste polymers into useful products. This chapter gives an overview about the recycling of reactive polymers including the different synthesis methods and applications of this type of polymers. The synthesis methods include post-polymerization functionalization, coordination polymerization, as well as free radical, anionic and cationic procedures. This chapter also highlights the fields of application of functional polymers, including surface modifications of polymers, as well as polymer nanoparticles to be suitable for use in

---

A. M. M. Saleh (✉)
Petroleum Applications Department, Asphalt Lab, Egyptian Petroleum Research Institute,
Cairo, Egypt

R. K. Farag
Petroleum Applications Department, Additives Lab, Egyptian Petroleum Research Institute,
Cairo, Egypt

T. J. Gutiérrez (ed.), *Reactive and Functional Polymers Volume Four*,
https://doi.org/10.1007/978-3-030-52052-6_6

extra-technical industries such as membranes, biomedical equipments, among others. The surface modification will include both plasma and ultraviolet (UV) irradiation, atomic layer deposition, electrochemistry, oxidation, reduction, hydrolysis, use of radicals and grafting 'on' or 'from' polymers. Finally, this chapter provides an updated survey on the recovery and recycling of reactive and functional polymers. Other diverse options for the management of polymer waste can be done *via* reuse, chemical and mechanical recycling, as well as the possible application of recycled polymers in different applications such as building construction, road paving, and various other industrial applications were discussed here.

Keywords Plastic wastes · Polymer recycling

6.1 Introduction

Reactive or functional polymers are defined as macromolecules that have unusual and unique properties necessary for special uses (Bergbeiter and Martin 1989; Arshady 1997). The characteristics of the reactive polymers depend on the presence of polar functional groups, which are generally different from the already existing polymer backbone. The addition of polar or ionic functional groups on hydrocarbon backbones or functionalization of polar polymer chains with hydrophobic groups are some examples of this dissimilarity. However, chemical dissimilarity or heterogeneity improves the reactivity and compatibility of the polymers. An advantage of the presence of functional groups is their ability to form self-assemblies or supramolecular structures through chemical or physical stimuli, which can lead to the formation of smart material. Most functional polymers are formed from simple linear backbones in different forms such as chain-end (telechelic), in-chain, block, graft and special structures (Fréchet 1994) such as three-dimensional polymers: star and hyperbranched polymers (Kim and Webster 1990; Malmström and Hult 1997; Turner and Voit 1997) and dendrimers (tree-like structures) (Tomalia et al. 1985). Low cost, ease of processing and unique mechanical properties are the main advantages of functional polymers. The properties mentioned above can be adjusted according to the desired application.

6.2 Polymer Functionalization Methods

Functionalization methods to modify the nonreactive polymer are categorized into three broad categories, such as direct polymerization, coordination and post polymerization. On the other hand, direct polymerization method is classified into anionic, cationic, grafting and free radical methods, while post polymerization proceeds into

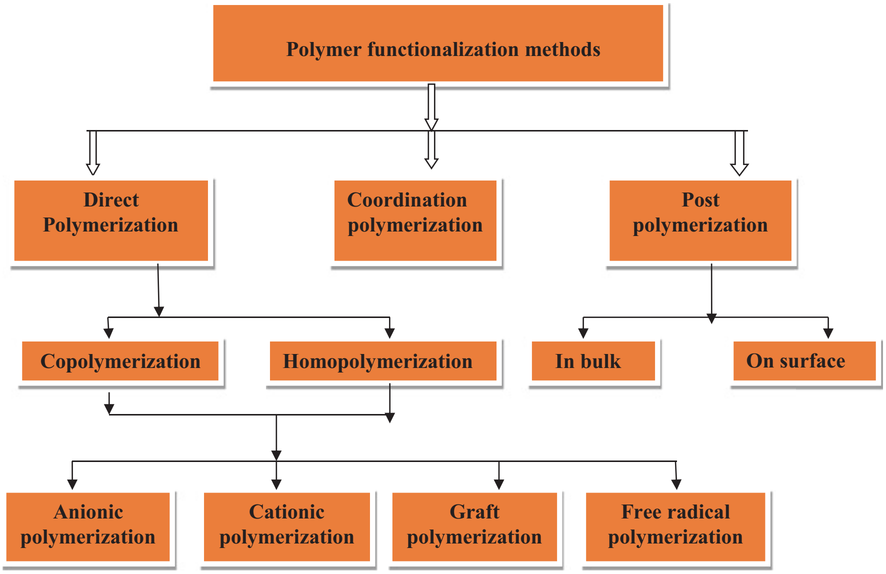

Fig. 6.1 Direct methods of polymer functionalization

two routes namely in bulk and on surface of the pre-existing polymer. All the polymer functionalization methods are shown in Fig. 6.1 and will be illustrated in the following subsection.

6.2.1 Direct Polymer Functionalization

Polymer functionalization by direct methods are classified broadly into homo and copolymerization techniques. Homopolymerization functionalization deals with the single type of monomer or polymer. Otherwise, copolymerization deals with more than one type of polymers. In direct copolymerization polymer functionalization, more than one comonomers are used to build the particular copolymer through chemical reaction. The formation of copolymer depends on various factors such as comonomer nature, alternativity, statistics and indiscriminate. The composition and characteristics of the prepared copolymers are also affected by ratio of reactivity of the reacted comonomers and accordingly affect on field application of the resultant material. Copolymerization of maleic anhydride (MA) with styrene (St) to prepare copolymer namely poly(St-alt-MA) is an example of direct copolymerization. In this reaction, MA works as it is a reactive anhydride, and therefore, it is possible to react with different types of nucleophiles such as alcohols or amines (Bonilla-Cruz et al. 2007; Hurtgen et al. 2011). The two types of direct polymerization are explained as follows:

6.2.1.1 Anionic Polymerization

Anionic polymerization functionalization is believed to be the most precise procedure of ‘living’ procedure and has highest degree of control within polymerization methods. This procedure proceeds without chain transfer and termination, producing polymers with expected molecular weight (Mw), narrow molecular weight distribution (MWD or polydispersity index—PDI = weight-average apparent molecular weight (M_w)/number-average apparent molecular weight (M_n)), distinct architectures, as well as the degree of functionalization purity is high. Often, anionic polymerization in not suitable preparation method for the preparation of linear or star polymers with MWD < 1.1 and functional purity >95% (Hsieh and Quirk 1996). Anionic procedure is also usually used for manufacturing chain-end (telechelic) and in-chain functional polymers. As an example, termination of ‘living’ lithium macromolecules with electrophilic reagents can be terminated using anionic polymerization to prepare telechelic polymers in a wide variety.

6.2.1.2 Cationic Polymerization

In this type of polymerization, a cationic initiator is transferred to the pre-existing polymer or a monomer to be reactive pieces. The type of monomers suitable for cationic polymerization are limited to olefins. On the other hand, this method is not suitable for producing well defined polymers for rearrangement of molecules in addition to inter and intra-molecular transfer. Recently, several polymers are prepared using cationic polymerization by controlling both of initiation, propagation and termination approaches (living polymerization). An example of cationic polymerization, is the preparation of tetrahydrofuran, poly(isobutylene) and poly(*N*-vinylcarbazole) (Smith and Hubin 1973).

6.2.1.3 Graft Polymerization

This class of functionalization is often used to form comb or reed polymers and consisting of one of the three approaches:

1. *In situ* homo or copolymer grafting synthesis containing the functional group has long or a small chain to a unit of the backbone of desired polymer chain to graft (starting from technique) (Bonilla-Cruz et al. 2013).
2. The atom of backbone that has the affinity to change is reacted or interchanged by the functional monomer or reactive groups.
3. Grafting a polymer with another one having a functional species, reactive groups or an initiator. The resultant polymer can have different structures such as regular or brushes, depending on both of graft distance and reactivity of the copolymers.

Examples of polymerization grafting is functionalization of poly(isoprene) and poly(butadiene) (PB) with some kinds of nitroxide moieties (Bonilla-Cruz et al. 2010). Another example is grafting of single-wall carbon nanotube with poly(styrene) (PS) (Qin et al. 2004). Also, synthesis of cylindrical molecular brushes have density of grafting well controlled and low dispersity using the new techniques of grafting namely reversible addition fragmentation chain transfer (RAFT) and ring-opening metathesis polymerization (ROMP) methods (Li et al. 2009).

6.2.1.4 Free-Radical Polymerization

Free-radical polymerization is usually used, practically in many products and in the preparation of laboratory polymers in high degree of control, by using free-radical polymerization, which can be formed in bulk or suspension, several functional groups can be afford to non-reactive polymers (Boutevin and Pietrasanta 1989; Moad and Solomon 2006). Otherwise, the control difficulty of dispersity, chain building, as well as the end group of the final resultant polymer are the major disadvantages of free-radical polymerization. Termination and propagation have high effect on effectiveness and growing of resultant polymers. Telomerization is a type of free radical polymerization in which the used agent for chain transfer has low Mw and high reactivity (Busfield et al. 1998). Almost all telomeres are used in telechelic preparation methods, as well as addition/fragmentation (Krstina et al. 1995). The control of this type of direct or indirect polymerization were studied by many researchers (Georges et al. 1993, 1997; Hawker 1994, 1995, 1996; Wang and Matyjaszewski 1995a, b; Percec and Barboiu 1995; Kato et al. 1995). Reversibility and rapid growth of inactive species, and the covalent atom that bonded to the reactive radical species has great effect on free radical efficiency. The termination reaction process between the growing radical moieties is affected by the reaction velocity and direction. Recently, ‘living’ polymerization is used instead of anionic or cationic techniques to produce well controlled polymer from points of views of low MWD, Mws, architectures, chain ends and capability of incorporating a wide range of functional groups. An example of free-radical functionalization is a combination of a conventional radical initiator, benzoyl peroxide, with 2,2,6,6-tetramethyllpiperidinoxyl (TEMPO) to obtain a well controlled free radical polymerization of benzoyl peroxide from points of view of molecular weight and chain functionalization, TEMPO is added to the initiator (Georges et al. 1993, 1997). Another example is, aminophenol protected with f-butoxycarbonyl (f-BOC), which can be coupled with the bromo-substituted TEMPO derivative in order to give the functionalized initiator. TEMPO is also used for the preparation of polyfunctional molecules bearing multiple initiating centers. Three arm star PS can be prepared by using polyfunctional molecules carrying several centers of initiators. Similarly, atom transfer radical polymerization (ATRP) has been used by Wang and Matyjaszewski (1995a, b) for the synthesis of PS and polyacrylates with controlled Mws.

6.2.2 Coordination Polymerization Functionalization

Coordination polymerization is used especially for functionalization of transition metals with catalyst. The importance of this route comes from the difficulty of using the ordinary methods of functionalization of transition that poisoned with heteroatoms such as N and O. One of two routes must be followed to maintain this type of functionalization, such as taking care of the monomer itself or modifying the catalyst used. Ziegler-Natta polymerization by Ti/Al systems, metallocene polymerization with Ti, Zr, Hf catalysts, or metathesis polymerization with W, Mo, Re metals are some examples of coordination functionalization. Modification of Ziegler-Natta polymerization catalyst involves metals, ligands and/or anions. For examples, Ni, Pd late transition metals (Brookhart et al. 1994a, b; Abu-Surrah et al. 1996; Johnson et al. 1996) and lanthanides (e.g. Sm) (Boffa and Novak 1994, 1997a, b) tend to be more tolerant of polar functionalities than are early transition metals (e.g. Ti, Zr, Hf). When the transition metal center is chosen further to the right in the periodic table, it becomes softer and contains more d-electrons, thereby favoring complexation with softer bases like olefins rather than harder oxygen containing functional groups.

6.2.3 Post functionalization

This type of functionalization based on orienting or conversion achievable of a non-reactive polymer bearing a chemoselective finger that is inert towards the ordinary polymerization conditions to reactive form. This method is carried out by direct or copolymerization procedures, and are affected by the tolerance of the functional group, as well as the orthogonal technique. However, post functionalization is classified as surface and bulk approaches, and are illustrated in the next subsection.

6.2.3.1 Surface Functionalization

This type of functionalization is used to activate polymers that do not react in different ways such as modifying the end of the already existing polymer, doubting that the chain will grow, or adding functional chemical groups or agent after breaking the chain.

6.2.3.2 Bulk Functionalization

In this type of polymerization, the functional group is embedded inside the network structure of the pre-existing polymer itself. Chemically crosslinked polymer is an clear example of bulk polymerization. In this type of functionalization, a crosslinking approach is used, which is usually a chemical reaction to bond two polymers. The cross-link may be covalent or ionic bonds. The characteristics of the prepared crosslinked polymer depends on crosslink density. Heat, pressure, pH change or irradiation are necessary initiator factors for the crosslinking reaction to start. An example of crosslinking using a chemical reaction is mixing of partially or un-polymerized resin with some crosslinking agents. In case of crosslinking thermoplastic materials, a radiation source as gamma radiation or ultraviolet (UV) light can be used. It must be mentioned here that, physical crosslinks are formed where the chemical reaction is covalent. In case of exposing the polymers desired to be crosslinked to atmospheric oxygen, the resultant polymers will be oxidative crosslinked and an oxidizing agent as hydrogen peroxide can be used to speed up the reaction. The synthetically crosslinked polymers are used in different applications such as car tires and forming polyacrylamide gels. Ethylene vinyl acetate is an examples of polymers that are crosslinked and used in solar panels.

6.3 Chemical Modification of Polymers

Chemical modification of polymer is achieved to functionalize any small molecule by a chemical reaction. This modification can be carried out in bulk, solution or on surface of the molecule. The reactivity of the synthesized functional group is affected and controlled by some factors such as the type of neighboring groups, polymer backbone type and morphology, as well as the solubility/miscibility of reactant and catalyst phases. However, reactions on polymer cause its crosslinking with other polymer to complicate and its chain to cleave. Different methods for performing chemical modification of the polymer are illustrated below:

6.3.1 Chemical Modification of Polymer in Solution

Solution reaction of polydienes (polyolefins) is a well known example of chemical modification. In this reaction, various types of modification are clearly detected such as isomerization, cyclization, hydrogenation, epoxidation, and reacting with carbenes or enophiles (Schulz et al. 1982; Schulz and Patil 1988). The resultant modified polyolefins have higher glass transition temperature (T_g) values, and consequently different mechanical, physical, chemical and electronic characteristics are obtained compared to an unmodified one, the modification process increases the field applications of the prepared materials. Otherwise, the ease of processing, recyclability, as well as low cost are unique properties of modified polyolefines, despite the modification sometimes they limit the reactivity of functional groups, and consequently, affect some particular uses such as adhesion, dying and painting.

6.3.2 *Chemical Modification of Polymer in Bulk*

Bulk modification of polymers by reactive extrusion (REx) represents a technologically attractive and relatively simple method. Modification is achieved during the forming process (extrusion or injection moulding) without the need of an additional modification step. It is important to choose reactive modifiers showing high compatibility with the polymer matrix in order to avoid agglomeration and negative effects on the mechanical properties of the bulk. For example, REx of stabilizers containing a polymerizable functional groups could be a very interesting approach to overcome the problem of the physical loss of these additives. The grafted stabilizers cannot be detached from the polymer matrix except through severance of chemical bonds and should, therefore, lead to highly substantive and effective stabilization systems, especially in an aggressive leaching environment (Gutiérrez & Alvarez 2017a, b, c; Herniou et al. 2019; Gutiérrez et al. 2017; Gutiérrez et al. 2021).

6.3.3 *Chemical Modification of Polymer on Surface*

Surface functionalization is a procedure used for modifying only the polymer surface without affecting its bulk characteristics. The change in polymer interfacial properties is a result of surface functionalization that can be denoted by wettability (this can be confirmed by change in the contact angle (WCA) values). However, surface modification of polymer has a great effect on its properties such as adhesion (Kaczinski and Dwight 1993; Kaboorani and Riedl 2011), biocompatibility, permeability (Le Roux et al. 1994), wettability (Costello and McCarthy 1987; Whitesides and Ferguson 1988), printability (Harth and Hibst 1993), weatherability (Jagur-Grodzinski 1992) or friction (Bee and McCarthy 1990).

As an example of surface functionalization is free-radical grafting of polyolefin by reaction with MA. The resultant modified polyolefin will contain amine groups, which are chemically versatile, although it causes corruption in expected Mw and functional-group distribution inside the polymer (Ward and McCarthy 1990; Garbassi et al. 1995). It is worth mentioning that after polydienes and polyolefins have been modified in solution, and it is also possible that a surface modification route can be carried out. An example of surface modification are polar functional group-modified polyolefins, which have been introduced on to syndiotactic 1,2-polybutadiene surfaces by photolytic addition of thiols, as well as treatment with aqueous permanganate.

6.4 Surface Modification Techniques

Modification of polymer surface is an important factor in development of polymer science because most of them are inert or weak reactive to materials used in industrial applications. However, polymers are considered one of the most important materials in our life day such as poly(ethylene) (PE), poly(propylene) (PP), etc., which are used in different applications such as gears, cars, clothes, electric cables for electricity, medical tools, among others. Generally, polymer surface modification is carried out in one and/or two ways with the aim of increasing its resistivity to environmental conditions or to impart or alter special characteristics for a specific application. An obvious example of surface care is painting the steel surface of cars in order to resist rust or corrosion caused by weather conditions. On the other hand, the use of polymers in medical applications such as cardiac supports, drug delivery, and in the electric field as electrical sensors are examples of surface modification to impart some properties for specific application.

In this section, different surface modification techniques as plasma, electrochemistry, chemical oxidation, chemical reduction, hydrolysis and aminolysis are explained as follows:

6.4.1 Plasma Technique

Plasma is defined as the forth state of matter (gas, liquid, solid and plasma). It is formed as a partly ionized gas, which contains energetic electrons, charged ions, free radicals and neutral particles (atoms and molecules). Some of these particles may be in an energetic state and when return to their earth state *via* emission of photons, which produces the typical plasma light emission. However, plasmas are formed by exciting gases into energetic states by using radio-frequency, microwaves or electrons from a hot filament discharge (Lieberman and Lichtenberg 2005). The most popular type of plasmas used in surface modification or treated are cold non-equilibrium, because they do no break the chemical bonds of the desired polymer to modify or destroy its surface.

A cold plasma can also be generated by using Corona discharge method, which is used for different industrial applications. In this method, the gas is ionized around a conductor, keeping a high potential energy. An example of Corona technique is surface modification of poly(dimethylsiloxane) (PDMS) (Eifert et al. 2015). Plasma can modify the surface polymer in two ways. The first way is using simple gases such as Ar, H_2O, O_2, N_2, … etc., which produce reactive pieces that react with the polymer surface. Second way, in the case of organic molecules to generate the plasma, a polymeric film is formed on to the polymer surface.

6.4.2 Electrochemistry Technique

In electrochemical technique, the polymer surface is activated by missing or gaining electrons using an electrical circuit. The polymer can be anode or cathode in the circuit depending on its place, in addition to the composition of another type of electrode in the electrical chain. An example of treatment of the polymer surface using the electrochemistry technique is the activation of poly(tetrafluoroethylene) (PTFE) (Combellas et al. 2004). Firstly, the surface of PTFE is reduced by Pt electrode either in contact with or within a distance of ~10 μm. The second case, is considered as a scanning electrochemical microscopy (SECM) pattern. The reduction of PTFE is obtained by two methods, such as the choice of benzonitrile, e.g. an electrochemically reversible redox couple (benzonitrile/benzonitrile radical anion, $E° = -2.05$ V/Ag/AgCl in paretic medium) or by using a solution of solvated electrons, prepared in liquid ammonia by electrochemistry. Upon electron transfer, the C-F bond is cleaved and the radical anion is reoxidized to benzonitrile, which diffuses to the electrode, thus reducing the pieces. The reduction results is a reactive n-doped polymeric carbon surface. The results of the reaction are unsaturated and oxygen functions, or a bonded polyacrylic acid film in the presence of acrylic acid. Also, nitro or bromophenyl groups attached to the carbon in the presence of 4-nitro or 4-bromobenzenediazonium and Au, Ag or Cu metallic deposits in the presence of the corresponding ions may be the result of the reduction.

6.4.3 Chemical Oxidation

Surface treatment of a polymer by chemical oxidation depends on its reaction with the oxidizing agent to form an oxygen functional group. Oxidation of PE with chromic acid and piranha solutions is an example of this type of surface functionalization. However, this method is resembled for using oxygen plasma or UV radiation methods as other means of surface functionalization of PE from points of view of surface roughness, WCAs and surface concentration of carboxylate groups. It was found that UV radiation method is the best rather than the other methods namely chemical oxidation and oxygen plasma (Barish and Goddard 2011a, b), and oxidation (Han et al. 2010) of PS-*b*-poly(ethylene-*co*-butylene)-*b*-PS (SEBS) by $KMnO_4$ or $KMnO_4/H_2SO_4$ provided predominantly surface O-C and O-C=O functions along with a small fraction of O–H and Mn–O groups, as a result the WCA values decreased from 106° to 45°. The most famous oxidizing agent, as it forms the structure of functional groups of peroxides. For example, peroxide is produced on the surface and inside the polymer structure in case of oxidizing PUR polymer, where less than 15% is located on the surface and the total concentration of 2.5×10^{-9} mol/cm^2 (Fujimoto et al. 1993). Another example for chemical oxidation is using ~200 nm-diameter porous anodized aluminum membranes as molds, in which PE and PTFE were cast by heating, where Al membrane, a structured polymeric surface was produced. Further oxidation of the resultant structured PE with $KClO_4/H_2SO_4$, caused its surface to be superhydrophobic polymer and the WCA values decreased from of 172° to 0° (Lee and McCarthy 2007). Recently, chemical oxidation is used for protecting food packaging materials of PE type without reacting with food itself, where peroxides are formed on its surface, thus causing radicals to react with poly(ethylene glycol) (PEG) diacrylate to give PEG-modified PE, which can be reacted with ethylenediamine (as a model of a bioactive molecule) through a Michael addition reaction (Barish and Goddard 2011a, b).

6.4.4 Chemical Reduction

Chemical reduction is used to treat the polymer surface by using a reduction agent in gaseous or liquid form, thus adding to the desired polymer containing ester or ketone functional groups in the chain to obtain a hydroxyl functional group. As an example, small particles of PEEK can be reduced by using a reduction agent as $NaBH_4$ in dimethyl sulfoxide (DMSO) at 120 °C to obtain the OH groups (Díez-Pascual et al. 2009). The obtained modified polymer can be further modified to produce soluble particles, which can be used for special applications in biocompatible systems (Henneuse-Boxus et al. 1998). In this sense, sodium borohydride, hydroquinone, glucose, pyrrole and alkaline solutions are strong reduction agents.

6.4.5 Hydrolysis and Aminolysis

Aminolysis is any compound treated with ammonia or an amine and causes causes polymers to be divided into two parts containing reactive amino groups. Hydrolysis means the formation of chemical bonds by nucleophiles in water or ruptures by substitution, elimination and fragmentation reactions.

Some examples of aminolysis and hydrolysis in polymer surface modification are as follows:

- Poly(ethylene terephthalate) (PET) polymer contains an ester group that can be hydrolyzed in a 2N NaOH solution at 70 °C, thus producing -COO- or -COOH terminal groups onto its surface. The reaction product is dependent further reprotonation with acetic acid (Chen and McCarthy 1998; Roux and Demoustier-Champagne 2003).
- In addition, superhydrophilic and superhydrophobic meltblown poly(butylene terephthalate) (PBT) fiber mats can be produced after being hydrolyzed and reacted in concentrated NaOH. The mat becomes superhydrophilic and perfluoroamine superhydrophobic. This type of treatment causes about 60% of the original polymer to degrade after 30 min (Wang et al. 2014). On the other hand, some examples of polymer surface modification using aminolysis techniques can be shown below:
- Aminolysis of poly(lactic-*co*-glycolic acid) (PLGA) with ethylenediamine (0.05 M) for a time period less than 20 min when hydroxyl and amino groups are formed onto the surface (Croll et al. 2004).

- A PET supported thin silica film (PET-(SiO_2)X-OH) can be produced *via* aminolysis of PET with the amino groups of 3-aminopropyltriethoxysilane (APTES) to produce PET-CONH(CH_2)$_3$Si(OH)$_3$ and tetraethyl orthosilicate (TEOS), which are deposited onto the surface. Both prepared surfaces can be reacted with silane coupling agents in a way similar to oxidized silicon wafers (Fadeev and McCarthy 1998). APTES is also used to modify poly(ethylene naphthalate) (PEN) films to form strong Si–O–Si bonds in adhesive materials (Hu et al. 2002).

6.4.6 Reaction with Radicals, Carbenes and Nitrenes

Reaction with radicals, carbenes and nitrenes is a modification method of polymer surface, which is similar to grafting. In this method, two approaches are followed namely: 'grafting on' and 'grafting from'. Examples of 'grafting on' route using radicals, carbenes and nitrenes can be represented by the following examples:

The use of radicals for the modification of poly(methylmethacrylate) (PMMA) with perfluoroalkyl groups can generally be produced *via* radicals using homolytic dediazonation of diazonium salts. Modification of PMMA with perfluoroalkyl groups starts from the deposition of amine group (NH_2-C_6H_4-C10F21) on its surface in isopentyl nitrite at 60 °C, and then the perfluoroalkyl diazonium salt formed is decomposed to produce perfluoroaryl radical. The radicals produced binds to PMMA surface and become hydrophobic (WCA = 108°) (Chehimi et al. 2014). The iodine atom of alkyl radicals can also be produced from a sterically hindered aryl radical that cannot react with surfaces, but it removes an iodine atom from an alkyl iodide (Hetemi et al. 2016). These radicals react onto the surface of PE and PMMA. The carboxylic groups can be further modified by esterification or amidation with PEG, anthraquinone groups or a dye (e.g. modification of the PE surface with neutral red *via* alkyl radicals).

The carbenes can be obtained from the thermal decomposition of bis(aryldiazomethane) at 120 °C, thus modifying PS or polyacrylate beads (Yang and Moloney 2016). The modified beads can be colored by the use of diazonium salts. The colored modified polymer is an example of complex surface modification.

Modification of the functional surface of PMMA occurs by using nitrene as modifying agent. This agent contains phosphorylcholine and azido groups and is used by its deposition on to the surface of the polymer to be modified (Fukazawa and Ishihara 2013). The agent is cleaved upon irradiation at 254 nm, nitrene is produced as a highly reactive agent, which is inserted into the carbon-hydrogen covalent bond of the desired polymer.

Generally, 'grafting on' reaction causes the modified polymers to have better and adhesion properties. Upon modification, the WCA values from PE decreased from ~100° to ~65°. An example of photochemical 'grafting from' reactions is atom transfer radical polymerization (ATRP). This method is used to grow polymers from surfaces, e.g the modification of nanoporous PB (Guo et al. 2010). Two different methods can be used for the modification of nanoporous PB. The first is by reacting the terminal double bonds of PB to obtain, finally C-Br groups onto the surface. The second method is the photochemical reaction of a benzophenone modified with a C-Br bond, thus allowing the initiation of the ATRP reaction with poly(ethylene glycol) methacrylate (PEGMA). ATRP of a PEG monomer (MPEG) onto the surface of PB is another example of 'grafting from' reaction.

6.5 Recycling of Reactive Polymers

In recent years, concern has grown about the problems of waste in the world and its effect on the environmentally. Polymers are used throughoutour life in different applications and represent one of the most difficult materials to degrade in a short period of time, and therefore, are accumulated in stockpiles in the environment so that different forms are considered with the aim of recycling and reducing waste discarded in the environment, thus helping to maintain the health of our life as much as possible. However, the management of this type of waste includes source reduction (produce less waste), reuse, recycling and compositing (Medina 1997). The waste has some potential negative effects on the environment such as occupation of space that can be used for other purposes, pollution and degradation of aesthetic quality of the environment, generation of harmful odors and support of disease vectors. The polymeric wastes can be categorized according to the source of generation, the acceptability of reuse, hazard effect on human and life, and the nature of the waste. There are different ways to manage the waste such as source reduction to decrease the space needed to landfill, reuse of scrap materials, especially those discarded from construction and demolition, recycling of some materials such as PET, and processing such as sizing. In this part of our chapter, the types of polymers that are used for various applications in our lives are discussed, as well as the recycling methods of reactive polymers, including some examples. Finally, the section focuses on the use of recycled reactive polymers in infrastructure applications as a case study.

6.5.1 Polymers for Industrial Applications

Polymeric materials can be grouped into two categories: thermosets and thermoplastics. Thermoset polymers are formed *via* an irreversible polymerization reaction. However, thermoset polymers are cured by heating or chemical agents. These polymers are characterized by being infusible and insoluble. In contrast, thermoplastics are prepared from linear molecular chains. This type of polymers soften on heating and harden on cooling. Thermoplastic polymers are distinguished by their durability, lightness, low cost, high resistance to corrosion and strength, and user-friendly design. Otherwise, thermoplastic polymers are classified into three groups: crystalline, amorphous and semicrystalline. Crystalline thermoplastics are semi-transparent and have regular molecular chains, as well as having high impact resistance compared to other polymers. PP, and low and high-density polyethylene (LDPE and HDPE) are examples of crystalline thermoplastic polymers. Amorphous thermoplastics are characterized by their transparency and random arrangement of molecules, e.g. poly(vinyl chloride) (PVC), PMMA, poly(carbonate) (PC), PS and acrylonitrile butadiene styrene (ABS), while semi-crystalline polymers have been characterized by their collective properties for the other types. Polyesters, PBT and poly(amide-imide) (PAI) are examples of semi-crystalline polymers, which have unique characteristics suitable for different applications (Collins and Metzger 1970; Le Duigou et al. 2008; Pillin et al. 2008; Hamad et al. 2011). The injection modeling process is the main technique of polymer processing, which allows the fabrication of different kinds of parts, such as the computer mouse (Brandrup et al. 1996; Lee et al. 2002; Yarahmadi et al. 2003; Augier et al. 2007).

6.5.2 Reactive Polymer Recycling Techniques

Different techniques are used to decrease the accumulation of plastics, such as chemical and mechanical recycling, and energy recovery to produce useful materials, which can be used for other purposes under defined conditions (Waldman and De Paoli 1998; Kartalis et al. 2000; de la Puente et al. 2002; Hájeková and Bajus 2005; Kabdi and Belhaneche-Bensemra 2008; Vallim et al. 2009; Jin et al. 2012; Petchwattana et al. 2012). The recycling and reuse of waste material is known as a green bio-industry. The plastic is difficult to be naturally degraded in a short period of time and takes a long time, at least 50 years, to corrode. Plastics are known to cleave in the environment by four mechanisms: photodegradation, thermo-oxidation, hydrolytic and biodegradation by microorganisms. The natural degradation of plastic begins with photodegradation *via* UV light from the sun. Firstly, the polymer absorbs oxygen from air using UV light, which is considered as a source of energy necessary for starting degradation, thus leading directly to second step (thermo-oxidative degradation), where polymer become brittle, as their molecular chains broken into smaller pieces, and the Mw decreases as the pieces are ready for attacking of the microorganisms starting the fourth and final stage of degradation. The microorganisms change the carbon atoms in the polymer chains into carbon dioxide or to be incorporated into biomolecules. This process is very long and can take more than 50 years (Elmaghor et al. 2003). Thus, some recycling technique must be suitable to dispose of plastic polymers. In fact, it is well known plastics are stable and monomer recovery is very poor.

Initially, incineration was used to dispose of thermoplastic wastes, but this method caused emissions of noxious and toxic gases such as CO in the air, as well as incineration ashes that contained lead and cadmium. Thermoplastic polymers type are suitable for recycling for their unique properties as mentioned above. Different characteristics of thermoplastic polymers are considerated to determine the suitability of the polymer to be recycled such as density, T_g, mechanical properties and cost of the recycling process. For example, the density of the polymer can affect the strength of the final product, which is formed when LDPE and PP are used in the linen reinforcement. The T_g is vital for defining the shape and motion of recycled polymer, specially for the amorphous type, the dimensions and motion of polymer molecules do not change. The mechanical properties are also important for determining both the tensile strength and tensile modulus (Achilias et al. 2007a, b, 2009; Tri Phuong et al. 2008; Vicente et al. 2009; Yang et al. 2009; Wei et al. 2010; Aurrekoetxea et al. 2001). The cost of the plastic recycling process should also be as low as possible. It should be mentioned here that recycling method decreases the environment pollution, as well as conserving the energy necessary for incineration and keeping the material for a longer period of time (Brennan et al. 2002; Gao et al. 2003; Bourmaud and Baley 2009; Bahlouli et al. 2012).

6.5.2.1 Mechanical Recycling

The mechanical recycling method deals with the reuse of the waste polymer without using any chemical reaction. Mechanical recycling methods can be basically classified into two routes: primary and secondary recycling.

1. **Primary Recycling**

   Primary recycling is a simple and low-cost recycling process in which the waste is reused in its original form and structure. The drawback of primary recycle is the limitation of recycling cycles for each waste product (Zaidi et al. 2010).

2. **Secondary Recycling**

   In this technique, simple processing routes can be used such as melting and sizing without changing the structure of the waste, thus recycling processing is limited only to thermoplastic polymers. Thermoplastic polymers can be recycled by extrusion after the waste is classified, cleaned, washed and cut into small pieces to be later melted. Another form of secondary recycling is mixing the waste with another material to obtain the desired properties.

   It is worth mentioning that the drawback of the mechanical recycling technique is that the characteristics of the waste change after each recycling cycle, since the Mw decreases dramatically. It is recommended to use chain extender compounds or to reprocess with vacuum degassing with this technique. Generally, this technique is preferable due to its low cost, despite the fact that it requires large investments (Elmaghor et al. 2003).

6.5.2.2 Chemical Recycling

Chemical recycling occurs by using different chemical reactions (e.g. glycolysis, hydrolysis and pyrolysis) in order to change the structure of the waste to be converted into monomers or partially depolymerized into oligomers. The resulting monomers and oligomers can be used to produce new polymeric products (Zaidi et al. 2010). Other chemical reactions used for polymer recycling are gasification, methanolysis, thermal and catalytic cracking. However, all forms of degradation reactions such as photodegradation, ultrasonic degradation and microwave reactor degradation are also used to destroy the chemical structure of the polymer. In fact, chemical recycling is difficult to use everywhere, because it requires a lot of investment and expert personnel. Glycolysis and methanolysis are the most widely used chemical recycling methods (Lee et al. 2002; Arandes et al. 2003; Williams and Bagri 2004). For example, PET can be prepared into different products depending on the type of reagent used in chemical recycling. PET is sometimes hydrolyzed using water or acids, or glycolyzed using glycols or alcohols to form an alcoholysis reaction. In case of hydrolysis, the PET waste can react with water under different pH conditions and the product is completely depolymerized from the reagent into its monomers. The hydrolysis reaction conditions such as high temperature (ranging from 200 to 250 °C) and pressures (between 1.4 and 2 MPa) limit the use of this method due to its high cost. In alkaline hydrolysis of PET flakes, aqueous solutions such as NaOH or KOH at 4–20 wt.% are used. An example of alkaline hydrolysis of waste PET that happens after waste soft-drink bottles was washed, dried and cut into small pieces and subjected to alkaline hydrolysis (aqueous NaOH solutions) at a temperature ranging between 120 and 200 °C, or using a non-aqueous KOH solution in methyl cello solution at 110–120 °C. Under conditions, sulfuric acid is used to separate high purity terephthalic acid (TPA). In this method, about 2% isophthalic acid mixture is obtained together with the pure 98% TPA, and the calculated activation energy was 99 kJ/mol (Achilias et al. 2007a, b). The possibility of simultaneously recycling PET and PVC from PVC-coated woven fabrics was also demonstrated by García et al. (2009a, b) *via* alkaline hydrolysis. However, other mineral acids such as nitric or phosphoric acids are used in the acid hydrolysis method. The acid hydrolysis condition is based on the type of acid. For example, in the decomposition of PET powder from waste bottles using nitric and sulfuric acids, the reaction temperatures are between 70 and 100 °C, (Boronat et al. 2009; García et al. 2009a, b) and 30 °C (Pérez et al. 2010), respectively. In case of neutral hydrolysis, hot water or steam is used. Autoclaves at temperatures between 200 and 300 °C and pressures of 1–4 MPa are the reaction conditions. This method is highly effective at temperatures above 245 °C, where the the efficiency exceeds 95%. According to Karahaliou and Tarantili (2009) neutral hydrolysis is believed to be highly efficient and is used instead of other hydrolysis methods, because it is more environmentally friendly even though the impurity of the reaction product is not high. The chemical recycling of PET by glycolysis involves the insertion of ethylene glycol (EG) into the PET chains to give bis(hydroxyethyl) terephthalate (BHET), which is a substrate for the synthesis of PET and other oligomers (Chen et al. 2011; Scaffaro et al. 2012). Keeping this in view, Yeh et al. (2009) reported the glycolysis of PET using various ionic basic liquids as catalysts, resulting in a higher catalytic activity using 1-butyl-3-methylimidazolium hydroxyl ([Bmim]OH) compared to 1-butyl-3-methylimidazolium bicarbonate ([Bmim]HCO_3), 1-butyl-3-methylimidazolium chloride ([Bmim]Cl) and 1-butyl-3-methylimidazolium bromide ([Bmim]Br). Bai et al. (2012) also reported that the purity of the glycolysis reaction with ionic liquids was modest compared to those using traditional compounds (e.g. metal acetate). Generally, the reactivity of the glycolyzed agent depends on temperature and catalysis, in addition to the physicochemical properties of the glycol used (Fraisse et al. 2005; Szabo et al. 2011). In chemical recycling *via* methanolysis of PET using methanol, the reaction conditions are temperatures between 180 and 280 °C and pressures from 2 to 4 MPa, thus yielding dimethyl terephthalate (DMT) and EG, while Du et al. (2011) reported that the ideal conditions for the methanolysis reaction are temperature between 260 and 270 ° C, pressure from 9.0 to 11.0 MPa and a methanol/PET ratio from 6 to 8. The resulting DMT can be purified by distillation before reusing it to produce PET (Elmaghor et al. 2004). On the other hand, polyolefin are an important group of thermoplastics used throughout the world, and they cannot be decomposed using simple chemicals into their monomers due to the random scission of the C-C bonds (Saleh et al. 2015). In this case, pyrolysis is used to produce oil and gaseous fractions to be used as feedstock for the production of new plastics. LDPE, HDPE and PP can be recycled using large amounts of organic solvents, dissolution/reprecipitation techniques (mechanical recycling) and pyrolysis (chemical/feedstock recycling). In case of mechanical recycling, large amounts of organic solvents must be used to obtain a high purity polymer. Therefore, chemical recycling is the most preferable technique. Pyrolysis technique is effective in PP than LDPE, and finally HDPE, and the decrease in thermostability in case of producing branched polymer (Hidaka et al. 2009). In case of PS degradation, toluene is an effective solvent used in the recovery of St from PS at 310–370 °C and 6.0 MPa pressure (Hata et al. 2002).

6.5.2.3 Energy Recovery or Quaternary Recycling

This method relies on recycling the polymer by recovering its energy content through incineration to decrease its volume. The disadvantage of incineration is emission of some toxic substances as dioxins. Therefore, it is neither healthy nor acceptable despite being a source of energy generation from polymers.

Of all the recycling methods mentioned above, the chemical technique seems to be the only acceptable one, because it produces the monomers from which the polymer can be formulated (Navarro et al. 2008; Shi et al. 2011; Tsintzou et al. 2012).

6.6 Recycled Reactive Polymers for Infrastructure Applications: A Case Study

As mentioned above, reactive polymers have unique properties from the point of view of their chemical, mechanical and thermal properties, as they are valuable materials and should be conserved as much as possible. The most reactive polymers are suitable for recycling and using as raw materials for infrastructure applications such as coatings and road paving. Polyester, and PET resins and fibers, as well as sometimes functionalized thermoset polymers such as waste car tires can be recycled and reused as a valuable material for other purposes. Polyester resins are unsaturated synthetic polymers, which are obtained by the reaction of dibasic organic acids and polyhydric alcohols. Polyester resins are used in a wide variety of applications such as toner of laser printers, fiberglass reinforced plastic (FRP) pipe applications, and as overlays on roads and bridges. These resins have unique properties such as resistance to heat up to 80 °C, to water, to chemicals, to weathering and ageing, to shrinkage, as well as being low cost and having good wetting to glass fibers. However, polyester resins have some disadvantages such as strong odor, difficult to mix, need proper precautions and weakly bonded to some substrates. Polyester wastes as fibers and spent toner carpet waste fibers have been used as asphalt modifiers for preparing hot mixes asphalt for road paving or coating both of concrete and steel construction. Such wastes are considered as asphalt and concrete reinforcement agents (Martínez-Barrera et al. 2005; Gencel et al. 2010; Essawy et al. 2013). Asphalt produced from petroleum distillation is a viscoelastic material containing saturated, aromatic, resin and asphaltene (SARA) fractions (Essawy et al. 2013). It is thus suitable to be mixed with a variety of not so reactive polymers such as HDPE, PP, LDPE, among others. The benefit of modifying asphalt from its blends with polymers is to increase its softening point to be able to withstand the obvious increase in ambient temperature and temperature variations. The waste PE fibers discarded from the carpet industry can be used in a percentage ranging from 5 to 10wt.% to be mixed with asphalt at a temperature between 160 and 180 ° C in order to reduce the cost of paving and maintenance, as well as reducing the land space necessary for filling land with non-degradable pollutants.

Virgin and recycled reactive polymers are generally considered as novel modifiers for asphalt with the goal of improving mix compatibility and decreasing modifier amount. Covalent bonds are formed between the asphalt and the unsaturated part of the additive (Selvavathi et al. 2002; Singh et al. 2003, 2004; Polacco et al. 2004a, b; Navarro et al. 2007).

The improvement of the properties of asphalt from the reaction of PANI and HCl allowed to give a reactive polymer with a low processing temperature, as a result of the chemical reactions between the -NH groups of the reactive polymer with the polar groups (-OH) of bituminous compounds. The modified asphalt (PMA) has been tested by Elnaggar et al. (2012) using electrochemical measurements in order to be used as a coating for carbon steel. In this sense, Elnaggar et al. (2012) concluded that PMA is suitable to be used as a coating.

The use of asphalt for concrete applications as a coating is an effective element because asphalt is an adhesive and hydrophobic material and inert to most chemicals and anticorrosive substances, but its softness and low resistance to temperature change reduces its possibility of use for this application. Different attempts have been made to increase the field applications of asphalt due to its low cost and versatility, especially in the coating of concrete and steel structures by using unsaturated PP ester (Polacco et al. 2005; El-Wahab et al. 2013; ELsawy et al. 2016). With this in mind, PET wastes have been added to the asphalt by two different methods: wet and dry. Under wet processing conditions, PET wastes are added to the asphalt, while in the dry process they have been used as aggregate for the preparation of hot mixes. Waste PET is generally added to asphalt to improve its resistance to rutting and to increase pavement performance characteristics such as Marshall stability, stiffness and fatigue life (Garcia-Morales et al. 2006; Ahmadinia et al. 2011). The only drawback of prepared modified asphalt is phase separation due to the inhomogeneous distribution of PET wastes in the asphalt (Ameri and Nasr 2016; Sulyman et al. 2016). Therefore, the chemical treatment is considered more suitable for road pavement applications (Padhan et al. 2013; Gürü et al. 2014). Keeping this in mind, Tahvildari et al. (2010) depolymerized PET waste flakes using diethylene glycol (DEG), triethylene glycol (TEG) and propylene glycol (PG) separately in the presence of 0.5% manganese acetate (by weight of waste PET) under an atmosphere of N_2 at 200–210 °C for 4 h. The unsaturated polyesters prepared were added to the asphalt in various percentages ranging from 2 to 10% (w/w) in a wet process, and were characterized in terms of their physical and chemical properties. These authors obtained optimal properties using 4% (w/w) of any of the polymers. Bary et al. (2020) also reported a higher decomposition temperature, rutting parameter ($G^*/\text{Sin}\ \delta$), the values of the complex shear modulus (G^*) and lower phase angle (δ) for modified asphalt samples, thus achieving improve high temperature performance compared to the values of ordinary asphalt binders.

Scrap tire rubber has been used early to improve the aging resistance of asphalt, because the complex crosslinked rubber in scrap tires and its antioxidant content prevent rubber decomposition (Kasa 1997; Wong and Wong 2007). As mentioned above, the heterogeneity between asphalt and rubber as a thermoset polymer, as well as the variation in Mw, lead to an immiscible mixture. The modification of the nano-size and the activation of the tire rubber surface from functional groups can be used to improve the compatibility of the mixture, as a result they can be used as a coating for steel and as a sealant for concrete (Lu and Isacsson 2000; Hussain and Elmasry 2013). The modification includes asphalt flexibility improvement, especially at low temperature for steel coating applications. The prepared coatings were tested using dynamic mechanical analysis (DMA). The results show that the mix improved the cracking resistance of asphalt at low temperature (Saleh et al. 2015).

6.7 Conclusions

This chapter highlights on the reactive and functional polymers that have superior properties such as corrosion resistance, high impact resistance, low density and light weight. The manuscript deals functional polymers from the point of view of functionalization methods, chemical modification, recycling and uses in infrastructure field as a case study. Furthermore, this gives an idea about the classification of the polymeric products into thermoset and thermoplastics, including the different synthesis methods and applications of reactive polymers. The synthesis methods include post-polymerization functionalization, coordination polymerization, as well as free radical, anionic and cationic procedures. The polymer functionalization methods such as direct polymerization, coordination and post polymerization were highlighted. On the other hand, direct polymerization methods namely anionic, cationic, grafting and free radical methods, in addition to post polymerization routes, such as in bulk and on surface of the pre-existing polymer were well defined. The broad classification of direct polymer functionalization methods such as homo and copolymerization techniques were also detailed. The chapter highlights on the application fields of functional polymers, including surface modifications of polymers. The surface modification includes both of plasma and UV irradiation, atomic layer deposition, electrochemistry, oxidation, reduction, hydrolysis and aminolysis, by using the radicals and grafting ‘on’ or ‘from’ polymers. Lastly, the chapter includes the definition of non-decaying waste disposal crises, such as polymers combined with a growing consumer population. It also gives an overview about the recycling methods of reactive polymers such as reuse, chemical and mechanical recycling, as well as the possible application of recycled polymers in different applications such as building construction, road paving, various industrial and indoor applications.

The chapter also explained the coordination polymerization functionalization especially used for functionalization of transition metals with catalyst. The categorization of polymeric waste was defined and its different ways to manage the waste such as source reduction, reuse of scrap materials, recycling of some materials and processing according to size were described. The mechanical recycling technique including primary and secondary routes, chemical recycling approaches, as well as energy recovery or quaternary recycling were defined here, including some examples. Finally, the chapter focused on the use of recycled reactive polymers for infrastructure applications as a case study.

Acknowledgments This chapter was supported by Egyptian Petroleum Research Institute.

Conflicts of Interest The authors declare no conflict of interest.

References

Achilias, D. S., Kanellopoulou, I., Megalokonomos, P., Antonakou, E., & Lappas, A. A. (2007a). Chemical recycling of polystyrene by pyrolysis: Potential use of the liquid product for the reproduction of polymer. *Macromolecular Materials and Engineering, 292*(8), 923–934. https://doi.org/10.1002/mame.200700058.

Achilias, D. S., Roupakias, C., Megalokonomos, P., Lappas, A. A., & Antonakou, E. V. (2007b). Chemical recycling of plastic wastes made from polyethylene (LDPE and HDPE) and polypropylene (PP). *Journal of Hazardous Materials, 149*(3), 536–542. https://doi.org/10.1016/j.jhazmat.2007.06.076.

Achilias, D. S., Giannoulis, A., & Papageorgiou, G. Z. (2009). Recycling of polymers from plastic packaging materials using the dissolution-reprecipitation technique. *Polymer Bulletin, 63*(3), 449–465. https://doi.org/10.1007/s00289-009-0104-5.

Abu-Surrah, A. S., Wursche, R., Rieger, B., Eckert, G., & Pechhold, W. (1996). Control of Molecular Weight in α-Olefin−Carbon Monoxide Alternating Copolymerization. A Way to High Molecular Weight Propene−Carbon Monoxide Thermoplastic Elastomers). *Macromolecules, 1996*(29), 13, 4806–4807. https://doi.org/10.1021/ma960008m.

Ahmadinia, E., Zargar, M., Karim, M. R., Abdelaziz, M., & Shafigh, P. (2011). Using waste plastic bottles as additive for stone mastic asphalt. *Materials & Design, 32*(10), 4844–4849. https://doi.org/10.1016/j.matdes.2011.06.016.

Ameri, M., & Nasr, D. (2016). Properties of asphalt modified with devulcanized polyethylene terephthalate. *Petroleum Science and Technology, 34*(16), 1424–1430. https://doi.org/10.1080/10916466.2016.1202968.

Arandes, J. M., Ereña, J., Azkoiti, M. J., Olazar, M., & Bilbao, J. (2003). Thermal recycling of polystyrene and polystyrene-butadiene dissolved in a light cycle oil. *Journal of Analytical and Applied Pyrolysis, 70*(2), 747–760. https://doi.org/10.1016/s0165-2370(03)00056-1.

Arshady, R. (1997) Desk reference of functional polymers: Syntheses and applications ACS: Washington, 1997. doi: https://doi.org/10.1021/ja9756230

Augier, L., Sperone, G., Vaca-Garcia, C., & Borredon, M. E. (2007). Influence of the wood fibre filler on the internal recycling of poly(vinyl chloride)-based composites. *Polymer Degradation and Stability, 92*(7), 1169–1176. https://doi.org/10.1016/j.polymdegradstab.2007.04.010.

Aurrekoetxea, J., Sarrionandia, M. A., Urrutibeascoa, I., & Maspoch, M. L. (2001). Effects of recycling on the microstructure and the mechanical properties of isotactic polypropylene. *Journal of Materials Science, 36*(11), 2607–2613. https://doi.org/10.1023/A:1017983907260.

Bahlouli, N., Pessey, D., Raveyre, C., Guillet, J., Ahzi, S., Dahoun, A., & Hiver, J. M. (2012). Recycling effects on the rheological and thermomechanical properties of polypropylene-based composites. *Materials & Design, 33*, 451–458. https://doi.org/10.1016/j.matdes.2011.04.049.

Bai, X. J., Wu, Z., & Feng, N. (2012). Degradation of ABS in ABS/$CaCO_3$ composites during reprocessing. *Advanced Materials Research, 455*, 845–850. https://doi.org/10.4028/www.scientific.net/amr.455-456.845.

Barish, J. A., & Goddard, J. M. (2011a). Polyethylene glycol grafted polyethylene: A versatile platform for nonmigratory active packaging applications. *Journal of Food Science, 76*(9), E586–E591. https://doi.org/10.1111/j.1750-3841.2011.02396.x.

Barish, J. A., & Goddard, J. M. (2011b). Topographical and chemical characterization of polymer surfaces modified by physical and chemical processes. *Journal of Applied Polymer Science, 120*(5), 2863–2871. https://doi.org/10.1002/app.33310.

Bary, E. A., Farag, R. K., Ragab, A. A., Abdel-monem, R. M., Abo-shanab, Z. L., & Saleh, A. M. M. (2020). Green asphalt construction with improved stability and dynamic mechanical properties. *Polymer Bulletin, 77*, 1729–1747. https://doi.org/10.1007/s00289-019-02821-z.

Bee, T. G., & McCarthy, T. J. (1990). Frictional studies of surface modified polychlorotrifluoroethylene. *Polymeric Materials Science and Engineering, 63*, 94–98.

Bergbeiter, B. E., & Martin, C. R. (1989). Functional Polymers An Overview. Plenum Press: New York.

Boffa, L. S., & Novak, B. M. (1994). Bimetallic samarium (III) initiators for the living polymerization of methacrylates and lactones. A new route into telechelic, triblock, and "link-functionalized" polymers. *Macromolecules, 27*(23), 6993–6995. https://doi.org/10.1021/ma00101a044.

Boffa, L. S., & Novak, B. M. (1997a). "Link-functionalized" polymers: An unusual macromolecular architecture through bifunctional initiation. *Macromolecules, 30*(12), 3494–3506. https://doi.org/10.1021/ma961805n.

Boffa, L. S., & Novak, B. M. (1997b). Bimetallic samarium (III) catalysts via electron transfer initiation: The facile synthesis of well-defined (meth)acrylate triblock copolymers. *Tetrahedron, 53*(45), 15367–15396. https://doi.org/10.1016/s0040-4020(97)00968-x.

Bonilla-Cruz, J., Caballero, L., Albores-Velasco, M., Saldívar-Guerra, E., Percino, J., & Chapela, V. (2007). Mechanism and kinetics of the induction period in nitroxide mediated thermal autopolymerizations. Application to the spontaneous copolymerization of styrene and maleic anhydride. *Macromolecular Symposia, 248*(1), 132–140. https://doi.org/10.1002/masy.200750214.

Bonilla-Cruz, J., Guerrero-Sánchez, C., Schubert, U. S., & Saldívar-Guerra, E. (2010). Controlled "grafting-from" of poly[styrene-*co*-maleic anhydride] onto polydienes using nitroxide chemistry. *European Polymer Journal, 46*(2), 298–312. https://doi.org/10.1016/j.eurpolymj.2009.10.009.

Bonilla-Cruz, J., Dehonor, M., Saldívar-Guerra, E., & González-Montiel, A. (2013). Polymer modification: Functionalization and grafting. In E. Saldívar-Guerra & E. Vivaldo-Lima (Eds.), *Handbook of polymer synthesis, characterization, and processing* (pp. 205–223). New York: Wiley. https://doi.org/10.1002/9781118480793.ch10.

Boronat, T., Segui, V. J., Peydro, M. A., & Reig, M. J. (2009). Influence of temperature and shear rate on the rheology and processability of reprocessed ABS in injection molding process. *Journal of Materials Processing Technology, 209*(5), 2735–2745. https://doi.org/10.1016/j.jmatprotec.2008.06.013.

Bourmaud, A., & Baley, C. (2009). Rigidity analysis of polypropylene/vegetal fibre composites after recycling. *Polymer Degradation and Stability, 94*(3), 297–305. https://doi.org/10.1016/j.polymdegradstab.2008.12.010.

Boutevin, B., & Pietrasanta, Y. (1989). Telomerization. In G. Allen & J. C. Bevington (Eds.), *Comprehensive polymer science and supplements* (Vol. 3, pp. 185–194). Oxford: Pergamon Press. https://doi.org/10.1016/b978-0-08-096701-1.00076-8.

Brandrup, J., Bittner, M., Michaeli, W., & Menges, G. (Eds.). (1996). *Recycling and recovery of plastics*. New York: Hanser.

Brennan, L. B., Isaac, D. H., & Arnold, J. C. (2002). Recycling of acrylonitrile-butadiene-styrene and high-impact polystyrene from waste computer equipment. *Journal of Applied Polymer Science, 86*(3), 572–578. https://doi.org/10.1002/app.10833.

Brookhart, M., Wagner, M. I., Balavoine, G. G., & Haddou, H. A. (1994a). Polymers with main-chain chirality. Synthesis of highly isotactic, optically active poly(4-tert-butylstyrene-alt-CO) using Pd(II) catalysts based on C2-symmetric bisoxazoline ligands. *Journal of the American Chemical Society, 116*(8), 3641–3642. https://doi.org/10.1021/ja00087a077.

Brookhart, M., DeSimone, J. M., Barborak, J. C., Rix, F. C., Tahiliani, M. K., & Wagner, D. (1994b). *Polymer Preprints, 35*(2), 530.

Busfield, W. K., Jenkins, I. D., Nakamura, T., Monteiro, M. J., Rizzardo, E., Sayama, S., Thang, S. H., Van Le, P., & Zayas-Holdsworth, C. I. (1998). Improving the knowledge and design of end groups in polymers produced by free radical polymerization. *Polymers for Advanced Technologies, 9*(1), 94–100. https://doi.org/10.1002/(sici)1099-1581(199801)9:1<94::aid-pat738>3.0.co;2-b.

Chehimi, M. M., Lamouri, A., Picot, M., & Pinson, J. (2014). Surface modification of polymers by reduction of diazonium salts: Polymethylmethacrylate as an example. *Journal of Materials Chemistry C, 2*(2), 356–363. https://doi.org/10.1039/c3tc31492h.

Chen, W., & McCarthy, T. J. (1998). Chemical surface modification of poly(ethylene terephthalate). *Macromolecules, 31*(11), 3648–3655. https://doi.org/10.1021/ma9710601.

Chen, S. C., Liao, W. H., Hsieh, M. W., Chien, R. D., & Lin, S. H. (2011). Influence of recycled ABS added to virgin polymers on the physical, mechanical properties and molding characteristics. *Polymer-Plastics Technology and Engineering, 50*(3), 306–311. https://doi.org/10.1080/03602559.2010.531869.

Collins, E. A., & Metzger, A. P. (1970). Polyvinylchloride melt rheology II-the influence of molecular weight on flow activation energy. *Polymer Engineering & Science, 10*(2), 57–65. https://doi.org/10.1002/pen.760100202.

Combellas, C., Fuchs, A., Kanoufi, F., Mazouzi, D., & Nunige, S. (2004). Surface modification of halogenated polymers. 6. Graft copolymerization of poly(tetrafluoroethylene) surfaces by polyacrylic acid. *Polymer, 45*(14), 4669–4675. https://doi.org/10.1016/j.polymer.2004.04.067.

Costello, C. A., & McCarthy, T. J. (1987). Surface-selective introduction of specific functionalities onto poly(tetrafluoroethylene). *Macromolecules, 20*(11), 2819–2828. https://doi.org/10.1021/ma00177a030.

Croll, T. I., O'Connor, A. J., Stevens, G. W., & Cooper-White, J. J. (2004). Controllable surface modification of poly(lactic-*co*-glycolic acid) (PLGA) by hydrolysis or aminolysis I: Physical, chemical, and theoretical aspects. *Biomacromolecules, 5*(2), 463–473. https://doi.org/10.1021/bm0343040.

Díez-Pascual, A. M., Martinez, G., & Gomez, M. A. (2009). Synthesis and characterization of poly(ether ether ketone) derivatives obtained by carbonyl reduction. *Macromolecules, 42*(18), 6885–6892. https://doi.org/10.1021/ma901208e.

Du, A. K., Zhou, Q., van Kasteren, J. M., & Wang, Y. Z. (2011). Fuel oil from ABS using a tandem PEG-enhanced denitrogenation-pyrolysis method: Thermal degradation of denitrogenated ABS. *Journal of Analytical and Applied Pyrolysis, 92*(1), 267–272. https://doi.org/10.1016/j.jaap.2011.06.006.

Eifert, A., Petit, J., Baier, T., Bonaccurso, E., & Hardt, S. (2015). Inscribing wettability gradients onto polymer substrates with different stiffness using corona discharge in point-to-plane geometry. *Applied Surface Science, 330*, 104–110. https://doi.org/10.1016/j.apsusc.2014.12.169.

Elmaghor, F., Zhang, L., & Li, H. (2003). Recycling of high density polyethylene/poly(vinyl chloride)/polystyrene ternary mixture with the aid of high energy radiation and compatibilizers. *Journal of Applied Polymer Science, 88*(12), 2756–2762. https://doi.org/10.1002/app.11985.

Elmaghor, F., Zhang, L., Fan, R., & Li, H. (2004). Recycling of polycarbonate by blending with maleic anhydride grafted ABS. *Polymer, 45*(19), 6719–6724. https://doi.org/10.1016/j.polymer.2004.07.022.

Elnaggar, E. M., Nassar, H. S., Migahed, M. A., Elkady, G. M., Elsherif, H., & Saleh, A. M. (2012). Nano reactive and nonreactive polymers as asphalt modifiers for anticorrosion application. *Al-Azhar Bulletin of Science-Basic Science Sector, 23*(1-A), 75–90. https://doi.org/10.21608/absb.2011.7191.

Elsawy, M. M., Taher, M. S., Ebraheme, A. A., Farag, R. K., & Saleh, A. M. M. (2016). Improvement performance of soft asphalt for coating applications. *Construction and Building Materials, 128*, 47–56. https://doi.org/10.1016/j.conbuildmat.2016.10.057.

El-Wahab, H. A., Saleh, A. M. M., Wassel, M. A., Elkady, G., Khalaf, N. S., & Ahmed, S. (2013). Preparation and evaluation of a new anti-corrosive coating based on asphalt cement blended with polyesteramide resin for steel protection. *Progress in Organic Coatings, 76*(10), 1363–1368. https://doi.org/10.1016/j.porgcoat.2013.04.010.

Essawy, A. I., Saleh, A. M. M., Zaky, M. T., Farag, R. K., & Ragab, A. A. (2013). Environmentally friendly road construction. *Egyptian Journal of Petroleum, 22*(1), 189–198. https://doi.org/10.1016/j.ejpe.2012.09.010.

Fadeev, A. Y., & McCarthy, T. J. (1998). Surface modification of poly(ethylene terephthalate) to prepare surfaces with silica-like reactivity. *Langmuir, 14*(19), 5586–5593. https://doi.org/10.1021/la980512f.

Fraisse, F., Verney, V., Commereuc, S., & Obadal, M. (2005). Recycling of poly(ethylene terephthalate)/polycarbonate blends. *Polymer Degradation and Stability, 90*(2), 250–255. https://doi.org/10.1016/j.polymdegradstab.02.019.

Fréchet, J. M. (1994). Functional polymers and dendrimers: Reactivity, molecular architecture, and interfacial energy. *Science, 263*(5154), 1710–1715. https://doi.org/10.1126/science.8134834.

Fujimoto, K., Takebayashi, Y., Inoue, H., & Ikada, Y. (1993). Ozone-induced graft polymerization onto polymer surface. *Journal of Polymer Science Part A: Polymer Chemistry, 31*(4), 1035–1043. https://doi.org/10.1002/pola.1993.080310426.

Fukazawa, K., & Ishihara, K. (2013). Synthesis of photoreactive phospholipid polymers for use in versatile surface modification of various materials to obtain extreme wettability. *ACS Applied Materials & Interfaces, 5*(15), 6832–6836. https://doi.org/10.1021/am402051e.

Gao, Z., Kaneko, T., Amasaki, I., & Nakada, M. (2003). A kinetic study of thermal degradation of polypropylene. *Polymer Degradation and Stability, 80*(2), 269–274. https://doi.org/10.1016/s0165-2370(98)00131-4.

Garbassi, F., Morra, M., & Occhiello, E. (1995). Polymer surfaces: From physics to technology. *Polymer International, 36*(3), 300–300. https://doi.org/10.1002/pi.1995.210360314.

García, M. T., Duque, G., Gracia, I., de Lucas, A., & Rodríguez, J. F. (2009a). Recycling extruded polystyrene by dissolution with suitable solvents. *Journal of Material Cycles and Waste Management, 11*(1), 2–5. https://doi.org/10.1007/s10163-008-0210-8.

García, M. T., Gracia, I., Duque, G., de Lucas, A., & Rodríguez, J. F. (2009b). Study of the solubility and stability of polystyrene wastes in a dissolution recycling process. *Waste Management, 29*(6), 1814–1818. https://doi.org/10.1016/j.wasman.2009.01.001.

Garcia-Morales, M., Partal, P., Navarro, F. J., & Gallegos, C. (2006). Effect of waste polymer addition on the rheology of modified bitumen. *Fuel, 85*(7-8), 936–943. https://doi.org/10.1016/j.fuel.2005.09.015.

Gencel, O., Brostow, W., Ozel, C., & Filiz, M. (2010). Concretes containing hematite for use as shielding barriers. *Materials Science, 16*(3), 249–256. Retrieved from https://pdfs.semanticscholar.org/d64c/79f59519c5e32e5af071a14e724bad87fa89.pdf.

Georges, M. K., Veregin, R. P., Kazmaier, P. M., & Hamer, G. K. (1993). Narrow molecular weight resins by a free-radical polymerization process. *Macromolecules, 26*(11), 2987–2988. https://doi.org/10.1021/ma00063a054.

George, S., George, J., & Tomas, S. (1997). Reactive compatibilization of immiscible polymer blends, Chapter 44 in ”Handbook of Engineering Polymeric Materials”, Marcel Dekker Inc, New York, Basel, Hong Kong.

Guo, F., Jankova, K., Schulte, L., Vigild, M. E., & Ndoni, S. (2010). Surface modification of nanoporous 1,2-polybutadiene by atom transfer radical polymerization or click chemistry. *Langmuir, 26*(3), 2008–2013. https://doi.org/10.1021/la9025443.

Gürü, M., Çubuk, M. K., Arslan, D., Farzanian, S. A., & Bilici, I. (2014). An approach to the usage of polyethylene terephthalate (PET) waste as roadway pavement material. *Journal of Hazardous Materials, 279*, 302–310. https://doi.org/10.1016/j.jhazmat.2014.07.018.

Gutiérrez, T. J., & Alvarez, V. A. (2017a). Properties of native and oxidized corn starch/polystyrene blends under conditions of reactive extrusion using zinc octanoate as a catalyst. *Reactive and Functional Polymers, 112*, 33–44. https://doi.org/10.1016/j.reactfunctpolym.2017.01.002.

Gutiérrez, T. J., & Alvarez, V. A. (2017b). Eco-friendly films prepared from plantain flour/PCL blends under reactive extrusion conditions using zirconium octanoate as a catalyst. *Carbohydrate Polymers, 178*, 260–269. https://doi.org/10.1016/j.carbpol.2017.09.026.

Gutiérrez, T. J., & Alvarez, V. A. (2017c). Data on physicochemical properties of active films derived from plantain flour/PCL blends developed under reactive extrusion conditions. *Data in Brief, 15*, 445–448. https://doi.org/10.1016/j.dib.2017.09.071.

Gutiérrez, T. J., Guarás, M. P., Vera, A., & Alvarez. (2017). Chapter 9. Reactive extrusion for the production of starch-based biopackaging. In M. A. Masuelli (Ed.), *Biopackaging* (pp. 287–315). Miami, EE.UU. ISBN: 978-1-4987-4968-8: CRC Press Taylor & Francis Group. https://doi.org/10.1201/9781315152349-9.

Gutiérrez, T. J., Mendieta, J. R., & Ortega-Toro, R. (2021). In-depth study from gluten/PCL-based food packaging films obtained under reactive extrusion conditions using chrome octanoate as a potential food grade catalyst. *Food Hydrocolloids, 11*, 106255. https://doi.org/10.1016/j.foodhyd.2020.106255.

Hájeková, E., & Bajus, M. (2005). Recycling of low-density polyethylene and polypropylene via copyrolysis of polyalkene oil/waxes with naphtha: Product distribution and coke formation. *Journal of Analytical and Applied Pyrolysis, 74*(1-2), 270–281. https://doi.org/10.1016/j.jaap.2004.11.016.

Hamad, K., Kaseem, M., & Deri, F. (2011). Effect of recycling on rheological and mechanical properties of poly(lactic acid)/polystyrene polymer blend. *Journal of Materials Science, 46*(9), 3013–3019. https://doi.org/10.1007/s10853-010-5179-8.

Han, X., Zhou, Y., Hu, J., & Liu, H. (2010). Surface modification and characterization of SEBS films obtained by *in situ* and *ex situ* oxidization with potassium permanganate. *Journal of Polymer Science Part B: Polymer Physics, 48*(21), 2262–2273. https://doi.org/10.1002/polb.22109.

Harth, K., & Hibst, H. (1993). Surface modification of polypropylene in oxygen and nitrogen plasmas. *Surface and Coatings Technology, 59*(1-3), 350–355. https://doi.org/10.1016/0257-8972(93)90111-z.

Hata, S., Goto, H., Yamada, E., & Oku, A. (2002). Chemical conversion of poly(carbonate) to 1,3-dimethyl-2-imidazolidinone (DMI) and bisphenol A: A practical approach to the chemical recycling of plastic wastes. *Polymer, 43*(7), 2109–2116. https://doi.org/10.1016/s0032-3861(01)00800-x.

Hawker, C. J. (1994). Molecular weight control by a "living" free-radical polymerization process. *Journal of the American Chemical Society, 116*(24), 11185–11186. https://doi.org/10.1021/ja00103a055.

Hawker, C. J. (1995). Architectural control in "living" free radical polymerizations: Preparation of star and graft polymers. *Angewandte Chemie International Edition in English, 34*(13-14), 1456–1459. https://doi.org/10.1002/anie.199514561.

Hawker, C. J. (1996). Advances in living free-radical polymerization: Architectural and structural control. *Trends in Polymer Science, 6*(4), 183–188.

Henneuse-Boxus, C., Boxus, T., Dulière, E., Pringalle, C., Tesolin, L., Adriaensen, Y., & Marchand-Brynaert, J. (1998). Surface amination of PEEK film by selective wet-chemistry. *Polymer, 39*(22), 5359–5369. https://doi.org/10.1016/s0032-3861(97)10216-6.

Herniou, C., Mendieta, J. R., & Gutiérrez, T. J. (2019). Characterization of biodegradable/non-compostable films made from cellulose acetate/corn starch blends processed under reactive extrusion conditions. *Food Hydrocolloids, 89*, 67–79. https://doi.org/10.1016/j.foodhyd.2018.10.024.

Hetemi, D., Médard, J., Kanoufi, F., Combellas, C., Pinson, J., & Podvorica, F. I. (2016). Surface modification of polymers by reaction of alkyl radicals. *Langmuir, 32*(2), 512–518. https://doi.org/10.1021/acs.langmuir.5b03669.

Hidaka, K., Iwakawa, Y., Maoka, T., Tanimoto, F., & Oku, A. (2009). Viable chemical recycling of poly(carbonate) as a phosgene equivalent illustrated by the coproduction of bisphenol A and carbohydrate carbonates. *Journal of Material Cycles and Waste Management, 11*(1), 6–10. https://doi.org/10.1007/s10163-008-0211-7.

Hsieh, H., & Quirk, R. P. (1996). *Anionic polymerization: Principles and practical applications*. Boca Raton: CRC Press.

Hu, B., Siddiqui, J. A., & Ottenbrite, R. M. (2002). Adhesive properties of silanol surface modified poly(ethylene naphthalate) film. *Macromolecular Chemistry and Physics, 203*(10-11), 1631–1635. https://doi.org/10.1002/1521-3935(200207)203:10/11<1631::aid-acp1631>3.0.co;2-c.

Hurtgen, M., Debuigne, A., Fustin, C. A., Jérôme, C., & Detrembleur, C. (2011). Organometallic-mediated radical polymerization: Unusual route toward (quasi-) diblock graft copolymers starting from a mixture of monomers of opposed reactivity. *Macromolecules, 44*(12), 4623–4631. https://doi.org/10.1021/ma200845m.

Hussain, A. I., & Elmasry, S. A. (2013). Chemically modified crumb rubber effects on rubberized asphalt properties. *International Journal of Environmental Sciences, 2*(4), 158–162. Retrieved from http://www.bu.edu.eg/portal/uploads/engineering,%20shoubra/civil%20engineering/2487/publications/sameh%20ahmed%20fahmy%20el-masry_vol-2-4-5-ijes.pdf.

Jagur-Grodzinski, J. (1992). Modification of polymers under heterogeneous conditions. *Progress in Polymer Science, 17*(3), 361–415. https://doi.org/10.1016/0079-6700(92)90020-y.

Jin, H., Gonzalez-Gutierrez, J., Oblak, P., Zupančič, B., & Emri, I. (2012). The effect of extensive mechanical recycling on the properties of low density polyethylene. *Polymer Degradation and Stability, 97*(11), 2262–2272. https://doi.org/10.1016/j.polymdegradstab.2013.09.025.

Johnson, L. K., Mecking, S., & Brookhart, M. (1996). Copolymerization of ethylene and propylene with functionalized vinyl monomers by palladium (II) catalysts. *Journal of the American Chemical Society, 118*(1), 267–268. https://doi.org/10.1021/ja953247i.

Kabdi, S. A., & Belhaneche-Bensemra, N. (2008). Compatibilization of regenerated low density polyethylene/poly(vinyl chloride) blends. *Journal of Applied Polymer Science, 110*(3), 1750–1755. https://doi.org/10.1002/app.28175.

Kaboorani, A., & Riedl, B. (2011). Effects of adding nano-clay on performance of polyvinyl acetate (PVA) as a wood adhesive. *Composites Part A: Applied Science and Manufacturing, 42*(8), 1031–1039. https://doi.org/10.1016/j.compositesa.2011.04.007.

Kaczinski, M. B., & Dwight, D. W. (1993). Enhancement of polymer film adhesion using acid-base interactions determined by contact angle measurements. *Journal of Adhesion Science and Technology, 7*(3), 165–177. https://doi.org/10.1163/156856193x00637.

Karahaliou, E. K., & Tarantili, P. A. (2009). Stability of ABS compounds subjected to repeated cycles of extrusion processing. *Polymer Engineering & Science, 49*(11), 2269–2275. https://doi.org/10.1002/pen.21480.

Kartalis, C. N., Papaspyrides, C. D., & Pfaendner, R. (2000). Recycling of post-used PE packaging film using the restabilization technique. *Polymer Degradation and Stability, 70*(2), 189–197. https://doi.org/10.1016/s0141-3910(00)00106-3.

Kasa, Z. (1997). *Preparation and usage of crumb rubber modified asphalts. Research report*. Veszprem: University of Pannonia.

Kato, M., Kamigaito, M., Sawamoto, M., & Higashimura, T. (1995). Polymerization of methyl methacrylate with the carbon tetrachloride/dichlorotris-(triphenylphosphine) ruthenium (II)/methylaluminum bis(2,6-di-tert-butylphenoxide) initiating system: Possibility of living radical polymerization. *Macromolecules, 28*(5), 1721–1723. https://doi.org/10.1021/ma00109a056.

Kim, Y. H., & Webster, O. W. (1990). Water soluble hyperbranched polyphenylene: "a unimolecular micelle?". *Journal of the American Chemical Society, 112*(11), 4592–4593. https://doi.org/10.1021/ja00167a094.

Krstina, J., Moad, G., Rizzardo, E., Winzor, C. L., Berge, C. T., & Fryd, M. (1995). Narrow polydispersity block copolymers by free-radical polymerization in the presence of macromonomers. *Macromolecules, 28*(15), 5381–5385. https://doi.org/10.1021/ma00119a034.

Le Duigou, A., Pillin, I., Bourmaud, A., Davies, P., & Baley, C. (2008). Effect of recycling on mechanical behaviour of biocompostable flax/poly(L-lactide) composites. *Composites Part A: Applied Science and Manufacturing, 39*(9), 1471–1478. https://doi.org/10.1016/j.compositesa.2008.05.008.

Le Roux, J. D., Paul, D. R., Arendt, M. F., Yuan, Y., & Cabasso, I. (1994). Surface fluorination of poly(phenylene oxide) composite membranes: Part II. Characterization of the fluorinated layer. *Journal of Membrane Science, 90*(1-2), 37–53. https://doi.org/10.1016/0376-7388(94)80032-4.

Lee, J. A., & McCarthy, T. J. (2007). Polymer surface modification: Topography effects leading to extreme wettability behavior. *Macromolecules, 40*(11), 3965–3969. https://doi.org/10.1021/ma070061i.

Lee, S. Y., Yoon, J. H., Kim, J. R., & Park, D. W. (2002). Degradation of polystyrene using clinoptilolite catalysts. *Journal of Analytical and Applied Pyrolysis, 64*(1), 71–83. https://doi.org/10.1016/s0165-2370(01)00171-1.

Li, Z., Zhang, K., Ma, J., Cheng, C., & Wooley, K. L. (2009). Facile syntheses of cylindrical molecular brushes by a sequential RAFT and ROMP "grafting-through" methodology. *Journal of Polymer Science Part A: Polymer Chemistry, 47*(20), 5557–5563. https://doi.org/10.1002/pola.23626.

Lieberman, M. A., & Lichtenberg, A. J. (2005). Principles of Plasma Discharges and Materials Processing, Second Edition, John Wiley & Sons, Inc. https://doi.org/10.1002/0471724254.

Lu, X., & Isacsson, U. (2000). Modification of road bitumens with thermoplastic polymers. *Polymer Testing, 20*(1), 77–86. https://doi.org/10.1016/s0142-9418(00)00004-0.

Malmström, E., & Hult, A. (1997). Hyperbranched polymers. *Journal of Macromolecular Science, Part C: Polymer Reviews, 37*(3), 555–579. https://doi.org/10.1080/15321799708018375.

Martínez-Barrera, G., Vigueras-Santiago, E., Hernández-López, S., Martínez-Barrera, G., Brostow, W., & Menchaca-Campos, C. (2005). Mechanical improvement of concrete by irradiated polypropylene fibers. *Polymer Engineering & Science, 45*(10), 1426–1431. https://doi.org/10.1002/pen.

Medina, M. (1997). The effect of income on municipal solid waste generation rates for countries of varying levels of economic development: A model. *Journal of Solid Waste Technology and Management, 24*(3).

Moad, G., & Solomon, D. H. (Eds.). (2006). *The chemistry of radical polymerization*. Amsterdam: Elsevier. https://doi.org/10.1016/b978-0-08-044288-4.x5015-8.

Navarro, F. J., Partal, P., Martínez-Boza, F. J., & Gallegos, C. (2007). Influence of processing conditions on the rheological behavior of crumb tire rubber-modified bitumen. *Journal of Applied Polymer Science, 104*(3), 1683–1691. https://doi.org/10.1002/app.25800.

Navarro, R., Ferrandiz, S., Lopez, J., & Seguí, V. J. (2008). The influence of polyethylene in the mechanical recycling of polyethylene terephthalate. *Journal of Materials Processing Technology, 195*(1-3), 110–116. https://doi.org/10.1016/j.jmatprotec.2007.04.126.

Padhan, R. K., Gupta, A. A., Badoni, R. P., & Bhatnagar, A. K. (2013). Poly(ethylene terephthalate) waste derived chemicals as an antistripping additive for bitumen–An environment friendly approach for disposal of environmentally hazardous material. *Polymer Degradation and Stability, 98*(12), 2592–2601. https://doi.org/10.1016/j.polymdegradstab.2013.09.019.

Percec, V., & Barboiu, B. (1995). "Living" radical polymerization of styrene initiated by arenesulfonyl chlorides and CuI(bpy)nCl. *Macromolecules, 28*(23), 7970–7972. https://doi.org/10.1021/ma00127a057.

Pérez, J. M., Vilas, J. L., Laza, J. M., Arnaiz, S., Mijangos, F., Bilbao, E., & León, L. M. (2010). Effect of reprocessing and accelerated weathering on ABS properties. *Journal of Polymers and the Environment, 18*(1), 71–78. https://doi.org/10.1007/s10924-009-0154-7.

Petchwattana, N., Covavisaruch, S., & Sanetuntikul, J. (2012). Recycling of wood-plastic composites prepared from poly(vinyl chloride) and wood flour. *Construction and Building Materials, 28*(1), 557–560. https://doi.org/10.1016/j.conbuildmat.2011.08.024.

Pillin, I., Montrelay, N., Bourmaud, A., & Grohens, Y. (2008). Effect of thermo-mechanical cycles on the physico-chemical properties of poly(lactic acid). *Polymer Degradation and Stability, 93*(2), 321–328. https://doi.org/10.1016/j.polymdegradstab.2007.12.005.

Polacco, G., Stastna, J., Biondi, D., Antonelli, F., Vlachovicova, Z., & Zanzotto, L. (2004a). Rheology of asphalts modified with glycidylmethacrylate functionalized polymers. *Journal of Colloid and Interface Science, 280*(2), 366–373. https://doi.org/10.1016/j.jcis.2004.08.043.

Polacco, G., Stastna, J., Vlachovicova, Z., Biondi, D., & Zanzotto, L. (2004b). Temporary networks in polymer-modified asphalts. *Polymer Engineering & Science, 44*(12), 2185–2193. https://doi.org/10.1002/pen.20246.

Polacco, G., Berlincioni, S., Biondi, D., Stastna, J., & Zanzotto, L. (2005). Asphalt modification with different polyethylene-based polymers. *European Polymer Journal, 41*(12), 2831–2844. https://doi.org/10.1016/j.eurpolymj.2005.05.034.

de la Puente, G., Klocker, C., & Sedran, U. (2002). Conversion of waste plastics into fuels: Recycling polyethylene in FCC. *Applied Catalysis B: Environmental, 36*(4), 279–285. https://doi.org/10.1016/s0926-3373(01)00287-9.

Qin, S., Qin, D., Ford, W. T., Resasco, D. E., & Herrera, J. E. (2004). Functionalization of single-walled carbon nanotubes with polystyrene via grafting to and grafting from methods. *Macromolecules, 37*(3), 752–757. https://doi.org/10.1021/ma035214q.

Roux, S., & Demoustier-Champagne, S. (2003). Surface-initiated polymerization from poly(ethylene terephthalate). *Journal of Polymer Science Part A: Polymer Chemistry, 41*(9), 1347–1359. https://doi.org/10.1002/pola.10686.

Saleh, A. M., Farag, R. K., Kandil, U. F., Nageeb, H. M., Reda, M., & Center, P. N. (2015). Utilization of reactive rubber nanoparticles and waste polymers in improving asphalt performance. In *10th International Conference on Composite Science and Technology ICCST/10*.

Scaffaro, R., Botta, L., & Di Benedetto, G. (2012). Physical properties of virgin-recycled ABS blends: Effect of post-consumer content and of reprocessing cycles. *European Polymer Journal, 48*(3), 637–648. https://doi.org/10.1016/j.eurpolymj.2011.12.018.

Schulz, D. N., & Patil, A. O. (1988). Chemical modification of synthetic elastomers. In A. K. Bhowmick & H. Stephens (Eds.), *Handbook of elastomers* (pp. 75–100). New York: M. Dekker.

Schulz, D. N., Turner, S. R., & Golub, M. A. (1982). Recent advances in the chemical modification of unsaturated polymers. *Rubber Chemistry and Technology, 55*(3), 809–859. https://doi.org/10.5254/1.3535904.

Selvavathi, V., Sekar, V. A., Sriram, V., & Sairam, B. (2002). Modifications of bitumen by elastomer and reactive polymer-A comparative study. *Petroleum Science and Technology, 20*(5-6), 535–547. https://doi.org/10.1081/lft-120003577.

Shi, G., He, L. J., Chen, C. Z., Liu, J. F., Liu, Q. Z., & Chen, H. Y. (2011). A novel nanocomposite based on recycled poly (ethylene terephthalate)/ABS blends and nano-SiO_2. *Advanced Materials Research, 150*, 857–860. https://doi.org/10.4028/www.scientific.net/amr.150-151.857.

Singh, B., Tarannum, H., & Gupta, M. (2003). Use of isocyanate production waste in the preparation of improved waterproofing bitumen. *Journal of Applied Polymer Science, 90*(5), 1365–1377. https://doi.org/10.1002/app.12808.

Singh, B., Gupta, M., & Tarannum, H. (2004). Evaluation of TDI production waste as a modifier for bituminous waterproofing. *Construction and Building Materials, 18*(8), 591–601. https://doi.org/10.1016/j.conbuildmat.2004.04.017.

Smith, S., & Hubin, A. J. (1973). The preparation and chemistry of dicationically active polymers of tetrahydrofuran. *Journal of Macromolecular Science: Part A - Chemistry, 7*(7), 1399–1413. https://doi.org/10.1080/10601327308060509.

Sulyman, M., Haponiuk, J., & Formela, K. (2016). Utilization of recycled polyethylene terephthalate (PET) in engineering materials: A review. *International Journal of Environmental Science and Development, 7*(2), 100–108. https://doi.org/10.7763/ijesd.2016.v7.749.

Szabo, E., Olah, M., Ronkay, F., Miskolczi, N., & Blazso, M. (2011). Characterization of the liquid product recovered through pyrolysis of PMMA-ABS waste. *Journal of Analytical and Applied Pyrolysis, 92*(1), 19–24. https://doi.org/10.1016/j.jaap.2011.04.008.

Tahvildari, K., Mozafari, S., & Tarinsun, N. (2010). Chemical recycling of poly ethylene terphthalat to obtain unsaturated polyester resins. *Journal of Applied Chemical Research, 12*, 59–68. https://doi.org/10.1039/c5gc01048a.

Thiemens, M. H., Jackson, T., Mauersberger, K., Schueler, B., & Morton, J. (1991), Oxygen isotope fractionation in stratospheric CO_2, *Geophysical Research Letters*, *18*(4), 669–672. https://doi.org/10.1029/91gl00121

Tomalia, D. A., Baker, H., Dewald, J., Hall, M., Kallos, G., Martin, S., Roeck, J., Ryder, J., & Smith, P. (1985). A new class of polymers: Starburst-dendritic macromolecules. *Polymer Journal, 17*(1), 117–132. https://doi.org/10.1295/polymj.17.117.

Tri Phuong, N., Gilbert, V., & Chuong, B. (2008). Preparation of recycled polypropylene/organophilic modified layered silicates nanocomposites Part I: The recycling process of polypropylene and the mechanical properties of recycled polypropylene/organoclay nanocomposites. *Journal of Reinforced Plastics and Composites, 27*(18), 1983–2000. https://doi.org/10.1177/0731684407086326.

Tsintzou, G. P., Antonakou, E. V., & Achilias, D. S. (2012). Environmentally friendly chemical recycling of poly(bisphenol-A carbonate) through phase transfer-catalysed alkaline hydrolysis under microwave irradiation. *Journal of Hazardous Materials, 241*, 137–145. https://doi.org/10.1016/j.jhazmat.2012.09.027.

Turner, S. R., & Voit, B. I. (1997). Hyperbranched polymers. *Polymer News, 22*(6), 197–202.

Vallim, M. R., Araujo, J. R., Spinacé, M. A. S., & De Paoli, M. A. (2009). Polyamide-6/high-density polyethylene blend using recycled high-density polyethylene as compatibilizer: Morphology, mechanical properties, and thermal stability. *Polymer Engineering & Science, 49*(10), 2005–2014. https://doi.org/10.1002/pen.21439.

Vicente, G., Aguado, J., Serrano, D. P., & Sánchez, N. (2009). HDPE chemical recycling promoted by phenol solvent. *Journal of Analytical and Applied Pyrolysis, 85*(1-2), 366–371. https://doi.org/10.1016/j.jaap.2008.10.007.

Waldman, W. R., & De Paoli, M. A. (1998). Thermo-mechanical degradation of polypropylene, low-density polyethylene and their 1:1 blend. *Polymer Degradation and Stability, 60*(2-3), 301–308. https://doi.org/10.1016/s0141-3910(97)00083-9.

Wang, J. S., & Matyjaszewski, K. (1995a). Controlled/"living" radical polymerization. atom transfer radical polymerization in the presence of transition-metal complexes. *Journal of the American Chemical Society, 117*(20), 5614–5615. https://doi.org/10.1021/ja00125a035.

Wang, J. S., & Matyjaszewski, K. (1995b). "Living"/controlled radical polymerization. Transition-metal-catalyzed atom transfer radical polymerization in the presence of a conventional radical initiator. *Macromolecules, 28*(22), 7572–7573. https://doi.org/10.1021/ma00126a041.

Wang, Z., Macosko, C. W., & Bates, F. S. (2014). Tuning surface properties of poly(butylene terephthalate) melt blown fibers by alkaline hydrolysis and fluorination. *ACS Applied Materials & Interfaces, 6*(14), 11640–11648. https://doi.org/10.1021/am502398u.

Ward, W. J., & McCarthy, T. J. (1990). In J. I. Kroschwitz (Ed.), *Encyclopedia of polymer science and engineering* (p. 1152). New York: John Wiley.

Wei, T. T., Wu, K. J., Lee, S. L., & Lin, Y. H. (2010). Chemical recycling of post-consumer polymer waste over fluidizing cracking catalysts for producing chemicals and hydrocarbon fuels. *Resources, Conservation and Recycling, 54*(11), 952–961. https://doi.org/10.1016/j.resconrec.2010.02.002.

Whitesides, G. M., & Ferguson, G. S. (1988). *Chemtracts. Organic chemistry* (Vol. 1, p. 171). New York: Chemtracts.

Williams, P. T., & Bagri, R. (2004). Hydrocarbon gases and oils from the recycling of polystyrene waste by catalytic pyrolysis. *International Journal of Energy Research, 28*(1), 31–44. https://doi.org/10.1002/er.949.

Wong, C. C., & Wong, W.-g. (2007). Effect of crumb rubber modifiers on high temperature susceptibility of wearing course mixtures. *Construction and Building Materials, 21*(8), 1741–1745. https://doi.org/10.1016/j.conbuildmat.2006.05.020.

Yang, P., & Moloney, M. G. (2016). Surface modification of polymers with bis(arylcarbene)s from bis(aryldiazomethane)s: Preparation, dyeing and characterization. *RSC Advances, 6*(112), 111276–111290. https://doi.org/10.1039/c6ra24392d.

Yang, J., Liang, J. Z., & Tang, C. Y. (2009). Studies on melt flow properties during capillary extrusion of PP/Al$(OH)_3$/Mg$(OH)_2$ flame retardant composites. *Polymer Testing, 28*(8), 907–911. https://doi.org/10.1016/j.polymertesting.2009.08.005.

Yarahmadi, N., Jakubowicz, I., & Martinsson, L. (2003). PVC floorings as post-consumer products for mechanical recycling and energy recovery. *Polymer Degradation and Stability, 79*(3), 439–448. https://doi.org/10.1016/s0141-3910(02)00360-9.

Yeh, S. K., Agarwal, S., & Gupta, R. K. (2009). Wood-plastic composites formulated with virgin and recycled ABS. *Composites Science and Technology, 69*(13), 2225–2230. https://doi.org/10.1016/j.compscitech.2009.06.007.

Zaidi, L., Kaci, M., Bruzaud, S., Bourmaud, A., & Grohens, Y. (2010). Effect of natural weather on the structure and properties of polylactide/cloisite 30B nanocomposites. *Polymer Degradation and Stability, 95*(9), 1751–1758. https://doi.org/10.1016/j.polymdegradstab.2010.05.014.

Chapter 7
Readily Recyclable Thermosets Based on Dynamic Covalent Bonds

Sheng Wang, Songqi Ma, and Jin Zhu

Abstract Thermosetting polymers have played an important and irreplaceable role, such as adhesives, coatings, composites, etc., while they are difficult to be recycled due to their permanent crosslinked networks. The last few years have witnessed the rapid development of thermosetting polymers based on dynamic covalent bonds, also known as covalent adaptable networks (CANs), which could be easily recycled (reprocessable, weldable or even degradable). The need to develop easily recyclable thermosetting polymers based on dynamic covalent bonds, as well as a summary of the research progress is highlighted in this chapter. The easily recyclable thermosets are divided into three categories based on: (1) the dynamic associative exchange reaction, (2) the dynamic dissociative exchange reaction or (3) two mechanisms together exchange reaction. The recycling methods and mechanisms, and research progress of each category of recyclable thermosets are described in this chapter, as well as the applications of the recyclable thermosets are also summarized. Finally, the conclusions and perspectives are highlighted.

Keywords Covalent adaptable networks (CANs) · Malleable thermosets · Thermosetting polymers · Vitrimers

---

S. Wang
Key Laboratory of Bio-based Polymeric Materials Technology and Application of Zhejiang Province, Division of Polymers and Composites, Ningbo Institute of Materials Technology and Engineering, Chinese Academy of Sciences, Ningbo, P. R. China

University of Chinese Academy of Sciences, Beijing, P. R. China

S. Ma (✉) · J. Zhu
Key Laboratory of Bio-based Polymeric Materials Technology and Application of Zhejiang Province, Division of Polymers and Composites, Ningbo Institute of Materials Technology and Engineering, Chinese Academy of Sciences, Ningbo, P. R. China
e-mail: masongqi@nimte.ac.cn

T. J. Gutiérrez (ed.), *Reactive and Functional Polymers Volume Four*,
https://doi.org/10.1007/978-3-030-52052-6_7

7.1 Introduction

Thermosetting polymers (thermosets) are those irreversibly hardened polymers by curing solid or liquid monomers or prepolymers or resins. Due to their chemically crosslinked, insoluble and infusible three-dimensional networks, thermosetting polymers have played an important and irreplaceable role in many applications, such as high-performance adhesives, coatings, composites, rubbers, solar cell encapsulants and light-emitting diode lenses (Ma et al. 2016; Ma and Webster 2018; Wang et al. 2018c). In the early 1980s, the rapid development of the polymer industry had led to the production and consumption of polymers superior to those of steel (Zhang et al. 2018c). However, the resulting challenge is the increasing environmental pollution and the crisis of fossil resources. Thermosetting polymers compared to thermoplastics are much more difficult to be recycled due to their irreversible covalent networks, which is unfavorable for their sustainable development (Ma and Webster 2018). Although some of thermosetting materials are recycled in lower value applications, most of them are landfilled or incinerated. Developing strategies to recycle thermosetting polymers effectively and valuablely remains a formidable challenge.

The last few years have witnessed the rapid development of malleable thermosetting polymers based on dynamic covalent bonds, also known as covalent adaptable networks (CANs). Through the reliable and efficient exchange between different dynamic cross-link points, the macroscopic flow of CANs can be achieved without losing the original properties permanently, thus achieving the recycling of thermosetting polymers (Denissen et al. 2016). In addition, under external stimuli such as heat (Röttger et al. 2017), light (Ji et al. 2014), pH (Wang et al. 2019), etc., dynamic covalent bonds can be cleaved or attacked by other compounds, as a result, CANs can be degraded and dissolved in solvents.

Based on different exchange mechanisms, CANs can be classified into two categories (Fig. 7.1). The first category is the associative CANs, also known as vitrimers, which is based on an associative exchange mechanism (Fig. 7.1a). In this mechanism, CANs show fixed cross-link densities and do not depolymerize under external stimuli. Montarnal et al. (2011) reported on the seminal vitrimers based on transesterification and first proposed the concept of vitrimer. Since then, different dynamic covalent bonds or reactions based on associative exchange mechanism such as aminal (Chao and Zhang 2019), boronic ester (Cromwell et al. 2015), hydrazide Michael adduct (Cromwell et al. 2015), siloxane exchange (Zheng and McCarthy 2012), transalkylation (Obadia et al. 2015), transcarbonation (Snyder et al. 2018), transthioesterification (Wang et al. 2018b), vinylogous urethane exchange (Denissen et al. 2015), etc., have been widely studied. Another category is the dissociative CANs which is based on dissociative exchange mechanism (Fig. 7.1b). In this mechanism, the cross-link points are broken first and then are formed again in another place. The typical example is the reversible Diels-Alder reaction of furan-maleimide system (Chen et al. 2002). In addition, some dynamic covalent structures such as Schiff base and disulfide, have two mechanisms at the same time.

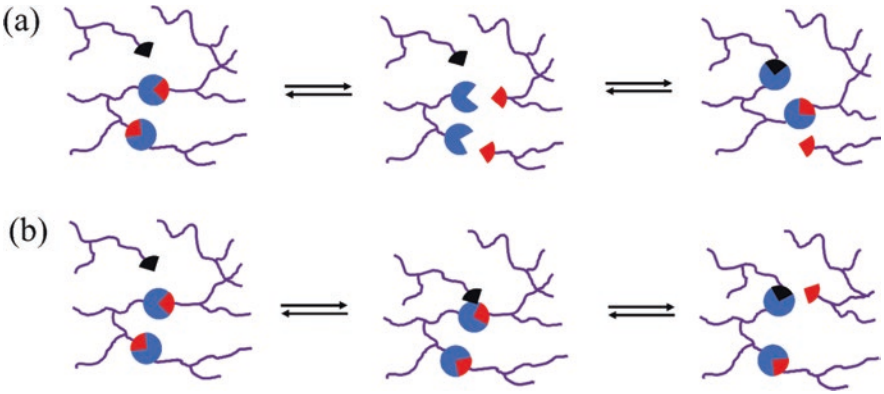

Fig. 7.1 Two different exchange mechanisms of CANs: (**a**) associative exchange mechanism and (**b**) dissociative exchange mechanism. Reproduced with permission from Denissen et al. (2016)

Several high-level reviews have summarized the CANs in different aspects (Bowman and Kloxin 2012; Kloxin and Bowman 2013; Roy et al. 2015; Denissen et al. 2016; Zou et al. 2017; Fortman et al. 2018a; Zhang et al. 2018c). However, to our best knowledge, there has not yet been a chapter or review focusing on the recycling of thermosetting polymers (by reprocessing, welding or degradation, not including self-healing) with dynamic covalent bonds. In this chapter, the easily recyclable thermosetting polymers will be divided into three categories based on dynamic associative exchange reaction, dynamic dissociative exchange reaction and dynamic associative and dissociative exchange reactions simultaneously. The synthetic routes, mechanical and thermal properties, recycling methods and recycling mechanisms, as well as research progress of each category will be described. The applications of the easily recyclable thermosetting polymers based on dynamic covalent bonds will also be highlighted.

7.2 Readily Recyclable Thermosets Based on the Dynamic Associative Exchange Reactions

7.2.1 *Transesterification*

The dynamic transesterification reaction is the process from an alcohol and an ester to form a new ester and a new alcohol, and this reaction usually requires high temperatures and often catalyzed by the addition of Lewis acids or Bronsted bases (Fig. 7.2) (Otera 1993).

Montarnal et al. (2011) proposed for the first time the concept of vitrimers by using the zinc acetate ($Zn(ac)_2$) and zinc acetyl acetonate ($Zn(acac)_2$) catalyzed transesterification in covalently crosslinked acid-epoxy and anhydride-epoxy thermosetting polymers (Fig. 7.3a). Through transesterification at elevated

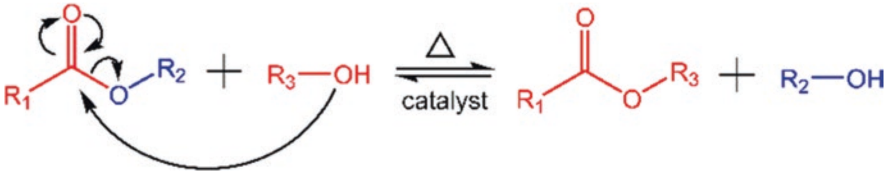

Fig. 7.2 Thermal-induced catalytic transesterification. Reproduced with permission from Otera (1993)

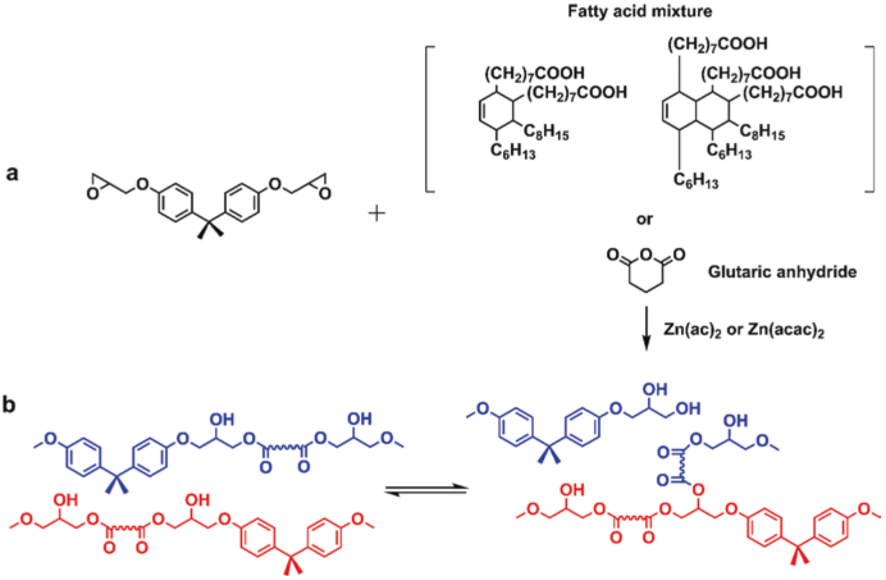

Fig. 7.3 (**a**) Preparation of covalently crosslinked acid-epoxy and anhydride-epoxy thermosetting polymers and (**b**) exchange process *via* transesterification in hydroxy-ester networks. Reproduced with permission from Montarnal et al. (2011)

temperatures between the alcohol and the ester generated by the curing reaction (Fig. 7.3b), the thermosetting polymers showed Arrhenius-like temperature-dependent stress relaxation, and the reprocess recycling of thermosetting polymers was achieved without losing the network integrity. Capelot et al. (2012) also found that changing the nature and content of the catalysts, the transesterification rate, glass transition temperature (T_g) and topology freezing transition temperature (T_v) could be well controlled in epoxy-based vitrimers.

As the acid-epoxy and anhydride-epoxy networks are easy to be prepared directly from commercial raw materials, readily recyclable thermosetting polymers based on transesterification have been widely investigated. Table 7.1 summarizes the properties of readily recyclable thermosetting polymers based on transesterification.

Table 7.1 The properties of readily recyclable thermosets based on transesterification

Curing sy stems	Raw materials	Transesterification catalyst	T_g (°C)	YM (MPa)	σ_m (MPa)	Recycling method	References
Acid-epoxy	Fatty acid mixture/DGEBA	$Zn(ac)_2$	–	4	9	Injection molding	Montarnal et al. (2011)
		$Zn(ac)_2$	30	11	6	Degradation at 180 °C for 6 h in excessive of ethylene glycol.	Shi et al. (2017)
		$Zn(ac)_2$	30–37	1000–3000	15–25	Welding at 190 °C for 5–30 min under pressure.	Legrand and Soulié-Ziakovic (2016)
		$Zn(ac)_2$	30	–	–	Degradation at 180 °C for 4 h in excessive of ethylene glycol	Yu et al. (2016)
	Citric acid/epoxidized soybean oil	Not used	0–30	–	–	Welding at 160 °C for 2 h under pressure.	Altuna et al. (2013)
	Adipic acid/DGEBA/CNT	TBD	45	–	25	Welding at room temperature for 1 min under light.	Yang et al. (2014)
	Adipic acid/DGEBA/Diamine/CNT	TBD	40	600	14	Hot press at 200 °C for 10 min under 2 MPa pressure.	Chen et al. (2017a)
						Welding at room temperature for 15 or 30 s under light.	
	Dodecanedioic acid/epoxidized natural rubber/diamine/CNT	$Zn(ac)_2$	−21.6 to −6.3	2	1.5	Hot press at 200 °C for 20 min under 15 MPa pressure.	Feng et al. (2019a)
						Welding at room temperature for 15 min under light or at 200 °C for 15–30 min.	
	Carboxyl-functionalized carbon black/epoxidized natural rubber	$Zn(ac)_2$	–	1.7–11.3	10.3–22.8	Hot pressed at 180 °C for 5–90 min under 20 MPa pressure.	Qiu et al. (2018)
	Carboxyl-functionalized tunicate cellulose nanocrystals/epoxidized natural rubber	$Zn(ac)_2$	−21.4 to −3.7	–	5.5	Hot pressed at 180 °C for 40 min under 15 MPa pressure.	Cao et al. (2019)
						Welding at 160 °C for 3 h.	
	Carboxyl-functionalized styrene-butadiene rubber/epoxy functionalized silica	TBD	−5	1.6–3.4	3–9.5	Hot pressed at 180 °C for 10 min.	Liu et al. (2018a)
	Carboxyl-functionalized lignin/epoxidized PEG	$Zn(acac)_2$	36.5–75.9	–	–	Degradation in 0.1 M NaOH solution for 10 min.	Hao et al. (2019)

(continued)

Table 7.1 (continued)

Curing sy stems	Raw materials	Transesterification catalyst	T_g (°C)	YM (MPa)	σ_m (MPa)	Recycling method	References
Anhydride-epoxy	Glutaric anhydride/DGEBA	$Zn(acac)_2$	80	1800	55	Hot pressed at 240 °C for 3 min.	Montarnal et al. (2011)
	Succinic anhydride/eugenol derive epoxy	$Zn(acac)_2$	42–58	–	–	Hot pressed at 200 °C for 1 h.	Liu et al. (2017a)
						Degradation at 160 °C for 5 h in ethanol.	
	Succinic anhydride/hyperbranched epoxy	Not used	70–96	2250–2560	46.5–54	Welding at 150 °C for 1 h.	Han et al. (2018)
	Glutaric anhydride/DGEBA/glycerol	Not used	44–105	–	–	Hot pressed at 170 °C for 5 h under 10 MPa pressure.	Liu et al. (2019)
	Phthalic anhydride/DGEBA	$Zn(acac)_2$	98	–	41.2	Hot pressed at 90–210 °C for 1–10 h under 3–12 MPa pressure.	Lu et al. (2017)
Acrylate	Diacrylate/acrylate	$Zn(acac)_2$	55	900	15	Hot pressed at 200 °C for 2 h under 500 MPa pressure.	Zhang et al. (2018a)
PBT-triol	PBT/glycerol	$Zn(acac)_2$	56–82	–	–	Hot pressed at 250 °C for 25 min under pressure.	Zhou et al. (2017)
Diisocyanate-hydroxyl	Hydroxyl terminated PLA/ methylenediphenyl diisocyanate	$Sn(Oct)_2$	60–75	1700	55	Welding at 140 °C for 30 min under 4 MPa pressure.	Brutman et al. (2014)
Siloxane-vinyl	PHMS/vinyl compounds (catalyst: Pt(cod) Cl_2)	Not used	4	–	–	Welding at 120 °C for 30 min.	Ube et al. (2016)

DGEBA: diglycidyl ether of bisphenol A, PEG: poly(ethylene glycol), PHMS: poly(hydrogenmethylsiloxane), PLA: poly(lactic acid), TBD: triazabicyclodecene, YM: Young's modulus, σ_m: tensile strength

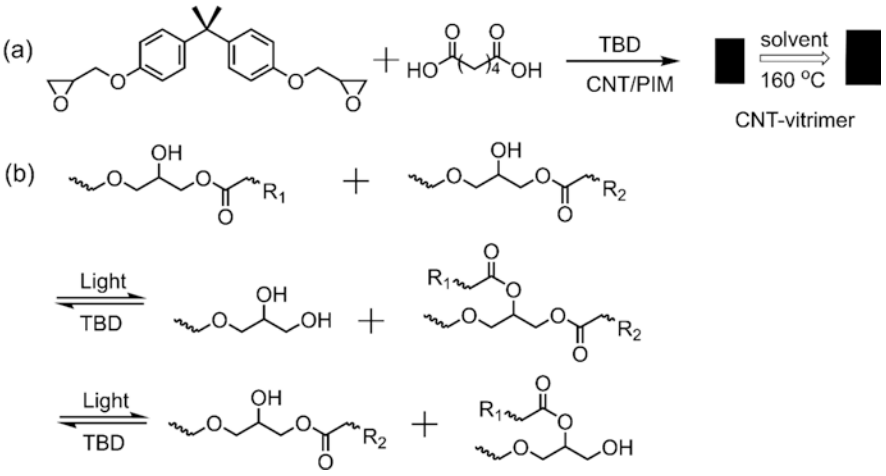

Fig. 7.4 (**a**) Preparation route of CNT-vitrimer composites; (**b**) Illustration of light-induced transesterifications in the presence of CNTs. Reproduced with permission from Yang et al. (2014)

In addition to acid-epoxy or anhydride-epoxy systems, ultra-violet (UV) cured acrylate (Zhang et al. 2018a), glycerol crosslinked poly(*p*-phenylene-2,6-benzobisthiazolediyl) (PBT) (Zhou et al. 2017), hydroxyl terminated polylactide-diisocyanate (Brutman et al. 2014) and siloxane-vinyl (Ube et al. 2016) systems have also been used to prepare recyclable thermosetting polymers based on transesterification.

In addition to heat, light can also be used for recycling of thermosetting polymers based on transesterification (Yang et al. 2014; Chen et al. 2017a; Feng et al. 2019a). Yang et al. (2014) reported for the first time the photothermal effect of carbon nanotubes (CNTs) in acid-epoxy based CNT-vitrimer composites. CNT-vitrimer composites were prepared by reacting adipic acid with DGEBA (Fig. 7.4a), and using triazabicyclodecene (TBD) as a catalyst for transesterification. Through the photothermal effect of CNTs, the hydroxyl groups and ester bonds in the composites could be dynamically exchanged under light (Fig. 7.4b), as a result, the composites could be recycled under light.

As mentioned above, the recycling of thermosetting polymers can be achieved by transesterification in the presence of catalysts. However, catalysts are usually toxic and have the problem of solubility (Denissen et al. 2016; Fortman et al. 2018a). In addition, the recycling of thermosetting polymers based on transesterification is generally depending largely on the type and amount of catalysts. So far, three methods have been used to prepare catalyst-free vitrimers base on transesterification. One method is *via* the protonation of the carboxylic acid, thus achieving the self-catalysis of the acid-epoxy vitrimers. Altuna et al. (2013) prepared the acid-epoxy vitrimers *via* the reaction between citric acid and epoxidized soybean oil in water. By means of the protonation of carboxylic acid in water, the self-catalysis of transesterification was achieved and the vitrimers showed a stress relaxation behavior and could be welded at 160 °C for 2 h. The second method is by introducing highly reactive phenolic hydroxyl groups. With this in mind, Ube et al. (2016) prepared crosslinked liquid-crystalline polymers containing ester bonds and phenolic hydroxyl groups *via* the hydrosilylation reaction between poly(hydrogenmethylsiloxane) (PHMS) and vinyl compounds, which could be welded at 120 °C for 30 min *via* the transesterification between ester bonds and phenolic hydroxyl groups in the absence of catalyst. The third method is *via* introducing a large amount of hydroxyl groups. Zhang' group demonstrated this method *via* hyperbranched epoxy with abundant hydroxyl groups (Han et al. 2018) or the addition of glycerol (Liu et al. 2019) into anhydride-epoxy networks. Hyperbranched epoxy vitrimers exhibited excellent mechanical properties and thermal stability similar to the conventional epoxy materials, but the method of adding glycerol greatly sacrificed the thermal and mechanical properties for the epoxy networks.

Readily recyclable thermosetting polymers based on transesterification have been used in 3D printing materials (Shi et al. 2017; Zhang et al. 2018a), recyclable carbon fiber-reinforced thermoset (CFRT) composites (Yu et al. 2016) and removable coatings (Hao et al. 2019). Keeping this in view, Yu et al. (2016) prepared a thermosetting polymer through the reaction between DGEBA and fatty acids using $Zn(ac)_2$ as catalyst. These authors suggested that the CFRT composite could be recovered to clean carbon fibers with the same dimensions and mechanical properties as the new ones when immersed in ethylene glycol at 180 °C for 4 h, following the transesterification between thermosetting matrix with ethylene glycol (Yu et al. 2016). The degraded resins could be reused to prepare a new generation of composites. Thus, a CFRT composite with a recyclability close to 100% could be achieved with this method.

In summary, thermosetting polymers based on transesterification, especially the acid-epoxy and anhydride-epoxy systems, have availability of monomers, ease of preparation, which makes them readily up-scalable and show great potential for industrial applications. However, compared to conventional thermosetting polymers, the thermal and mechanical properties ($T_g < 105$ °C, $\sigma_m < 55$ MPa) of them are relatively lower. In addition, most systems require a transesterification catalyst, which is usually toxic and has the problem of solubility, catalyst-free systems are only achieved *via* the protonation of carboxylic acid or the introduction of phenolic hydroxyl or a large amount of alcoholic hydroxyl groups, more universal catalyst-free systems need to be developed. Furthermore, reprocessing requires high temperatures (>90 °C) for transesterification-based systems. These issues should be addressed in future.

7.2.2 Transcarbonation

Analogous to transesterification, transcarbonation is the exchange reaction between a carbonate and a free hydroxyl group to form a new carbonate and a new free hydroxyl group (Fig. 7.5). Snyder et al. (2018) reported hydroxyl-functionalized thermosetting polycarbonates which underwent dynamic transcarbonation in the

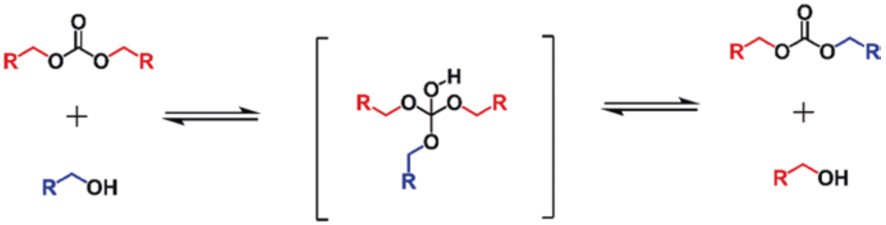

Fig. 7.5 Transcarbonation exchange reaction. Reproduced with permission from Snyder et al. (2018)

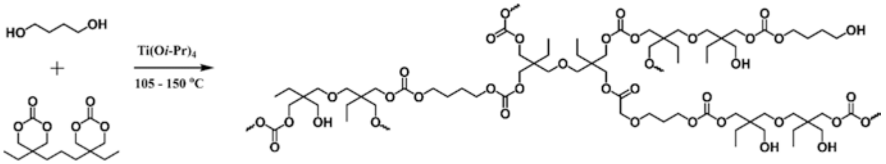

Fig. 7.6 Preparation route of the hydroxyl-functionalized thermosetting polycarbonate. Reproduced with permission from Snyder et al. (2018)

presence of catalyst ($Ti(Oi\text{-}Pr)_4$) at elevated temperatures (Fig. 7.6). The transcarbonation rate, thermal and mechanical properties (T_g: 15–35 °C, YM: 100–1200 MPa and σ_m: 7–36 MPa) of the thermosetting polymers could be easily tuned by adjusting the catalyst load and the feed ratio of monomers. The Arrhenius stress relaxation activation energy (E_a) was in the range of 93–123 kJ/mol. In addition, these thermosetting polymers could be reprocessed by hot pressing at 140 °C for 7 h under 5–10 MPa pressure and degraded at 160 °C for 4 h in ethylene glycol or at 90 °C for 36 h in 1 M HCl *via* acid-catalyzed hydrolysis to obtain pure monomer precursors with about 80% recovery.

7.2.3 Boronic Ester Exchange

Boronic acid derivatives such as boronate esters and boroxine have been used as dynamic covalent bonds in crosslinked networks. Table 7.2 summarizes the properties of recyclable thermosetting polymers based on boronic ester. Cromwell et al. (2015) reported for the first time networks of recyclable polyolefins based on the transesterification of boronic ester from difunctional boronic ester cross-linkers and 1,2-diol moieties. The boronic ester transesterification rate could be adjusted by the structures, which varied the malleability and the efficiency of self-healing of the networks. In addition, in tertiary amine-containing networks, the pieces cut from samples could be reprocessed by hot pressing at 80 °C. However, in the absence of tertiary amines, poor malleability was observed, suggesting an amine-catalyzed boronic ester transesterification mechanism. Later, Röttger et al. (2017) reported the

Table 7.2 The properties of recyclable thermosetting polymers based on boronic ester

Raw materials	T_g (°C)	YM (MPa)	σ_m (MPa)	Recycling method	Recycling mechanisms	References
Diol containing polycyclooctene/telechelic divalent boronic esters	–	3.23–4.86	1.12–1.97	Hot pressed at 50 °C for 16 h under pressure.	Boronic ester transesterification	Cromwell et al. (2015)
Pendant dioxaborolane—containing functional polymers/bis-dioxaborolane	–	–	18	Injection at 180 and 200 °C.	Dioxaborolane metathesis	Röttger et al. (2017)
				Welding.	Dioxaborolane metathesis	
Diboronic acid/pyridine or 4-undecylpyridine	26–47	559–768	17.8–32.9	Hot pressed at 100 °C.	Boroxine exchange	Ogden and Guan (2018)
				Degradation at 100 °C for 1 h in water.	Boroxine hydrolysis	
Styrenebutadiene rubber/thiols-containing boronic ester	−10 to 0	1.86–2.43	1.7–2.68	Hot pressed at 160 °C for 1 h under 10 MPa pressure.	Dioxaborolane metathesis	Chen et al. (2018b)
				Welding at 25–80 °C for 1–24 h.	Dioxaborolane metathesis	
Novolac resin/phenylboronic acid	62	–	–	Degradation at room temperature in ethanol	Boronic ester transesterification	Wang et al. (2018d)

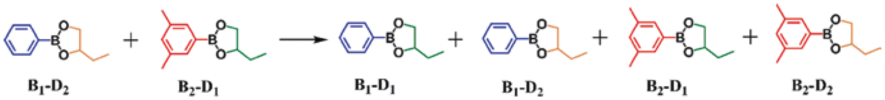

Fig. 7.7 Metathesis of dioxaborolanes B1-D2 and B2-D1. Reproduced with permission from Röttger et al. (2017)

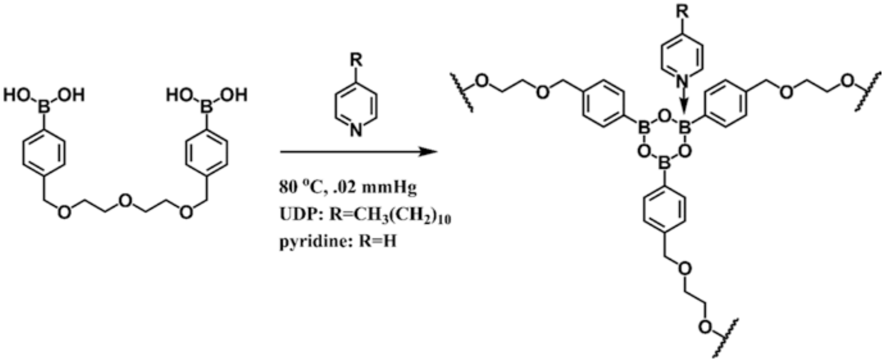

Fig. 7.8 Synthesis of thermosetting boroxine. Reproduced with permission from Ogden and Guan (2018)

readily recyclable thermosetting polymers based on the metathesis of dioxaborolanes without catalyst (Fig. 7.7). Two complementary approaches to the synthesis of copolymers containing pendant dioxaborolanes and grafting of dioxaborolanes onto commercial thermoplastic polymers were used to prepare dioxaborolane-containing polymers by reactive processing, then the metathesis reaction was used to both cross-link the polymers and assure fluctuations in the topology of the network and vitrimer behavior. Compared with the corresponding commodity plastics, dioxaborolane-based thermosetting polymers exhibited excellent solvent and environmental stress-cracking resistance, and better dimensional stability and resistance to high temperature melting. Furthermore, the thermosetting polymers could be reprocessed by conventional thermoplastic processing techniques, such as extrusion and injection molding at more than 130 °C. These results demonstrated the great potential for the preparation of vitrimers from conventional plastics.

In addition to reprocessing, crosslinked boronate esters can be fully recovered to the original monomers. Ogden and Guan (2018) prepared the thermosetting boroxine using a method of trimerization of boronic acid facilitated by ligand (Fig. 7.8). The thermosetting boroxine showed high malleability with the activation energy of the relaxation process of 79.5 kJ/mol, which led to easy reprocessing at 80 °C. Even more interesting, the thermosetting boroxine was relatively stable under moderate humidity conditions, while it was found to be fully dissolved in boiling water, and the original monomer was recovered, which opens a door for possible recycling of thermosetting polymers.

An application of recyclable thermosetting polymers based on boronic ester is to produce recyclable CFRT composites. Wang et al. (2018d) directly crosslinked conventional Novolac resin (NR) with phenylboronic acid (PBA) to prepare thermosetting polymers, which could be dissolved in ethanol through the transesterification between boronic ester and ethanol at room temperature. The NR/PBA-based CFRT composites could be recycled by the same method and the recovered carbon fiber maintained the structure and performance of the original.

In summary, thermosetting polymers based on boronic ester show excellent mechanical properties, malleability, reprocessability, universality, and in some systems, monomer recovery can be achieved with only boiling water. However, the boronic ester is water sensitive and its hydrolysis stability needs to be improved (Cash et al. 2018). In addition, their possible applications also need to be exploited.

7.2.4 *Aminal Exchange*

Aminals, also known as *N*,*N*-acetals, can be formed as the main product by condensation reaction of formaldehyde with primary amines or aldehydes with secondary amines through the highly reactive methylenimine towards the nucleophilic addition (Fig. 7.9a) (Buchs et al. 2011; Chao and Zhang 2019). Aminal exchange is the reaction between an aminal and another aminal to form a new aminal (Fig. 7.9b) (Chao and Zhang 2019). Chao and Zhang (2019) reported for the first time the dynamic polyaminals containing secondary amine-derived aminal bonds through the condensation of formaldehyde and secondary amines (Fig. 7.10). The polyaminals showed a fast stress relaxation behavior in the range of 50–75 °C with the

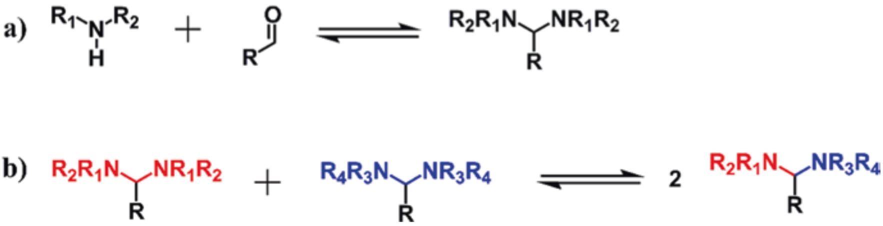

Fig. 7.9 (**a**) Aminals formation and (**b**) aminal exchange. Reproduced with permission from Chao and Zhang (2019)

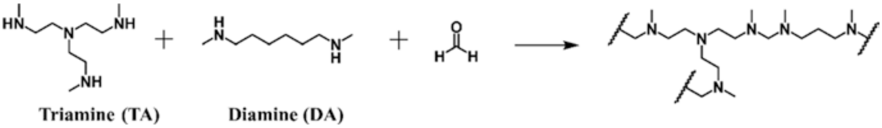

Fig. 7.10 Preparation route of dynamic covalent networks containing secondary amine-derived aminal bonds. Reproduced with permission from Chao and Zhang (2019)

activation energies of bond exchange of 52–80 kJ/mol. In addition, the polyaminals could be reprocessed and welded at 80 °C for 1 h. However, the thermal and mechanical properties of the networks were relatively poor (T_g: −51.1 to −76.6 °C, YM: 31–230 KPa, σ_m: 0.45–0.8 MPa) (Chao and Zhang 2019).

7.2.5 *Vinylogous Urethane Exchange*

Another promising chemistry exploiting the nucleophilicity of amines is the catalyst-free transamination of vinylogous urethanes, which has also been used to produce readily recyclable thermosetting polymers (Denissen et al. 2015; Stukenbroeker et al. 2017; Guerre et al. 2018; Liu et al. 2018b; Lessard et al. 2019). Vinylogous urethanes can be synthesized *via* the condensation of an acetoacetate ester and a primary amine, and the exchange reaction between a vinylogous urethane and a primary amine usually occurs at a temperature above 100 °C without a catalyst (Fig. 7.11). Table 7.3 summarizes the properties of recyclable thermosetting polymers based on vinylogous urethane exchange.

Denissen et al. (2015) synthesized the recyclable thermosetting polymers based on vinylogous urethane *via* the condensation of acetoacetate esters and excess polyfunctional amines (excess amines to keep residual free amines) (Fig. 7.12). These vitrimers showed fast stress relaxation rates without catalysts and could be reprocessed for five generations of reprocessing without significant chemical or mechanical change. In addition, at a given temperature, the exchange rate of vinylogous urethane exchange in thermosets could be tuned in an order of magnitude by adding acidic or basic additives, which is capable of promoting or inhibiting this reaction (Denissen et al. 2017). Recyclable thermosets based on vinylogous urethane can also be prepared by other methods, such as grafting acetoacetate esters (Guerre et al. 2018; Liu et al. 2018b; Lessard et al. 2019) or amino groups (Stukenbroeker et al. 2017) onto linear polymers and then crosslinked by acetoacetate esters or amines. Interestingly, Guerre et al. (2018) reported fluorinated vitrimers prepared by reaction between acetoacetate ester-containing perfluoropolyethers and triamine,

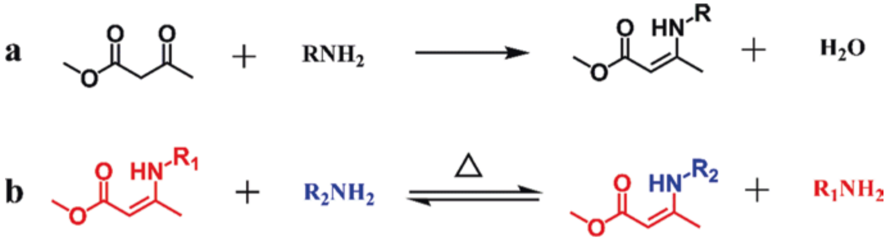

Fig. 7.11 (**a**) Synthesis of vinylogous urethane and (**b**) transamination of vinylogous urethanes without catalyst. Reproduced with permission from Denissen et al. (2015)

Table 7.3 The properties of recyclable thermosetting polymers based on vinylogous urethane exchange

Curing systems	Curing system	T_g (°C)	YM (MPa)	σ_m (MPa)	Recycling method	References
Acetoacetate ester—amine	Diacetoacetate ester/triamine/diamine	87	2100	91	Hot pressed at 150 °C for 30 min.	Denissen et al. (2015)
	Acetoacetate ester modified PBD/diamine	8–24	4.4–43.4	2.7–11.3	Hot pressed at 150 °C for 30 min under 10 MPa pressure.	Liu et al. (2018b)
					Welding at 140 °C for 15 min.	
					Degradation at 150 °C for 30 min in benzylamine or NMP.	
	Acetoacetate ester modified linear polymer/triamine	110	–	–	Hot pressed at 160 °C for 4 h.	Lessard et al. (2019)
					Degradation at 80 °C for 3–18 h in acetonitrile.	
	Acetoacetate ester modified perfluoropolyethers/triamine	−100 to −40	–	1	Hot pressed at 80 °C for overnight.	Guerre et al. (2018)
Vinylogous urethane-amine	Amine containing-polydimethylsiloxane/bis-vinylogous urethane	−118 to −117	0.007–0.135	–	Hot pressed at 90 °C for 3 h.	Stukenbroeker et al. (2017)

NMP: 1-methyl-2-pyrrolidone; PBD: Poly(polybutadiene)

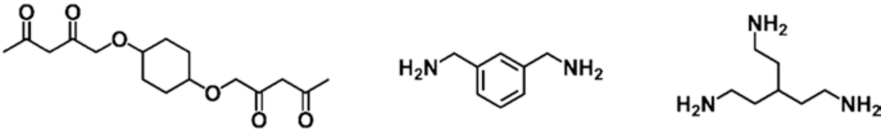

Fig. 7.12 Monomers used for the preparation of recyclable thermosets based on vinylogous urethane. Reproduced with permission from Denissen et al. (2015)

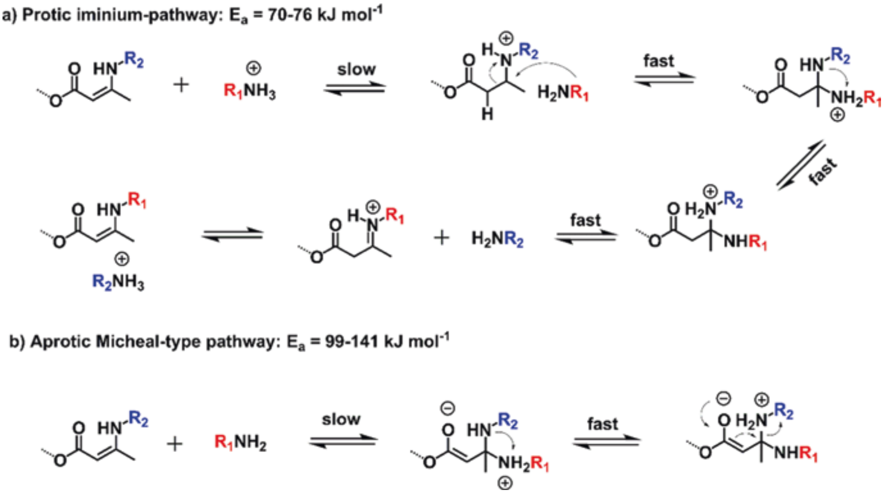

Fig. 7.13 Two different exchange mechanisms in a recyclable thermosetting polymer based on vinylogous urethane. Reproduced with permission from Guerre et al. (2018)

and found that the exchange of dual bonds coexisted, showed different temperature-dependent stress relaxations, and different activation energies (60 kJ/mol *vs.* 130–170 kJ/mol) were calculated for different exchange pathways (Fig. 7.13).

7.2.6 Vinylogous Urea Exchange

Analogous to vinylogous urethane exchange, vinylogous urea exchange is the reaction between a vinylogous urea and a primary amine (Fig. 7.14), the exchange rates could be greatly increased by the acid catalyst (Denissen et al. 2018). Denissen et al. (2018) prepared poly(vinylogous) urea vitrimers by the reaction between diacetoacetate ester, triamine and diamine using 0.5 mol.% of *p*-toluenesulfonic acid (*p*-TsOH) as a catalyst, which showed excellent mechanical and thermal properties with a YM of 2.2 GPa and T_g of 110 °C and a fast stress relaxation above T_g. The fully cured glass fiber-reinforced composite still allowed efficient thermal fusion, as well as thermoforming, and could be recycled *via* solvolysis at 100 °C for 15 min in a solution of *N*-methyl pyrrolidone with a primary amine.

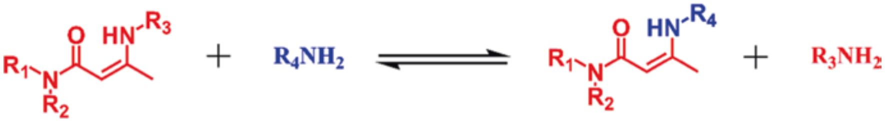

Fig. 7.14 Vinylogous urea exchange. Reproduced with permission from Denissen et al. (2018)

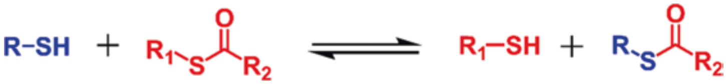

Fig. 7.15 Transthioesterification between a thiol and a thioester to form a new thiol and a new thioester. Reproduced with permission from Wang et al. (2018b)

7.2.7 Transthioesterification

Transthioesterification is the reaction of a thiol and a thioester to form a new thiol and a new thioester (Fig. 7.15). Wang et al. (2018b) prepared the recyclable thermosetting polymers based on transthioesterification through the photopolymerization between several thiol monomers and a thioester diallyl ether with various stoichiometric ratios, and methylhydroquinone was used as a photoinitiator. The prepared thermosetting polymers could be degraded into oligomers *via* thiol-excess transthioesterification in the presence of acetone and triethylamine, and then be rephotopolymerized in almost indistinguishable thermosetting polymers compared to the originals. The prepared filler-reinforced composites could also be recycled in the same way. However, the thermal and mechanical properties (T_g: −28 to 7 °C, YM: ~8 MPa, σ_m: ~1 MPa) of the recyclable thermosetting polymers based on transthioesterification were poor, which should be improved in the future.

7.2.8 Transalkylation

Two types of transalkylation have been used to prepare the recyclable thermosetting polymers. The first is the transalkylation of triazolium salts, which is the exchange reaction between the 1,2,3-triazolium salts and alkyl halide (Fig. 7.16). With this in mind, Obadia et al. (2015) reported the recyclable thermosetting poly(1,2,3-triazolium) based on transalkylation containing pendant alkyl halide chains, 1,2,3-triazolium salts and triazolines. Such poly(1,2,3-triazolium) networks were synthesized by a one-pot process of simultaneous polyaddition of a-azide-u-alkyne monomers and crosslinking with difunctional quaternizing agent 1,6-dibromohexane without catalyst (Fig. 7.17). The prepared poly(1,2,3-triazolium) showed a fast stress relaxation and the calculated E_a was around 140 kJ/mol. The stress relaxation

Fig. 7.16 Transalkylation of triazolium salts between 1,2,3-triazolium salts and alkyl halide. Reproduced with permission from Obadia et al. (2015)

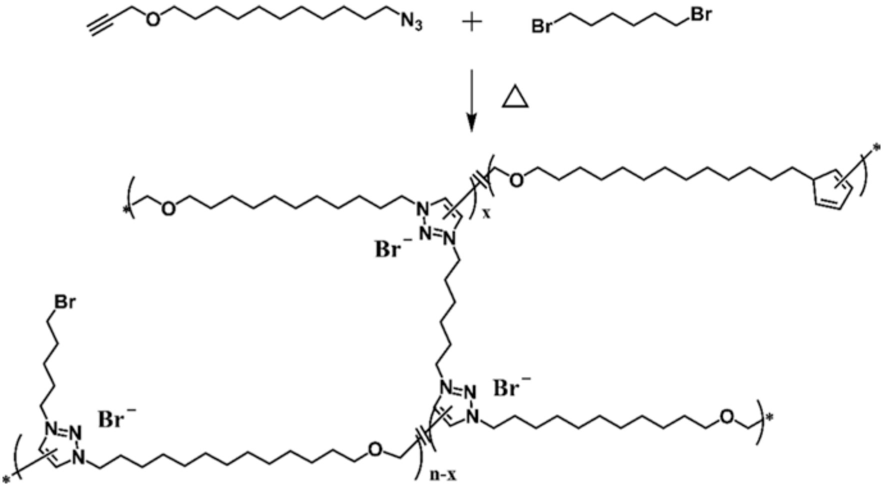

Fig. 7.17 Preparation of poly(1,2,3-triazolium) networks by a one-pot process of simultaneous polyaddition of α-azide-ω-alkyne monomers and crosslinking with difunctional quaternizing agent 1,6-dibromohexane. Reproduced with permission from Obadia et al. (2015)

Fig. 7.18 Transalkylation of trialkylsulfonium salts between trialkylsulfonium salts and thioethers. Reproduced with permission from Hendriks et al. (2017)

rate could be adjusted by the choice of counter-ions ($Br^- \gg I^- > MsO^-$). In addition, poly(1,2,3-triazolium) could be recycled by depolymerization of networks by adding 1-bromopentane or dihalogenated monomers or reprocessed *via* hot pressing at 170 °C for 60 min. Later, Obadia et al. (2017) also found that the Arrhenius activation energies of poly(1,2,3-triazolium) could be tuned by varying the ratios of α-azide-ω-alkyne monomers and difunctional halogen compound in the initial formulation.

Another type is the transalkylation of trialkylsulfonium salts, which is the exchange reaction between trialkylsulfonium salts and thioethers (Fig. 7.18). Hendriks et al. (2017) prepared recyclable thermosetting poly(thioether) *via* the

Table 7.4 The properties of recyclable thermosetting polymers based on transalkylation

Curing system	T_g (°C)	YM (MPa)	σ_m (MPa)	Recycling method	Recycling mechanisms	References
α-azide-ω-alkyne/1,6-dibromohexane	−11	8	1.2	Hot pressed at 170 °C for 60 min under 200 bar pressure.	Transalkylation of triazolium salts.	Obadia et al. (2015)
				Degradation at 110 °C for 24–96 h in α-azide-ω-alkyne or 1,6-dibromohexane or 1-bromopentane		
Octanedithiol/octadiene/trithiol	−20	41	7.5	Hot pressed at 160 °C for 40 min.	Transalkylation of trialkylsulfonium salts.	Hendriks et al. (2017)

reaction between octanedithiol, octadiene and trithiol with butyl brosylate as an alkylating agent in the absence of catalyst. The prepared poly(thioether) networks showed a stress relaxation behavior with the E_a calculated around 113 kJ/mol, which was lower than that of the transalkylation of triazolium salts in poly(1,2,3-triazolium) networks. In addition, the poly(thioether) networks could be reprocessed four times without an obvious decrease in thermal stability and T_g. However, an increase of YM and decrease of σ_m were observed due to the increase of the cross-link density.

Table 7.4 summarizes the properties of recyclable thermosetting polymers based on transalkylation. The preparation of polyionic networks is an easy one-pot process: catalyst-free and solvent-free. However, the alkylating reagents used are expensive and hazardous, and the thermal and mechanical properties of the polyionic networks are poor. In addition, the application of the recyclable polyionic networks has never been explored.

7.2.9 Siloxane Exchange

The Si-O-Si bond is stable toward air, water and radical coupling conditions, but can go through exchange with silonates (Fig. 7.19). Table 7.5 summarizes the properties of recyclable thermosetting polymers based on the exchange of siloxane. Keeping this in view, Zheng and McCarthy (2012) reported the recyclable thermosetting poly(dimethylsiloxane) (PDMS) based on siloxane-silonate exchange catalyzed by either acids or bases. The thermosetting PDMSs were prepared *via* the ring-opening polymerization of octamethylcyclotetrasiloxane, which could be welded at 90 °C for 24 h. Later, the effect of cross-link density and catalyst content

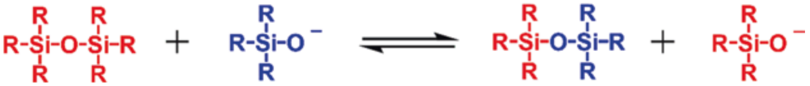

Fig. 7.19 Siloxane-silonate exchange. Reproduced with permission from Zheng and McCarthy (2012)

on the properties of the crosslinked PDMS networks were studied by Schmolke et al. (2015). By increasing the catalyst ratios or reducing the cross-link density, the crosslinked PDMS networks exhibited the faster relaxation rates. The PDMS networks were able to quickly stress relaxation (1.92 s) at 5 °C, by especially increasing the catalyst ratios to 3.25 mol.%. However, the increase of catalyst content or the reduction in cross-link density reduced the mechanical properties of the PDMS networks.

These recyclable thermosetting polymers based on the siloxane-silonate exchange are promising, since they exhibit the fastest stress relaxation rates in all reported vitrimers or vitrimer-like materials and quantitative reprocessing could be achieved. In addition, polysiloxanes are nontoxic. However, in order to expand their applications, the rapid siloxane exchange must be coupled with more rigid structures to avoid stress relaxation at service temperatures. Nishimura et al. (2017) used silyl ether as a robust dynamic covalent bond to produce malleable and reprocessable thermosets (Fig. 7.20). The stress relaxation rate could be accelerated by almost three orders of magnitude by introducing a neighboring amino moiety. The calculated E_a and the topology-freezing transition temperature of the silyl ether-based network with amino moiety are around 81 kJ/mol and 47 °C, respectively, and those of the silyl ether-based network without amino moiety are around 174 kJ/mol and 117 °C, respectively. In addition, the thermosetting polymers could be reprocessed by hot pressing without an obvious decrease in T_g. Later, Wu et al. (2019) prepared recyclable elastomer/silica hybrids through the reaction between epoxidized natural rubber and silica in the presence of Lewis acid, which could also be reprocessed by hot pressing.

7.2.10 Hydrazide Michael Adduct Exchange

The exchange of hydrazide Michael adduct is the reaction between a hydrazide Michael adduct and a hydrazide to form a new hydrazide Michael adduct and a new hydrazide without catalyst (Fig. 7.21). Debnath et al. (2018) synthesized recyclable thermosetting polymers based on exchange of hydrazide Michael adduct *via* the Michael adduct reaction between hydrazide-containing linear polymer and tetraethyl-2,2′-[1,4-phenylenebis(methanylylidene)] dimalonate (TPMD) (Fig. 7.22). The T_g, YM and σ_m of the prepared thermosetting polymers were 46–67 °C, 7.8–23.8 MPa and 700–2500 MPa, which could be tuned by adjusting the cross-link density. The calculated E_a of the prepared thermosetting polymers was around

Table 7.5 The properties of recyclable thermosetting polymers based on siloxane exchange

Recycling mechanisms	Raw materials	Catalyst	T_g (°C)	YM (MPa)	σ_m (MPa)	Recycling method	References
Siloxane-Silonate Exchange	Octamethyl-cyclotetrasiloxane	Bases	−192.5	–	–	Welding at 90 °C for 24 h.	Zheng and McCarthy (2012)
	DGEBAEO/anion oligoaminopropylmethylsiloxanediol	Not used	83	2200	45	Hot pressed at 130 °C for 40 min under 10 MPa pressure.	Wu et al. (2018)
						Welding at 110 °C for 24 h.	
	Aminopropyl terminated PDMS/trimethylolpropane triacrylate	Tetramethylammonium hydroxide	–	–	1.08	Welding at 105 °C for 24 h.	Li et al. (2018b)
Silyl ether exchange	Hydroxyl-containing PS/bis-γ-NH or bis-C10	Not used	123–125	12–20	1000–1400	Hot pressed at 160 or 190 °C for 6 h.	Nishimura et al. (2017)
	Epoxidized natural rubber/silica	$AlCl_3$	5–40	–	7–18.2	Hot pressed at 160 °C for 30 min.	Wu et al. (2019)

DGEBAEO: Diglycidyl ether of ethoxylated bisphenol A, PS: poly(styrene)

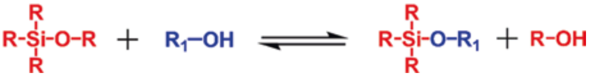

Fig. 7.20 Silyl ether exchange. Reproduced with permission from Nishimura et al. (2017)

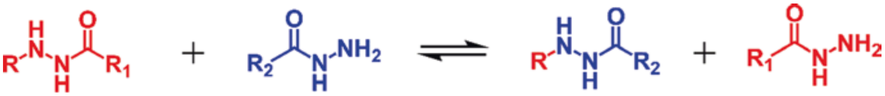

Fig. 7.21 Exchange of hydrazide Michael adduct. Reproduced with permission from Debnath et al. (2018)

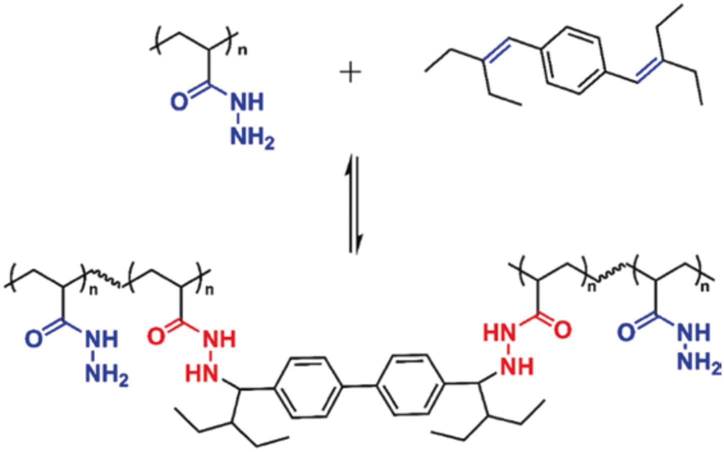

Fig. 7.22 Synthetic route of thermosetting polymers containing hydrazide Michael adduct *via* the Michael adduct reaction between hydrazide-containing linear polymer and TPMD. Reproduced with permission from Debnath et al. (2018)

109.5 kJ/mol. In addition, the thermosetting polymers could be reprocessed by following two steps: softened by dipping in a THF:H_2O (95:5, v:v) mixture for 3 h, and pressing at 25 °C for 48 h under a 1 kg load.

7.2.11 Diselenide Bond Metathesis

The bond energy of diselenide bonds is 172 kJ/mol, which is lower than that of disulfide bonds (240 kJ/mol), which suggests that the metathesis of diselenide bonds (Fig. 7.23) can occur under much milder conditions compared to metathesis of disulfide bonds (Ji et al. 2014). Thus, diselenide bond-containing thermosetting polymers are widely used to achieve the self-healing feature under light in the

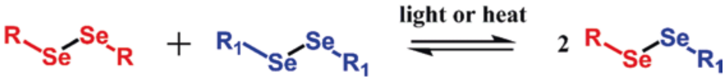

Fig. 7.23 Metathesis of diselenide bonds. Reproduced with permission from Ji et al. (2014)

Table 7.6 The properties of recyclable thermosetting polymers based on diselenide bonds

Raw materials	T_g (°C)	Recycling method	References
Selenolactone/triamine/linear polyetheramine	–	Reprocess at room temperature for 10 min under UV radiation.	Pan et al. (2017)
Tris-isocyanate-terminated prepolymer/bis-isocyanate-terminated prepolymer/diselenide bond-containing diamine	30	Welding at room temperature for 30 s.	An et al. (2017)
		Hot pressed at 100 °C.	
γ-butyroselenolactone/triol	–	Reprocess at room temperature for 10 min under UV radiation or at 70 °C for 20 min.	Wang et al. (2018a)

absence of catalyst (Ji et al. 2014, 2015; Suzuki et al. 2018). In recent years, recyclable thermosetting polymers based on diselenide bonds have also been developed, their properties are summarized in Table 7.6. Pan et al. (2017) reported the thermosetting polymers *via* the reaction between selenolactone, triamine and a linear polyetheramine, followed by the oxidation by H_2O_2 in tetrahydrofuran, which could be reprocessed under UV for 10 min. Later, Wang et al. (2018a) prepared diselenide-containing crosslinked polyesters by similar steps *via* the ring-opening reaction of γ-butyroselenolactone by ethylene glycol followed by the oxidation using H_2O_2 in tetrahydrofuran, which could be reprocessed at room temperature for 10 min under UV radiation or at 70 °C for 20 min. An et al. (2017) also found that the reprocessing of the thermosetting polymers based on aromatic diselenide is easier than that of the thermosetting polymers based on aromatic disulfide.

7.2.12 *Transcarbamoylation*

Isocyanate is usually used for the preparation of the thermosetting poly(urethane) (PU). However, regulators in Europe and United States are working to reduce or eliminate their use in PU synthesis due to the toxicity by using isocyanates (Fortman et al. 2018a). It is thus imperative to develop alternative chemicals to prepare thermosetting PU. One way for preparing thermosetting PU without using isocyanate is through the reaction between amines and cyclic carbonates, and the prepared thermosetting PUs could be recycled through associative transcarbamoylation (Fig. 7.24). The properties of recyclable thermosetting polymers based on transcarbamoylation are summarized in Table 7.7. In this sense, Fortman et al. (2015) reported for the first time the transcarbamoylation-based recyclable thermosetting

Fig. 7.24 Associative transcarbamoylation. Reproduced with permission from Fortman et al. (2015)

Table 7.7 The properties of recyclable thermosets based on transcarbamoylation

Curing systems	Catalyst	T_g (°C)	YM (MPa)	σ_m (MPa)	Recycling method	Reference
Bis(six-membered cyclic carbonate)/ triamines	Not used	54	2200	72	Hot pressed at 160 °C for 8 h under 4 MPa pressure.	Fortman et al. (2015)
					Degradation at 180 °C for 4 h in tetraethylene glycol	
	Not used	7–54	600–3000	1.9–80	Hot pressed at 160 °C under 4 MPa pressure.	Fortman et al. (2017)
Bis(five-membered cyclic carbonate)/ triamine	Dibutyltin dilaurate	−16 to 30	–	1.7–9.7	Hot pressed at 140 °C for 2 h under 11 MPa pressure.	Chen et al. (2017b)

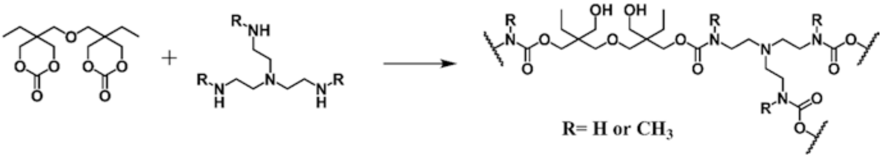

Fig. 7.25 Preparation of recyclable thermosetting PUs through the reaction between bis(cyclic carbonate) and tris(2-aminoethyl)amine or tris[2-(methylamino)ethyl]amine without catalyst. Reproduced with permission from Fortman et al. (2015)

PUs through the reaction between bis(cyclic carbonate) and tris(2-aminoethyl) amine or tris[2-(methylamino)ethyl]amine without catalyst (Fig. 7.25). These authors reported that a thermosetting PU showed excellent mechanical properties with a YM of around 2200 MPa, strain at break (ε_b) of about 6.9 ± 3.8% and σ_m of around 72 MPa, and could be reprocessed by hot pressing at 160 °C for 8 h or degraded by tetraethylene glycol at 180 °C for 4 h, which is relatively demanding. Chen et al. (2017b) also achieved quantitative reprocessing for five-membered cyclic carbonate-based thermosetting PUs by hot pressing at 140 °C for 2 h. However, their thermal and mechanical properties were relatively low, and catalyst was used for the formation of the networks. In line with this, Fortman et al. (2017) observed limited thermal stability of β-hydroxyurethanes in thermosetting PUs, as a result, the reprocessing was limited to PU elastomers.

Fig. 7.26 Alkene metathesis. Reproduced with permission from Lu et al. (2012)

7.2.13 Olefin Metathesis

Olefin metathesis is the reaction between strong C-C double bonds catalyzed by transition-metal (Fig. 7.26). With this in mind, Lu and Guan (2012) reported two papers on olefin metathesis in crosslinked thermosetting PBDs using the second-generation Grubbs catalyst. This catalyst compared to classical metathesis catalysts is compatible with functional group, and stable to air and moisture, due to the efficient bond exchange, the prepared thermosetting polymers showed a rapid stress relaxation and creep at low temperatures, and quantitative welding was observed between cut samples at room temperature for 3 h under 20 kPa pressure with only 0.005 mol% catalyst. However, the mechanical properties of these thermosetting PBDs were relatively poor with σ_m of ~0.5 MPa. Later, Neal et al. (2015) improved the mechanical properties (YM: 2.34–2.51 MPa, σ_m: 1.31–1.66 MPa) of these thermosetting polymers by incorporating secondary amide side chains into the network, and the toughness was also improved through the hydrogen bonding of the secondary amide side chains. This strategy showed potential to improve mechanical properties of other CANs.

In summary, the second-generation Grubbs catalyst-catalyzed olefin metathesis shows great potential for the recycling of thermosetting polymers at room temperature. However, creep at low temperature is not desirable for most applications of thermosetting polymers, which should be addressed in the future. Only elastomers have been used to demonstrate the viability of the olefin metathesis to recycle thermosetting polymers, therefore, it is necessary to design more rigid structures.

7.3 Readily Recyclable Thermosets Based on Dynamic Dissociative Exchange Reaction

7.3.1 Reversible Diels-Alder Reaction

The reversible Diels-Alder (DA) [4 + 2] reaction involves the Diels-Alder addition between a dienophile and a diene to produce a cycloadduct, and retro Diels-Alder reaction (rDA) of the DA cycloadduct to the dienophile and diene at a higher temperature. Thermodynamics and kinetics of DA reactions vary with different dieneophiles and dienes, regiochemistry and steric bulk of their cycloadducts. Furan-maleimide system has been widely studied due to its easy access and the rapid occurrence of cycloadduct formation. The DA reaction of furan-maleimide

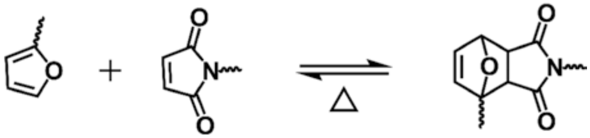

Fig. 7.27 Reversible Diels-Alder reaction. Reproduced with permission from Chen et al. (2002)

system commonly occurs at around <60 °C, and the rDA often happens at around >100 °C (Fig. 7.27). Table 7.8 summarizes the recyclable thermosetting polymers based on reversible DA reaction.

Recyclable thermosetting polymers based on the reversible DA reaction between furans and maleimides was reported by Craven (1969) for the first time in a U.S. patent filed by du Pont de Nemours and Company, and subsequently, many other recyclable thermosetting polymers based on this link were widely reported. Two main routes have been used to prepare the recyclable thermosetting polymers with DA structure. One route is through the reaction between multifunctional furans and multifunctional maleimides (Chen et al. 2002; Liu and Hsieh 2006; Ikeda et al. 2013; Cai et al. 2017; Duval et al. 2017; Lei et al. 2017). A typical example is the networks prepared *via* the reaction between trifunctional maleimide and tetrafunctional furan, which show approx. 40% and 50% mending efficiency after heating at 120 °C for 2 h and 150 °C for 2 h, respectively (Chen et al. 2002). Another pathway is to use the DA structure as cross-link points, which has been used to produce recyclable thermosetting polymers from epoxy resin (McElhanon et al. 2002; Kuang et al. 2015), PBD (Bai et al. 2015; Trovatti et al. 2015), PCL (Mallek et al. 2013), PLA (Yamashiro et al. 2008, 2009), poly(ethylene adipate) (Watanabe and Yoshie 2006; Yoshie et al. 2010), poly(*N*-acetylethylenimine) (Chujo et al. 1990), poly(β-thioether ester) (Zhang and Dumont 2018), poly(amide) (Luo et al. 2018b), poly(ketone) (Zhang et al. 2009), PS (Canary and Stevens 1992), and PU (Swanson et al. 2010). Taking recyclable crosslinked PBD as an example, Trovatti et al. (2015) incorporated furan as side groups into PBD *via* thiol-ene reaction between PBD unsaturations and furfuryl thiol, and subsequently crosslinked furan-PBD with an aromatic bismaleimide (Fig. 7.28). The prepared crosslinked PBD could be recycled at 110 °C in a matter of hours *via* the rDA reaction. By tuning the amount of pendent furan and the furan/bismaleimide ratios, the mechanical properties of the crosslinked PBD could be tailored (Bai et al. 2015).

In some cases, rDA can compromise the thermosetting polymers at high temperatures (>100 °C) through depolymerization of the polymer skeleton or crosslinkers, which affects the thermal stability of the thermosetting polymers based on DA reaction. Although, many applications of thermosetting polymers do not require high heat-resistance. The reversible DA reaction occurs under relatively mild conditions without solvent or catalyst, and has been used for recycling of several commercial polymers, indicating great potential for industrial applications.

Table 7.8 The properties of recyclable thermosetting polymers based on Diels-Alder reaction

Curing systems	Raw materials	T_g (°C)	YM (MPa)	σ_m (MPa)	Recycling method	References
Multifunctional furans-multifunctional maleimides	Tetrafunctional furan/trifunctional maleimide.	–	4720	68	Welding at 120 °C for 2 h and 150 °C for 2 h.	Chen et al. (2002)
	Trifunctional furan/trifunctional maleimide.	–	–	–	Degradation at 90 °C for 1 h in NMP.	Liu and Hsieh (2006)
	Tetrafunctional furans/ tetrafunctional maleimide or bismaleimide.	−47.2 to −25.2	10–200	1–10	Degradation at 80 °C for 24 h in DMF.	Ikeda et al. (2013)
	Tetrafunctional furans/ bismaleimide/graphene.	100	511–1546	14.1–36.8	Reprocess at room temperature for 4 min under light.	Cai et al. (2017)
	Tetrafunctional furan modified tannins/bismaleimide.	4	–	–	Degradation at 120 °C for 1 h.	Duval et al. (2017)
	Maleimide modified lignin/ multifunctional furans.	−11.9 to 22.9	0.4–13.6	0.4–3.6	Hot pressed at 130 °C for 30 min, and then cured in the oven at 60 °C for 48 h and at room temperature for 24 h.	Lei et al. (2017)
					Welding at 120 °C for 20 min, 60 °C for overnight, and room temperature for 24 h.	
Furan modified linear polymer-maleimide modified linear polymer	Furan modified poly(*N*-acetylethylenimine)/maleimide modified poly(*N*-acetylethylenimine).	–	–	–	Degradation at 120 °C for >2 h.	Chujo et al. (1990)
	Furan modified copolymer/ maleimide modified PS.	–	–	–	Degradation at 150 °C for 2.5 min in glycerin.	Canary and Stevens (1992)

Furan modified linear polymer-maleimide	Bisfuran terminated poly(ethylene adipate)/trimaleimide.	−34	–	–	Degradation at 145 °C for 20 min.	Watanabe and Yoshie (2006)
	Bisfuran terminated poly(ethylene adipate)/tris-maleimide.	−34	89	27	Welding at 60 °C for 5 days.	Yoshie et al. (2010)
	Furan-modified PLA/ bismaleimides or trimaleimide.	51.5–66.1	–	–	Degradation at 160 °C.	Yamashiro et al. (2008)
	Furan-modified PLA/ bismaleimides or trimaleimide.	54–65	–	–	Degradation at 160 °C for 10 min.	Yamashiro et al. (2009)
	Furan-modified PBD/ bismaleimide.	−80	–	–	Degradation at 110 °C within hours.	Trovatti et al. (2015)
	Furan-modified polyamides/ bismaleimide.	128–147	960–2599	44.2–87.9	Degradation at 130 °C for 30 min in NMP.	Luo et al. (2018b)
	Furan-modified polyketones/ bismaleimide.	87–100	–	–	Hot pressed at 120 °C for 20 min under 4 MPa pressure. Degradation at 150 °C for 5 min.	Zhang et al. (2009)
	Furan-modified PCL/ trimaleimide.	–	–	–	Degradation at 90 °C for 1 h or 2 h in DMF.	Mallek et al. (2013)
	Furan-modified PBD/ bismaleimide.	−92.4 to 97.2	2–48.4	1.92–5.59	Hot pressed at 160 °C for 5 min under 5 MPa. Degradation at 160 °C.	Bai et al. (2015)
	Furan-modified poly(thioether ester)/bismaleimide.	−32.3 to 27.7	1.1–4.3	1.3–5.7	Degradation at 130 °C for 2 h in DMF.	Zhang and Dumont (2018)
Epoxy-amine	DA cycloadduct-containing epoxy/amines.	85	33.5–39	–	Degradation at 90 °C in *n*-butanol.	McElhanon et al. (2002)
	DA cycloadduct-containing diamine/DGEBA.	52	–	–	Welding at 120 and 150 °C for 20 min, and 75 °C for 1 h. Hot pressed at 120 and 140 °C for 5 min.	Kuang et al. (2015)
Isocyanate-hydroxyl	Diisocyanate/DA cycloadduct-containing diols/hydroxyl-terminated PBD.	–	–	–	Degradation at 130 °C for 45 min.	Swanson et al. (2010)
Free radical polymerization of acrylate	DA cycloadduct-containing diacrylate/acrylate.	−15	–	0.2–0.25	Welding at 90 °C for 7 h.	Zhang et al. (2015)

DMF: *N*,*N*-dimethylformamide, PCL: poly(ε-caprolactone)

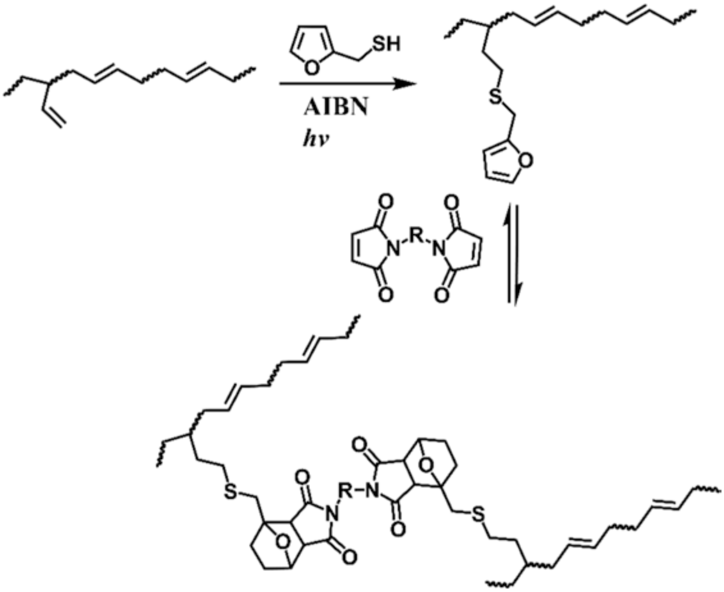

Fig. 7.28 Synthetic route of recyclable crosslinked PBD. Reproduced with permission from Trovatti et al. (2015)

7.3.2 Alkoxyamine Equilibrium

Dynamic alkoxyamine bonds can undergo reversible homolytic bond cleavage to produce stable, nitroxyl/aminoxyl and carbon-centered radicals at mild temperatures (around 100 °C) (Fig. 7.29). Table 7.9 summarizes the recyclable thermosetting polymers based on transalkylation. In the first studies, 2,2,6,6-tetramethyl-1-piperidinyloxy (TEMPO) moieties were used as crosslinking agents for poly(methyl methacrylate) (Higaki et al. 2006), PS (Yuan et al. 2011; Wang et al. 2012) or PU (Yuan et al. 2014) to achieve the self-healing function of thermosetting polymers through dynamic alkoxyamine bonds. Later, Jin et al. (2016) prepared recyclable crosslinked styrene-butadiene rubbers using the commercial TEMPO-substituted methacrylate *via* an one-step controlled curing process. The thermosetting polymers showed a tunable performance and could be quantitative reprocessed by hot pressing at 140 °C for 40 min or 130 °C for 30 min. This approach shows enormous potential as TEMPO can be directly used in networks based on controlled radical polymerization or embedded into conventional polymers based on acrylic, styrenic or other olefinic monomers. Zhang et al. (2016b) also prepared the crosslinked methyl methacrylate thermosetting polymers based on dynamic alkoxyamine bonds and three methods (reprocessing, welding, degradation) were used to achieve the recycling of the thermosetting polymers.

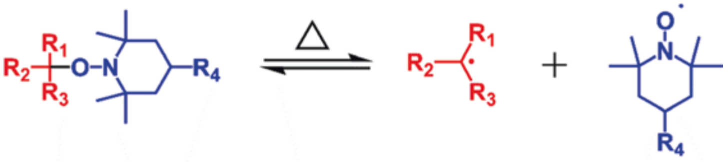

Fig. 7.29 Alkoxyamine equilibrium. Reproduced with permission from Jin et al. (2016)

Table 7.9 The properties of recyclable thermosetting polymers based on dynamic alkoxyamines

Raw materials	T_g (°C)	YM (MPa)	σ_m (MPa)	Recycling method	References
TEMPO-substituted methacrylate/*n*-butyl acrylate/styrene	30–60	21–91	3.1–3.6	Hot pressed at 130 °C for 30 min or 140 °C for 40 min.	Jin et al. (2016)
Alkoxyamine containing methacrylate ester/ thiols	27–34	–	0.36–0.72	Hot pressed t 80 °C for 2.5 h under 3 MPa pressure.	Zhang et al. (2016b)
				Welding at 80 °C for 4 h	
				Degradation at 100 °C for 6 h in DMF with an excess amount of TEMPO.	

7.3.3 Urea/Urethane Exchange

Crosslinked polyureas and PUs have been widely used to prepared vitrimers. Much of the work has been focused on introducing dynamic covalent bonds into polyurea or PU networks or through transcarbamoylation to achieve the recycling of thermosetting polyureas or PUs. This section will focus on the recycling of thermosetting polyureas or PUs directly based on urethane or urea bonds. Table 7.10 summarizes the properties of recyclable thermosetting polymers based on urea/urethane exchange.

One approach for recycling of thermosetting PUs is directly through the dissociative exchange of urethane (Fig. 7.30). Zheng et al. (2016) found for the first time that thermosetting PUs and polyurethanes in the presence of dibutyltin dilaurate as a catalyst showed a temperature-dependent stress relaxation behavior with an E_a range from 113.6 to 130.5 kJ/mol and plasticity at elevated temperatures. This relaxation behavior occurred in the absence of free alcohol, which suggests that tin-catalyzed urethane exchange is the main mechanism. Although the urethane exchange is carried out through a dissociative mechanism, the thermosetting PUs showed a vitrimer-like behavior because only a small amount of urethane bonds were dissociated at elevated temperatures (Fortman et al. 2018a, b). Later, Yan et al. (2017) prepared a biobased thermosetting PU using castor oil as raw material and demonstrated its recyclability *via* hot pressing and welding by using dibutyltin dilaurate as a catalyst.

Table 7.10 The properties of recyclable thermosetting polymers based on urea/urethane exchange

Recycling mechanisms	Raw materials	Catalyst	T_g (°C)	YM (MPa)	σ_m (MPa)	Recycling method	References
Urethane exchange	Diisocyanate/PEG 2000/castor oil.	Dibutyltin dilaurate	37		7–10	Hot pressed at 180 °C for 2 h under 4 MPa pressure.	Yan et al. (2017)
						Welding at 140–160 °C for 2–30 min.	
Oxime-enabled urethane exchange	Diisocyanate/amino-alcohols containing compounds.	Not used	25–48	130–344	34–49	Hot pressed at 120 °C for 30 min under 10 MPa pressure.	Liu et al. (2017b)
Hindered-urea exchange	Diisocyanate/hindered diamines/diol/triol.	Not used	−78 to −49		0.62–0.93	Welding at 37 °C for 12 h	Ying et al. (2014)
	Triisocyanate/2-(*tert*-butylamino)-ethanol.	Not used	53	1870	40	Hot press at 100 °C for 20 min under 300 kPa pressure	Zhang et al. (2016a)
						Welding at 100 °C for 20 min	
						Degradation at 60 °C for 5 h in $CHCl_3$	

Another approach is *via* introducing oxime to prepare recyclable thermosetting PUs based on dissociative oxime-enabled urethane exchange without catalyst (Fig. 7.31). Liu et al. (2017b) reported the crosslinked poly(oxime-urethanes) (POUs) *via* the reaction between hexamethylene diisocyanate (THDI) and multifunctional oximes. The POUs showed a rapid stress relaxation with an E_a range from 98 to 110 kJ/mol and could be reprocessed by hot pressing at 120 °C for 30 min under a 10 MPa pressure. In addition, kinetics experiments and calculations of functional density theory suggested that the oxime was more reactive in the formation of urethane bonds and also improved the dynamic nature of conventional urethane bonds.

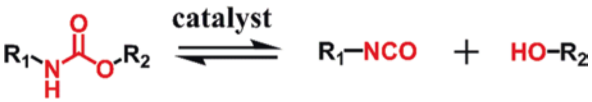

Fig. 7.30 Dissociative urethane exchange. Reproduced with permission from Zheng et al. (2016)

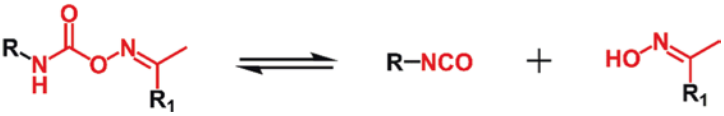

Fig. 7.31 Dissociative oxime-enabled urethane exchange. Reproduced with permission from Liu et al. (2017b)

Fig. 7.32 Dissociative hindered-urea exchange. Reproduced with permission from Ying et al. (2014)

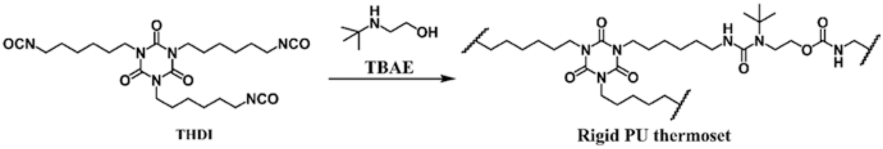

Fig. 7.33 Preparation route of the rigid thermosetting polyurea *via* the reaction between TBAE and THDI. Reproduced with permission from Zhang et al. (2016a)

In addition, thermosetting polyureas can also be recycled at milder temperatures through the more readily dissociative hindered-urea exchange without catalyst (Fig. 7.32). Ying et al. (2014) designed three thermosetting polyureas with hindered urea bonds through the reaction between diamine, diisocyanate, diol and triol, which showed a self-healing behavior at low temperature *via* the hindered-urea exchange. Later, Zhang et al. (2016a) reported a rigid thermosetting polyurea prepared *via* the reaction between 1-(*tert*-butyl)-1-ethylurea (TBAE) and a tri-functional homopolymer of THDI (Fig. 7.33), which could be reprocessed five times by hot pressing above T_g or welded at 37 °C for 5 days. Furthermore, the thermosetting polyurea could be degraded by excess TBAE and re-crosslinked by THDI.

7.4 Readily Recyclable Thermosets Based on Dynamic Associative and Dissociative Exchange Reactions at the Same Time

7.4.1 *Schiff Base Exchange*

Schiff base is the one of the most used dynamic covalent bonds, which includes three distinct processes: dissociative imine condensation/hydrolysis (Fig. 7.34a), associative imine exchange (Fig. 7.34b) and associative imine metathesis (Fig. 7.34c) (Wang et al. 2019). The exchange or hydrolysis of Schiff base often occurs under relatively mild conditions without catalyst, and can be controlled by several external stimuli such as heat, pH or water content. Similar to transesterification, the wide variety of commercial dialdehydes and diamines makes polyimines easy to prepare. Several reports have reported that polyimines or thermosets containing Schiff base are superior malleable, recyclable and degradable materials without catalyst (Taynton et al. 2014, 2016a, b; Van et al. 2014; Chao et al. 2016; Li et al. 2016; Lei et al. 2017; Wang et al. 2018c, 2019; Zhao and Abu-Omar 2018; Zheng et al. 2018a, b; Zou et al. 2018; Feng et al. 2019b; Mai et al. 2019). In addition, the recovery of the original monomers can also be achieved through imine hydrolysis (Van et al. 2014; Wang et al. 2019). Table 7.11 summarizes the properties of readily recyclable thermosetting polymers based on Schiff base.

Zhang's group first reported on recyclable crosslinked polyimine (Taynton et al. 2014). The polyimine was prepared directly through condensation reaction between aldehyde groups and amino groups (Fig. 7.35). At elevated temperatures, cross-linked polyimine exhibited Arrhenius type malleability through imine exchange or imine metathesis, which led to high recycling efficiency during four times of reprocess. The cross-linked polyimine can also be reshaped or recycled using only water at ambient temperature through imine condensation/hydrolysis, which leads to green recycling of the material. Similar structures have also been used to study the chemomechanics of the moisture-induced malleability of polyimines and revealed

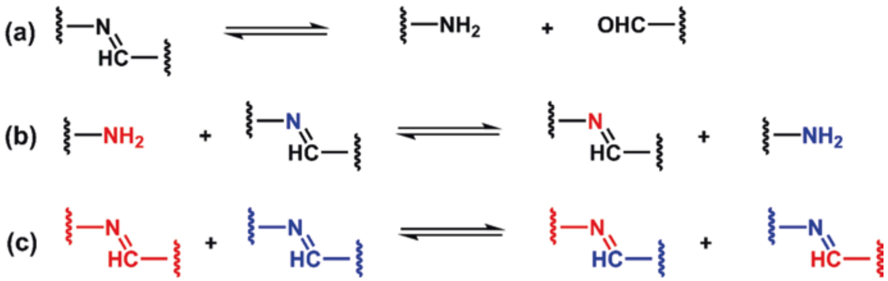

Fig. 7.34 Schiff base exchange mechanism: (**a**) imine condensation/hydrolysis, (**b**) imine exchange and (**c**) imine metathesis. Reproduced with permission from Wang et al. (2018c)

Table 7.11 The properties of readily recyclable thermosets based on Schiff base

Curing system	Raw materials	T_g (°C)	YM (MPa)	σ_m (MPa)	Recycling method	Recycling mechanisms	References
Dialdehydes-triamine-diamine	TPAL/TREN/DETA	56	1500	40	Hot pressed at 80 °C for 40 min under 90 kPa pressure.	Imine exchange or imine metathesis.	Taynton et al. (2014)
					Water press at room temperature for 24 h under 90 kPa pressure.	Imine condensation/hydrolysis.	
		–	1000–1500	30–35	Welding at 80 °C for 4 min by adding amines.	Imine Exchange.	Zou et al. (2018)
					Degradation by adding amines.		
	TPAL/TREN/diamines	47–120	14–1050	11–65	Welding at room temperature or 77 °C for 1 h.	Imine condensation/hydrolysis.	Taynton et al. (2016b)
		18–135	130–1000	10–64	Hot pressed at 110 °C under <0.1 MPa pressure.	Imine exchange or imine metathesis.	Taynton et al. (2016a)
					Degradation at room temperature for 24 h in DETA.	Imine Exchange.	
		7.3–61.4	–	4.3–165.6	Hot pressed at 120 °C for 5 min under 10 MPa pressure.	Imine exchange or imine metathesis.	Li et al. (2016)
					Degradation at room temperature for 48 h in acid solution (pH = 1).	Imine hydrolysis.	
		45–274	263–1960	21.4–94.1	Welding at 50 °C, 60 °C, 80 °C for each temperature 2 h by one drop of DETA solution.	Imine exchange.	Lei et al. (2017)
					Degradation at 55 °C for 24 h in DMF solution containing amines	Imine exchange.	
		72–102	–	40–50	Water welding at 80 °C for 15 min or 70 °C for 10 min.	Imine exchange.	Zheng et al. (2018b)
					Hot welding at 110 °C for 30 min and 80 °C for 20 min.		
					Degradation in amines.		
	Vanillin based dialdehydes/TREN/DETA	48–64	580–724	47.4–57.1	Hot pressed at 150 °C for 10 min under 10 MPa pressure.	Imine exchange or imine metathesis.	Van et al. (2014)
					Welding at 150 °C for 1 h under 200 g weight.		
					Degradation at 50 °C for 1 h in HCl solution	Imine hydrolysis.	
	TPAL/TREN/amine terminated PDMS	−107.5 to −105.2	0.6–21	0.39–2.8	Hot pressed at 100 °C for 15 min under 15 MPa pressure.	Imine exchange or imine metathesis.	Feng et al. (2019b)
					Water press at room temperature for 6 h.	Imine condensation/hydrolysis.	
					Welding at 100 °C for 30 min.	Imine exchange or imine metathesis.	
	TPAL/TREN/PPD	76–102	1580	40–49	Welding at 80 °C for 15 min with 200 g loading or at 110 °C for 30 min with 200 g loading.	Imine exchange or imine metathesis.	Zheng et al. (2018a)
					Degradation in ethylenediamine.	Imine exchange.	
	Dialdehydes/a dimeric and trimeric mixture	−10	4.4	0.69	Hot pressed at 120 °C for 10 min.	Imine exchange or imine metathesis.	Dhers et al. (2019)

(continued)

Table 7.11 (continued)

Curing system	Raw materials	T_g (°C)	YM (MPa)	σ_m (MPa)	Recycling method	Recycling mechanisms	References
Trialdehyde-diamine	Vanillin based trialdehyde/diamines	87–178	1426–1925	35.2–69.2	Hot pressed at 180 °C for 2–10 min under 15 MPa pressure.	Imine exchange or imine metathesis.	Wang et al. (2018c)
					Degradation at room temperature for 48 min to 21 h 15 min in 1 M HCl solution.	Imine hydrolysis.	
	TFB/amine terminated PEO	–	–	–	Welding at 50 °C for 5 min.	Imine exchange.	Chao et al. (2016)
					Degradation at 50 °C for 4 h in water.	Imine hydrolysis.	
Epoxy-hydroxyl	DGEBA/Schiff base containing diol	87	–	85	Welding at 110 °C for 15 min.	Imine exchange or imine metathesis.	Mai et al. (2019)
					Degradation at 70 °C for 8 h in 0.1 M HCl solution.	Imine hydrolysis.	
Epoxy-amine	Vanillin based epoxy/PACM	172	2112	81	Hot press at 180 °C for 20 min under 15 MPa pressure.	Imine exchange or imine metathesis.	Wang et al. (2019)
					Degradation at room temperature for 237–982 min in 0.1 or 1 M HCl solution.	Imine hydrolysis.	
	Vanillin based Schiff base-containing epoxy/D400	74	1500	45	Welding at 120 °C for 4 h.	Imine exchange or imine metathesis	Zhao and Abu-Omar (2018)
					Degradation at 65 °C for 30 min in 0.25 M HCl solution.	Imine hydrolysis	

D400: polyfunctional amine (Jeffamine, Mw = 400), DETA: diethylene triamine, PACM: 4,4′-methylenebiscyclohexanamine, PEO: poly(ethylene oxide), PPD: *p*-phenylenediamine, TFB: 1,3,5-triformylbenzene, TPAL: terephthalaldehyde, TREN: tris(2-aminoethyl)amine

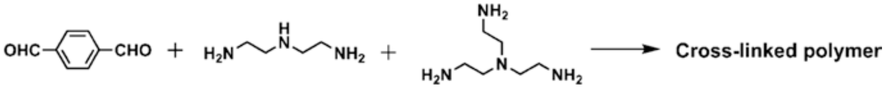

Fig. 7.35 Synthesis of cross-linked polyimine. Reproduced with permission from Taynton et al. (2014)

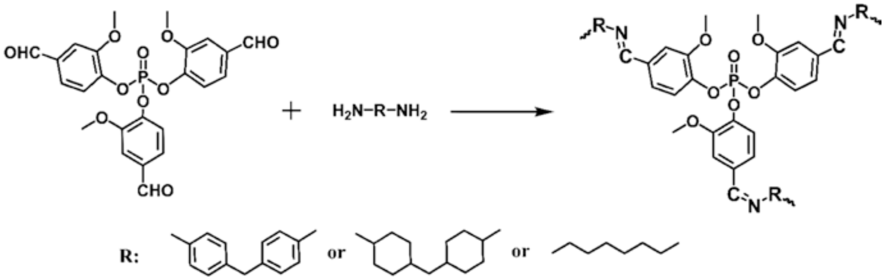

Fig. 7.36 Preparation of Schiff base CANs. Reproduced with permission from Wang et al. (2018c)

that both temperature and moisture could improve the malleability of polyimine networks (Luo et al. 2018a).

In a more recent work, Wang et al. (2018c) synthesized a novel Schiff base precursor from an abundant and renewable lignin derivative, vanillin, through the condensation reaction between phosphorus oxychloride and vanillin, and also prepared malleable Schiff Base CANs (Fig. 7.36). The Schiff base CANs not only showed excellent performance with high strength, T_g and YM, but could also be readily recycled by two hot pressing methods within 2–10 min at 180 °C and hydrolyzing to original Schiff base precursor with a high recovery rate of around 70% under mild conditions. In addition, an excellent flame retardancy as high as UL-94 V0 rate during vertical burning was achieved for these Schiff base CANs, addressing the fire safety issue of conventional thermosetting polymers.

Readily recyclable thermosetting polymers based on Schiff base have been used in electronic skin (Zou et al. 2018) and carbon fiber reinforced thermoset (CFRT) composites (Taynton et al. 2016a; Wang et al. 2019). Zhang's group used the commercial dialdehydes/diamine/triamine systems to achieve repair and recycling of electronic skin and CFRT composite (Zou et al. 2018). Epoxy resins represent for 90% of thermosetting polymers used in CFRT composites due to their excellent properties. With this in mind, Wang et al. (2019) used epoxy resins containing Schiff base structures combining the properties of epoxy resins and polyimines to prepare high-performance, readily recyclable CFRT composites. The Schiff base epoxy resin was prepared through an easy method involving the *in-situ* formation of a Schiff base during the curing process of a monofunctional epoxy monomer containing a formyl group (Fig. 7.37). Through the imine exchange or imine metathesis, the Schiff base epoxy resin showed superior malleability with a T_v of around 70 °C. In

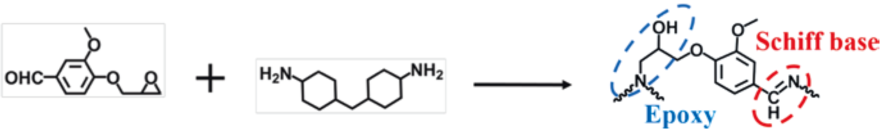

Fig. 7.37 Preparation route of Schiff base epoxy resin. Reproduced with permission from Wang et al. (2019)

addition, the CFRT composite prepared could be degraded under mild conditions at room temperature and the reclaimed carbon fibers maintained the chemical structure, textile structure, surface morphology and mechanical properties compared to the original carbon fibers.

In summary, thermosetting polymers based on Schiff base have several advantages, such as catalyst-free, easy to prepare, fast degradation, moisture-sensitive and rapid reprocessing, which makes them widely reported and show the potential of some high-tech applications such as electronic skin and CFRT composites. However, some side reactions (self-crosslinking of Schiff base, reaction between amine and Schiff base, oxidation, etc.) may occur during the reprocessing at high temperature, resulting in an increase in the brittleness of the materials, which is unfavorable for its use (Wang et al. 2018c, 2019). In addition, rapid relaxation is beneficial for reprocessing materials, but also limits the use of materials at high temperatures.

7.4.2 Disulfide Exchange

Due to the great significance of vulcanized rubbers in the industry, the dynamic sulfur-sulfur bonds have been widely studied. Recent reports show that the behavior of disulfide exchange involves several mechanisms depending on the substitution patterns and service conditions of the disulfides. The simplest mechanism is the reduction of disulfides to two thiols and oxidation of thiols to disulfides again *via* a dissociative mechanism (Fig. 7.38a). The mechanism for dissociative exchange of radical disulfide is the opening of disulfides to stabilized thiyl radicals and the formation of new disulfides by UV radiation or heat (Fig. 7.38b), or by the addition of a radical initiator (Fig. 7.38c). The mechanism of exchange of associative anionic disulfide is the disulfide bond attacked by the thiolate anion to form new thiolate anions and disulfide bond, where the thiolate anion is generated by the addition of catalysts or under basic conditions (Fig. 7.38d). The associative aromatic disulfide metathesis at room temperature has also been reported (Fig. 7.38e). In addition, the associative exchange of disulfides-thiols can also occur through the reaction between disulfides and free thiols (Fig. 7.38f). The disulfide exchange is one of the most commonly used dynamic covalent bonds for self-healing thermosetting polymers due to the low energy barrier of the disulfide exchange. However, this section pays more attention to the recycling (reprocessing, welding or degradation) of thermosetting polymers containing S-S bonds which are summarized in Table 7.12.

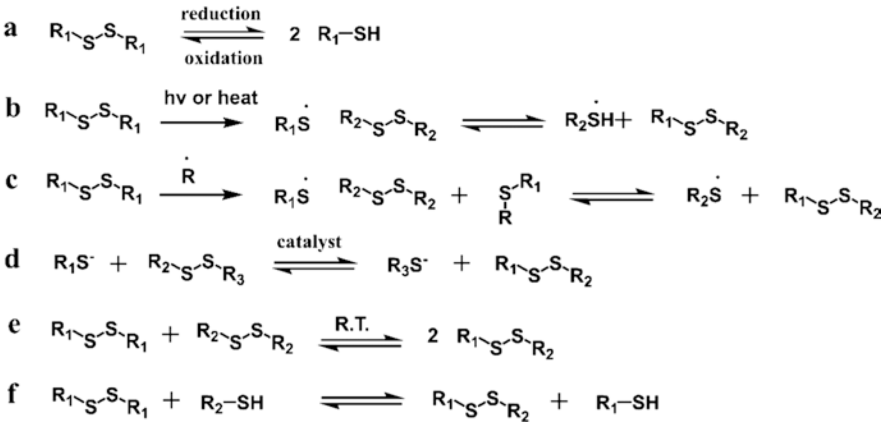

Fig. 7.38 (**a**–**f**) Different mechanisms of disulfide exchange

In 1990, two papers on the recyclable epoxy thermosetting polymers containing disulfide bonds by reducing disulfides to two thiols and reoxidizing of thiols to disulfides using tributyl phosphine as a catalyst were reported (Sastri and Tesoro 1990; Tesoro and Sastri 1990). Due to the toxicity and poor compatibility of the catalyst, recent works have been focused on the development of catalyst-free disulfide exchange systems. In particular, the use of aromatic disulfides instead of aliphatic disulfides could significantly increase the rate of bond exchange, giving thermosetting polymers with excellent reprocessing capacity in the absence of catalyst (Rekondo et al. 2014; Azcune and Odriozola 2016; de Luzuriaga et al. 2016; Kim et al. 2018). Rekondo et al. (2014) demonstrated reprocessable thermosetting poly(urea-urethane)s through aromatic disulfide metathesis. Due to the network reshuffling and the dynamic hydrogen bond formation, the thermosets show a quantitative welding at room temperature. Hydrogen bonds prevent the network from flowing at low temperatures, as a result, little stress relaxation is observed at room temperature. Although most disulfide exchanges follow dissociative mechanisms, Pepels et al. (2013) prepared epoxy thermosetting polymers by the reaction between epoxy and polysulfides, and demonstrated the ability to reprocess through the reaction of disulfides with thiols, which depended much of the pH. These thermosetting polymers could be welded *via* associative cross-linkers exchange at room temperature, which has potential benefits compared to dissociative processes. However, thiols are susceptible to oxidation, which may limit their applications.

Recyclable thermosetting polymers based on the disulfide exchange have been used as a possible application to prepare reprogrammable and reprocessable liquid crystal elastomer (Wang et al. 2017), reprocessable self-powered wearable electronics (Deng et al. 2018) and recyclable fiber-reinforced thermoset (FRT) composites (de Luzuriaga et al. 2016). Keeping this in view, de Luzuriaga et al. (2016) prepared the epoxy thermoset through the curing reaction between DGEBA and 4-aminophenyl disulfide with excellent mechanical and thermal properties, and showed a rapid stress relaxation behavior above T_g with an E_a around 55 kJ/mol. The prepared FRT

Table 7.12 The properties of recyclable thermosets based on disulfide exchange

Curing system	Raw materials	T_g (°C)	YM (MPa)	σ_m (MPa)	Recycling method	Recycling mechanisms	References
Epoxy-amine	DGEBA/disulfide-containing diamines.	96–180	–	–	Degradation at 160 °C for 6 days in diglyme.	Disulfide reduction (catalyst: TBP).	Tesoro and Sastri (1990)
	DGEBA/disulfide-containing diamines.	116–140	–	–	Degradation at 160 °C for 55 min in diglyme.	Disulfide reduction (catalyst: TBP).	Sastri and Tesoro (1990)
	Disulfide-containing epoxy/disulfide-containing diamine.	133	2200	38	Hot pressed at 180 °C for 20 min under 20 MPa pressure.	Radical disulfide exchange.	Zhou et al. (2018)
					Degradation at 50 °C for 20 h in DMF solution with dithiothreitol.	Disulfides-thiols exchange.	
	Isosorbide based epoxy/disulfide-containing diamine.	40.6–60	1990	11	Hot press at 100 °C for 1 h	Radical disulfide exchange.	Ma et al. (2017)
					Degradation in 5 wt.% NaOH aqueous solution for 3 h.	Alkaline hydrolysis.	
	DGEBA/disulfide-containing diamine.	130	2600	88	Hot pressed at 200 °C for 5 min under 100 bar pressure.	Radical disulfide exchange.	de Luzuriaga et al. (2016)
					Degradation at room temperature for 24 h in DMF with 2-mercaptoethanol.	Thiol-disulfide exchange.	
Epoxy-thiol	Epoxy/polysulfides.	–	–	0.25–0.3	Welding	Disulfides-thiols exchange.	Pepels et al. (2013)
	DGEBA/disulfide-containing polysulfides/trithiol (catalyst: TDAP).	–	–	1.3	Welding at 95 °C for 20 min.	Anionic disulfide exchange.	Deng et al. (2018)
Epoxy-acid	Epoxidized natural rubber/disulfide-containing carboxylic acid.	–	1.67	5.3	Hot pressed at 180 °C for 40 min under 8 tons pressure.	Radical disulfide exchange.	Imbernon et al. (2015)

Isocyanate-amine	Triisocyanate/diisocyanate/disulfide-containing diamine.	–	–	8	Hot pressed at 150 °C and 10 MPa for 10 min.	Radical disulfide exchange.	Li et al. (2018a)
					Degradation at 150 °C in DMSO.	Disulfide reduction.	
	Triisocyanate/biisocyanate/disulfide-containing diamine.	−45	–	0.8	Hot pressed at 150 °C for 20 min under 30 bar pressure.	Radical disulfide exchange.	Martin et al. (2014)
	Castor oil/biisocyanate/disulfide-containing diamine.	−10 to 60	5.31–249	0.81–11.82	Hot pressed at 180 °C.	Radical disulfide exchange.	Chen et al. (2018a)
	Triisocyanate/biisocyanate/disulfide-containing diamine.	–	–	0.8	Welding at room temperature for 1–24 h.	Disulfide metathesis.	Rekondo et al. (2014)
Isocyanate-hydroxyl	Diisocyanate/disulfide-containing diols.	−8.2	1.45	6.76	Welding at room temperature for 2–6 h.	Disulfide metathesis.	Kim et al. (2018)
Isocyanate-amine-hydroxyl	HDI/thiuram disulfide-containing diols/TEG/TEA.	−42 to −34	0.6–10.8	0.3–2.1	Welding at room temperature for 24 h under light.	Radical disulfide exchange.	Amamoto et al. (2012)
Cyclic carbonate-amine	Bis(cyclic carbonate)/disulfide-containing diamine/TREN.	49–66	2000	35	Hot pressed at 150 °C for 30 min under 5–10 MPa pressure.	Radical disulfide exchange.	Fortman et al. (2018a, b)
Acrylate-thiol	Disulfide-containing diacrylate/triacrylate/dithiol/tetrathiol (catalyst: 1-methylimidazole).	−19.3 to −15.6	56–110	4.4–8.6	Hot pressed at 60 °C for 30 min under 10 MPa pressure.	Radical disulfide exchange.	Zhang et al. (2018b)
					Welding at 60 °C for 1 h.	Radical disulfide exchange.	
					Degradation at room temperature by TBP or triols.	Disulfide reduction or disulfides-thiols exchange.	
Acrylate	Alkyl disulfide-containing diacrylate.	20	–	7.5	Hot pressed at 120 °C for 12 h under 70 kPa pressure.	Radical disulfide exchange.	Takahashi et al. (2017)
					Welding at 120 °C for 7 h under 70 kPa pressure.	Radical disulfide exchange.	

DMSO: Dimethylsulfoxide, TBP: tributyl phosphine, TDAP: 2,4,6-tris-dimethylaminomethyl phenol, TEA: triethanolamine, TEG: tetra(ethylene glycol), TREN: tris(2-aminoethyl)amine composites could be reprocessed at 210 °C through hot pressing and recycled in a thiol-containing solution at room temperature through disulfides-thiols exchange. Even more interestingly, the epoxy thermoset could be used to prepare enduring prepregs of CFRT composites to solve the problem of limited shelf-life and out-life of prepregs.

In summary, recyclable thermosetting polymers based on disulfide exchange have many advantages, such as the ability to control the structure, low temperature and fast rate for disulfide exchange, excellent recyclability and universality of sulfur-containing compounds. In addition, due to the wide use of commercial sulfur-containing crosslinked materials, their feasible recycling would be of great benefit to the environment.

7.5 Conclusions and Perspectives

In this chapter, the readily recyclable thermosetting polymers based on dynamic associative, dissociative or dynamic associative and dissociative at the same time exchange reaction have been presented. The synthetic routes, mechanical and thermal properties, recycling methods, recycling mechanisms, research progress and applications of each category of recyclable thermosetting polymers have been described.

Thermosetting polymers based on different dynamic bonds exhibit different synthetic routes, mechanical and thermal properties, recycling methods and mechanisms. In general, the thermosetting polymers based on dynamic covalent bonds, especially with associative mechanism, can maintain its structural stability over the temperature range of use. While under certain stimuli, they are able to change their topological networks, thus achieving the recycling of thermosetting polymers. In addition, several works have introduced biobased raw materials such as furan compound (Duval et al. 2017), lignin (Hao et al. 2019), soybean oil (Altuna et al. 2013) and vanillin (Wang et al. 2018c, 2019) to prepare biobased recyclable thermosetting polymers based on dynamic covalent bonds, which is beneficial for a more sustainable development. In addition, the readily recyclable thermosetting polymers show great potential in unique applications, such as 3D printing materials, liquid-crystalline elastomer actuators, recyclable fiber-reinforced composites, removable coatings and wearable electronics. However, most reported readily recyclable thermosetting polymers have several disadvantages, such as poor overall performance, especially the thermal stability, use of catalyst, complex and inefficient recycling, expensive cost, etc. In addition, until now, most thermosetting polymers based on dynamic covalent bonds have not yet been used for industrial applications. More efforts should thus be made to address the problems and improve the sustainability of recyclable thermosetting polymers. The development of thermosetting polymers combining controlled recyclability and improved overall performance has significant value for polymer science and industrial applications.

Acknowledgements This work was financially supported by National Natural Science Foundation of China (No. 51773216), Youth Innovation Promotion Association, CAS (No. 2018335).

Conflicts of Interest The authors declare no conflict of interest.

References

Altuna, F. I., Pettarin, V., & Williams, R. J. J. (2013). Self-healable polymer networks based on the cross-linking of epoxidised soybean oil by an aqueous citric acid solution. *Green Chemistry, 15*(12), 3360–3366. https://doi.org/10.1039/c3gc41384e.

Amamoto, Y., Otsuka, H., Takahara, A., & Matyjaszewski, K. (2012). Self-healing of covalently cross-linked polymers by reshuffling thiuram disulfide moieties in air under visible light. *Advanced Materials, 24*(29), 3975–3980. https://doi.org/10.1002/adma.201201928.

An, X., Aguirresarobe, R. H., Irusta, L., Ruipérez, F., Matxain, J. M., Pan, X., Aramburu, N., Mecerreyes, D., Sardon, H., & Zhu, J. (2017). Aromatic diselenide crosslinkers to enhance the reprocessability and self-healing of polyurethane thermosets. *Polymer Chemistry, 8*(23), 3641–3646. https://doi.org/10.1039/c7py00448f.

Azcune, I., & Odriozola, I. (2016). Aromatic disulfide crosslinks in polymer systems: Self-healing, reprocessability, recyclability and more. *European Polymer Journal, 84*, 147–160. https://doi.org/10.1016/j.eurpolymj.2016.09.023.

Bai, J., Li, H., Shi, Z., & Yin, J. (2015). An eco-friendly scheme for the cross-linked polybutadiene elastomer via thiol–ene and Diels–Alder click chemistry. *Macromolecules, 48*(11), 3539–3546. https://doi.org/10.1021/acs.macromol.5b00389.

Bowman, C. N., & Kloxin, C. J. (2012). Covalent adaptable networks: Reversible bond structures incorporated in polymer networks. *Angewandte Chemie International Edition, 51*(18), 4272–4274. https://doi.org/10.1002/anie.201200708.

Brutman, J. P., Delgado, P. A., & Hillmyer, M. A. (2014). Polylactide vitrimers. *ACS Macro Letters, 3*(7), 607–610. https://doi.org/10.1021/mz500269w.

Buchs, B., Godin, G., Trachsel, A., Laumer, J.-Y. d. S., Lehn, J.-M., & Herrmann, A. (2011). Reversible aminal formation: Controlling the evaporation of bioactive volatiles by dynamic combinatorial/covalent chemistry. *European Journal of Organic Chemistry, 2011*(4), 681–695. https://doi.org/10.1002/ejoc.201001433.

Cai, C., Zhang, Y., Zou, X., Zhang, R., Wang, X., Wu, Q., & Sun, P. (2017). Rapid self-healing and recycling of multiple-responsive mechanically enhanced epoxy resin/graphene nanocomposites. *RSC Advances, 7*(73), 46336–46343. https://doi.org/10.1039/c7ra09258j.

Canary, S. A., & Stevens, M. P. (1992). Thermally reversible crosslinking of polystyrene via the furan–maleimide Diels–Alder reaction. *Journal of Polymer Science Part A: Polymer Chemistry, 30*(8), 1755–1760. https://doi.org/10.1002/pola.1992.080300829.

Cao, L., Fan, J., Huang, J., & Chen, Y. (2019). A robust and stretchable cross-linked rubber network with recyclable and self-healable capabilities based on dynamic covalent bonds. *Journal of Materials Chemistry A, 7*(9), 4922–4933. https://doi.org/10.1039/c8ta11587g.

Capelot, M., Unterlass, M. M., Tournilhac, F., & Leibler, L. (2012). Catalytic control of the vitrimer glass transition. *ACS Macro Letters, 1*(7), 789–792. https://doi.org/10.1021/mz300239f.

Cash, J. J., Kubo, T., Dobbins, D. J., & Sumerlin, B. S. (2018). Maximizing the symbiosis of static and dynamic bonds in self-healing boronic ester networks. *Polymer Chemistry, 9*(15), 2011–2020. https://doi.org/10.1039/c8py00123e.

Chao, A., & Zhang, D. (2019). Investigation of secondary amine-derived aminal bond exchange toward the development of covalent adaptable networks. *Macromolecules, 52*(2), 495–503. https://doi.org/10.1021/acs.macromol.8b02654.

Chao, A., Negulescu, I., & Zhang, D. (2016). Dynamic covalent polymer networks based on degenerative imine bond exchange: Tuning the malleability and self-healing properties by solvent. *Macromolecules, 49*(17), 6277–6284. https://doi.org/10.1021/acs.macromol.6b01443.

Chen, X., Dam, M. A., Ono, K., Mal, A., Shen, H., Nutt, S. R., Sheran, K., & Wudl, F. (2002). A thermally re-mendable cross-linked polymeric material. *Science, 295*(5560), 1698–1702. https://doi.org/10.1126/science.1065879.

Chen, Q., Yu, X., Pei, Z., Yang, Y., Wei, Y., & Ji, Y. (2017a). Multi-stimuli responsive and multi-functional oligoaniline-modified vitrimers. *Chemical Science, 8*(1), 724–733. https://doi.org/10.1039/c6sc02855a.

Chen, X., Li, L., Jin, K., & Torkelson, J. M. (2017b). Reprocessable polyhydroxyurethane networks exhibiting full property recovery and concurrent associative and dissociative dynamic chemistry via transcarbamoylation and reversible cyclic carbonate aminolysis. *Polymer Chemistry, 8*(41), 6349–6355. https://doi.org/10.1039/c7py01160a.

Chen, J.-H., Hu, D.-D., Li, Y.-D., Meng, F., Zhu, J., & Zeng, J.-B. (2018a). Castor oil derived poly(urethane urea) networks with reprocessibility and enhanced mechanical properties. *Polymer, 143*, 79–86. https://doi.org/10.1016/j.polymer.2018.04.013.

Chen, Y., Tang, Z., Zhang, X., Liu, Y., Wu, S., & Guo, B. (2018b). Covalently cross-linked elastomers with self-healing and malleable abilities enabled by boronic ester bonds. *ACS Applied Materials & Interfaces, 10*(28), 24224–24231. https://doi.org/10.1021/acsami.8b09863.

Chujo, Y., Sada, K., & Saegusa, T. (1990). Reversible gelation of polyoxazoline by means of Diels-Alder reaction. *Macromolecules, 23*(10), 2636–2641. https://doi.org/10.1021/ma00212a007.

Craven, J. M. (1969). Cross-linked thermally reversible polymers produced from condensation polymers with pendant furan groups cross-linked with maleimides. U.S. *Patent No. 3,435,003*. Washington, DC: U.S. Patent and Trademark Office.

Cromwell, O. R., Chung, J., & Guan, Z. (2015). Malleable and self-healing covalent polymer networks through tunable dynamic boronic ester bonds. *Journal of the American Chemical Society, 137*(20), 6492–6495. https://doi.org/10.1021/jacs.5b03551.

Debnath, S., Ujjwal, R. R., & Ojha, U. (2018). Self-healable and recyclable dynamic covalent networks based on room temperature exchangeable hydrazide michael adduct linkages. *Macromolecules, 51*(23), 9961–9973. https://doi.org/10.1021/acs.macromol.8b01827.

Deng, J., Kuang, X., Liu, R., Ding, W., Wang, A. C., Lai, Y. C., Dong, K., Wen, Z., Wang, Y., Wang, L., Qi, H. J., Zhang, T., & Wang, Z. L. (2018). Vitrimer elastomer-based jigsaw puzzle-like healable triboelectric nanogenerator for self-powered wearable electronics. *Advanced Materials, 30*(14), 1705918. https://doi.org/10.1002/adma.201705918.

Denissen, W., Rivero, G., Nicolaÿ, R., Leibler, L., Winne, J. M., & Du Prez, F. E. (2015). Vinylogous urethane vitrimers. *Advanced Functional Materials, 25*(16), 2451–2457. https://doi.org/10.1002/adfm.201404553.

Denissen, W., Winne, J. M., & Du Prez, F. E. (2016). Vitrimers: Permanent organic networks with glass-like fluidity. *Chemical Science, 7*(1), 30–38. https://doi.org/10.1039/c5sc02223a.

Denissen, W., Droesbeke, M., Nicolay, R., Leibler, L., Winne, J. M., & Du Prez, F. E. (2017). Chemical control of the viscoelastic properties of vinylogous urethane vitrimers. *Nature Communications, 8*, 14857. https://doi.org/10.1038/ncomms14857.

Denissen, W., De Baere, I., Van Paepegem, W., Leibler, L., Winne, J., & Du Prez, F. E. (2018). Vinylogous urea vitrimers and their application in fiber reinforced composites. *Macromolecules, 51*(5), 2054–2064. https://doi.org/10.1021/acs.macromol.7b02407.

Dhers, S., Vantomme, G., & Avérous, L. (2019). A fully bio-based polyimine vitrimer derived from fructose. *Green Chemistry, 21*(7), 1596–1601. https://doi.org/10.1039/c9gc00540d.

Duval, A., Couture, G., Caillol, S., & Avérous, L. (2017). Biobased and aromatic reversible thermoset networks from condensed tannins via the Diels–Alder reaction. *ACS Sustainable Chemistry & Engineering, 5*(1), 1199–1207. https://doi.org/10.1021/acssuschemeng.6b02596.

Feng, Z., Hu, J., Zuo, H., Ning, N., Zhang, L., Yu, B., & Tian, M. (2019a). Photothermal-induced self-healable and reconfigurable shape memory bio-based elastomer with recyclable ability. *ACS Applied Materials & Interfaces, 11*(1), 1469–1479. https://doi.org/10.1021/acsami.8b18002.

Feng, Z., Yu, B., Hu, J., Zuo, H., Li, J., Sun, H., Ning, N., Tian, M., & Zhang, L. (2019b). Multifunctional vitrimer-like polydimethylsiloxane (PDMS): Recyclable, self-healable, and water-driven malleable covalent networks based on dynamic imine bond. *Industrial & Engineering Chemistry Research, 58*(3), 1212–1221. https://doi.org/10.1021/acs.iecr.8b05309.

Fortman, D. J., Brutman, J. P., Cramer, C. J., Hillmyer, M. A., & Dichtel, W. R. (2015). Mechanically activated, catalyst-free polyhydroxyurethane vitrimers. *Journal of the American Chemical Society, 137*(44), 14019–14022. https://doi.org/10.1021/jacs.5b08084.

Fortman, D. J., Brutman, J. P., Hillmyer, M. A., & Dichtel, W. R. (2017). Structural effects on the reprocessability and stress relaxation of crosslinked polyhydroxyurethanes. *Journal of Applied Polymer Science, 134*(45), 44984. https://doi.org/10.1002/app.44984.

Fortman, D. J., Brutman, J. P., De Hoe, G. X., Snyder, R. L., Dichtel, W. R., & Hillmyer, M. A. (2018a). Approaches to sustainable and continually recyclable cross-linked polymers. *ACS Sustainable Chemistry & Engineering, 6*(9), 11145–11159. https://doi.org/10.1021/acssuschemeng.8b02355.

Fortman, D. J., Snyder, R. L., Sheppard, D. T., & Dichtel, W. R. (2018b). Rapidly reprocessable cross-linked polyhydroxyurethanes based on disulfide exchange. *ACS Macro Letters, 7*(10), 1226–1231. https://doi.org/10.1021/acsmacrolett.8b00667.

Guerre, M., Taplan, C., Nicolay, R., Winne, J. M., & Du Prez, F. E. (2018). Fluorinated vitrimer elastomers with a dual temperature response. *Journal of the American Chemical Society, 140*(41), 13272–13284. https://doi.org/10.1021/jacs.8b07094.

Han, J., Liu, T., Hao, C., Zhang, S., Guo, B., & Zhang, J. (2018). A catalyst-free epoxy vitrimer system based on multifunctional hyperbranched polymer. *Macromolecules, 51*(17), 6789–6799. https://doi.org/10.1021/acs.macromol.8b01424.

Hao, C., Liu, T., Zhang, S., Brown, L., Li, R., Xin, J., Zhong, T., Jiang, L., & Zhang, J. (2019). A high-lignin-content, removable, and glycol-assisted repairable coating based on dynamic covalent bonds. *ChemSusChem, 12*(5), 1049–1058. https://doi.org/10.1002/cssc.201802615.

Hendriks, B., Waelkens, J., Winne, J. M., & Du Prez, F. E. (2017). Poly(thioether) vitrimers via transalkylation of trialkylsulfonium salts. *ACS Macro Letters, 6*(9), 930–934. https://doi.org/10.1021/acsmacrolett.7b00494.

Higaki, Y., Otsuka, H., & Takahara, A. (2006). A thermodynamic polymer cross-linking system based on radically exchangeable covalent bonds. *Macromolecules, 39*(6), 2121–2125. https://doi.org/10.1021/ma052093g.

Ikeda, T., Oikawa, D., Shimasaki, T., Teramoto, N., & Shibata, M. (2013). Organogelation behavior, thermal and mechanical properties of polymer network formed by the Diels–Alder reaction of furan- and maleimide-terminated four-arm star-shaped ε-caprolactone oligomers. *Polymer, 54*(13), 3206–3216. https://doi.org/10.1016/j.polymer.2013.04.052.

Imbernon, L., Oikonomou, E. K., Norvez, S., & Leibler, L. (2015). Chemically crosslinked yet reprocessable epoxidized natural rubber via thermo-activated disulfide rearrangements. *Polymer Chemistry, 6*(23), 4271–4278. https://doi.org/10.1039/c5py00459d.

Ji, S., Cao, W., Yu, Y., & Xu, H. (2014). Dynamic diselenide bonds: Exchange reaction induced by visible light without catalysis. *Angewandte Chemie International Edition, 53*(26), 6781–6785. https://doi.org/10.1002/anie.201403442.

Ji, S., Xia, J., & Xu, H. (2015). Dynamic chemistry of selenium: Se–N and Se–Se dynamic covalent bonds in polymeric systems. *ACS Macro Letters, 5*(1), 78–82. https://doi.org/10.1021/acsmacrolett.5b00849.

Jin, K., Li, L., & Torkelson, J. M. (2016). Recyclable crosslinked polymer networks via one-step controlled radical polymerization. *Advanced Materials, 28*(31), 6746–6750. https://doi.org/10.1002/adma.201600871.

Kim, S.-M., Jeon, H., Shin, S.-H., Park, S.-A., Jegal, J., Hwang, S. Y., Oh, D. X., & Park, J. (2018). Superior toughness and fast self-healing at room temperature engineered by transparent elastomers. *Advanced Materials, 30*(1), 1705145. https://doi.org/10.1002/adma.201705145.

Kloxin, C. J., & Bowman, C. N. (2013). Covalent adaptable networks: Smart, reconfigurable and responsive network systems. *Chemical Society Reviews, 42*(17), 7161–7173. https://doi.org/10.1039/c3cs60046g.

Kuang, X., Liu, G., Dong, X., Liu, X., Xu, J., & Wang, D. (2015). Facile fabrication of fast recyclable and multiple self-healing epoxy materials through diels-alder adduct cross-linker. *Journal of Polymer Science Part A: Polymer Chemistry, 53*(18), 2094–2103. https://doi.org/10.1002/pola.27655.

Legrand, A., & Soulié-Ziakovic, C. (2016). Silica–epoxy vitrimer nanocomposites. *Macromolecules, 49*(16), 5893–5902. https://doi.org/10.1021/acs.macromol.6b00826.

Lei, X., Jin, Y., Sun, H., & Zhang, W. (2017). Rehealable imide–imine hybrid polymers with full recyclability. *Journal of Materials Chemistry A, 5*(40), 21140–21145. https://doi.org/10.1039/c7ta07076d.

Lessard, J. J., Garcia, L. F., Easterling, C. P., Sims, M. B., Bentz, K. C., Arencibia, S., Savin, D. A., & Sumerlin, B. S. (2019). Catalyst-free vitrimers from vinyl polymers. *Macromolecules, 52*(5), 2105–2111. https://doi.org/10.1021/acs.macromol.8b02477.

Li, H., Bai, J., Shi, Z., & Yin, J. (2016). Environmental friendly polymers based on schiff-base reaction with self-healing, remolding and degradable ability. *Polymer, 85*(24), 106–113. https://doi.org/10.1016/j.polymer.2016.01.050.

Li, T., Xie, Z., Xu, J., Weng, Y., & Guo, B.-H. (2018a). Design of a self-healing cross-linked polyurea with dynamic cross-links based on disulfide bonds and hydrogen bonding. *European Polymer Journal, 107*, 249–257. https://doi.org/10.1016/j.eurpolymj.2018.08.005.

Li, X., Yu, R., Zhao, T., Zhang, Y., Yang, X., Zhao, X., & Huang, W. (2018b). A self-healing polysiloxane elastomer based on siloxane equilibration synthesized through amino-ene Michael addition reaction. *European Polymer Journal, 108*, 399–405. https://doi.org/10.1016/j.eurpolymj.2018.09.021.

Liu, Y.-L., & Hsieh, C.-Y. (2006). Crosslinked epoxy materials exhibiting thermal remendablility and removability from multifunctional maleimide and furan compounds. *Journal of Polymer Science Part A: Polymer Chemistry, 44*(2), 905–913. https://doi.org/10.1002/pola.21184.

Liu, T., Hao, C., Wang, L., Li, Y., Liu, W., Xin, J., & Zhang, J. (2017a). Eugenol-derived biobased epoxy: Shape memory, repairing, and recyclability. *Macromolecules, 50*(21), 8588–8597. https://doi.org/10.1021/acs.macromol.7b01889.

Liu, W.-X., Zhang, C., Zhang, H., Zhao, N., Yu, Z.-X., & Xu, J. (2017b). Oxime-based and catalyst-free dynamic covalent polyurethanes. *Journal of the American Chemical Society, 139*(25), 8678–8684. https://doi.org/10.1021/jacs.7b03967.

Liu, Y., Tang, Z., Chen, Y., Zhang, C., & Guo, B. (2018a). Engineering of β-hydroxyl esters into elastomer-nanoparticle interface toward malleable, robust, and reprocessable vitrimer composites. *ACS Applied Materials & Interfaces, 10*(3), 2992–3001. https://doi.org/10.1021/acsami.7b17465.

Liu, Z., Zhang, C., Shi, Z., Yin, J., & Tian, M. (2018b). Tailoring vinylogous urethane chemistry for the cross-linked polybutadiene: Wide freedom design, multiple recycling methods, good shape memory behavior. *Polymer, 148*, 202–210. https://doi.org/10.1016/j.polymer.2018.06.042.

Liu, T., Zhang, S., Hao, C., Verdi, C., Liu, W., Liu, H., & Zhang, J. (2019). Glycerol induced catalyst-free curing of epoxy and vitrimer preparation. *Macromolecular Rapid Communications, 40*(7), e1800889. https://doi.org/10.1002/marc.201800889.

Lu, Y.-X., & Guan, Z. (2012). Olefin metathesis for effective polymer healing via dynamic exchange of strong carbon-carbon double bonds. *Journal of the American Chemical Society, 134*(34), 14226–14231. https://doi.org/10.1021/ja306287s.

Lu, Y.-X., Tournilhac, F., Leibler, L., & Guan, Z. (2012). Making insoluble polymer networks malleable via olefin metathesis. *Journal of the American Chemical Society, 134*(20), 8424–8427. https://doi.org/10.1021/ja303356z.

Lu, L., Pan, J., & Li, G. (2017). Recyclable high-performance epoxy based on transesterification reaction. *Journal of Materials Chemistry A, 5*(40), 21505–21513. https://doi.org/10.1039/c7ta06397k.

Luo, C., Lei, Z., Mao, Y., Shi, X., Zhang, W., & Yu, K. (2018a). Chemomechanics in the moisture-induced malleability of polyimine-based covalent adaptable networks. *Macromolecules, 51*(23), 9825–9838. https://doi.org/10.1021/acs.macromol.8b02046.

Luo, K., Li, J., Duan, G., Wang, Y., Yu, J., Zhu, J., & Hu, Z. (2018b). Comb-shaped aromatic polyamide cross-linked by Diels-Alder chemistry: Towards recyclable and high-performance thermosets. *Polymer, 142*, 33–42. https://doi.org/10.1016/j.polymer.2018.03.026.

de Luzuriaga, A. R., Martin, R., Markaide, N., Rekondo, A., Cabanero, G., Rodriguez, J., & Odriozola, I. (2016). Epoxy resin with exchangeable disulfide crosslinks to obtain reprocessable, repairable and recyclable fiber-reinforced thermoset composites. *Materials Horizons, 3*(3), 241–247. https://doi.org/10.1039/c6mh00029k.

Ma, S., & Webster, D. C. (2018). Degradable thermosets based on labile bonds or linkages: A review. *Progress in Polymer Science, 76*, 65–110. https://doi.org/10.1016/j.progpolymsci.2017.07.008.

Ma, S., Li, T., Liu, X., & Zhu, J. (2016). Research progress on bio-based thermosetting resins. *Polymer International, 65*(2), 164–173. https://doi.org/10.1002/pi.5027.

Ma, Z., Wang, Y., Zhu, J., Yu, J., & Hu, Z. (2017). Bio-based epoxy vitrimers: Reprocessibility, controllable shape memory, and degradability. *Journal of Polymer Science Part A: Polymer Chemistry, 55*(10), 1790–1799. https://doi.org/10.1002/pola.28544.

Mai, V.-D., Shin, S.-R., Lee, D.-S., & Kang, I. (2019). Thermal healing, reshaping and ecofriendly recycling of epoxy resin crosslinked with Schiff base of vanillin and hexane-1,6-diamine. *Polymers, 11*(2), 293. https://doi.org/10.3390/polym11020293.

Mallek, H., Jegat, C., Mignard, N., Abid, M., Abid, S., & Taha, M. (2013). Reversibly crosslinked self-healing PCL-based networks. *Journal of Applied Polymer Science, 129*(9), 954–964. https://doi.org/10.1002/app.38595.

Martin, R., Rekondo, A., de Luzuriaga, A. R., Cabanero, G., Grande, H. J., & Odriozola, I. (2014). The processability of a poly(urea-urethane) elastomer reversibly crosslinked with aromatic disulfide bridges. *Journal of Materials Chemistry A, 2*(16), 5710–5715. https://doi.org/10.1039/c3ta14927g.

McElhanon, J. R., Russick, E. M., Wheeler, D. R., Loy, D. A., & Aubert, J. H. (2002). Removable foams based on an epoxy resin incorporating reversible Diels-Alder adducts. *Journal of Applied Polymer Science, 85*(7), 1496–1502. https://doi.org/10.1002/app.10753.

Montarnal, D., Capelot, M., Tournilhac, F., & Leibler, L. (2011). Silica-like malleable materials from permanent organic networks. *Science, 334*(6058), 965–968. https://doi.org/10.1126/science.1212648.

Neal, J. A., Mozhdehi, D., & Guan, Z. (2015). Enhancing mechanical performance of a covalent self-healing material by sacrificial noncovalent bonds. *Journal of the American Chemical Society, 137*(14), 4846–4850. https://doi.org/10.1021/jacs.5b01601.

Nishimura, Y., Chung, J., Muradyan, H., & Guan, Z. (2017). Silyl ether as a robust and thermally stable dynamic covalent motif for malleable polymer design. *Journal of the American Chemical Society, 139*(42), 14881–14884. https://doi.org/10.1021/jacs.7b08826.

Obadia, M. M., Mudraboyina, B. P., Serghei, A., Montarnal, D., & Drockenmuller, E. (2015). Reprocessing and recycling of highly cross-linked ion-conducting networks through transalkylation exchanges of C–N bonds. *Journal of the American Chemical Society, 137*(18), 6078–6083. https://doi.org/10.1021/jacs.5b02653.

Obadia, M. M., Jourdain, A., Cassagnau, P., Montarnal, D., & Drockenmuller, E. (2017). Tuning the viscosity profile of ionic vitrimers incorporating 1,2,3-triazolium cross-links. *Advanced Functional Materials, 27*(45), 1703258. https://doi.org/10.1002/adfm.201703258.

Ogden, W. A., & Guan, Z. (2018). Recyclable, strong, and highly malleable thermosets based on boroxine networks. *Journal of the American Chemical Society, 140*(20), 6217–6220. https://doi.org/10.1021/jacs.8b03257.

Otera, J. (1993). Transesterification. *Chemical Reviews, 93*(4), 1449–1470. https://doi.org/10.1021/cr00020a004.

Pan, X., Driessen, F., Zhu, X., & Du Prez, F. E. (2017). Selenolactone as a building block toward dynamic diselenide-containing polymer architectures with controllable topology. *ACS Macro Letters, 6*(2), 89–92. https://doi.org/10.1021/acsmacrolett.6b00944.

Pepels, M., Filot, I., Klumperman, B., & Goossens, H. (2013). Self-healing systems based on disulfide-thiol exchange reactions. *Polymer Chemistry, 4*(18), 4955–4965. https://doi.org/10.1039/c3py00087g.

Qiu, M., Wu, S., Fang, S., Tang, Z., & Guo, B. (2018). Sustainable, recyclable and robust elastomers enabled by exchangeable interfacial cross-linking. *Journal of Materials Chemistry A, 6*(28), 13607–13612. https://doi.org/10.1039/c8ta04173c.

Rekondo, A., Martin, R., de Luzuriaga, A. R., Cabanero, G., Grande, H. J., & Odriozola, I. (2014). Catalyst-free room-temperature self-healing elastomers based on aromatic disulfide metathesis. *Materials Horizons, 1*(2), 237–240. https://doi.org/10.1039/c3mh00061c.

Röttger, M., Domenech, T., van der Weegen, R., Breuillac, A., Nicolaÿ, R., & Leibler, L. (2017). High-performance vitrimers from commodity thermoplastics through dioxaborolane metathesis. *Science, 356*(6333), 62–65. https://doi.org/10.1126/science.aah5281.

Roy, N., Bruchmannb, B., & Lehn, J.-M. (2015). DYNAMERS: Dynamic polymers as self-healing materials. *Chemical Society Reviews, 44*(11), 3786–3807. https://doi.org/10.1039/c5cs00194c.

Sastri, V. R., & Tesoro, G. C. (1990). Reversible crosslinking in epoxy resins. II. New approaches. *Journal of Applied Polymer Science, 39*(7), 1439–1457. https://doi.org/10.1002/app.1990.070390703.

Schmolke, W., Perne, N., & Seiffert, S. (2015). Dynamically cross-linked polydimethylsiloxane networks with ambient-temperature self-Healing. *Macromolecules, 48*(24), 8781–8788. https://doi.org/10.1021/acs.macromol.5b01666.

Shi, Q., Yu, K., Kuang, X., Mu, X., Dunn, C. K., Dunn, M. L., Wang, T., & Jerry Qi, H. (2017). Recyclable 3D printing of vitrimer epoxy. *Materials Horizons, 4*(4), 598–607. https://doi.org/10.1039/c7mh00043j.

Snyder, R. L., Fortman, D. J., De Hoe, G. X., Hillmyer, M. A., & Dichtel, W. R. (2018). Reprocessable acid-degradable polycarbonate vitrimers. *Macromolecules, 51*(2), 389–397. https://doi.org/10.1021/acs.macromol.7b02299.

Stukenbroeker, T., Wang, W., Winne, J. M., Du Prez, F. E., Nicolaÿ, R., & Leibler, L. (2017). Polydimethylsiloxane quenchable vitrimers. *Polymer Chemistry, 8*(43), 6590–6593. https://doi.org/10.1039/c7py01488k.

Suzuki, N., Takahashi, A., Ohishi, T., Goseki, R., & Otsuka, H. (2018). Enhancement of the stimuli-responsiveness and photo-stability of dynamic diselenide bonds and diselenide-containing polymers by neighboring aromatic groups. *Polymer, 154*, 281–290. https://doi.org/10.1016/j.polymer.2018.09.022.

Swanson, J. P., Rozvadovsky, S., Seppala, J. E., Mackay, M. E., Jensen, R. E., & Costanzo, P. J. (2010). Development of polymeric phase change materials on the basis of Diels–Alder chemistry. *Macromolecules, 43*(14), 6135–6141. https://doi.org/10.1021/ma100836c.

Takahashi, A., Goseki, R., Ito, K., & Otsuka, H. (2017). Thermally healable and reprocessable bis(hindered amino)disulfide-cross-linked polymethacrylate networks. *ACS Macro Letters, 6*(11), 1280–1284. https://doi.org/10.1021/acsmacrolett.7b00762.

Taynton, P., Yu, K., Shoemaker, R. K., Jin, Y., Qi, H. J., & Zhang, W. (2014). Heat- or water-driven malleability in a highly recyclable covalent network polymer. *Advanced Materials, 26*(23), 3938–3942. https://doi.org/10.1002/adma.201400317.

Taynton, P., Ni, H., Zhu, C., Yu, K., Loob, S., Jin, Y., Qi, H. J., & Zhang, W. (2016a). Repairable woven carbon fiber composites with full recyclability enabled by malleable polyimine networks. *Advanced Materials, 28*(15), 2904–2909. https://doi.org/10.1002/adma.201505245.

Taynton, P., Zhu, C., Loob, S., Shoemaker, R., Pritchard, J., Jin, Y., & Zhang, W. (2016b). Re-healable polyimine thermosets: Polymer composition and moisture sensitivity. *Polymer Chemistry, 7*(46), 7052–7056. https://doi.org/10.1039/c6py01395c.

Tesoro, G. C., & Sastri, V. R. (1990). Reversible crosslinking in epoxy resins. I. Feasibility studies. *Journal of Applied Polymer Science, 39*(7), 1425–1437. https://doi.org/10.1002/app.1990.070390702.

Trovatti, E., Lacerda, T. M., Carvalho, A. J. F., & Gandini, A. (2015). Recycling tires? Reversible crosslinking of poly(butadiene). *Advanced Materials, 27*(13), 2242–2245. https://doi.org/10.1002/adma.201405801.

Ube, T., Kawasaki, K., & Ikeda, T. (2016). Photomobile liquid-crystalline elastomers with rearrangeable networks. *Advanced Materials, 28*(37), 8212–8217. https://doi.org/10.1002/adma.201602745.

Van, A., Chiou, K., & Ishida, H. (2014). Use of renewable resource vanillin for the preparation of benzoxazine resin and reactive monomeric surfactant containing oxazine ring. *Polymer, 55*(6), 1443–1451. https://doi.org/10.1016/j.polymer.2014.01.041.

Wang, F., Rong, M. Z., & Zhang, M. Q. (2012). Reversibility of solid state radical reactions in thermally remendable polymers with C–ON bonds. *Journal of Materials Chemistry, 22*(26), 13076. https://doi.org/10.1039/c2jm30578j.

Wang, Z., Tian, H., He, Q., & Cai, S. (2017). Reprogrammable, reprocessible, and self-healable liquid crystal elastomer with exchangeable disulfide bonds. *ACS Applied Materials & Interfaces, 9*(38), 33119–33128. https://doi.org/10.1021/acsami.7b09246.

Wang, C., An, X., Pang, M., Zhang, Z., Zhu, X., Zhu, J., Du Prez, F. E., & Pan, X. (2018a). Dynamic diselenide-containing polyesters from alcoholysis/oxidation of γ-butyroselenolactone. *Polymer Chemistry, 9*(29), 4044–4051. https://doi.org/10.1039/c8py00736e.

Wang, C., Goldman, T. M., Worrell, B. T., McBride, M. K., Alim, M. D., & Bowman, C. N. (2018b). Recyclable and repolymerizable thiol–X photopolymers. *Materials Horizons, 5*(6), 1042–1046. https://doi.org/10.1039/c8mh00724a.

Wang, S., Ma, S., Li, Q., Yuan, W., Wang, B., & Zhu, J. (2018c). Robust, fire-safe, monomer-recovery, highly malleable thermosets from renewable bioresources. *Macromolecules, 51*(20), 8001–8012. https://doi.org/10.1021/acs.macromol.8b01601.

Wang, S., Xing, X., Zhang, X., Wang, X., & Jing, X. (2018d). Room-temperature fully recyclable carbon fibre reinforced phenolic composites through dynamic covalent boronic ester bonds. *Journal of Materials Chemistry A, 6*(23), 10868–10878. https://doi.org/10.1039/c8ta01801d.

Wang, S., Ma, S., Li, Q., Xu, X., Wang, B., Yuan, W., Zhou, S., You, S., & Zhu, J. (2019). Facile in situ preparation of high-performance epoxy vitrimer from renewable resources and its application in nondestructive recyclable carbon fiber composite. *Green Chemistry, 21*(6), 1484–1497. https://doi.org/10.1039/c8gc03477j.

Watanabe, M., & Yoshie, N. (2006). Synthesis and properties of readily recyclable polymers from bisfuranic terminated poly(ethylene adipate) and multi-maleimide linkers. *Polymer, 47*(14), 4946–4952. https://doi.org/10.1016/j.polymer.2006.05.036.

Wu, X., Yang, X., Huang, W., Yu, R., Zhao, X., & Zhang, Y. (2018). A facile access to Stiff epoxy vitrimer with excellent mechanical properties *via* siloxane equilibration. *Journal of Materials Chemistry A, 6*(22), 10184–10188. https://doi.org/10.1039/c8ta02102c.

Wu, S., Yang, Z., Fang, S., Tang, Z., Liu, F., & Guo, B. (2019). Malleable organic/inorganic thermosetting hybrids enabled by exchangeable silyl ether interfaces. *Journal of Materials Chemistry A, 7*(4), 1459–1467. https://doi.org/10.1039/c8ta09866b.

Yamashiro, M., Inoue, K., & Iji, M. (2008). Recyclable shape-memory and mechanical strength of poly(lactic acid) compounds cross-linked by thermo-reversible Diels-Alder reaction. *Polymer Journal, 40*(7), 657–662. https://doi.org/10.1295/polymj.pj2008042.

Yamashiro, M., Inoue, K., & Iji, M. (2009). Recyclable shape-memory polymer: Poly(lactic acid) crosslinked by a thermoreversible Diels-Alder reaction. *Journal of Applied Polymer Science, 112*(2), 876–885. https://doi.org/10.1002/app.29469.

Yan, P., Zhao, W., Fu, X., Liu, Z., Kong, W., Zhou, C., & Lei, J. (2017). Multifunctional polyurethane-vitrimers completely based on transcarbamoylation of carbamates: Thermally-induced dual-shape memory effect and self-welding. *RSC Advances, 7*(43), 26858–26866. https://doi.org/10.1039/c7ra01711a.

Yang, Y., Pei, Z., Zhang, X., Tao, L., Wei, Y., & Ji, Y. (2014). Carbon nanotube-vitrimer composite for facile and efficient photo-welding of epoxy. *Chemical Science, 5*(9), 3486–3492. https://doi.org/10.1039/c4sc00543k.

Ying, H., Zhang, Y., & Cheng, J. (2014). Dynamic urea bond for the design of reversible and self-healing polymers. *Nature Communications, 5*, 3218. https://doi.org/10.1038/ncomms4218.

Yoshie, N., Watanabe, M., Araki, H., & Ishida, K. (2010). Thermo-responsive mending of polymers crosslinked by thermally reversible covalent bond: Polymers from bisfuranic terminated poly(ethylene adipate) and tris-maleimide. *Polymer Degradation and Stability, 95*(5), 826–829. https://doi.org/10.1016/j.polymdegradstab.2010.01.032.

Yu, K., Shi, Q., Dunn, M. L., Wang, T., & Qi, H. J. (2016). Carbon fiber reinforced thermoset composite with near 100% recyclability. *Advanced Functional Materials, 26*(33), 6098–6106. https://doi.org/10.1002/adfm.201602056.

Yuan, C. e., Rong, M. Z., Zhang, M. Q., Zhang, Z. P., & Yuan, Y. C. (2011). Self-healing of polymers via synchronous covalent bond fission/radical recombination. *Chemistry of Materials, 23*(22), 5076–5081. https://doi.org/10.1021/cm202635w.

Yuan, C. e., Rong, M. Z., & Zhang, M. Q. (2014). Self-healing polyurethane elastomer with thermally reversible alkoxyamines as crosslinkages. *Polymer, 55*(7), 1782–1791. https://doi.org/10.1016/j.polymer.2014.02.033.

Zhang, D., & Dumont, M.-J. (2018). Reprocessable 5-hydroxymethylfurfural derivative-based thermoset elastomers synthesized through the thiol-Michael and Diels–Alder reactions. *Journal of Materials Science, 53*(15), 11116–11129. https://doi.org/10.1007/s10853-018-2375-4.

Zhang, Y., Broekhuis, A. A., & Picchioni, F. (2009). Thermally self-healing polymeric materials: The next step to recycling thermoset polymers? *Macromolecules, 42*(6), 1906–1912. https://doi.org/10.1021/ma8027672.

Zhang, B., Digby, Z. A., Flum, J. A., Foster, E. M., Sparksb, J. L., & Konkolewicz, D. (2015). Self-healing, malleable and creep limiting materials using both supramolecular and reversible covalent linkages. *Polymer Chemistry, 6*(42), 7368–7372. https://doi.org/10.1039/c5py01214g.

Zhang, Y., Ying, H., Hart, K. R., Wu, Y., Hsu, A. J., Coppola, A. M., Kim, T. A., Yang, K., Sottos, N. R., White, S. R., & Cheng, J. (2016a). Malleable and recyclable poly(urea-urethane) thermosets bearing hindered urea bonds. *Advanced Materials, 28*(35), 7646–7651. https://doi.org/10.1002/adma.201601242.

Zhang, Z. P., Lu, Y., Rong, M. Z., & Zhang, M. Q. (2016b). A thermally remendable and reprocessable crosslinked methyl methacrylate polymer based on oxygen insensitive dynamic reversible C–ON bonds. *RSC Advances, 6*(8), 6350–6357. https://doi.org/10.1039/c5ra22275c.

Zhang, B., Kowsari, K., Serjouei, A., Dunn, M. L., & Ge, Q. (2018a). Reprocessable thermosets for sustainable three-dimensional printing. *Nature Communications, 9*(1), 1831. https://doi.org/10.1038/s41467-018-04292-8.

Zhang, L., Qiu, T., Zhu, Z., Guo, L., & Li, X. (2018b). Self-healing polycaprolactone networks through thermo-induced reversible disulfide bond formation. *Macromolecular Rapid Communications, 39*(20), 1800121. https://doi.org/10.1002/marc.201800121.

Zhang, Z. P., Rong, M. Z., & Zhang, M. Q. (2018c). Polymer engineering based on reversible covalent chemistry: A promising innovative pathway towards new materials and new functionalities. *Progress in Polymer Science, 80*, 39–93. https://doi.org/10.1016/j.progpolymsci.2018.03.002.

Zhao, S., & Abu-Omar, M. M. (2018). Recyclable and malleable epoxy thermoset bearing aromatic imine bonds. *Macromolecules, 51*(23), 9816–9824. https://doi.org/10.1021/acs.macromol.8b01976.

Zheng, P., & McCarthy, T. J. (2012). A surprise from 1954: Siloxane equilibration is a simple, robust, and obvious polymer self-healing mechanism. *Journal of the American Chemical Society, 134*(4), 2024–2027. https://doi.org/10.1021/ja2113257.

Zheng, N., Fang, Z., Zou, W., Zhao, Q., & Xie, T. (2016). Thermoset shape-memory polyurethane with intrinsic plasticity enabled by transcarbamoylation. *Angewandte Chemie International Edition, 55*(38), 11421–11425. https://doi.org/10.1002/anie.201602847.

Zheng, H., Liu, Q., Lei, X., Chen, Y., Zhang, B., & Zhang, Q. (2018a). A conjugation polyimine vitrimer: Fabrication and performance. *Journal of Polymer Science Part A: Polymer Chemistry, 56*(22), 2531–2538. https://doi.org/10.1002/pola.29232.

Zheng, H., Liu, Q., Lei, X., Chen, Y., Zhang, B., & Zhang, Q. (2018b). Performance-modified polyimine vitrimers: Flexibility, thermal stability and easy reprocessing. *Journal of Materials Science, 54*(3), 2690–2698. https://doi.org/10.1007/s10853-018-2962-4.

Zhou, Y., Goossens, J. G. P., Sijbesma, R. P., & Heuts, J. P. A. (2017). Poly(butylene terephthalate)/glycerol-based vitrimers via solid-state polymerization. *Macromolecules, 50*(17), 6742–6751. https://doi.org/10.1021/acs.macromol.7b01142.

Zhou, F., Guo, Z., Wang, W., Lei, X., Zhang, B., Zhang, H., & Zhang, Q. (2018). Preparation of self-healing, recyclable epoxy resins and low-electrical resistance composites based on double-disulfide bond exchange. *Composites Science and Technology, 167*, 79–85. https://doi.org/10.1016/j.compscitech.2018.07.041.

Zou, W., Dong, J., Luo, Y., Zhao, Q., & Xie, T. (2017). Dynamic covalent polymer networks: From old chemistry to modern day innovations. *Advanced Materials, 29*(14), 1606100. https://doi.org/10.1002/adma.201606100.

Zou, Z., Zhu, C., Li, Y., Lei, X., Zhang, W., & Xiao, J. (2018). Rehealable, fully recyclable, and malleable electronic skin enabled by dynamic covalent thermoset nanocomposite. *Science Advances, 4*(2), eaaq0508. https://doi.org/10.1126/sciadv.aaq0508.

Chapter 8
A Review to Guide Eco-Design of Reactive Polymer-Based Materials

Emma Delamarche, Valérie Massardier, Remy Bayard, and Edson Dos Santos

Abstract After decades of intensive use, polymer wastes are omnipresent and disturb natural environments such as oceans. Thus, sustainable materials must be developed, combining not only the use properties, but also their recycling or end of life in natural environments. This chapter focuses on the study of the parameters that influence the biodegradation of reactive polymer-based materials, either in the perspective of recycling or for the end of life in natural environments, including compostability. In fact, the hydrolysable bonds of reactive polymers, such as polyesters make them prone to hydrolysis that can be catalyzed enzymatically, either by enzymes naturally present in the environment or by other selected ones used in chemical reactors. Of course, the formulation of materials can also influence the degradation at end of life. In this sense, the controlled end of life in natural environment must correspond to several advantages, such as increasing soil fertility and lower volumes of discarded plastic materials, while enzyme catalyzed hydrolysis in chemical reactors allows recover chemical building blocks such as monomers and oligomers. Finally, a critical analysis of the parameters influencing the degradation

---

E. Delamarche
Ingénierie des Matériaux Polymères, INSA Lyon, CNRS UMR 5223, Université de Lyon,
Villeurbanne, France

DEEP Déchets Eaux Environnement Pollutions, EA 7429, INSA Lyon, Université de Lyon,
Villeurbanne, France

V. Massardier (✉)
Ingénierie des Matériaux Polymères, INSA Lyon, CNRS UMR 5223, Université de Lyon,
Villeurbanne, France

INSA de Lyon, Université de Lyon, Lyon, France
e-mail: valerie.massardier@insa-lyon.fr

R. Bayard
DEEP Déchets Eaux Environnement Pollutions, EA 7429, INSA Lyon, Université de Lyon,
Villeurbanne, France

E. D. Santos
Ingénierie des Matériaux Polymères, INSA Lyon, CNRS UMR 5223, Université de Lyon,
Villeurbanne, France

T. J. Gutiérrez (ed.), *Reactive and Functional Polymers Volume Four*,
https://doi.org/10.1007/978-3-030-52052-6_8

of reactive polymer-based materials will allow to give recommendations for their eco-design.

Keywords Biodegradation · Enzyme catalyzed hydrolysis · Natural environments · Recycling

8.1 Introduction

After decades of development of industrial production and consumption of manufactured plastic products, the management of their end of life remains a great challenge for our planet. In fact, there is a real awareness of the environmental problems of the treatment and recovery of the plastic waste we produce and, more particularly, end-of-life plastics that are ubiquitous in our lives. Now, their presence in all ecosystems is known, and their interactions with the living world are still being studied to understand the consequences. It is thus necessary to develop sustainable materials, which combine not only acceptable use properties, but also the recyclability or the ability to biodegrade in natural environments (Sombrio et al. 2017; Gutiérrez 2018a).

Nowadays, most of plastics on the market are petroleum-based organic polymers. Large amounts of plastics waste are disseminated in the environment and are associated with the problematic pollution of air, soil and water. Biobased plastics are considered an interesting alternative because they have several advantages, including the biogenic source of organic carbon, chemical composition, synthesis or process method, economic importance, as well as their applications, and potential biodegradability (Gutiérrez 2018b; Herniou-Julien et al. 2019). Its world production is growing, while its end of life is not sufficiently controlled (Li et al. 2018). Many studies have focused on replacing petroleum-based materials by renewable alternatives, as well as anticipating the end-of-life in order to generate materials adequate for recycling options in the circular economy (Zhu et al. 2016). There is a number of advantages in the use of biodegradable polymers, such as the increase in soil fertility, the accumulation of low volumes of plastic materials discarded in the environment, as well as the reduction of waste management costs (Gross and Kalra 2002; Merino et al. 2018a, 2019a). With respect to the seas, a study estimated that in 2014 more than five trillion pieces of plastics floated in the oceans (Plastiques: derrière les déchets, un gisement d'industries 2018).

On the other hand, plastic particles are defined as those with a length less than 5 mm (Li et al. 2018). These microplastics lead to a growing scientific and social awareness, as they are disseminated on air, earth and water (oceans…). Thus, with respect to pollution by microplastics and plastics, it could be interesting that polymer materials biodegrade more easily in the environment, without generating toxic products.

From the perspective of circular economy, functional polymers can undergo mechanical recycling, which is, a priori, a fairly simple route, with an economical interest and a reduced environmental impact compared to depolymerization (Shen et al. 2010). Nevertheless, the hydrolysable bonds of functional polymers such as polyesters make these polymers prone to chemical degradation *via* hydrolysis or enzyme-catalyzed hydrolysis in order to recover building blocks (Engineer et al. 2011). Depolymerization is particularly interesting for thermoset polymers, for which recycling is not obvious since they are not likely to undergo mechanical recycling using melt processing.

This chapter presents the general definition of biodegradable polymers *via* enzyme catalyzed hydrolysis. In the second part of this chapter, the main parameters influencing polymer degradation are displayed. The third part was then dedicated to enzyme catalyzed hydrolysis to recover building blocks from the perspective of a circular economy. The fourth part of this chapter presents typical end-of-life tests (composting, soil burial) with the objective of predicting behaviors under natural conditions. The synthesis of the first four parts leads to discuss the eco-design of polymer-based materials in order to tune their biodegradability.

The purpose of this chapter is to guide the eco-design of reactive polymer-based materials in order to facilitate their end of life (1) for the recovery of chemical building blocks by enzyme catalyzed hydrolysis or (2) by biodegradation under natural environments.

8.1.1 Biodegradable Polymers

Replacing fossil polymers with biobased polymers is one of the main research attempts in the modern plastic industry. Natural polymers represent a specific class of materials among polymers based on natural resources. These polymers occur in nature as macromolecules and are often physically or chemically modified (Imre and Pukánszky 2015).

The global consumption of biodegradable polymers has increased from 14 million kg in 1996 to approx. 68 million kg in 2001 (Demirbas 2007). Target markets for biobased polymers include packaging materials, disposable nonwovens and hygiene products, consumer and agricultural tools (Gutiérrez and Alvarez 2018; Gutiérrez et al. 2019; Merino et al. 2018b, 2019b). The commercialization of biobased polymers is, however, hampered by competition with commodity plastics which are inexpensive and familiar to the customer (Gross and Kalra 2002).

Polyesters constitute a large family of biodegradable polymers. They contain ester bonds in their structure, which are easily hydrolysable and reasonably biodegradable. The most commonly used biodegradable polymers can be divided into two groups: aliphatic (such as poly(butylene succinate) (PBS), poly(hydroxyalkanoates) (PHAs), poly(lactic acid) (PLA), poly(ε-caprolactone) (PCL), among others) and aromatics (such as aliphatic-aromatic copolyester (AAC)) (Walter et al. 1995; Vieira et al. 2013; Żenkiewicz et al. 2013; Gutiérrez and Alvarez

2017a, b, c; Gutiérrez 2018c; Gutiérrez et al. 2021). Polyesters such as PBS are considered particularly interesting due to their potential ability for biodegradation, thermal stability, relatively high melting temperature (T_m) and easy thermal processability (Zeng et al. 2016). As another biodegradable polymer, PLA has attracted a lot of attention due to its ability to replace some current commodity plastics (Sudesh and Iwata 2008; Matta et al. 2014).

Biobased synthetic polymers can be produced with different characteristics such as biodegradability, crystallinity, solubility, glass transition temperature (T_g) and T_m according to their synthetic form and/or the obtaining conditions. These specificities may affect the biodegradability of polymers (Vieira et al. 2013; Díaz et al. 2014; Pellis et al. 2016).

Functional polymers are good candidates for depolymerization through hydrolysis or glycolysis. However, they can also be recycled by being melted again to form new materials. Polyesters such as poly(ethylene terephthalate) (PET) are prone to hydrolysis and it can be useful to maintain or increase chain lengths with chain extenders, in the perspective of mechanical recycling (Lacoste et al. 2005).

There are two different sources for the mechanical recycling of plastics. The first refers to wastes coming directly from industrial production rejections, where there is no contamination, making them often rather easy to recycle, while post-consumer plastic wastes which may have a high level of pollution, are more difficult and expensive to recycle (Begley and Hollifield 1995; Forlin and Faria 2002). The presence of other types of materials, such as aluminum, glass, paint, paper, steel, etc. can be considered contaminants of plastic packaging with respect to their recycling, which may make their mechanical recycling difficult (Huber and Franz 1997; Forlin and Faria 2002).

8.1.2 Definitions of Biodegradation and Enzyme Catalyzed Hydrolysis

8.1.2.1 Biodegradation

In this chapter, the following terms are defined as follows:

- **Degradation or deterioration** refers to any evolution of the properties of the material through aging (fragmentation, loss of mechanical properties, mass loss, molecular weight (Mw), etc.). **Disintegration** refers to an advanced stage of degradation, where fragmentation is important and the material is divided into very small fragments (ISO/FDIS 16929:2013 2013).
- **Biodegradation** is the process of degradation of a polymer material to generally obtain water, carbon dioxide (CO_2) and/or methane (CH_4), and biomass as degradation products *via* the action of microorganisms. Biodegradation is carried out through different steps. First, fragmentation occurs, which increases the surface area, thus allowing microorganisms to adhere. Fragmentation can be caused by physical means (grinding) and/or chemical degradation (hydrolysis), which leads to a polymer of lower average Mw, easier to be processed by microorgan-

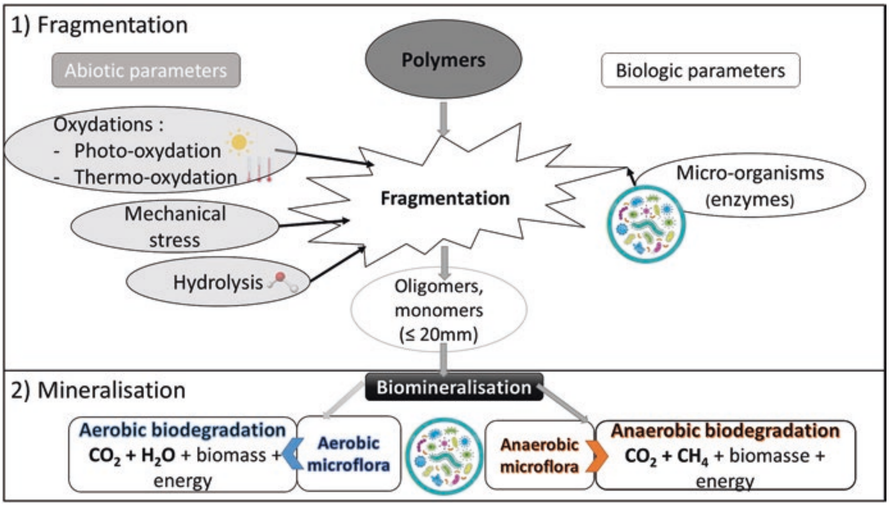

Fig. 8.1 Main steps of the degradation of polymer materials

isms (Witt et al. 1996). Then, bioassimilation or biomineralization, occurs: fragments and oligomers are mineralized by microorganisms into simple molecules and biomass (Witt et al. 1996; Castelan 2010; Mierzwa-Hersztek et al. 2019).

The most common definition of a biodegradable polymer is 'a degradable polymer wherein the primary degradation mechanism is through the action of metabolism by microorganisms' (Leja and Lewandowicz 2010). The biodegradation rate depends on humidity, temperature, number and type of microorganisms, and is often fast if all three requirements are present.

Polymer degradation takes place in several different ways, depending on the structure and exposure conditions (Fig. 8.1). Degradation results from an irreversible change, which leads to a loss of mass and, eventually, to failure. The most common types of degradation occur through chemical reactions, but there are some important examples of degradation, which result only from physical changes (Hawkins 1984; Ohkita and Lee 2006).

The first degradation mechanism is physical/physical-chemical degradation. Mechanical degradation can take place due to compression, shear forces and/or tension. Mechanical factors are not predominant during the biodegradation process, but the damages caused by this mechanism can activate or accelerate it. Under field conditions, mechanical stresses act in synergy with the other abiotic parameters such as chemicals, solar radiation and temperature (Hawkins 1984; Lucas et al. 2008).

The second degradation mechanism is photodegradation, also known as photo-oxidation. These processes are influenced by the light intensity and the temperature, and can lead to dramatic decreases of the Mw, as well as changes in Mw distribution (MWD or polydispersity index—PDI = weight-average apparent molecular weight (M_w)/number-average apparent molecular weight (M_n)) (Weiland et al. 1995;

Feldman 2002; Koutny et al. 2006). In aqueous media, compared to air, photodegradation of polymers is much slower (Andrady et al. 1993). Oxodegradable plastic materials are usually polyolefins with additives (pro-oxidants), which induce a fragmentation process when exposed to ultra-violet (UV) radiations, which causes oxidation. Such materials are fragmentable, and produced fragments have been found to remain in the environment (Bioplastics 2015; Selke et al. 2015).

Another well-known mechanism is thermal degradation, which should be considered in the thermophilic composting (Beyler and Hirschler 2002; Lucas et al. 2008; Ojumu et al. 2004). Atmospheric pollutants and agrochemicals can also interact with polymers, thus changing the macromolecules properties, i.e. they can change the bonds, attack and break them, producing free radicals, and causing the material degradation (Muller et al. 2001; Lucas et al. 2008).

8.1.2.2 Enzyme Catalyzed Hydrolysis

Functional polymers containing hydrolysable covalent bonds such as amide, anhydride, carbamide (urea), ester amide (urethane), ester and ether groups, etc. can undergo chemical degradation *via* enzymatic hydrolysis (Le Digabel and Avérous 2006). Hydrolysis depends on parameters such as concentration, pH, temperature, time and water activity. For most biodegradable materials, especially artificial polymers, passive hydrolysis is the most important degradation mechanism (Göpferich 1996; Tengborg et al. 2001; Angelidaki and Sanders 2004). Glycolysis can also be efficient for cutting chains. The selected enzymes can be efficient catalysts for such hydrolysis or glycolysis.

8.2 Main Parameters in Polymer Degradation

8.2.1 Polymer Characteristics

8.2.1.1 Molar Mass

It is generally admitted that polymer degradation occurs more rapidly in lower Mw polymers. For example, Husarova et al. (2014) observed that PLA exhibiting a low average Mw was degraded faster than high Mw PLA under composting conditions and abiotic aqueous conditions. Bernhard et al. (2008) also observed that anaerobic degradation was slower for high Mw poly(ethylene glycol) (PEG). These authors observed that the lag phase raised with the increase in Mw (Bernhard et al. 2008).

The influence of Mw can be explained by several reasons:

- Polymer materials initially having a rather low average Mw, reaches faster low Mws through degradation. Since low Mws lead to materials having poor mechanical properties (Nunes et al. 1982), these materials appear macroscopically deteriorated (through a loss of mechanical properties, cracks, fragmentation, etc.).

- Polymers exhibiting low Mws may show a lower T_g (Fox and Flory 1950). If the T_g is close to room temperature, it significantly affects the degradation (Park 1994).
- Under biotic conditions, certain polymer-based materials having a high average Mw are not easily attacked by microorganisms. Witt et al. (1996) observed that small copolyesters and oligomers are more easily degraded by microorganisms, due to their solubility in water, which leads to fast mineralization. Schliecker et al. (2003) found that PLAs that had a number average Mw of 830 Da are water soluble. More recently, Husarova et al. (2014) also suggested that low Mw polymer chains can be better substrates for microorganisms.

8.2.1.2 Macroscopic Shape

It has been observed that materials having a high specific surface area degrade faster in biotic media. Husarova et al. (2014) made this observation with PLA under composting conditions. Rudnik and Briassoulis (2011b) also observed the same behavior under soil burial conditions with PLA. In marine water, Volova et al. (2010) and Deroiné (2014) observed a faster degradation of PHA films than pellets or massive samples. In fact, in a biotic environment, the higher the specific surface area, the better microorganisms can adhere to the surface, which leads to faster degradation.

In abiotic environment, the influence of morphology depends on the degradation mechanisms, and conflicting results have been found in the literature. For example, Husarova et al. (2014) observed in the case of abiotic hydrolysis of PLA, a faster degradation for samples exhibiting a higher specific surface area, while Deroiné (2014) did not observe any influence of the geometry, because the degradation occurred within the samples and not on their surface. In fact, degradation rate in abiotic hydrolysis of PLA can be higher within the material due to the autocatalytic effect (degradation products are trapped within the sample), which leads to a ‘hollow structure’ (Grizzi et al. 1995). Dvorackova et al. (2015) studied PBS and obtained a greater weight loss in abiotic hydrolysis for thin PBS films than for thick films. However, Deroiné (2014) did not observe influence of the geometry in the abiotic hydrolysis of PHA.

8.2.1.3 Crystallinity

It has been observed that the degradation rate is lower for polymers exhibiting a high degree of crystallinity, because the crystalline regions are less accessible to enzymes (Pantani and Sorrentino 2013) and water (Zhou and Xanthos 2008; Pantani and Sorrentino 2013). In fact, amorphous PLA is degraded faster than semi-crystalline PLA in abiotic medium (Zhou and Xanthos 2008), as well as in aerobic degradation under composting conditions (Pantani and Sorrentino 2013). Tserki et al. (2006) studied the biodegradation of poly(butylene succinate-*co*-adipate)

(PBSA) copolyesters under soil burial conditions and identified the crystallinity as the dominant factor controlling the biodegradation rate.

The crystalline structure, for a same degree of crystallinity, also influences the degradation rate. Cho et al. (2001) used thermal treatments on PBS to achieve different crystalline structures and observed that the hydrolysis degradation rate was influenced by the thermal history, and therefore, the crystalline structure.

8.2.1.4 Hydrophobicity

Hydrophobicity and water adsorption also influence the degradability of polymer-based materials, especially those that undergo hydrolysis. Keeping this in view, Höglund et al. (2010) reported that the degradability rate decreases with increasing hydrophobicity.

Most of the plastics found in the environment, such as PET, poly(ethylene) (PE), poly(propylene) (PP) and poly(styrene) (PS) are hydrophobic. The UV irradiation (photo-oxidation) can also oxidize their surface (Andrady 2011), and often leads to mass loss, since oxidized groups are more prone to biodeterioration *via* the formation of bacterial biofilm. Photo-degradation of suspended plastics in water is slower than in air (Andrady et al. 1993).

8.2.2 Environmental Conditions

8.2.2.1 Humidity

Humidity influences the degradation rate by increasing the hydrolysis rate and by allowing the activity and transport of microorganisms. Gu et al. (1994) conducted degradation experiments on cellulose acetate films in composting reactors with different humidity percentages and found that moisture significantly accelerated degradation.

8.2.2.2 pH

Another factor influencing the degradation rate is the pH. For example, Makino et al. (1986) and Schliecker et al. (2003) observed that PLA was degraded more rapidly under alkaline conditions than under neutral or acidic conditions. Schliecker et al. (2003) also found that PLA undergoes chain-end cleavage under acidic conditions, and a random chain cleavage under alkaline conditions, while the solubility of PLA oligomers depended on the pH. Meanwhile, Xu and Guo (2010) also reported that PBS undergoes faster degradation in alkaline media.

In fact, hydrolysis of polyesters is faster under alkaline conditions. According to Abeysinghe et al. (1982) and Gu et al. (2001), this is because of the formation of a resonance-stabilized carboxylate anion that can react with the alcohol functions. Ester hydrolysis in neutral and acidic solutions is reversible. For this reason, recombinations could slow down the degradation of polyesters in neutral and acidic solutions. In alkaline solutions, hydrolysis is irreversible. Another explanation could be that hydrogen bonds (in polymers that exhibit hydrogen bonds) are destroyed in alkaline media, which leads to a less dense structure that increases the accessibility (Chu 1981b).

8.2.2.3 Temperature

Higher temperatures often lead to faster degradation. At temperatures above the T_g of a given polymer material, chain mobility is increased, which facilitates the access for enzymes (Weinberger et al. 2017). Chain mobility also facilitates water absorption (Siparsky et al. 1997). For this reason, at temperatures below their T_g, polyesters such as PLA do not easily degrade, while they are significantly degraded at temperatures close to their T_g (Agarwal et al. 1998; Itävaara et al. 2002; Yagi et al. 2009; Karamanlioglu and Robson 2013).

Abiotic hydrolysis rate increases with temperature, since the reaction kinetics and water diffusion depend on temperature (Siparsky et al. 1997; Schliecker et al. 2003). In biotic degradation, hydrolysis is the first limiting step of the degradation of polyesters such as PLA (Husarova et al. 2014), and at higher temperatures lead to faster hydrolysis, and therefore, the production of oligomers that can be degraded by microorganisms is faster (Witt et al. 1996).

8.2.2.4 Others

- Oxygen: degradation can be influenced by the presence (aerobic conditions) or the absence of oxygen (anaerobic conditions). In this context, Itävaara et al. (2002) observed a faster biodegradation of PLA under anaerobic thermophilic conditions. These authors suggested that this was due to the lactic acid produced, which could be a more favorable substrate for anaerobic microorganisms (Zellner et al. 1994; Itävaara et al. 2002). On the contrary, PBS can be easily degraded under mesophilic and thermophilic aerobic conditions, but not under mesophilic anaerobic conditions (Shin et al. 1997; Cho et al. 2011; Dvorackova et al. 2015).
- Ionic strength: Makino et al. (1986) observed that PLA microcapsules were degraded faster in high ionic strength solutions. These authors also studied the effect of pH and suggested that pH and ionic strength changed the electric potential distribution (Makino et al. 1986).
- Concentration of species: Makino et al. (1986) observed that the concentration of salt in buffered solution has an impact on the degradation rate of PLA microcapsules. The degradation takes place faster in a concentrated buffer solution, supposedly because this concentrated buffer solution leads to the conversion of acidic degradation products into neutral salts (Chu 1981a; Makino et al. 1986).

- C/N ratio: polymer biodegradation depends on the concentration and nature of other nutrients in the environment, which may or may not be preferred by microorganisms (Gu et al. 1994).
- Marine/saline conditions: degradation in seawater may take place differently from degradation in pure water (Kasuya et al. 1998). Kasuya et al. (1998) tested different polyesters and observed that poly(ethylene succinate) (PES) was completely degraded in freshwater but was almost not degraded in seawater. These authors suggested that this was due to the fact that the population of microorganisms is different, depending on the water source (Kasuya et al. 1998). Bernhard et al. (2008) also observed that PEG was degraded faster in freshwater than in marine water.
- Microorganisms in the environment: Kasuya et al. (1998) observed that the biodegradability of polyesters in natural water depends on the source of the water. Boyandin et al. (2012) also observed a significant influence of the population of microorganisms on the degradation of PHAs in soil.

8.3 Enzyme Catalyzed Hydrolysis for Recovery of Building Blocks

The objective of enzymatic degradation with selected enzymes is the recovery of the building blocks, that can be used to elaborate new materials. Enzymatic catalysis is particularly indicated for hydrolysable polymers, such as polyesters, and is a means to accelerate degradation. Nevertheless, compared to chemical hydrolysis, reaction catalyzed by enzymes can be carried out under mild conditions that are quite selective. For example, a lipase of *Pseudomonas cepacia* can selectively degrade PBS and not PLA, at low temperature, while chemical hydrolysis would hydrolyze both polymers simultaneously.

8.3.1 Enzymatic Degradation Mechanisms

Hydrolysis is defined as a breakdown of polymer bonds by the gradual diffusion of water into the polymer matrix (Azevedo and Reis 2004; Lyu and Untereker 2009). Hydrolytic degradation is an autocatalytic process, where the carboxylic acids produced catalyze further hydrolysis. The diffusion reaction phenomenon determines the means by which this pathway proceeds. The advantage of surface degradation is the predictability of the process (Li 1998; Castilla-Cortázar et al. 2012).

Enzymatic hydrolysis of polymer materials is not a homogeneous process because of the mode of interaction between the enzymes and the polymer chains and typically involves several steps: (1) diffusion of the enzyme from the bulk solution to the solid surface, (2) adsorption of the enzyme on the substrate, resulting in the formation of an enzyme-substrate complex, (3) catalysis of the hydrolysis reaction and (4) diffusion of the soluble degradation products from the solid substrate to the solution. The rate of the global reaction is controlled by the slowest step (Rahmouni et al. 2001; Azevedo and Reis 2004).

Enzymatic hydrolysis can take place in two different ways. First, exoenzymes, secreted by cells, thus allowing the degradation of macromolecules that cannot penetrate the cellular membrane, specifically hydrolyze the ester bonds located at the chain-ends, releasing monomers. This mechanism only slightly affects the Mw of the polymer, while one can observe an overall mass loss. The second case corresponds to the use of endoenzymes, which are intracellular enzymes that work in the intracellular medium in which they are produced. Selected endoenzymes can cause the rupture of random ester bonds of carbon chains of polyesters, thus releasing polymers of lower Mws. This results in a significant decrease in the M_w of the residual polymer (Lenz 1993; Yang and Pan 2015; Thirunavukarasu et al. 2016).

Taniguchi et al. (2002) analyzed the effects of the enzymatic degradation of PBS films and fibers by lipase from *Pseudomonas cepacia* at 50 °C and pH 6. These authors observed that PBS fibers were less degraded than PBS films (PBS film lost 76% of its mass compared to only 6% for the fibers). This difference can be attributed to the fact that PBS fibers have a higher degree of crystallinity than films. In addition to the chemical structure, the degree of crystallinity is indeed the factor that most influences enzymatic hydrolysis of PBS. Therefore, for aliphatic copolymers, such as PBS-*co*-ethylene succinate or PBSA: the higher the degree of crystallinity, the lower the mass loss (Mochizuki and Hirami 1996; Xu et al. 2008). As a result, PBSA and PBS undergo approximately the same type of enzymatic hydrolysis with similar degrees of crystallinity.

Enzymes catalyzed degradation experiments are often carried out using enzymes such as cutinases, lipases and proteinases, which are used on polymers based on PLA or starch.

8.3.2 Enzymatic Degradation Essays

Among the main biobased polymers are functional polymers based on polyesters, which are easily hydrolysable (Walter et al. 1995; Vieira et al. 2013; Żenkiewicz et al. 2013). Such synthetic polymers can show versatile characteristics such as crystallinity, solubility, T_g and T_m, which can be considered an advantage over natural biodegradable polymers such as chitosan (Cs), gelatin and others (Vieira et al. 2013; Díaz et al. 2014; Pellis et al. 2016). Especially, crystallinity can significantly modify the hydrolysis rates.

pH values that are too acidic or alkaline can affect the efficiency of enzymes. An adequate pH must thus be chosen based on the intrinsic properties of the enzyme and the type of experiment involved. The incubation temperature is also a key factor when enzymatic tests are performed. Temperature can also inhibit the enzyme activity if is poorly chosen. However, higher temperatures can significantly increase the kinetics of the reaction. The substrate and enzyme concentrations must also be regulated, and the initial rate of an enzymatic reaction is generally proportional to the enzyme concentration.

Other factors that must be controlled in an enzymatic degradation assay are incubation time, solution components and the use of cofactors. In general, longer incubation times lead to more advanced enzymatic degradation. However, at a certain stage, the enzyme loses its effectiveness. The compounds in solution (bacteriostatic product, type of buffer, among others) must be adapted to the enzymes used. As for cofactors, these depend on the enzyme and the type of experiment performed, but they can be essential if the enzyme needs to be activated by them.

The enzymatically catalyzed degradation products often dissolve in the aqueous medium of the reaction and contain carbon (Fig. 8.2). Therefore, the total organic carbon (TOC) analysis of the dissolved carbon in solution after experiment is useful.

Enzymatic degradation starts rather on the surface of the polymer (mass loss and surface erosion), because, at first, enzymes cannot penetrate the very compact matrix of the material. After degradation, three types of analyzes can be carried out mainly following the enzymatic tests implemented:

- A macroscopic analysis to check with the naked eye if the samples or solutions have changed appearance (color, strength, among others) for further analysis.
- An analysis of the mass loss ratio of the samples between before and after incubation.
- A TOC analysis of dissolved carbon in solution to confirm the effects of mass loss (PBS and PLA are approx. 50% carbon).

Spectroscopic analyses such as Fourier transform infrared (FTIR) and nuclear magnetic resonance (NMR) spectroscopies can also be carried out to assess changes in chemical structure.

Fig. 8.2 Enzyme catalyzed hydrolysis of polyester films

8.3.3 *Enzymatic Degradation as a Recycling Route*

Enzymatic degradation could be used as a recycling route for polymers. It is possible to recover oligomers and monomers that can be further polymerized. This was assessed by Matsumura et al. (2002) who used a lipase to degrade PCL and recover polymerizable monomers and oligomers. This is particularly interesting for the recycling of complex materials containing several polymers, which are not easily separated. With this in mind, Gamerith et al. (2017) worked on the use of a cutinase to recycle PET from polymer blends and identified key parameters, such as particle size, temperature and the presence of inhibitor constituents such as bis(2-hydroxyethyl) terephthalate. Desrousseaux et al. (2017) also developed a bacterial enzymatic product, which was able to depolymerize up to 97% of polyester-based bottles, in particular those containing PET and/or PLA in 16 h.

8.3.4 *Enzymatic Degradation as a Means to Assess Biodegradability*

Enzymatic hydrolysis is an effective and rapid degradation process. It is often conducted in order to evaluate the potential biodegradability of a given material in the environment. For example, Ju et al. (2015) made P(3HB-*co*-4HB)/PLA blends and conducted enzymatic degradation experiments. These authors found that degradation was accelerated when polymers were blended, due to the increase in the specific surface area (Ju et al. 2015). However, since enzymes are quite specific with a given substrate, the results may not reflect the behavior of the material in a real environment.

8.4 Assessing Biodegradability: End of Life in Environments Aiming to Be Representative of Natural Conditions

The degradation of polymer materials can be studied at different scales and under different environments and conditions, with the aim of being representative of natural conditions.

8.4.1 *Disintegration Experiments*

Degradation or disintegration experiments, based on the characterization of polymer samples before and after aging, can be conducted in any environment, at any scale (aqueous medium, composting facility, soil burial, etc.). Mainly fragmentation

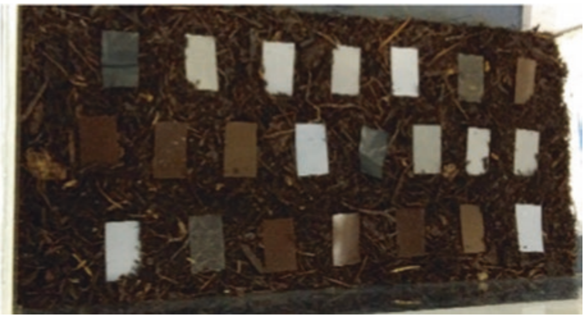

Fig. 8.3 Samples before burial under compost conditions for disintegration experiment

and mass loss are studied. Some disintegration experiments constitute standards, such as standards ISO 16929 or ISO 20200, which suggest a disintegration test in compost, monitored using odor detection, visual appearance and mass loss, the latter used to determine a degree of disintegration. Standard ISO 846 specifies a protocol for the evaluation of degradation under soil burial conditions, which was applied by Tserki et al. (2006).

However, fragmentation and mass loss alone do not prove that chemical degradation occurs. In fact, following the evolution of molar masses by using steric exclusion chromatography (SEC) is mandatory, as well as spectroscopy techniques to follow the increase in end-of-chain groups.

In addition, in the case of composites, a polymer material can be partially degraded macroscopically, but generates remaining fragments. For example, Goheen and Wool (1991) observed that PE remained intact after the aging of PE/starch blends under soil burial conditions, while the starch was easily degraded.

As a conclusion, disintegration experiments give an idea of the material behavior in natural environment (Fig. 8.3). Thus, they are still widely used to study new formulations of potentially biodegradable polymers (Arrieta et al. 2014a, b). However, the test does not provide information about microorganisms capable of mineralizing fragments, monomers, oligomers and/or degradation products. Different monitoring techniques should thus be used in order to prove the assimilation of a polymer material.

8.4.2 Biodegradation Experiments

Microbial activity under aerobic or anaerobic conditions are often considered as valuable preliminary tests.

8.4.2.1 Aerobic Conditions

Aerobic biodegradation occurs in aerated environments, and therefore, respirometric techniques are still used. A respirometer is a device used to measure the oxygen consumption, or CO_2 production. The standard ISO 14851 describes the determination of the definitive aerobic biodegradability of plastic materials in an aqueous medium by measuring the oxygen demand (OD) in a closed respirometer. Known biodegradable materials, such as cellulose powder, and non-degradable materials, such as PE, are used as references. In this sense, the tested material is immersed in an aqueous medium (mineral medium) inoculated with sludge from sewage. The oxygen consumption is measured in each flask, e.g. by monitoring the pressure (with a CO_2 trap) (Fig. 8.4). After subtracting the biological oxygen demand (BOD) of the flasks containing only the inoculum, the BOD of the sample is divided by the theoretical OD to determine a percentage of biodegradability.

The theoretical oxygen demand (TOD—mg O_2/mg sample) is calculated as follows:

$$TOD = \frac{16 \times \left(2c + 0.5\left(h - cl - 3n\right) + 3s + 2.5p + 0.5na - o\right)}{M} \tag{8.1}$$

where M is the molar mass of a substance $C_cH_hCl_{cl}N_nS_{es}P_pNa_{na}O_o$.

Other standards specifying the evaluation of the biodegradability of materials after oxygen consumption include standards ISO 14855-1 under composting conditions, ISO 17556 in soil, ISO 18830 in seawater and sediments.

CO_2 production can also be studied, and evaluation techniques are specified by standards ISO 19679 in seawater and sediments, as well as ASTM D-5338 or ISO 14855-2 in compost. Given the mass fraction of carbon in the material (X_c is determined from chemical formula or elemental analysis) and the theoretical amount of CO_2 (TCO_2) produced can be calculated using the following equation:

Fig. 8.4 Measuring heads used to monitor O_2 production

$$TCO_2 = m_{material} \times X_c \times \frac{M(CO_2)}{M(C)} \tag{8.2}$$

After subtracting the amount of CO_2 produced in the flasks containing only the inoculum, the CO_2 production of the flask containing the tested material is divided by the TCO_2 produced, to determine a percentage of biodegradability. Some studies evaluating biodegradability using a respirometer have been conducted by Bernhard et al. (2008) and Hablot et al. (2014) for PEG and PLA/PHA blends, respectively.

8.4.2.2 Anaerobic Conditions

In anaerobic media, there is no oxygen present in the system. The biodegradation of polymer materials is evaluated through biogas production: CH_4 and CO_2. The tested samples are disposed in medium inoculated with anaerobic sludge. Biodegradable materials such as cellulose powder and non-degradable materials such as PE are used as references. Microorganisms transform organic matter into CH_4 and CO_2. Biogas production is monitored using pressure or volumetric measurements. The amount of carbon in the gaseous volume (in the form CH_4 and CO_2) can be calculated using the ideal gas law. The percentage of biodegradation is calculated by dividing the amount of carbon converted into gas by the amount of carbon in the tested material. Standard ISO 14853 describes a biodegradation experiment in anaerobic aqueous medium, and standard ISO 15985 specifies a protocol for high solid content household waste. In this regard, recent studies assessing the polymer biodegradability under anaerobic conditions include the biodegradation of PBS (Dvorackova et al. 2015) and PLA/LA blends (Lee et al. 2016).

8.4.2.3 Ecotoxicity

Ecotoxicity refers to the potential to affect ecosystems (Gutiérrez 2018a, b). The ecotoxicity of polymer materials and their degradation products can be evaluated using several protocols such as:

- The standardized luminescent bacteria test (ISO 11348-3 1998), which was used by Tuominen et al. (2002) employing *Vibrio fischeri* as bioluminescent bacteria. An inhibition of light production in the presence of the compound tested can reveal a possible toxicity. This essay is conducted widely to evaluate ecotoxicity of compounds due to their numerous advantages, which include a short test duration, low cost and sensitivity (Abbas et al. 2018).
- Plant growth studies. For example, Tuominen et al. (2002) evaluated the ecotoxicity in the soil containing degradation products using as biomarkers the number of seedlings emerged and the mass of the part of the plant that is on the soil surface in barley, cress, and radish crops.

- Contact with animals, such as daphnia (Witt et al. 2001), fish (standards OECD 203 and 204) or earthworms in a soil (Jayasekara et al. 2003), where behavior, health and reproduction are usually studied.

8.4.3 Definitions in Standards

Degradation essays can be conducted under mesophilic (at temperatures between 20 and 40 °C) or thermophilic (above 40 °C) conditions. However, most of the experiments assessing the degradation of polymers under thermophilic conditions take place around 58 °C. Different microorganisms can be used under mesophilic and thermophilic conditions.

Composting is an aerobic process where organic matter is biodegraded, thus forming an organic soil conditioner (ISO 17088). During the composting process, microbial activity leads to a significant rise in temperature (Bayard and Gourdon 2010). Thus, under industrial composting conditions, thermophilic conditions are reached, which does not usually occur under home composting conditions (Barrena et al. 2014). Composting could be a potential route for biological recycling of certain biodegradable polymers. However, compostability should be assessed.

Industrial compostability, is described in European standard EN13432, or standard ISO 17088. To be qualified as compostable in industrial facilities, a plastic material must show a biodegradability of more than 90% in 6 months at 58 °C (essay described in standard ISO 14855), and a fragmentation (less than 2 mm fragments) in 3 months (prEN 14045). The compost, after experiment, must exhibit a low concentration of heavy metals and its quality must remain unchanged (assessed through ecotoxicity tests monitoring plant growth). Then, plastic degradation must induce no significant change of nutrients (N, P, etc.) in compost.

As said earlier, **home compostability**, implies lower temperatures. French standard NF T-51-800 describes specifications for home composting. A biodegradability essay (standard ISO 14855) must be conducted at 25 °C instead of 58 °C. The disintegration essay (such as the one described in standard ISO 20200) must be carried out at 25 °C as well.

The degradation of polymers in soil is studied to assess the end-of-life of plastic waste, in the case where there is lost involuntarily in the environment or if they are disposed in landfills. The standards are used to establish the degradability of polymers under soil burial conditions. As under composting conditions, disintegration tests, as well as biodegradation tests using respirometric devices, can be conducted to evaluate the end-of-life behavior in the soil. The European standard TC 249 WG 9, specifies the requirements that mush comprise a biodegradation test in a respirometer at around 20–30 °C (ISO 17566), which leads to at least 90% biodegradation in 2 years, and the control of the soil quality (control of hazardous substances and ecotoxicity tests).

Biogasification of organic waste in biogas, such as methane, is another potential route for polymer recycling. To assess biodegradability in an anaerobic digester, the standards specify protocols using anaerobic sewage sludge (ISO 13975, ISO 15985).

8.5 Ecodesign: How to Tune Biodegradability in Natural Environments?

As discussed above, thermoplastic functional polymers, such as polyesters, are often good candidates for mechanical recycling or depolymerization (enzyme catalyzed hydrolysis, glycolysis, hydrolysis, etc.). However, thermoset polymers, such as polyurethanes and epoxy resins are quite difficult to recycle. Polyurethanes can be depolymerized by glycolysis, but there are only few studies addressing the enzyme catalyzed depolymerization reaction (Magnin et al. 2019).

Regarding the anticipation of the end of the useful life of thermoset and thermoplastic polymers, eco-design with the insertion of ‘easy-to-break functions’ in the polymer chains should facilitate the recovery of building blocks in the perspective of a circular economy.

Improving the assimilation of polymer materials is an important challenge. The main parameters used to control biodegradability in polymers are listed in the next section. Selected articles refer to studies of polymer disintegration in water media (biotic and/or abiotic hydrolysis), under soil or under composting conditions. Biodegradation studies under aerobic or anaerobic conditions will also be analyzed in the following sections. In this part, publications assessing enzymatic catalyzed degradation are not included, since the specificity of enzymes for a given polymer may give incorrect tendencies, considering complex polymer materials.

8.5.1 Chemical Nature

8.5.1.1 Chemical Bonds

It is known that specific chemical bonds between repeated units are easily broken, and checking that decomposition products are not toxic or eco-toxic when eliminated in the environment is necessary.

- Hydrolysable bonds include amide, anhydride, carbamide, ester, ether and urethane functions (Lucas et al. 2008). In this sense, Göpferich (1996) reviewed and listed the half-lives associated with the hydrolysis of various chemical bonds. The anhydride bonds and ortho ester bonds, followed by ester and amide bonds, are easily hydrolyzed (Göpferich 1996).
- Certain types of bonds, such as esters can be photodegraded, which can lead to chain scissions or crosslinking (Lucas et al. 2008).

8.5.1.2 Repeating Unit

The nature of the bond itself does not control the macroscopic degradation of the polymer, but also the repeating unit can affect biodegradation. For example, steric hindrance can slow down degradation kinetics (Göpferich 1996). Polyesters exhibiting side chains tend to be more difficult to be assimilated than those without side chains (Tokiwa et al. 2009). The general degradability properties of common polyesters are listed in Table 8.1.

With respect to polyesters, aromatic polyesters such as PET are known for not being easily degraded, but they have good mechanical properties. However, many aliphatic polyesters are easily degraded, but have low mechanical properties. Thus, the degradability can be tuned in order to obtain satisfactory properties of the material. In this sense, it is possible to design aliphatic/aromatic co-polyesters and adjust the aliphatic/aromatic ratio to achieve the desired properties. Some examples in this field were listed by Muller et al. (2001). More recently, Hermanova et al. (2015) manufactured poly(ethylene terephthalate-*co*-lactate) copolymers and found that aliphatic units improved hydrolytic degradation and biodegradation.

Totaro et al. (2014) also found that stereochemistry and ionic chain terminals influence the degradability, while Zhou and Xanthos (2008) observed that PDLA was hydrolyzed faster than PLLA. This possibly because PDLA is more amorphous than PLLA. With respect to PHA, Boyandin et al. (2012) observed that PHBV copolymers are degraded more rapidly in the soil than PHB. Once again, the most amorphous polymer material (PHBV) was more rapidly degraded.

8.5.2 Formulation

8.5.2.1 Blends with Other Polyesters

Many attempts have been made to tune the biodegradability properties of polyesters using different blends.

Polyester Blends

Several studies about PLA/PHA blends have been published. Contradictory results show that the degradation is complex and depends on the experimental conditions (temperature, etc.), as well as the type of added polymer. For example, Arrieta et al. (2014b) found that the PHB in PLA acted as a nucleating agent which increased the crystallinity and slowed down the degradation rate of PLA under composting conditions. On the contrary, Zhang and Thomas (2011) conducted composting experiments on PLA/PHB blends, and observed that PHB, despite acting as a nucleating agent for PLA, induced a higher weight loss. Weng et al. (2013b) who studied P(3HB-*co*-4HB)/PLA blends, observed that the degradation rate in soil increased

Table 8.1 Polyesters commonly considered as biodegradable

Polymer	Conditions	Biodegradability	References
PLA	Mesophilic conditions: domestic compost, seawater, soil burial and anaerobic conditions.	Poor	Shogren et al. (2003) Yagi et al. (2009) Rudnik and Briassoulis (2011b) Greene (2012)
PLA	Thermophilic conditions: anaerobic conditions and industrial composting facilities.	Good	Ho et al. (1999) Kale et al. (2007) Yagi et al. (2009)
PBS	Aerobic mesophilic conditions: activated sludge, composting facility, soil burial and water environments.	Little/partial degradation.	Shin et al. (1997) Kasuya et al. (1998) Cho et al. (2011) Yang et al. (2004)
	Aerobic thermophilic conditions: abiotic water environments and industrial composting facility.	Partial degradation.	Yang et al. (2004) Kunioka et al. (2009) Dvorackova et al. (2015)
	Anaerobic mesophilic conditions: activated sludge.	Poor	Shin et al. (1997) Cho et al. (2011)
	Anaerobic thermophilic conditions: activated sludge.	Partial degradation.	Dvorackova et al. (2015)
PHAs	Aerobic mesophilic conditions: composting conditions and soil landfill.	Good/slow, depending on the type of PHA.	Mergaert et al. (1992) Rudnik and Briassoulis (2011a) Zhang et al. (2011) Boyandin et al. (2012)
	Thermophilic conditions: industrial composting facility.	Good	Weng et al. (2010, 2011)
	Anaerobic conditions: marine sediments and sludge.	Good	Shin et al. (1997) Abou-Zeid et al. (2001) Federle et al. (2002)
	Lake, marine environment and river water.	Partial-Good	Kasuya et al. (1998) Greene (2012) Deroiné et al. (2015)
	Sterilized water	Poor	Kasuya et al. (1998)

(continued)

Table 8.1 (continued)

Polymer	Conditions	Biodegradability	References
Poly(butylene adipate-*co*-terephthalate) (PBAT)	Thermophilic conditions: composting conditions.	Good	Kijchavengkul et al. (2008) Stloukal et al. (2012)
	Soil burial	Depends on environmental parameters	Rychter et al. (2010) Weng et al. (2013a) Wang et al. (2015)
	Anaerobic mesophilic conditions.	Slow	Abou-Zeid et al. (2004)
PCL	Aerobic thermophilic conditions: composting conditions.	Good	Yang et al. (2004) Hoshino et al. (2007)
	Anaerobic mesophilic conditions: digester sludge.	Poor/slow	Day et al. (1994) Gartiser et al. (1998) Abou-Zeid et al. (2001) Federle et al. (2002)
	Soil burial conditions	Slow	Solaro et al. (1998)

while raising the PHA content. As confirmed by Weng et al. (2013b) and Dharmalingam et al. (2015), PHA is preferentially degraded by microorganisms in PLA/P(3HB-*co*-4HB) blends, which leads to an erosion phenomenon, while the PLA hydrolysis is carried out in the bulk.

Starch Blends

Starch is a natural polysaccharide, which is hydrophilic and easily biodegradable (Gutiérrez et al. 2014; Suárez and Gutiérrez 2017), and is often blended with other polymers to increase the biodegradability of starch-containing blends (Gutiérrez and Alvarez 2017d).

The polyolefins have been blended with starch in order to accelerate their degradation. Since starch is easily deteriorated by microorganisms, after starch is decomposed, the remaining material exhibits a higher specific surface area, which is easier to degrade or fragment (Żuchowska et al. 1999). However, although fragmentation occurs, the remaining polyolefin phases could not be more decomposed (Goheen and Wool 1991).

Starch can also be blended with polyesters to improve their degradability properties and processability (Bastioli 1998). Petinakis et al. (2010) observed that the biodegradation rate (measured using respirometric devices) was higher for PLA/starch composites than for pure PLA under composting conditions. Ratto et al. (1999) studied PBSE/starch blends and observed higher biodegradation rates in soil as the starch content increased in the blend. Shogren et al. (2003) studied PLA/poly(hydroxyester-ether)/starch blends and found that the rate of weight loss in soil was the highest for PLA/PHEE/starch blend, and the lowest for pure PLA. However, the weight loss was only due to starch (Shogren et al. 2003). In summary, starch should only be blended with biodegradable and nontoxic polymers in order to obtain compostable composite blends.

8.5.2.2 Influence of Additives or Fillers

Compatibilizer

In the case of immiscible blends, the addition of a compatibilizing agent increases the mechanical properties by providing interfacial adhesion, but this affects the degradability of the material. With this in mind, Ohkita and Lee (2006) suggested that biodegradability can be tuned with the degree of interfacial adhesion given by a compatibilizer.

Singh et al. (2003) also studied PCL/starch blends and observed that degradation was improved as a result of lower interfacial tension. In addition, the degradability of PCL under composting conditions was dependent on the compatibilization efficiency, rather than starch concentration: a strong adhesion reduced the degradation rate (Singh et al. 2003). Ohkita and Lee (2006) studied PLA/starch blends compatibilized with lysine diisocyanate (burial tests) and observed that adding lysine diisocyanate reduced the degradability of the PLA matrix.

Plasticizer

A plasticizer is an aggregate added with the objective of reducing the T_g of a polymer material. For that reason, as seen above, the addition of a plasticizer can cause an increase in the degradability rate. Keeping this in view, Arrieta et al. (2014c) used limonene as a plasticizing agent for PLA/PHB blends and observed faster hydrolysis. Arrieta et al. (2014b) also studied PEG and acetyltributyl citrate (ATBC) as plasticizers in PLA/PHB blends and found that the added plasticizers migrated from the polymer blend during degradation under composting conditions, which increased the available surface for hydrolysis process, resulting in an improved rate of disintegration. However, Höglund et al. (2010) plasticized pure PLA with ATBC and observed a slower hydrolysis process. This was explained by the fact that ATBC is quite hydrophobic, and therefore, the increased hydrophobicity of the material led to difficult water absorption (Höglund et al. 2010).

Clays

Clays (nanoclays or microclays) are mineral fillers which are often added to polymers in order to increase their mechanical properties (higher Young's modulus) (Nieddu et al. 2009). They can also improve the thermomechanical stability during processing (Zhou and Xanthos 2008). It has been observed from the literature that adding clays into polymer materials can improve their degradability (Ray et al. 2002; Stloukal et al. 2012). In line with this, Nieddu et al. (2009) observed that fluorohectorite, montmorillonite (Mnt) and sepiolite improved the degradation of PLA. Zhou and Xanthos (2008) also observed that micro and nanoclays (Mnt) increased the rate of chemical hydrolysis of PLA.

Clays modify the degradability of polymer materials for different reasons:

- They modify hydrophobicity and water adsorption, due to their hydroxyl groups (Ray et al. 2002). Zhou and Xanthos (2008) observed that nanoclays and microclays improved water adsorption. Paul et al. (2005) studied the hydrolytic degradation of PLA and found that the more hydrophilic the filler is, the higher degradability the material exhibits.
- The structure of nanocomposites is also another factor (Paul et al. 2005). Nieddu et al. (2009) conducted *in vitro* biodegradation experiments on PLA/clays blends. These authors found that the degradation rate was dependent on the interactions between the filler and the matrix, and that the intercalated composites exhibited a higher degradation rate (Nieddu et al. 2009). Zhou and Xanthos (2008) studied the influence of nanoclays on the hydrolytic degradation of PLA and found that the degradation rate was higher for nanocomposites than for pure PLA, and slightly lower for microcomposites, although they exhibit a greater water adsorption.

Cellulose and Wood Derivates

Wood-based fillers are used as biobased reinforcements in polymers. For example, wood flour has been added into the PLA matrix and it was found that the biodegradation rate increases under composting conditions, by facilitating the water penetration into the polymer matrix, and therefore, bacterial growth (Mathew et al. 2005; Petinakis et al. 2010). Similar experiments were performed by Kim et al. (2006) with PBS and wood flour.

Cellulose nanocrystals (CNCs) have also been used as interesting fillers, as they can provide high stiffness to polymers. For example, Arrieta et al. (2014a) found that the thermal stability of the PLA decreased, while the disintegration rate increased under composting conditions. This was possibly due to the presence of hydroxyl groups that catalyze hydrolysis.

Grafting and Functionalization

Grafting has been investigated in order to tune the properties of polymers. For example, Wang et al. (2017) grafted PEG onto PLA in order to increase the hydrophilicity of PLA, which reduced its T_g and increased its hydrolysis rate. Yang et al. (2015) grafted degradation products of PHB onto PLA to increase ductility and toughness, which also increased the hydrolysis rate.

Many studies have focused on grafting acrylic acid (AA) and methacrylate derivatives onto polymers. In this context, Moreno-Chulim et al. (2003) evaluated the biodegradation of AA-grafted starch by fungus *Aspergillus niger*, and observed that AA grafting induced a modification of the shape of the starch particles and delayed the biodegradation. Wu (2005) also grafted AA in order to improve the compatibility of PLA/starch blends, and noted that grafting improves starch dispersion, processability, water resistance and reduced the degradation rate under soil burial conditions.

Grafting PHBV with 2-hydroxyethyl methacrylate (HEMA) leads to a decrease of the aerobic biodegradability by increasing the grafted content (Lao et al. 2009). With this in mind, Mitomo et al. (1995) grafted methyl methacrylate (MMA) and HEMA onto PHB and PHBV. These authors found that the MMA grafting decreased the enzymatic biodegradability, while grafting HEMA improved the enzymatic degradability by increasing the wettability.

On the other hand, the hydrophobicity of grafted polymers influences the biodegradability (Mitomo et al. 1995). Harish Prashanth et al. (2005) polymerized MMA onto Cs. These authors conducted tests of enzymatic and bacterial degradation, and observed preferential degradation of chitosan parts, but this did not imply that the PMMA parts were not degradable under other conditions (Harish Prashanth et al. 2005).

Stabilizers

Stabilizers are commonly used to avoid polymer degradation during processing. Stloukal et al. (2015) worked on an aromatic carbodiimide-based anti-hydrolysis agent in PLA, and observed that the addition of stabilizer decreased the biodegradation and hydrolysis rate of PLA. These authors used mineral fillers to counteract this effect (Stloukal et al. 2015).

Others

Lee et al. (2016) added lactic acid monomers into a PLA matrix, then conducted an anaerobic biodegradation experiment, and found that lactic acid monomers facilitate the attachment of microorganisms to the surface, leading to an improved biodegradability.

Luo et al. (2012) added titanium dioxide (TiO_2) nanoparticles into PLA and found that the hydrolysis rate was accelerated by the addition of TiO_2. Like clays, these nanofillers affect the water adsorption and hydrolysis takes place at the interface of the matrix and the fillers (Luo et al. 2012).

Ionic liquids can be used as additives to tune properties of polymers (Delamarche 2020). Park and Xanthos (2009) studied ionic liquids as plasticizers and lubricants for PLA, and found that some ionic liquids could improve the rate of hydrolysis of PLA.

8.6 Conclusion

Controlling end-of-life behavior of polymers is a complex task that requires multidisciplinary approaches, in order to give answers to the critical question: what material and life properties for which end-of-life scenario?

Of course, end-of-life must be anticipated when designing the material. Recycling must be preferred for the circular economy, as it is expected to generate less burdens than to produce a virgin material. Enzyme catalyzed hydrolysis offers the advantages of being selective under mild conditions, and to allow recovery of building blocks, that can be further reacted for the production of new materials.

Unfortunately, part of polymer-based products is disseminated on air, earth and water. It is thus necessary to design materials combining good performance with the ability to biodegrade in nature. Biobased materials formulations can offer a good compromise to achieve those two objectives. In order to tune both objectives, biobased polymers with adapted formulation composition are often good candidates. The prediction of the end of life in each environment can be evaluated by using standard biodegradation tests.

Acknowledgments The authors would like to thank the French Ministry of High Education and Research for PhD grant funding.

Conflicts of Interest The authors declare no conflict of interest.

References

Abbas, M., Adil, M., Ehtisham-ul-Haque, S., Munir, B., Yameen, M., Ghaffar, A., Shar, G. A., Asif Tahir, M., & Iqbal, M. (2018). Vibrio fischeri bioluminescence inhibition assay for ecotoxicity assessment: A review. *Science of the Total Environment, 626*, 1295–1309. https://doi.org/10.1016/j.scitotenv.2018.01.066.

Abeysinghe, H. P., Edwards, W., Pritchard, G., & Swampillai, G. J. (1982). Degradation of crosslinked resins in water and electrolyte solutions. *Polymer, 23*(12), 1785–1790. https://doi.org/10.1016/0032-3861(82)90123-9.

Abou-Zeid, D. M., Muller, R., & Deckwer, W. D. (2001). Degradation of natural and synthetic polyester under anaerobic conditions. *Journal of Biotechnology, 86*(2), 113–126. https://doi.org/10.1016/s0168-1656(00)00406-5.

Abou-Zeid, D. M., Müller, R. J., & Deckwer, W. D. (2004). Biodegradation of aliphatic homopolyesters and aliphatic-aromatic copolyesters by anaerobic microorganisms. *Biomacromolecules, 5*(5), 1687–1697. https://doi.org/10.1021/bm0499334.

Agarwal, M., Koelling, K. W., & Chalmers, J. J. (1998). Characterization of the degradation of polylactic acid polymer in a solid substrate environment. *Biotechnology Progress, 14*(3), 517–526. https://doi.org/10.1021/bp980015p.

Andrady, A. L. (2011). Microplastics in the marine environment. *Marine Pollution Bulletin, 62*(8), 1596–1605. https://doi.org/10.1016/j.marpolbul.2011.05.030.

Andrady, A. L., Pegram, J. E., & Song, Y. (1993). Studies on enhanced degradable plastics. II. Weathering of enhanced photodegradable polyethylenes under marine and freshwater floating exposure. *Journal of Environmental Polymer Degradation, 1*(2), 117–126. https://doi.org/10.1007/bf01418205.

Angelidaki, I., & Sanders, W. (2004). Assessment of the anaerobic biodegradability of macropollutants. *Reviews in Environmental Science and Biotechnology, 3*, 117–129. https://doi.org/10.1007/s11157-004-2502-3.

Arrieta, M. P., Fortunati, E., Dominici, F., Rayón, E., López, J., & Kenny, J. M. (2014a). PLA-PHB/cellulose based films: Mechanical, barrier and disintegration properties. *Polymer Degradation and Stability, 107*, 139–149. https://doi.org/10.1016/j.polymdegradstab.2014.05.010.

Arrieta, M. P., Lopez, J., Rayon, E., & Jiménez, A. (2014b). Disintegrability under composting conditions of plasticized PLA-PHB blends. *Polymer Degradation and Stability, 108*, 307–318. https://doi.org/10.1016/j.polymdegradstab.2014.01.034.

Arrieta, M. P., Lopez, J., Hernandez, A., & Rayon, E. (2014c). Ternary PLA-PHB-Limonene blends intended for biodegradable food packaging applications. *European Polymer Journal, 50*(1), 255–270. https://doi.org/10.1016/j.eurpolymj.2013.11.009.

Azevedo, H., & Reis, R. (2004). Understanding the enzymatic degradation of biodegradable polymers and strategies to control their degradation rate. In R. L. Reis & J. San Román (Eds.), *Biodegradable systems in tissue engineering and regenerative medicine* (pp. 177–202). Boca Raton: CRC Press. https://doi.org/10.1201/9780203491232.ch12.

Barrena, R., Font, X., Gabarrell, X., & Sánchez, A. (2014). Home composting versus industrial composting: Influence of composting system on compost quality with focus on compost stability. *Waste Management, 34*(7), 1109–1116. https://doi.org/10.1016/j.wasman.2014.02.008.

Bastioli, C. (1998). Properties and applications of Mater-Bi starch-based materials. *Polymer Degradation and Stability, 59*, 263–272. https://doi.org/10.1016/b978-0-444-81708-2.50049-x.

Bayard, R., & Gourdon, R. (2010). Traitement biologique des déchets. *Techniques de l'Ingénieur, 30*(1), 22. https://doi.org/10.1051/asees/2009005.

Begley, T. H., & Hollifield, H. C. (1995). Food packaging made from recycled polymers: Functional barrier considerations. In C. P. Rader, S. D. Baldwin, D. D. Cornell, G. D. Sadler, & R. F. Stockel (Eds.), *Plastics, rubber, and paper recycling: A pragmatic approach* (pp. 445–457). Washington: American Chemical Society. https://doi.org/10.1021/bk-1995-0609.ch036.

Bernhard, M., Eubeler, J. P., Zok, S., & Knepper, T. P. (2008). Aerobic biodegradation of polyethylene glycols of different molecular weights in wastewater and seawater. *Water Research, 42*(19), 4791–4801. https://doi.org/10.1016/j.watres.2008.08.028.

Beyler, C. L., & Hirschler, M. M. (2002). Thermal decomposition of polymers. *SFPE Handbook of Fire Protection Engineering, 2*, 111–131.

Bioplastics, E. (2015). *"Oxo-biodegradable" plastics and other plastics with additive for degradation*.

Boyandin, A. N., Prudnikova, S. V., Filipenko, M. L., Khrapov, E. A., Vasil'ev, A. D., & Volova, T. G. (2012). Biodegradation of polyhydroxyalkanoates by soil microbial communities of different structures and detection of PHA degrading microorganisms. *Applied Biochemistry and Microbiology, 48*(1), 28–36. https://doi.org/10.1134/S0003683812010024.

Castelan, G. (2010). Polymères biodégradables. *Techniques de l'Ingénieur, 33*.

Castilla-Cortázar, I., Más-Estellés, J., Meseguer-Dueñas, J. M., Escobar Ivirico, J. L., Marí, B., & Vidaurre, A. (2012). Hydrolytic and enzymatic degradation of a poly(ε-caprolactone) network. *Polymer Degradation and Stability, 97*(8), 1241–1248. https://doi.org/10.1016/j.polymdegradstab.2012.05.038.

Cho, K., Lee, J., & Kwon, K. (2001). Hydrolytic degradation behavior of poly(butylene succinate)s with different crystalline morphologies. *Journal of Applied Polymer Science, 79*(6), 1025–1033. https://doi.org/10.1002/1097-4628(20010207)79:6<1025::aid-app50>3.0.co;2-7.

Cho, H. S., Moon, H. S., Kim, M., Nam, K., & Kim, J. Y. (2011). Biodegradability and biodegradation rate of poly(caprolactone)-starch blend and poly(butylene succinate) biodegradable polymer under aerobic and anaerobic environment. *Waste Management, 31*(3), 475–480. https://doi.org/10.1016/j.wasman.2010.10.029.

Chu, C. C. (1981a). An *in-vitro* study of the effect of buffer on the degradation of poly(glycolic acid) sutures. *Journal of Biomedical Materials Research, 15*(1), 19–27. https://doi.org/10.1002/jbm.820150106.

Chu, C. C. (1981b). The *in-vitro* degradation of poly(glycolic acid) sutures — Effect of pH. *Journal of Biomedical Materials Research, 15*(6), 795–804. https://doi.org/10.1002/jbm.820150604.

Day, M., Shaw, K., & Cooney, D. (1994). Biodegradability: An assessment of commercial polymers according to the Canadian method for anaerobic conditions. *Journal of Environmental Polymer Degradation, 2*(2), 121–127. https://doi.org/10.1007/bf02074780.

Demirbas, A. (2007). Biodegradable plastics from renewable resources. *Energy Sources, Part A: Recovery, Utilization, and Environmental Effects, 29*(5), 419–424. https://doi.org/10.1080/009083190965820.

Delamarche E, Mattlet A, Livi S, Gérard J-F, Bayard R and Massardier V (2020) Tailoring Biodegradability of Poly(Butylene Succinate)/Poly(Lactic Acid) Blends With a Deep Eutectic Solvent. Front. Mater. 7:7. https://doi.org/10.3389/fmats.2020.00007.

Deroiné, M. (2014). *Étude du vieillissement de biopolymères en milieu marin*. Unpublished doctoral dissertation, Université de Bretagne Sud.

Deroiné, M., César, G., Le Duigou, A., Davies, P., & Bruzaud, S. (2015). Natural degradation and biodegradation of poly(3-hydroxybutyrate-co-3-hydroxyvalerate) in liquid and solid marine environments. *Journal of Polymers and the Environment, 23*(4), 493–505. https://doi.org/10.1007/s10924-015-0736-5.

Desrousseaux, M.-L., Texier, H., Duquesne, S., Marty, A., Aloui Dalibey, M., & Chateau, M. (2017). *Patent No. WO2017198786 (A1)*.

Dharmalingam, S., Hayes, D. G., Wadsworth, L. C., Dunlap, R. N., DeBruyn, J. M., Lee, J., & Wszelaki, A. L. (2015). Soil degradation of polylactic acid/polyhydroxyalkanoate-based nonwoven mulches. *Journal of Polymers and the Environment, 23*(3), 302–315. https://doi.org/10.1007/s10924-015-0716-9.

Díaz, A., Katsarava, R., & Puiggalí, J. (2014). Synthesis, properties and applications of biodegradable polymers derived from diols and dicarboxylic acids: From polyesters to poly(ester amide)s. *International Journal of Molecular Sciences, 15*(5), 7064–7123. https://doi.org/10.3390/ijms15057064.

Dvorackova, M., Svoboda, P., Kostka, L., & Pekarova, S. (2015). Influence of biodegradation in thermophilic anaerobic aqueous conditions on crystallization of poly(butylene succinate). *Polymer Testing, 47*, 59–70. https://doi.org/10.1016/j.polymertesting.2015.08.006.

Engineer, C., Parikh, J. K., & Raval, A. (2011). Review on hydrolytic degradation behavior of biodegradable polymers from controlled drug delivery system review on hydrolytic degradation behavior of biodegradable polymers from controlled drug delivery system. *Trends in Biomaterials and Artificial Organs, 25*(2), 79–85. Retrieved from http://medind.nic.in/taa/t11/i2/taat11i2p79.pdf.

Federle, T. W., Barlaz, M. A., Pettigrew, C. A., Kerr, K. M., Kemper, J. J., Nuck, B. A., & Schechtman, L. A. (2002). Anaerobic biodegradation of aliphatic polyesters: Poly(3-hydroxybutyrate-*co*-3-hydroxyoctanoate) and poly(ε-caprolactone). *Biomacromolecules, 3*(4), 813–822. https://doi.org/10.1021/bm025520w.

Feldman, D. (2002). Polymer weathering: photo-oxidation. *Journal of Polymers and the Environment, 10*(4), 163–173. https://doi.org/10.1023/A:1021148205366.

Forlin, F. J., & Faria, J. D. A. F. (2002). Considerações sobre a reciclagem de embalagens plásticas. *Polímeros, 12*(1), 1–10. https://doi.org/10.1590/s0104-14282002000100006.

Fox, T. G., & Flory, P. J. (1950). Second-order transition temperatures and related properties of polystyrene. I. Influence of molecular weight. *Journal of Applied Physics, 21*(6), 581–591. https://doi.org/10.1063/1.1699711.

Gamerith, C., Zartl, B., Pellis, A., Guillamot, F., Marty, A., Acero, E. H., & Guebitz, G. M. (2017). Enzymatic recovery of polyester building blocks from polymer blends. *Process Biochemistry, 59*(Part A), 58–64. https://doi.org/10.1016/j.procbio.2017.01.004.

Gartiser, S., Wallrabenstein, M., & Stiene, G. (1998). Assessment of several test methods for the determination of the anaerobic biodegradability of polymers. *Journal of Environmental Polymer Degradation, 6*(3), 159–173. https://doi.org/10.1023/a:1021869530253.

Goheen, S. M., & Wool, R. P. (1991). Degradation of polyethylene–starch blends in soil. *Journal of Applied Polymer Science, 42*(10), 2691–2701. https://doi.org/10.1002/app.1991.070421007.

Göpferich, A. (1996). Mechanisms of polymer degradation and erosion. *Biomaterials, 17*(2), 103–114. https://doi.org/10.1016/0142-9612(96)85755-3.

Greene, J. (2012). *PLA and PHA biodegradation in the marine environment*. Sacramento: Department of Resources Recycling and Recovery.

Grizzi, I., Garreau, H., Li, S., & Vert, M. (1995). Hydrolytic degradation of devices based on poly(dl-lactic acid) size-dependence. *Biomaterials, 16*(4), 305–311. https://doi.org/10.1016/0142-9612(95)93258-F.

Gross, R. A., & Kalra, B. (2002). Biodegradable polymers for the environment. *Green Chemistry, 297*(4), 803–807. https://doi.org/10.1126/science.297.5582.803.

Gu, J. D., Yang, S., Welton, R., Eberiel, D., McCarthy, S. P., & Gross, R. A. (1994). Effect of environmental parameters on the degradability of polymer films in laboratory-scale composting reactors. *Journal of Environmental Polymer Degradation, 2*(2), 129–135. https://doi.org/10.1007/bf02074781.

Gu, X., Raghavan, D., Nguyen, T., VanLandingham, M. R., & Yebassa, D. (2001). Characterization of polyester degradation using tapping mode atomic force microscopy: Exposure to alkaline solution at room temperature. *Polymer Degradation and Stability, 74*(1), 139–149. https://doi.org/10.1016/s0141-3910(01)00138-0.

Gutiérrez, T. J. (2018a). Chapter 9. Biodegradability and compostability of food nanopackaging materials. In G. Cirillo, M. A. Kozlowski, & U. G. Spizzirri (Eds.), *Composite materials for food packaging* (pp. 269–296). Hoboken: WILEY-Scrivener Publisher. https://doi.org/10.1002/9781119160243.ch9. ISBN: 978-1-119-16020-5.

Gutiérrez, T. J. (2018b). Are modified pumpkin flour/plum flour nanocomposite films biodegradable and compostable? *Food Hydrocolloids, 83*, 397–410. https://doi.org/10.1016/j.foodhyd.2018.05.035.

Gutiérrez, T. J. (2018c). Biological macromolecule composite films made from sagu starch and flour/poly(ε-caprolactone) blends processed by blending/thermo molding. *Journal Polymers and the Environment, 26*(9), 3902–3912. https://doi.org/10.1007/s10924-018-1268-6.

Gutiérrez, T. J., & Alvarez, V. A. (2017a). Eco-friendly films prepared from plantain flour/PCL blends under reactive extrusion conditions using zirconium octanoate as a catalyst. *Carbohydrate Polymers, 178*, 260–269. https://doi.org/10.1016/j.carbpol.2017.09.026.

Gutiérrez, T. J., & Alvarez, V. A. (2017b). Data on physicochemical properties of active films derived from plantain flour/PCL blends developed under reactive extrusion conditions. *Data in Brief, 15*, 445–448. https://doi.org/10.1016/j.dib.2017.09.071.

Gutiérrez, T. J., & Alvarez, V. A. (2017c). Films made by blending poly(ε-caprolactone) with starch and flour from sagu rhizome grown at the Venezuelan Amazons. *Journal Polymers and the Environment, 25*(3), 701–716. https://doi.org/10.1007/s10924-016-0861-9.

Gutiérrez, T. J., & Alvarez, V. A. (2017d). Properties of native and oxidized corn starch/polystyrene blends under conditions of reactive extrusion using zinc octanoate as a catalyst. *Reactive and Functional Polymers, 112*, 33–44. https://doi.org/10.1016/j.reactfunctpolym.2017.01.002.

Gutiérrez, T. J., & Alvarez, V. A. (2018). Bionanocomposite films developed from corn starch and natural and modified nano-clays with or without added blueberry extract. *Food Hydrocolloids, 77*, 407–420. https://doi.org/10.1016/j.foodhyd.2017.10.017.

Gutiérrez, T. J., Toro-Márquez, L. A., Merino, D., & Mendieta, J. R. (2019). Hydrogen-bonding interactions and compostability of bionanocomposite films prepared from corn starch and nano-fillers with and without added Jamaica flower extract. *Food Hydrocolloids, 89*, 283–293. https://doi.org/10.1016/j.foodhyd.2018.10.058.

Gutiérrez, T. J., Pérez, E., Guzmán, R., Tapia, M. S., & Famá, L. (2014). Physicochemical and functional properties of native and modified by crosslinking, dark-cush-cush yam (Dioscorea Trifida) and cassava (Manihot Esculenta) starch. *Journal of Polymer and Biopolymer Physics Chemistry, 2*(1), 1–5. https://doi.org/10.12691/jpbpc-2-1-1.

Gutiérrez, T. J., Mendieta, J. R., & Ortega-Toro, R. (2021). In-depth study from gluten/PCL-based food packaging films obtained under reactive extrusion conditions using chrome octanoate as a potential food grade catalyst. *Food Hydrocolloids, 11*, 106255. https://doi.org/10.1016/j.foodhyd.2020.106255.

Hablot, E., Dharmalingam, S., Hayes, D. G., Wadsworth, L. C., Blazy, C., & Narayan, R. (2014). Effect of simulated weathering on physicochemical properties and inherent biodegradation of PLA/PHA nonwoven mulches. *Journal of Polymers and the Environment, 22*(4), 417–429. https://doi.org/10.1007/s10924-014-0697-0.

Harish Prashanth, K. V., Lakshman, K., Shamala, T. R., & Tharanathan, R. N. (2005). Biodegradation of chitosan-graft-polymethylmethacrylate films. *International Biodeterioration and Biodegradation, 56*(2), 115–120. https://doi.org/10.1016/j.ibiod.2005.06.007.

Hawkins, W. L. (1984). Polymer degradation. In *Polymer degradation and stabilization. Polymers properties and applications* (Vol. 8, pp. 3–34). Berlin: Springer. https://doi.org/10.1007/978-3-642-69376-2_2.

Hermanova, S., Smejkalova, P., Merna, J., & Zarevucka, M. (2015). Biodegradation of waste PET based copolyesters in thermophilic anaerobic sludge. *Polymer Degradation and Stability, 111*, 176–184. https://doi.org/10.1016/j.polymdegradstab.2014.11.007.

Herniou-Julien, C., Mendieta, J. R., & Gutiérrez, T. J. (2019). Characterization of biodegradable/non-compostable films made from cellulose acetate/corn starch blends processed under reactive extrusion conditions. *Food Hydrocolloids, 89*, 67–79. https://doi.org/10.1016/j.foodhyd.2018.10.024.

Ho, K.-L. G., Pometto, A. L., Gadea-Rivas, A., Briceno, J. A., & Rojas, A. (1999). Degradation of polylactic acid (PLA) plastic in Costa Rican soil and Iowa State University compost rows. *Journal of Environmental Polymer Degradation, 7*(4), 173–177. https://doi.org/10.1023/a:1022874530586.

Höglund, A., Hakkarainen, M., & Albertsson, A. C. (2010). Migration and hydrolysis of hydrophobic polylactide plasticizer. *Biomacromolecules, 11*(1), 277–283. https://doi.org/10.1021/bm901157h.

Hoshino, A., Tsuji, M., Momochi, M., Mizutani, A., Sawada, H., Kohnami, S., Nakagomi, H., Ito, M., Saida, H., Ohnishi, M., Hirata, M., Kunioka, M., Funabash, M., & Uematsu, S. (2007). Study of the determination of the ultimate aerobic biodegradability of plastic materials under controlled composting conditions. *Journal of Polymers and the Environment, 15*(4), 275–280. https://doi.org/10.1007/s10924-007-0078-z.

Huber, M., & Franz, R. (1997). Studies on contamination of post consumer plastics from controlled resources for recycling into food packaging applications. *Deutsche Lebensmittel-Rundschau (Germany), 93*(10), 328.

Husarova, L., Pekarova, S., Stloukal, P., Kucharzcyk, P., Verney, V., Commereuc, S., Ramone, A., & Koutny, M. (2014). Identification of important abiotic and biotic factors in the biodegradation of poly(l-lactic acid). *International Journal of Biological Macromolecules, 71*, 155–162. https://doi.org/10.1016/j.ijbiomac.2014.04.050.

Imre, B., & Pukánszky, B. (2015). Compatibilization in bio-based and biodegradable polymer blends. *European Polymer Journal, 49*(6), 1215–1233. https://doi.org/10.1016/j.eurpolymj.2013.01.019.

ISO/FDIS 16929:2013. (2013). *Plastics — Determination of the degree of disintegration of plastic materials under defined composting conditions in a pilot-scale test*. Retrieved from https://www.iso.org/standard/62948.html.

Itävaara, M., Karjomaa, S., & Selin, J. F. (2002). Biodegradation of polylactide in aerobic and anaerobic thermophilic conditions. *Chemosphere, 46*(6), 879–885. https://doi.org/10.1016/s0045-6535(01)00163-1.

Jayasekara, R., Sheridan, S., Lourbakos, E., Beh, H., Christie, G. B. Y., Jenkins, M., Halley, P. B., McGlashan, S., & Lonergan, G. T. (2003). Biodegradation and ecotoxicity evaluation of a bionolle and starch blend and its degradation products in compost. *International Biodeterioration and Biodegradation, 51*(1), 77–81. https://doi.org/10.1016/s0964-8305(02)00090-2.

Ju, D., Han, L., Bian, J., Guo, Z., Li, F., Chen, S., & Dong, L. (2015). Enzymatic degradation and porous morphology of poly(l-lactide) and poly(3-hydroxybutyrate-*co*-4-hydroxybutyrate) blends. *RSC Advances, 5*(7), 5474–5483. https://doi.org/10.1039/c4ra12313a.

Kale, G., Auras, R., Singh, S. P., & Narayan, R. (2007). Biodegradability of polylactide bottles in real and simulated composting conditions. *Polymer Testing, 26*(8), 1049–1061. https://doi.org/10.1016/j.polymertesting.2007.07.006.

Karamanlioglu, M., & Robson, G. D. (2013). The influence of biotic and abiotic factors on the rate of degradation of poly(lactic) acid (PLA) coupons buried in compost and soil. *Polymer Degradation and Stability, 98*(10), 2063–2071. https://doi.org/10.1016/j.polymdegradstab.2013.07.004.

Kasuya, K., Takagi, K., Ishiwatari, S., Yoshidab, Y., & Doi, Y. (1998). Biodegradabilities of various aliphatic polyesters in natural waters. *Polymer Degradation and Stability, 59*(1-3), 327–332. https://doi.org/10.1016/s0141-3910(97)00155-9.

Kijchavengkul, T., Auras, R., Rubino, M., Ngouajio, M., & Fernandez, R. T. (2008). Assessment of aliphatic-aromatic copolyester biodegradable mulch films. Part I: Field study. *Chemosphere, 71*(9), 1607–1616. https://doi.org/10.1016/j.chemosphere.2008.01.037.

Kim, H. S., Kim, H. J., Lee, J. W., & Choi, I. G. (2006). Biodegradability of bio-flour filled biodegradable poly(butylene succinate) bio-composites in natural and compost soil. *Polymer Degradation and Stability, 91*(5), 1117–1127. https://doi.org/10.1016/j.polymdegradstab.2005.07.002.

Koutny, M., Lemaire, J., & Delort, A. M. (2006). Biodegradation of polyethylene films with prooxidant additives. *Chemosphere, 64*(8), 1243–1252. https://doi.org/10.1016/j.chemosphere.2005.12.060.

Kunioka, M., Ninomiya, F., & Funabashi, M. (2009). Biodegradation of poly(butylene succinate) powder in a controlled compost at 58 °C evaluated by naturally-occurring carbon 14 amounts in evolved CO_2 based on the ISO 14855-2 method. *International Journal of Molecular Sciences, 10*(10), 4267–4283. https://doi.org/10.3390/ijms10104267.

Lacoste, J. F., Bounor-legaré, V., Llauro, M. F., Monnet, C., Cassagnau, P., & Michel, A. (2005). Functionalization of poly(ethylene terephthalate) in the melt state: Chemical and rheological aspects. *Journal of Polymer Science, Part A: Polymer Chemistry, 43*(11), 2207–2223. https://doi.org/10.1002/pola.20696.

Lao, H.-K., Renard, E., Langlois, V., Vallée-Rehel, K., & Linossier, I. (2009). Surface functionalization of PHBV by HEMA grafting via UV treatment: Comparison with thermal free radical polymerization. *Journal of Applied Polymer, 116*(1), 288–297. https://doi.org/10.1002/app.31507.

Le Digabel, F., & Avérous, L. (2006). Effects of lignin content on the properties of lignocellulose-based biocomposites. *Carbohydrate Polymers, 66*(4), 537–545. https://doi.org/10.1016/j.carbpol.2006.04.023.

Lee, J. C., Moon, J. H., Jeong, J. H., Kim, M. Y., Kim, B. M., Choi, M. C., & Kim, J. R. (2016). Biodegradability of poly(lactic acid) (PLA)/lactic acid (LA) blends using anaerobic digester sludge. *Macromolecular Research, 24*(8), 741–747. https://doi.org/10.1007/s13233-016-4100-y.

Leja, K., & Lewandowicz, G. (2010). Polymer biodegradation and biodegradable polymers – A review. *Polish Journal of Environment Study, 19*(2), 255–266. Retrieved from http://yunus.hacettepe.edu.tr/~damlacetin/kmu407/index_dosyalar/2.%20makale.pdf.

Lenz, R. W. (1993). Biodegradable polymers. In R. S. Langer & N. A. Peppas (Eds.), *Biopolymers I. Advances in polymer science* (Vol. 107). Berlin: Springer. https://doi.org/10.1007/bfb0027550.

Li, S. (1998). Hydrolytic degradation characteristics of aliphatic polyesters derived from lactic and glycolic acids. *Journal of Biomedical Materials Research, 48*(3), 342–353. https://doi.org/10.1002/(sici)1097-4636(1999)48:3<342::aid-jbm20>3.0.co;2-7.

Li, J., Liu, H., & Paul Chen, J. (2018). Microplastics in freshwater systems: A review on occurrence, environmental effects, and methods for microplastics detection. *Water Research, 137*, 362–374. https://doi.org/10.1016/j.watres.2017.12.056.

Lucas, N., Bienaime, C., Belloy, C., Queneudec, M., Silvestre, F., & Nava-Saucedo, J. E. (2008). Polymer biodegradation: Mechanisms and estimation techniques - A review. *Chemosphere, 73*(4), 429–442. https://doi.org/10.1016/j.chemosphere.2008.06.064.

Luo, Y. B., Wang, X. L., & Wang, Y. Z. (2012). Effect of TiO_2 nanoparticles on the long-term hydrolytic degradation behavior of PLA. *Polymer Degradation and Stability, 97*(5), 721–728. https://doi.org/10.1016/j.polymdegradstab.2012.02.011.

Lyu, S., & Untereker, D. (2009). Degradability of polymers for implantable biomedical devices. *International Journal of Molecular Sciences, 10*(9), 4033–4065. https://doi.org/10.3390/ijms10094033.

Magnin, A., Pollet, E., Perrin, R., Ullmann, C., Persillon, C., Phalip, V., & Avérous, L. (2019). Enzymatic recycling of thermoplastic polyurethanes: Synergistic effect of an esterase and an amidase and recovery of building blocks. *Waste Management, 85*, 141–150. https://doi.org/10.1016/j.wasman.2018.12.024.

Makino, K., Ohshima, H., & Kondo, T. (1986). Mechanism of hydrolytic degradation of poly(l-lactide) microcapsules: Effects of ph, ionic strength and buffer concentration. *Journal of Microencapsulation, 3*(3), 203–212. https://doi.org/10.3109/02652048609031574.

Mathew, A. P., Oksman, K., & Sain, M. (2005). Mechanical properties of biodegradable composites from poly lactic acid (PLA) and microcrystalline cellulose (MCC). *Journal of Applied Polymer Science, 97*(5), 2014–2025. https://doi.org/10.1002/app.21779.

Matsumura, S., Ebata, H., & Toshima, K. (2002). A new strategy for sustainable polymer recycling using an enzyme: Poly(ε-caprolactone). *Macromolecular Rapid Communications, 21*(12), 860–863. https://doi.org/10.1002/1521-3927(20000801)21:12<860::aid-marc860>3.3.co;2-l.

Matta, A. K., Umamaheswara Rao, R., Suman, K. N. S., & Rambabu, V. (2014). Preparation and characterization of biodegradable PLA/PCL polymeric blends. *Procedia Materials Science, 6*, 1266–1270. https://doi.org/10.1016/j.mspro.2014.07.201.

Mergaert, J., Anderson, C., Wouters, A., Swings, J., & Kersters, K. (1992). Biodegradation of polyhydroxyalkanoates. *FEMS Microbiology Letters, 103*(2–4), 317–321. https://doi.org/10.1016/0378-1097(92)90325-I.

Merino, D., Gutiérrez, T. J., & Alvarez, V. A. (2019a). Structural and thermal properties of agricultural mulch films based on native and oxidized corn starch nanocomposites. *Starch-Stärke, 71*(7–8), 1800341. https://doi.org/10.1002/star.201800341.

Merino, D., Gutiérrez, T. J., & Alvarez, V. A. (2019b). Potential agricultural mulch films based on native and phosphorylated corn starch with and without surface functionalization with chitosan. *Journal Polymers and the Environment, 27*(1), 97–105. https://doi.org/10.1007/s10924-018-1325-1.

Merino, D., Mansilla, A. Y., Gutiérrez, T. J., Casalongué, C. A., & Alvarez, V. A. (2018a). Chitosan coated-phosphorylated starch films: Water interaction, transparency and antibacterial properties. *Reactive and Functional Polymers, 131*, 445–453. https://doi.org/10.1016/j.reactfunctpolym.2018.08.012.

Merino, D., Gutiérrez, T. J., Mansilla, A. Y., Casalongué, C. A., & Alvarez, V. A. (2018b). Critical evaluation of starch-based antibacterial nanocomposites as agricultural mulch films: Study on their interactions with water and light. *ACS Sustainable Chemistry & Engineering, 6*(11), 15662–15672. https://doi.org/10.1021/acssuschemeng.8b04162.

Mierzwa-Hersztek, M., Gondek, K., & Kopeć, M. (2019). Degradation of polyethylene and biocomponent-derived polymer materials: An overview. *Journal of Polymers and the Environment, 27*(3), 600–611. https://doi.org/10.1007/s10924-019-01368-4.

Mitomo, H., Enjoji, T., Watanabe, Y., Yoshii, F., Makuuchi, K., & Saito, T. (1995). Radiation-induced graft polymerization of poly(3-hydroxybutyrate) and its copolymer. *Journal of Macromolecular Science, Part A, 32*(3), 429–442. https://doi.org/10.1080/10601329808001959.

Mochizuki, M., & Hirami, M. (1996). Structural effects on biodegradation of aliphatic polyesters. *Polymers for Advanced Technologies, 8*, 203–209. https://doi.org/10.2115/fiber.52.5_p200.

Moreno-Chulim, M. V., Barahona-Perez, F., & Canche-Escamilla, G. (2003). Biodegradation of starch and acrylic-grafted starch by Aspergillus niger. *Journal of Applied Polymer Science, 89*(10), 2764–2770. https://doi.org/10.1002/app.12427.

Muller, R. J., Kleeberg, I., & Deckwer, W. D. (2001). Biodegradation of polyesters containing aromatic constituents. *Journal of Biotechnology, 86*(2), 87–95. https://doi.org/10.1016/s0168-1656(00)00407-7.

Nieddu, E., Mazzucco, L., Gentile, P., Benko, T., Balbo, V., Mandrile, R., & Ciardelli, G. (2009). Preparation and biodegradation of clay composites of PLA. *Reactive and Functional Polymers, 69*(6), 371–379. https://doi.org/10.1016/j.reactfunctpolym.2009.03.002.

Nunes, R. W., Martin, J. R., & Johnson, J. F. (1982). Influence of molecular weight and molecular weight distribution on mechanical properties of polymers. *Polymer Engineering & Science, 22*(4), 205–228. https://doi.org/10.1002/pen.760220402.

Ohkita, T., & Lee, S. (2006). Thermal degradation and biodegradability of poly(lactic acid)/corn starch biocomposites. *Journal of Applied Polymer Science, 100*(4), 3009–3017. https://doi.org/10.1002/app.23425.

Ojumu, T. V., Yu, J., & Solomo, B. O. (2004). Production of polyhydroxyalkanoates, a bacterial biodegradable polymer. *African Journal of Biotechnology, 3*(1), 18–24. https://doi.org/10.5897/ajb2004.000-2004.

Pantani, R., & Sorrentino, A. (2013). Influence of crystallinity on the biodegradation rate of injection-moulded poly(lactic acid) samples in controlled composting conditions. *Polymer Degradation and Stability, 98*(5), 1089–1096. https://doi.org/10.1016/j.polymdegradstab.2013.01.005.

Park, T. G. (1994). Degradation of poly(D,L-lactic acid) microspheres: Effect of molecular weight. *Journal of Controlled Release, 30*(2), 161–173. https://doi.org/10.1016/0168-3659(94)90263-1.

Park, K. I., & Xanthos, M. (2009). A study on the degradation of polylactic acid in the presence of phosphonium ionic liquids. *Polymer Degradation and Stability, 94*(5), 834–844. https://doi.org/10.1016/j.polymdegradstab.2009.01.030.

Paul, M. A., Delcourt, C., Alexandre, M., Degée, P., Monteverde, F., & Dubois, P. (2005). Polylactide/montmorillonite nanocomposites: Study of the hydrolytic degradation. *Polymer Degradation and Stability, 87*(3), 535–542. https://doi.org/10.1016/j.polymdegradstab.2004.10.011.

Pellis, A., Haernvall, K., Pichler, C. M., Ghazaryan, G., Breinbauer, R., & Guebitz, G. M. (2016). Enzymatic hydrolysis of poly(ethylene furanoate). *Journal of Biotechnology, 235*, 47–53. https://doi.org/10.1016/j.jbiotec.2016.02.006.

Petinakis, E., Liu, X., Yu, L., Way, C., Sangwan, P., Dean, K., Bateman, S., & Edward, G. (2010). Biodegradation and thermal decomposition of poly(lactic acid)-based materials reinforced by hydrophilic fillers. *Polymer Degradation and Stability, 95*(9), 1704–1707. https://doi.org/10.1016/j.polymdegradstab.2010.05.027.

Plastiques: Derrière les déchets, un gisement d'industries. (2018). Retrieved from https://www.ccimp.com/actualite/industrie-innovation/34155-plastiques-derriere-dechets-un-gisement-dindustries

Rahmouni, M., Chouinard, F., Nekka, F., Lenaerts, V., & Leroux, J. C. (2001). Enzymatic degradation of cross-linked high amylose starch tablets and its effect on in vitro release of sodium diclofenac. *European Journal of Pharmaceutics and Biopharmaceutics, 51*(3), 191–198. https://doi.org/10.1016/s0939-6411(01)00127-8.

Ratto, J. A., Stenhouse, P. J., Auerbach, M., Mitchell, J., & Farrell, R. (1999). Processing, performance and biodegradability of a thermoplastic aliphatic polyester/starch system. *Polymer, 40*(24), 6777–6788. https://doi.org/10.1016/s0032-3861(99)00014-2.

Ray, S. S., Yamada, K., Okamoto, M., & Ueda, K. (2002). New polylactide-layered silicate nanocomposites. 2. Concurrent improvements of material properties, biodegradability and melt rheology. *Polymer, 44*(3), 857–866. https://doi.org/10.1016/s0032-3861(02)00818-2.

Rudnik, E., & Briassoulis, D. (2011a). Comparative biodegradation in soil behaviour of two biodegradable polymers based on renewable resources. *Journal of Polymers and the Environment, 19*(1), 18–39. https://doi.org/10.1007/s10924-010-0243-7.

Rudnik, E., & Briassoulis, D. (2011b). Degradation behaviour of poly(lactic acid) films and fibres in soil under Mediterranean field conditions and laboratory simulations testing. *Industrial Crops and Products, 33*(3), 648–658. https://doi.org/10.1016/j.indcrop.2010.12.031.

Rychter, P., Kawalec, M., Sobota, M., Kurcok, P., & Kowalczuk, M. (2010). Study of aliphatic-aromatic copolyester degradation in sandy soil and its ecotoxicological impact. *Biomacromolecules, 11*(4), 839–847. https://doi.org/10.1021/bm901331t.

Schliecker, G., Schmidt, C., Fuchs, S., & Kissel, T. (2003). Characterization of a homologous series of D,L-lactic acid oligomers; a mechanistic study on the degradation kinetics in vitro. *Biomaterials, 24*(21), 3835–3844. https://doi.org/10.1016/s0142-9612(03)00243-6.

Selke, S., Auras, R., Nguyen, T. A., Castro Aguirre, E., Cheruvathur, R., & Liu, Y. (2015). Evaluation of biodegradation-promoting additives for plastics. *Environmental Science and Technology, 49*(6), 3769–3777. https://doi.org/10.1021/es504258u.

Shen, L., Worrell, E., & Patel, M. K. (2010). Open-loop recycling: A LCA case study of PET bottle-to-fibre recycling. *Resources, Conservation and Recycling, 55*(1), 34–52. https://doi.org/10.1016/j.resconrec.2010.06.014.

Shin, P., Kim, M., & Kim, J. (1997). Biodegradability of degradable plastics exposed to anaerobic digested sludge and simulated landfill conditions. *Journal of Polymers and the Environment, 5*(1), 33–39. https://doi.org/10.1007/bf02763566.

Shogren, R. L., Doane, W. M., Garlotta, D., Lawton, J. W., & Willett, J. L. (2003). Biodegradation of starch/polylactic acid/poly(hydroxyester-ether) composite bars in soil. *Polymer Degradation and Stability, 79*(3), 405–411. https://doi.org/10.1016/s0141-3910(02)00356-7.

Singh, R. P., Pandey, J. K., Rutot, D., Degée, P., & Dubois, P. (2003). Biodegradation of poly(ε-caprolactone)/starch blends and composites in composting and culture environments: The effect of compatibilization on the inherent biodegradability of the host polymer. *Carbohydrate Research, 338*(17), 1759–1769. https://doi.org/10.1016/S0008-6215(03)00236-2.

Siparsky, G. L., Voorhees, K. J., Dorgan, J. R., & Schilling, K. (1997). Water transport in polylactic acid (PLA), PLA/polycaprolactone copolymers, and PLA/polyethylene glycol blends. *Journal of Environmental Polymer Degradation, 5*(3), 125–136. https://doi.org/10.1007/bf02763656.

Solaro, R., Corti, A., & Chiellini, E. (1998). A new respirometric test simulating soil burial conditions for the evaluation of polymer biodegradation. *Journal of Environmental Polymer Degradation, 6*(4), 203–208. https://doi.org/10.1023/a:1021877732070.

Sombrio, B. R., Lima, A., Paula, A., Pezzin, T., & Apati, G. (2017). Produção de poli(3-hidroxibutirato) por Cupriavidus necator em batelada alimentada usando glicerol. *Polimeros, 27*, 110–115. https://doi.org/10.1590/0104-1428.2237.

Stloukal, P., Verney, V., Commereuc, S., Rychly, J., Matisova-Rychlá, L., Pis, V., & Koutny, M. (2012). Assessment of the interrelation between photooxidation and biodegradation of selected polyesters after artificial weathering. *Chemosphere, 88*(10), 1214–1219. https://doi.org/10.1016/j.chemosphere.2012.03.072.

Stloukal, P., Kalendova, A., Mattausch, H., Laske, S., Holzer, C., & Koutny, M. (2015). The influence of a hydrolysis-inhibiting additive on the degradation and biodegradation of PLA and its nanocomposites. *Polymer Testing, 41*, 124–132. https://doi.org/10.1016/j.polymertesting.2014.10.015.

Suárez, G., & Gutiérrez, T. J. (2017). Chapter 15. Recent advances in the development of biodegadable films and foams from cassava starch. In: Klein, C. (Ed)., *Handbook on cassava: Production, potential uses and recent advances*. Editorial Nova Science Publishers, Inc. New York. EE.UU. ISBN: 978-1-53610-307-6. pp. 297–312.

Sudesh, K., & Iwata, T. (2008). Sustainability of biobased and biodegradable plastics. *CLEAN - Soil, Air, Water, 36*(5–6), 433–442. https://doi.org/10.1002/clen.200700183.

Taniguchi, I., Nakano, S., Nakamura, T., El-salmawy, A., Miyamoto, M., & Kimura, Y. (2002). Mechanism of enzymatic hydrolysis of poly(butylene succinate) and poly(butylene succinate-*co*-L-lactate) with a Lipase from Pseudomonas cepacia. *Macromolecular Bioscience, 2*(9), 447–455. https://doi.org/10.1002/mabi.200290002.

Tengborg, C., Galbe, M., & Zacchi, G. (2001). Influence of enzyme loading and physical parameters on the enzymatic hydrolysis of steam-pretreated softwood. *Biotechnology Progress, 17*(1), 110–117. https://doi.org/10.1021/bp000145+.

Thirunavukarasu, K., Purushothaman, S., Sridevi, J., Aarthy, M., Gowthaman, M. K., Nakajima-kambe, T., & Ramudu, N. (2016). International Biodeterioration & Biodegradation Degradation of poly(butylene succinate) and poly(butylene succinate-co-butylene adipate) by a lipase from yeast Cryptococcus sp. grown on agro-industrial residues. *International Biodeterioration & Biodegradation, 110*, 99–107. https://doi.org/10.1016/j.ibiod.2016.03.005.

Tokiwa, Y., Calabia, B. P., Ugwu, C. U., & Aiba, S. (2009). Biodegradability of plastics. *International Journal of Molecular Sciences, 10*(9), 3722–3742. https://doi.org/10.3390/ijms10093722.

Totaro, G., Marchese, P., Banella, M. B., Sisti, L., Celli, A., Verney, V., & Commereuc, S. (2014). Ageing of PCCD aliphatic polyesters: Effect of stereochemistry and ionic chain terminals. *Journal of Photochemistry and Photobiology A: Chemistry, 292*, 42–48. https://doi.org/10.1016/j.jphotochem.2014.06.019.

Tserki, V., Matzinos, P., Pavlidou, E., Vachliotis, D., & Panayiotou, C. (2006). Biodegradable aliphatic polyesters. Part I. Properties and biodegradation of poly(butylene succinate-co-butylene adipate). *Polymer Degradation and Stability, 91*(2), 367–376. https://doi.org/10.1016/j.polymdegradstab.2005.04.035.

Tuominen, J., Kylma, J., Kapanen, A., Venelampi, O., Itävaara, M., & Seppälä, J. (2002). Biodegradation of lactic acid based polymers under controlled composting conditions and evaluation of the ecotoxicological impact. *Biomacromolecules, 3*(3), 445–455. https://doi.org/10.1021/bm0101522.

Vieira, A. C., Guedes, R. M., & Tita, V. (2013). Considerations for the design of polymeric biodegradable products. *Journal of Polymer Engineering, 33*(4), 293–302. https://doi.org/10.1515/polyeng-2012-0150.

Volova, T. G., Boyandin, A. N., Vasiliev, A. D., Karpov, V. A., Prudnikova, S. V., Mishukova, O. V., Boyarskikh, U. A., Filipenko, M. L., Rudnev, V. P., Bá Xuân, B., Việt Dũng, V., & Gitelson, I. I. (2010). Biodegradation of polyhydroxyalkanoates (PHAs) in tropical coastal waters and identification of PHA-degrading bacteria. *Polymer Degradation and Stability, 95*(12), 2350–2359. https://doi.org/10.1016/j.polymdegradstab.2010.08.023.

Walter, T., Augusta, J., Müller, R. J., Widdecke, H., & Klein, J. (1995). Enzymatic degradation of a model polyester by lipase from *Rhizopus delemar*. *Enzyme and Microbial Technology, 17*(3), 218–224. https://doi.org/10.1016/0141-0229(94)00007-e.

Wang, H., Wei, D., Zheng, A., & Xiao, H. (2015). Soil burial biodegradation of antimicrobial biodegradable PBAT films. *Polymer Degradation and Stability, 116*, 14–22. https://doi.org/10.1016/j.polymdegradstab.2015.03.007.

Wang, Y. p., Wei, X., Duan, J., Yang, J. h., Zhang, N., Huang, T., & Wang, Y. (2017). Greatly enhanced hydrolytic degradation ability of poly(L-lactide) achieved by adding poly(ethylene glycol). *Chinese Journal of Polymer Science, 35*(3), 386–399. https://doi.org/10.1007/s10118-017-1904-y.

Weiland, M., Daro, A., & David, C. (1995). Biodegradation of thermally oxidized polyethylene. *Polymer Degradation and Stability, 48*(2), 275–289. https://doi.org/10.1016/0141-3910(95)00040-s.

Weinberger, S., Canadell, J., Quartinello, F., Yeniad, B., Arias, A., Pellis, A., & Guebitz, G. (2017). Enzymatic degradation of poly(ethylene 2,5-furanoate) powders and amorphous films. *Catalysts, 7*(11), 318. https://doi.org/10.3390/catal7110318.

Weng, Y. X., Wang, Y., Wang, X. L., & Wang, Y. Z. (2010). Biodegradation behavior of PHBV films in a pilot-scale composting condition. *Polymer Testing, 29*(5), 579–587. https://doi.org/10.1016/j.polymertesting.2010.04.002.

Weng, Y. X., Wang, X. L., & Wang, Y. Z. (2011). Biodegradation behavior of PHAs with different chemical structures under controlled composting conditions. *Polymer Testing, 30*(4), 372–380. https://doi.org/10.1016/j.polymertesting.2011.02.001.

Weng, Y. X., Jin, Y. J., Meng, Q. Y., Wang, L., Zhang, M., & Wang, Y. Z. (2013a). Biodegradation behavior of poly(butylene adipate-co-terephthalate) (PBAT), poly(lactic acid) (PLA), and their blend under soil conditions. *Polymer Testing, 32*(5), 918–926. https://doi.org/10.1016/j.polymertesting.2013.05.001.

Weng, Y. X., Wang, L., Zhang, M., Wang, X. L., & Wang, Y. Z. (2013b). Biodegradation behavior of P(3HB,4HB)/PLA blends in real soil environments. *Polymer Testing, 32*(1), 60–70. https://doi.org/10.1016/j.polymertesting.2012.09.014.

Witt, U., Müller, R.-J., & Deckwer, W.-D. (1996). Evaluation of the biodegradability of copolyesters containing aromatic compounds by investigations of model oligomers. *Journal of Environmental Polymer Degradation, 4*(1), 9–20. https://doi.org/10.1007/bf02083878.

Witt, U., Einig, T., Yamamoto, M., Kleeberg, I., Deckwer, W. D., & Müller, R. J. (2001). Biodegradation of aliphatic-aromatic copolyesters: Evaluation of the final biodegradability and ecotoxicological impact of degradation intermediates. *Chemosphere, 44*(2), 289–299. https://doi.org/10.1016/s0045-6535(00)00162-4.

Wu, C. S. (2005). Improving polylactide/starch biocomposites by grafting polylactide with acrylic acid - Characterization and biodegradability assessment. *Macromolecular Bioscience, 5*(4), 352–361. https://doi.org/10.1002/mabi.200400159.

Xu, J., & Guo, B.-H. (2010). Microbial succinic acid, its polymer poly(butylene succinate), and applications. In *Plastics from bacteria: Natural functions and applications* (Vol. 14, pp. 85–119). New York: Springer. https://doi.org/10.1007/978-3-642-03287.

Xu, Y., Xu, J., Liu, D., Guo, B., & Xie, X. (2008). Synthesis and characterization of biodegradable poly(butylene succinate-*co*-propylene succinate)s. *Journal of Applied Polymer Science, 109*(3), 1881–1889. https://doi.org/10.1002/app.24544.

Yagi, H., Ninomiya, F., Funabashi, M., & Kunioka, M. (2009). Anaerobic biodegradation tests of poly(lactic acid) under mesophilic and thermophilic conditions using a new evaluation system for methane fermentation in anaerobic sludge. *International Journal of Molecular Sciences, 10*(9), 3824–3835. https://doi.org/10.3390/ijms10093824.

Yang, Q., & Pan, X. (2015). Correlation between lignin physicochemical properties and inhibition to enzymatic hydrolysis of cellulose. *Biotechnology and Bioengineering, 113*(6), 1213–1224. https://doi.org/10.1002/bit.25903.

Yang, H. S., Yoon, J. S., & Kim, M. N. (2004). Effects of storage of a mature compost on its potential for biodegradation of plastics. *Polymer Degradation and Stability, 84*(3), 411–417. https://doi.org/10.1016/j.polymdegradstab.2004.01.014.

Yang, X., Clénet, J., Xu, H., Odelius, K., & Hakkarainen, M. (2015). Two step extrusion process: From thermal recycling of PHB to plasticized PLA by reactive extrusion grafting of PHB degradation products onto PLA chains. *Macromolecules, 48*(8), 2509–2518. https://doi.org/10.1021/acs.macromol.5b00235.

Zellner, G., Neudörfer, F., & Diekmann, H. (1994). Degradation of lactate by an anaerobic mixed culture in a fluidized-bed reactor. *Water Research, 28*(6), 1337–1340. https://doi.org/10.1016/0043-1354(94)90299-2.

Zeng, R. T., Hu, W., Wang, M., Zhang, S. D., & Zeng, J. B. (2016). Morphology, rheological and crystallization behavior in non-covalently functionalized carbon nanotube reinforced poly(butylene succinate) nanocomposites with low percolation threshold. *Polymer Testing, 50*, 182–190. https://doi.org/10.1016/j.polymertesting.2016.01.003.

Żenkiewicz, M., Richert, A., Malinowski, R., & Moraczewski, K. (2013). A comparative analysis of mass losses of some aliphatic polyesters upon enzymatic degradation. *Polymer Testing, 32*(2), 209–214. https://doi.org/10.1016/j.polymertesting.2012.10.011.

Zhang, M., & Thomas, N. L. (2011). Blending polylactic acid with polyhydroxybutyrate: The effect on thermal, mechanical, and biodegradation properties. *Advances in Polymer Technology, 30*(2), 67–79. https://doi.org/10.1002/adv.20235.

Zhang, J., Lu, X. P., & Chu, T. L. (2011). Properties analysis of biodegradable material P(3HB-co-4HB). *Advanced Materials Research, 380*, 168–172. https://doi.org/10.4028/www.scientific.net/amr.380.168.

Zhou, Q., & Xanthos, M. (2008). Nanoclay and crystallinity effects on the hydrolytic degradation of polylactides. *Polymer Degradation and Stability, 93*(8), 1450–1459. https://doi.org/10.1016/j.polymdegradstab.2008.05.014.

Zhu, Y., Romain, C., & Williams, C. K. (2016). Sustainable polymers from renewable resources. *Nature, 540*(7633), 354–362. https://doi.org/10.1038/nature21001.

Żuchowska, D., Hlavatá, D., Steller, R., Adamiak, W., & Meissner, W. (1999). Physical structure of polyolefin-starch blends after ageing. *Polymer Degradation and Stability, 64*(2), 339–346. https://doi.org/10.1016/s0141-3910(98)00212-2.

Correction to: Surface Functionalization of Polymers

Deval Prasad Bhattarai, Pashupati Pokharel, and Dequan Xiao

Correction to:
Chapter 2 in: T. J. Gutiérrez (ed.), *Reactive and Functional Polymers Volume Four*, https://doi.org/10.1007/978-3-030-52052-6_2

The country in Dr. Deval Prasad Bhattarai affiliation is incorrectly mentioned as "India". However, the affiliation is corrected to Department of Chemistry, Amrit Campus, Tribhuvan University, Kathmandu, Nepal.

The updated online version of this chapter can be found at
https://doi.org/10.1007/978-3-030-52052-6_2

T. J. Gutiérrez (ed.), *Reactive and Functional Polymers Volume Four*,
https://doi.org/10.1007/978-3-030-52052-6_9

Index

A
Acetyltributyl citrate (ATBC), 228
Acrylic acid (AA), 230
Advanced materials, 7
Alkoxyamine equilibrium, 187
Amide functionalization (Amidation), 16
Amide-functionalized polymers, 16
Amine-functionalized PS NPs, 16
Aminolysis, 139
Anionic polymerization fuctionalization, 132
Anionic surface functionalization, 15
Antibacterial effect
    against *Staphylococcus aureus*, 39
    N-halamine-functionalized steel, 40
    polidopamine-coated PU films, 40
    QACs-decorated PS, 40
    thymol-decorated PPC, 39
Antibacterial implants, 37
Antimicrobial peptides (AMPs)
    microbes, 36
    microbicidal properties, implants, 36
    on Ti substrates, 37
Atomic force microscopy (AFM), 64
Azobenzene, 117

B
Bacterial cellulose nanocrystals (BCN), 43
Biobased plastics, 208
Biobased synthetic polymers, 210
Biodegradable polymers
    aerobic conditions, 221
    anaerobic conditions, 222
    definition, 210, 211
    disintegration experiments, 219, 220
    ecodesign (*see* Ecodesign)
    ecotoxicity, 222, 223
    global consumption, 209
    mechanism, 211, 212
    polyesters, 209, 210
    recycling, 208
    recycling plastics, 210
    replacing fossil, 209
    standards, 223
    use, 208
    via enzyme catalyzed hydrolysis, 209, 212
Biodegradation, 210
Biointerface engineering, 111
Biointerface strategy, 104
Biointerface technology, 109
Biological environment, 98
Biomedical applications, 13
Biomedical engineering, 115
Bis(hydroxyethyl) terephthalate (BHET), 145
Boronic acid derivatives, 167
Bottom-up methods, 113
Brain drug delivery, 11
Brownian motion, 77

C
Carbon fiber-reinforced thermoset (CFRT), 166, 193
Carboxylate functionalization, 17
Carboxymethylated cellulose nanofibrils (CMCNFs), 45
Catechol functionalization, 17
Cationic polymerization, 132
Cationic surface functionalization, 14
Cellulose materials, 43

T. J. Gutiérrez (ed.), *Reactive and Functional Polymers Volume Four*,
https://doi.org/10.1007/978-3-030-52052-6

Cellulose nanocrystals (CNCs), 43, 229
Cellulose nanofibers (CNFs), 44
Cellulose nanomaterials, 45
Chemical etching, 38
Chemical grafting method, 23
Chemical interface reactions
  acyllactam and amine, 57
  amine and anhydride, 58
  anhydride and epoxy, 58
  carbodiimide and carboxylic acid, 58
  carboxylic acid and isocyanate, 58
  carboxylic acid and oxazoline, 58
  functional groups, 57
  GMA-based reactions (*see* Glycidyl methacrylate (GMA))
  MA-based reactions (*see* Maleic anhydride (MA))
  reactive compatibilization, 57
Chemical reduction, 139
Clays, 229
CNC-PAPMA polymer, 14
Compatibilization
  efficiency, MA-*g*-PE, 65
  MA grafted PP, 62
  MA-*g*-HDPE substrate, 65
  MA-grafted sPS with PA6, 66
  PBT with GMA-modified PP, 71
  PP/PA6 systems, 66
  reactive compatibilization (*see* Reactive compatibilization)
Composting, 223
Conventional trypsinization, 116
Coordination polymerization
  in bulk-functionalization, 134
  chemical modification
    bulk, 136
    factors, 135
    solution reaction, 135
    surface, 136
  definition, 134
  on-surface-functionalization, 134
  post-functionalization, 134
Cotton fiber, 42
Covalent adaptable networks (CANs)
  categories, 160
  fixed cross-link densities, 160
  mechanism, 160, 161
  vitrimers, 160, 165, 169, 171
Covalent immobilizations, 36
Critical surface energy, 74
Cross-linked polyimine, 190, 193
Cyclodextrin polymer (CDP), 46

D
DDAA dimer, 101
Degradation essays, 223
Diclofenac, 41
Diels-Alder (DA), 182
Diene elastomers, 48
Diethylene glycol (DEG), 147
Differential scanning calorimetry (DSC), 64
Dimethyl sulfoxide (DMSO), 139
Dimethyl terephthalate (DMT), 145
Dispersion forces, 73
DNA double helix formation, 100
Dopamine-functionalized PMMA, 11
Dynamic associative exchange reactions
  boronic acid derivatives, 167–169
  diselenide bonds, 179, 180
  hydrazide Michael adduct, 177, 179
  olefin metathesis, 182
  siloxane, 176–179
  transalkylation, 174–176
  transcarbamoylation, 180, 181
  transcarbonation, 166, 167
  transesterification, 161–166
  transthioesterification, 174
  vinylogous urea, 173, 174
  vinylogous urethanes, 171, 173
Dynamic dissociative exchange reaction
  alkoxyamine equilibrium, 186, 187
  reversible DA, 182, 183, 185
  urea/urethane, 187–189
Dynamic mechanical analysis (DMA), 147
Dynamic transesterification reaction, 161

E
Ecodesign
  additives/filters
    cellulose/wood derivates, 229
    clays, 229
    compatibilizer, 228
    grafting, 230
    ionic liquids, 231
    plasticizer, 228
    stabilizers, 230
  chemical bonds, 224
  easy-to-break functions, 224
  formulation
    polyester blends, 225
    starch blends, 227, 228
  repeating unit, 225
Ecotoxicity, 222
Electrochemical polymerization, 113

Electrochemical technique, 137
Electrodeposition
  surface topography, 113
Electron beam lithography, 111
Electron microscopy techniques, 82
Electrosensitive polymers, 117
Electrosensitive systems, 118
Electrospinning, 22
Electro-spun fibers, 8
Enzymatic catalyzed hydrolysis
  advantages, 231
  biodegradability, 219
  essays, 217, 218
  mechanisms, 216, 217
  PBS, 217
  recycling route, 219
Enzyme immobilization, 22
Enzyme sensitive polymers, 118
Epoxypropyl trimethylammonium chloride (EPTMAC), 45
Esterification, 17
Ethylene-vinyl-acetat (EVA), 67
Ethylene-vinyl alcohol (EVOH), 50

F
Food packaging process, 12
Fourier transform infrared (FTIR), 60, 218
Free-radical polymerization, 133
Functional polymers, 209, 210
  SiO_2 NPs, 38
  surface modification (*see* Surface modification)
  surface-free functional groups, 38
  water purification, 43
Functionalization, 36
  MA onto polymer, 59
  PE/PP surface, 39
  PLGA NPs, 41
  polymeric nanomaterials, 41
  PP with MA, 59
  PPC surface, 39
  short alkyl chain, 40
  stainless steel surfaces, 40
  surface functionalization, 80
Functionalization methods
  anionic polymerization, 132
  cationic polymerization, 132
  definition, 130
  direct methods, 131
  direct polymerization, 148
  free-racial polymerization, 133
  graft polymerization, 132
  homopolymerization, 131
Functionalized GO nanosheets, 11

G
Gibbs elasticity, 83
Gibbs-Helmholtz equation, 56
Glycidyl methacrylate (GMA)
  compatibilization effect, S-MA and S-GMA copolymers, 67
  grafting onto polymers, 68, 69
  interface reaction with grafted polymers, 70–71
  non-functionalized polymers, 68
Gold NPs (Au NPs), 41
Graft polymerization, 23, 132–134
Grafting copolymerization, 42
Green bio-industry, 142

H
H-bond donors, 102
H-bonded hetero-complementary interactions, 102
H-bonding energy, 100
H-bonding interactions, 103
Hetero-complementary dimers, 101
Heteroternary complex, 105
Homo and copolymerization techniques, 131
Hyaluronic acid (HA), 41
Hybrid nanocarriers, 103
Hydrolysis, 23, 216
Hydrophobize polymer, 17
2-hydroxyethyl methacrylate (HEMA), 230
Hydroxyl functional group, 24

I
Interface adhesion, 57, 63, 67, 71, 72
Interface characterization
  by advanced mechanical testing, 84–86
  chemical and physical behavior, 82
  classical PP/PA polymer system, 82
  electron microscopy techniques, 82
  mechanical testing, 82
  by melt rheology, 83–84
  multilayer systems, 82
  plate-plate rheology measurements, 82
  polymer blends, 82
  rheological measurement, 82
Interface reaction
  chemical (*see* Chemical interface reactions)
  with GMA grafted polymers, 70–71
  in-situ formation of copolymers, 56
  interfacial diffusion and entanglement
    Brownian motion, 77
    entangled polymer chain dynamics, 78, 79

Interface reaction (*cont.*)
        interfacial diffusion dynamics, 79, 80
        polymer chains, 76
        short chain polymers, 77, 78
        surface activation by plasma, 80–81
    with MA grafted polymer
        amine end group, PA, 63
        bi-component fibers, 65
        compatibilization, 62
        compatibilization efficiency, MA-*g*-PE, 65
        compatibilized blend, 63
        DSC measurements, 64
        fracture toughness, 64
        FTIR spectroscopy, 63
        in-situ synthesized compatibilizer, 63
        MA-grafted poly(ethylene-*co*-octene), 67
        MA-PMMA copolymer, 67
        PAs in polyolefins, 66
        PBT and EVA copolymers, 67, 68
        PP crystallization, 64
        PP/MA-*g*-PP reactive blend processing, 65
        PP/PA6 blend, 63
    phase bonding, 56
    physical interactions
        chain diffusion and entanglement, 72
        dipoles, 72
        interface adhesion, 71
        interfacial energy, 74, 75
        polymer/reinforcement systems, 72
        surface energy, 72–74
    strategies to strengthen, 57
Interfacial adhesion process, 79
Interfacial characterization
    by nano-IR technique, 86–87
Interfacial energy, 74, 75
Interfacial wetting, 79

L
Lithography, 110, 111
    biomedical field, 110
    electron beam lithography, 111
    emergence, 110
    fabrication approach, 110
    photoreactive material, 111
Lower-critical solution temperature (LCST), 115

M
Macrocyclic host-guest interactions, 103
    binary complexes, 103
    nanocarriers, 103
    photoresponsive properties, 104
    poly-L-lysine, 104
MA-*g*-high-density PE (MA-*g*-HDPE), 65
Maleic anhydride (MA), 38, 39, 45, 131
    grafting, MA onto polymers, 59–62
    MA grafted polymer (*see* Interface reaction)
Mechanical recycling method, 143
Mechanical testing, 82, 85
Medical implants, 27
Metallic implants, 13
Metal-ligand coordination, 106
Metal-organic coordination, 106
Metal-organic coupling scheme, 106
Methyl methacrylate (MMA), 230
Microfluidic channels, 9
Microwave plasma-mediated surface reactions, 38
Modular self-assembly approach, 98
Molecular weight distribution (MWD), 132
Multilayer polymer system, 56
Multiphase polymeric systems, 56
Multiple H-bonds, 100
Multiple nanocarriers, 13, 14
Multiple responsive polymeric system, 118–119
Mussel-inspired polyglycerol (MI-PG), 18
Mutual diffusion, 80
Mw distribution (MWD), 211

N
N,*N*-acetals, 170
Nanoimprint, 112
    hydrophilic block, 112
Nano-IR technique, 86, 87
Nanoprinting surface, 112
Nano-scale analysis, 86–87
Non-covalent bonds, 100
Non-covalent interactions, 98
Non-covalent physical adsorption, 36
Non-dye anionic water pollutants, 46
Novolac resin (NR), 170
Nuclear magnetic resonance (NMR), 218

O

Olefin metathesis, 182
Orthogonal stimuli-responsive system, 119
Oxidation modification, 17
Ozone treatment method, 22

P

PET supported thin silica film (PET-(SiO_2) X-OH), 140
Petroleum-based organic polymers, 208
pH switchable, 117
Phenanthrene, 46
Phenylboronic acid (PBA), 170
Photodegradation/photo-oxidation, 211
Photolithography, 110
Photo-responsive molecules, 116
Photo-sensitive polymers, 116
  light, 116
pH-responsive drug delivery systems, 10
pH-sensitive polymers, 117
Physiological niche, 13
Plasma-induced effects, 12
Plasma treatment, 20, 27, 80, 81
Plasticizer, 228
Polar solids, 75
Polidopamine, 39
Poly(3-hexylthiophene) (P3HT), 49
Poly(butylene succinate) (PBS), 209
Poly(butylene terephthalate) (PBT), 67
Poly(dimethylsiloxane) (PDMS), 176
Poly(ethylene succinate) (PES), 216
Poly(ethylene terephthalate) (PET), 210
Poly(hydroxyalkanoates) (PHAs), 209
Poly(lactic acid) (PLA), 69, 209
poly(methylmethacrylate) (PMMA), 140
Poly(propylene carbonate) (PPC), 39
Poly(tetrafluoroethylene) (PTFE), 138
Poly(ε-caprolactone) (PCL), 209
Polyelectrolyte multilayers (PEMs), 105
Polyelectrolytes, 118
Polyester films, 46
Polylactic-*co*-glycolic acid (PLGA) NPs, 41
Polymer blends
  compatibility, 83
  and composites, 56
  interface characterization, 82
  interphase, 56
  properties, 56
Polymer composite materials, 11
Polymer degradation
  characteristics
    crystallinity, 213, 214
    hydrophobicity, 214
    macroscopic shape, 213
    molar mass, 212
  environmental conditions
    humidity, 214
    marine/saline, 216
    microorganisms, 216
    oxygen, 215
    pH, 214
    species, 215
    temperature, 215
Polymer grafting, 18
Polymer material (PHBV), 225
Polymer modified asphalt (PMA), 146
Polymer/reinforcement system, 75
Polymeric materials, 10
Polymeric nanomaterials, 10
Polymeric NPs, 13
Polymers
  free energy of mixture (ΔGm), 56
  functionalization and modification, 56
  melt flow behavior, 83, 84
  melting dynamics, 77
  multiphase polymeric systems, 56
  polymer interface (*see* Interface reaction)
Polymers, surface functionalization
  adsorption process, 10
  amine functionalized PS NPs, 16
  anionic groups, 15
  applications, 8
  approaches, 25–26
  assessment, 26
  biomedical applications, 13
  carboxylate groups, 17
  cationic moieties, 14
  chemical and physical changes, 26
  drug delivery vehicles, 10
  electronics, 11
  electrospinning, 22
  engineered material, 7
  esterification, 17
  food packaging process, 12
  forms and designs, 7
  fundamentals, 7
  GO-based PU nanocomposites, 19
  material surfaces, 7
  materials, 7
  microfluidic channels, 9
  nanomaterial, 7
  nanomaterials, 8
  ozone treatment method, 22
  PCL nanofibers, 10
  PEEK polymers, 24

Polymers, surface functionalization (*cont.*)
  PEO/PCL coating, 12
  phenotype and cell organization, 8
  physical applications, 7
  physicochemical characterizations, 26
  plasma, 20
  polymer grafting, 18
  properties, 7
  scope, 9
  silane group, 18
  spectroscopic signal, 26
  surface properties, 8
  synchrotron radiations, 27
  textile, 12
  ultrafiltration, 10
  UV treatment, 21
Polysaccharide graft copolymerization, 42, 43
Preparation techniques
  electrodeposition, 113
  LbL, 109
  lithography, 110
  nanoimprint, 112
  neuronal cells, 114
Protein adsorption, 8
Proton acceptor, 101

Q
Quaternary ammonium compounds (QACs), 37, 38, 40

R
Reactive and functional polymers, 1
Reactive compatibilization
  bi-component fibers, preparation, 65
  chemical interface reaction, 57
  covalent bonds, 57
  functional groups, 57
  glass transition temperature, 68
  GMA-*g*-LDPE with PA6, 70
  HDPE with PET, 67
  MA grafted PP and PA6, 62
  NR/PA6 system, 67
Reactive extrusion (REx), 136
Reactive polymers
  infrastructure applications, 146, 147
  techniques
    chemical, 144, 145
    energy recovering, 145
    mechanic, 143
    plastics, 142, 143
    thermoplatic polymers type, 143
Reactive/functional polymers, 130
Recycling polymers
  functionalization methods, 130
  industrial applications, 141, 142
  reactive, 141 (*see also* Reactive polymers)
  reactive/functional, 130
retro Diels-Alder reaction (rDA), 182
Reversible addition fragmentation chain transfer (RAFT), 133
Rheological measurement, 82
Ring-opening metathesis polymerization (ROMP) methods, 133
Rouse diffusion coefficient (DR), 77

S
Scanning electrochemical microscopy (SECM), 138
Scrap tire rubber, 147
Silica nanoparticles (SiO_2 NPs), 38
Silylation (silane grafting), 18
Si-O-Si bond, 176
Spray coating method, 18
Stabilizers, 230
Starch, 227
Stearic acid grafting, 12
Stem neuronal cells, 114
Steric exclusion chromatography (SEC), 220
Sterilization, 27
Stimuli-responsive polyelectrolytes, 105
Stimulus-response
  electrosensitive polymers, 117
  LCST, 115
  photo-sensitive polymers, 116
  PNIPAM, 115
  thermo-reversibility, 115
  thermosensitive, 115
Stimulus-responsive supramolecular interfaces, 100
Stimulus-sensitive polymer chains, 99
Styrene-GMA (S-GMA), 67, 70
Styrene-maleic anhydride (S-MA), 67
Sulfhydryl cotton fiber-based (SCF) materials, 42
Superhydrophobic surfaces, 12
Superhydrophobicity, 12
Supramolecular and switchable polymers, 104
Supramolecular block copolymers, 112
Supramolecular chemistry, 98
Supramolecular interactions, 98–100, 109
Supramolecular polymer interactions
  AOA layer, 103
  DDAA dimer, 101

  H-bonded rings, 102
  H-bonding interactions, 100
  hetero-complementary dimers, 101
  material functionalization, 101
  multiple H-bonds, 100
  SOA-AOA motif-copolymer, 103
  supramolecular interactions, 103
  UPy's tautomerized product, 101
Supramolecular polymers, 109, 113
Surface acetylation, 17
Surface acylation, 17
Surface characterization methods, 27
Surface energy, 72–74
Surface functionalization, 80, 136
Surface functionalization, polymeric nanomaterials, 40
Surface functionalized NPs, 11
Surface modification
  antimicrobial applications
    AMPs, 36
    antibiotics, 39
    ceramic nanocompounds, 38
    QACs, 37
    stainless steel surfaces, 40
    strategies, microbiological growth, 36
  desalination/purification applications (*see* Water desalination)
  drug delivery applications
    diclofenac, 41
    HA, 41
    PLGA NPs, 41
    pluronic, 40
    polymeric membranes, 40
    polymeric nanomaterials, 40
  improved coating applications, 48, 49
  radicals, carbenes, and nitrenes, 140, 141
  techniques
    aminolysis, 139, 140
    chemical oxidation, 138
    chemical reduction, 139
    electrochemical, 137, 138
    plasma, 137
  textile applications, 42
Surface modified NPs, 11
Surface properties, 7
Surface topography, 113
Swelling-shrinking, 117
Swelling-shrinking transition, 106
Switchable and supramolecular polymers, 99
Switchable bio-interfaces, 98
Switchable polymer layers, 109
Symmetric oligoamide (SOA), 102
Synthetic diene elastomers, 48

T
Tetraethyl-2,2′-[1,4-phenylenebis(methanyllidene)] dimalonate (TPMD), 177
2,2,6,6-tetramethyl-1-piperidinyloxy (TEMPO), 186
1-(*tert*-butyl)-1-ethylurea (TBAE), 189
Textile polymer composite, 85
Thermoplastic polymers, 143
Thermosetting polymers
  applications, 160, 198
  bonds, 198
  CANs, 160
  definition, 160
  dynamic associative exchange reactions, 161
  exchange reactions
    disulfide, 194, 195, 197, 198
    Schiff base, 190, 191, 193, 194
Titanium dioxide (TiO_2), 230
Top-down methods, 113
Transcarbonation, 166
Transcarbonation in the presence of catalyst ($Ti(O\textit{i}\text{-}Pr)_4$), 167
Transthioesterification, 174
Triazolinedione (TAD), 49
Triethylene glycol (TEG), 147
Tube model, 78, 79

U
Ultrafiltration, 10
Uniform dispersion, 11
Upper-critical solution temperature (UCST, 115
UPy-units, 101
UV treatment, 21

V
van der Waals forces, 98
Visible-light-responsive polymers, 104

W
Water contact angle (WCA), 73, 74, 81
Water desalination
  acid hydrolysis, 45
  CDP-coated electrospun PET nanofibers, 47
  cellulose materials, 43
  chemical modifications/functionalizations, 44

Water desalination (*cont.*)
  CMCNFs, 45
  heavy metal ions, removal, 46
  non-dye anionic water pollutants, 46
  PET-TSC chelating fibers, 47
  polymeric resins, 48
  and purification applications, 43, 44
  reactive molecules, 44
  removal of contaminants, 43
  resin beads, 48
  SNC-3-MPA synthesis, 46
  succinylation, 45
  superficially modified cellulose, 43
  surface modification, CNFs, 44
  TEMPO oxidation method, 45
  water and isocyanate (R-NCO), 45
Wetting, 72, 73, 75, 76, 79
Wood-based fillers, 229

X
X-ray photoelectron spectroscopy (XPS), 81, 107

Z
Zeta potential magnitude, 13
Zimm model, 78
Zwitter-ionic surface functionalization, 15